Behaviour of concrete frame structures under localised fire scenarios

Suryawan Murtiadi

School of Engineering & Applied Science

ASTON UNIVERSITY

Doctor of Philosophy

July 2007

ASTON UNIVERSITY

Behaviour of concrete frame structures under localised fire scenarios

Suryawan Murtiadi

2007

SUMMARY

Concrete structures have a favourable position in the building industry with regard to their performance of fire resistance. Consequently, the understanding of its behaviour under elevated temperature is essential for reliable analysis and safe design. This thesis encompasses an investigation of the behaviour of concrete frame structure under localised fire scenarios by implementing a constitutive model using finite-element computer program.

The investigation phase included properties of material at elevated temperature, description of computer program, thermal and structural analyses. Transient thermal properties of material have been employed in this study to achieve reasonable results. The finite-element computer package of ANSYS is utilized in the present analyses to examine the effect of fire on the concrete frame under five various fire scenarios. In addition, a report of full-scale BRE Cardington concrete building designed to Eurocode2 and BS8110 subjected to realistic compartment fire is also presented.

The transient analyses of present model included additional specific heat to the base value of dry concrete at temperature 100°C and 200°C. The combined convective-radiation heat transfer coefficient and transient thermal expansion have also considered in the analyses. For the analyses with the transient strains included, the constitutive model based on empirical formula in a full thermal strain-stress model proposed by Li and Purkiss (2005) is employed. Comparisons between the models with and without transient strains included are also discussed.

Results of present study indicate that the behaviour of complete structure is significantly different from the behaviour of individual isolated member based on current design methods. Although the current tabulated design procedures are conservative when the entire building performance is considered, it should be noted that the beneficial and detrimental effects of thermal expansion in complete structures should be taken into account. Therefore, developing new fire engineering methods from the study of complete structures rather than from individual isolated member behaviour is essential.

Keywords: Concrete, displacement, fire, finite-element, strain, stress.

ACKNOWLEDGEMENTS

This thesis was completed at Aston University in Birmingham, United Kingdom, for the degree of Doctor of Philosophy in Civil Engineering. Funding in the form of graduate fellowship from the Government of Republic Indonesia through the Engineering Education Development Project of Indonesia and has been managed under auspices of the British Council is gratefully acknowledged. Additional financial support from the School of Engineering & Applied Sciences, Aston University, is also indebted.

Grateful acknowledgements are also presented to Dr JA Purkiss and Dr LY Li for their patience, encouragements and affections under whose discussions, guidance and supervisions of the thesis was carried out. Acknowledgement is also addressed to Prof R J Kettle, Subject Group Convenor of Engineering Systems & Management, for his encouragements and the facilities provided. Remarkable thanks also made to Mr R Poole and Mr A Crowcombe, computer engineers, for their excellent technical supports and assistances during the computer works.

Especial thanks to my beloved mother, Hj. Mursidah, who relentlessly provided me with the moral support (regardless of those "steaming phone bills to Indonesia"). Grateful thanks to my wife, Sri Sugiyatmi, and my son, Handal Suryaputra, for their continuing encouragements and affections. I also extend my gratefulness to all of family member, especially my brothers and sisters, for their supports and fondness.

Last but certainly not least, I take this opportunity to express my profound gratitude to the Dean of Faculty of Engineering, colleagues and staffs at Mataram University for inspiring me to undertake this enormous challenge.

This thesis is dedicated to the memory of my beloved father,

RM.H. MASHURI WIRYOSAPUTRA

who passed away on 5th October 2005 during my struggle of finishing this thesis.

CONTENTS

LIST OF FIGURES

LIST OF TABLES

NOTATION

Roman Characters

A Area

a_c Thermal diffusivity of concrete

a_s Thermal diffusivity of steel

c Specific heat

c_p Specific heat of combined heat and mass transfer

$c_{p,dry}$ Specific heat of dry concrete

c_{add} Additional specific heat of mass transfer

$[C]$ Conductance matrix

$\frac{dT}{dx}$ Temperature gradient

E Integrity of the test specimen

E_c Young's modulus of concrete

e Emissivity

e_{free} Concrete water content by weight

f_{cu} Concrete design strength based on cube strength

$\bar{f}_c$ Concrete permissible stress

f_y Characteristic strength of steel reinforcement

f'_{max} Most positive (tensile) stress

f'_{min} Most negative (compressive) stress

I	Insulation of the fire test specimen
i, j	Indexes
l	Length or thickness
R	Stability of the fire test specimen, thermal resistance
Q	Quantity of heat
T	Temperature
T_∞	Temperature of surrounding environment
t	Time

Greek Characters

α	Coefficient of convective heat transfer
$\varepsilon_{cr,c}$	Creep strain of concrete
$\varepsilon_{tot,c}$	Total strain of concrete at elevated temperature
ε_{th}	Thermal strain
$\varepsilon_{th,c}$	Thermal strain of concrete
$\varepsilon_{tr,c}$	Transient strain of concrete
$\varepsilon_{\sigma,c}$	Stress strain of concrete
Φ	Radiation factor of the angle of the heat source
λ	Thermal conductivity
λ_c	Thermal conductivity of concrete
λ_s	Thermal conductivity of steel
υ	Poisson's ratio

ρ	Density
σ	Stefan-Boltzmann constant
Δl	Length increment
ΔT	Temperature increment
Δt	Time increment
Δx	Displacement in the X direction or horizontal direction
Δy	Displacement in the Y direction or vertical direction

Chapter 1 INTRODUCTION

1.1. General

The integrity and strength of building materials are strongly affected by their exposure to their environment. Exposure to high temperatures causes changes in performance of the materials due to changes in its structural behaviour. Concrete frame structures when subjected to fire are expected to experience a loss of strength. The loss of strength may or may not be recovered after cooling. The amount of loss and recovery depends on the type of material, the severity of the fire as measured by its temperature, and the duration of the exposure fire.

Severe temperature and prolonged exposure to fire will result in reductions of concrete compressive and tensile strengths. Elevated temperature will also cause aggregate splitting, spalling and cracking. Most fine cracks are confined to the surface where wide cracks or cracks near supports may cause a loss of anchorage or yielding of the steel reinforcement. These phenomena play as a significant role to the collapse of structures.

In general, as reported by Schneider (1990), when the concrete temperature rises above 100°C, the cement paste begins to dehydrate because the moisture is driven off. The particles of aggregate start to expand generating large differential strains and cause extensive micro cracking of the cement paste. Disintegration of the concrete eventually happens at this stage even though without suffer any losses of the concrete strength. The residual concrete strength of around 80-90% of the initial strength happens when temperature increase to 200°C.

Further increases of temperature above 300°C, some aggregates begin to break up while the yield strength of reinforcing steel begins to reduce. At this temperature, residual concrete strength is about 70% of its initial strength. The concrete strength as well as the strength of reinforcing steel reduces significantly when temperature rises between 500°C and 600°C. At this stage the residual concrete strength is around 30-40% while the strength of reinforcing steel reduces to about 50%. In compartment fires, the concrete temperatures can rise above 1200°C when most of the concrete particles fuse.

During the past decade, considerable attention has been given to the use of structural building components as physical barriers to prevent or delay the growth and spread of fire. The basis for the present study is to require special consideration by the designer for fire safety in buildings. This also applies to concrete structures which traditionally have a favourable position in the building industry regarding their performance of fire resistance.

Khoury (2000) reported that concrete mixes have been developed to provide structural strength and robustness under extreme fire loading. Deterioration of mechanical properties can be reduced by sensible design of the concrete mix. Behaviours of aggregate, cement paste, and the interaction between them should be taken into consideration. Desirable features of aggregate are: (a) high thermal stability to prevent break-up at low temperatures; (b) low thermal expansion to improves thermal compatibility with cement paste; (c) rough angular surface to improves physical bond with the paste; and (d) presence of reactive silica to improves chemical bond with the paste. For the cement blend, a low CaO/SiO_2 ratio (C/S ratio) is desirable to ensure a more beneficial hydrothermal reaction. The C/S ratio is reduced in practice by the use of cement replacements such as slag, pulverized fly ash and silica fume in the mix. He

tested that the use of slag produces the best results at high temperatures, followed by pulverized fly ash and then silica fume.

Supplementary polypropylene fibres are also required in the concrete mix to reduce spalling if concrete has low permeability from the use of silica fume for high-performance concrete. The relatively low performance of the silica fume cement paste at elevated temperature is contrary to its high durability performance at room temperature. The low performance may be attributed to the dense and low permeability structure of the paste which does not allow moisture to escape from the heated concrete resulting in high pore pressures and the development of micro-cracks. The uses of polypropylene fibres are considered for the purpose of increasing permeability during heating. Polypropylene fibres melt at approximately 160°C provide channels in the concrete for moisture to escape reducing pore pressures and the risk of spalling. A minimum dosage polypropylene fibre value of 2 kg/m^3 has been recommended in the Eurocode 2 (2002) for high strength concrete.

1.2. Scope of Research

A review of the effect of elevated temperature on the strength and material properties of structural concrete elements will be carried out. The process of heat transfer from exposed fire environment to the structural element as well as the heat transfer within the element itself will be presented. Modelling of concrete frame structures before and under fire will be initiated and analysed.

In order to analyse the thermal and structural responses, finite element computer software will be utilized using ANSYS. A suitable constitutive model for general

purpose finite element program will be implemented. By implementing the constitutive model, the behaviour of concrete frame structures subjected to fire can then be predicted accurately under variation of localised fire compartment scenarios.

1.3. Research Objectives

Previous researchers have dealt with the design aspects of structural elements such as beam, slab, and column when exposed to the effects of fire. This study is concerned with how those elements behave when connected together to form a complete structure. The continuity effects that are generated when elements are connected together can be taken advantage of in design. Better understanding of the interactions between different components when subject to fire is likely to prove more cost-effective. Therefore the performance of individual isolated components should not be a high priority.

Based on the above, the main objective of this research is to study and evaluate the behaviour of concrete frame structures subjected to localised fire scenarios. This major objective is not limited to but may contain the following objectives:

- To investigate the thermal behaviour of a concrete frame structure. The investigation includes the temperature distribution in the element and thermal expansions from the heated parts of the structure within localised fire scenarios.
- To analyse the structural behaviour and performance of the reinforced concrete beam-column connections subjected to fire. The analyses include horizontal and vertical displacements of the element. The beam and column are constructed with difference concrete materials, i.e. normal strength concrete for the beam and high-strength concrete for the column.

- To examine the stress analyses of the structure in which the properties of material, boundary conditions, and sequence of fire are varied. The examinations consist of analyses with and without transient strains included.

1.4. Format

This thesis can be divided into three main parts. Part I appears under Chapters 1, 2 and 3. Chapter 1 covers the introduction, the scope of research and the objective of the research. Chapter 2 covers the general discussion and the literature review. Chapter 3 covers the previous experimental investigation of a full-scale reinforced concrete building subjected to fire carried out by BRE at their laboratory in Cardington.

Part II appears under Chapters 4 and 5 which consist of computer analyses carried out to study the behaviour of concrete structures at elevated temperatures. The investigation have been presented using ANSYS program, which is based on finite element computer program. Chapter 4 covers the description of the computer program illustrated with conduction elements used by ANSYS. Chapter 5 covers the heat transfer analysis using the program and validating the result using finite element calculation.

Part III appears under Chapter 6 which covers the discussion of concrete frame structure under structural and thermal analysis. The preliminary analysis carried out at Aston University prior to the test of Cardington concrete frame will be presented with and without transient strains. And modelling of concrete frame structure as a substructure of the whole building will be investigated with and without transient strains included under variety of fire compartment scenarios.

Chapter 2 GENERAL DISCUSSION AND LITERATURE REVIEW

2.1. General

Green (2003) reported that in 1999 the UK was estimated to be spending £1.75 billion a year on fire protection within buildings. He suggested that current annual spending are about £2 billion while the Association of British Insurers estimated the cost of fires at £7 billion a year. Injuries resulting from fires, including domestic accident, rose by 1% to 17,200 during 2002 but were still below the average in recent years. Based on above data, everyone is calling for far more integrated approach to fire safety. The integration should be approached starting from the whole design to process of construction and continued maintenance. The structural fire safety can make contribution to the protection of the property and therefore, the insurance premium could also be reduced. A code of practice for protection of business published by Fire Protection Association (1999) could be used as guidance for the fire protection of buildings.

The Fire Protection Association (1965) described that fire is a chemical reaction in the process of burning when heat is released and the form of substance is destroyed. Fire can occur caused by three essential materials such as fuel, oxygen and initial source of heat as an ignition. In a building fire, the fuel would be present in the combustible structure or furniture and other materials content in the building while oxygen is present in the air. In fire statistics, the initial source of heat is generally occurs by accident through a variety of mechanism from appliances fault, electrical wiring, overheating of

mechanical plant etc. Arson, war and terrorism have also been the cause of many fires in buildings.

All fires create smoke. Smoke is dangerous even though the heat itself may not cause damage. Smoke consists of small carbonaceous particles suspended in the atmosphere that can obscure the passage of light preventing exit signs from being seen. Heavy smoke may also contribute to panic because of its effects on eyes, nose and throat. In this condition, occupants may be unable to reach a place of safety quickly enough or became trapped by the heavy smoke cutting off their escape route.

Concrete is a non-combustible material and a good insulator. However, there is significant loss of strength and significant large deformations of the structure which is sufficient to cause collapse when very high temperature is reached. The collapse can be caused by large compressive forces on vertical elements due to restraint of thermal expansion from entire structural elements especially from large thermal expansion of horizontal element such as slab.

In a concrete structure, steel reinforcement has little effect on the strength when exposed to temperature below 250°C. Higher temperature exposure causes reductions in Young's modulus, yield stress and ultimate strength. For steel reinforcement of various types the nominal yield stress is reduced significantly to 50% of its normal value at temperatures of 550°C. As this temperature can be reached very early in a fire, concrete cover and element size data are usually required to have an adequate fire resistance. However, we need to carefully consider that providing element fire design will not guarantee structure design.

During the past decades, the behaviour of concrete structures in fire has been investigated in the range of heavy smoke to major destruction. The investigation

included disintegration of reinforced concrete, yielding of steel reinforcements that cause large deflections, and buckling of structural elements, as well as damage to a variety of interior elements. The main objective of the investigation is to increase both live safety and property safety.

In the UK, the tests of real fire in the large-scale structures have been conducted to investigate whole building behaviour that could not be identified from standard fire test. The full-scale fire tests of eight-storey steel-composite building, six-storey timber framed building and seven-storey reinforced-concrete building have been carried out at BRE. These investigations will be discussed further in the next chapter.

Since an active or passive fire protection system may not be operational, it should be noted that the situation during construction or repair can be inherently more severe than for completed building. When buildings under construction, a substantial amount of highly combustible materials is often stored on the site, some site processes involve the use of naked flame. Muirhead (1993) explained that a full security system linked to any fire detection procedure through construction is necessary.

Several buildings experienced fire damage at the time of under construction have been highlighted by Robbin (1990) at the Broadgate Centre building, Bishop (1991) at Minster Court building, Rosato (1992) at London Underwritting Centre building and Byrd (1992) at Pavilion of Discovery building caused by drying sprinklers in Expo'92 burned. Malhotra (1986) assigned the summary of the considerations in fire safety engineering under two headings of active and passive measures. In the UK, requirement for structures under various type of occupancy is covered by BS 5588 Part 1–11, while regulatory control of current situation is covered by Read and Morris (1993) and guidance is also published by the Department of the Environment (1992).

2.2. Early Investigations

Numerous fire tests on concrete structures have been carried out throughout the history of reinforced concrete structures. The fire tests have been carried out both on concrete elements as individual structural members and when it is connected together to form whole structures. One of the earliest reports was published in London by Hyatt (1877) presented some experiments with Portland cement concrete on floor under elevated temperature.

Bottke (1931) investigated behaviour of reinforced concrete structures in fire. He attributed that the differential thermal expansion over the cross-section of heated concrete, especially the differential between the concrete and reinforcing steel, plays an important role to exacerbate the stresses of the structure. In general, the classification for fire resistance of a concrete structural member is based on the standard fire exposure according to ISO 834 (1987).

Concerning fires in concrete building, large numbers of reports dealing with structural analysis have also been published. Becker and Bresler (1974) presented an analysing reinforced concrete frame subjected to fires. They used computer program, FIRES-RC, related discretization techniques to approach the behaviour of the concrete structures. Anderberg (1976) established this computer program to include material behaviour on the analysis. These models have been developed at the Lund Institute of Technology in Sweden. Another establishment has also been presented as a revised version by Iding, Bresler and Nizamuddin (1977) with analytical method using computer program called FIRE-RCII. They replaced the secant stiffness approach by a

tangent stiffness solution approach for the linear variation of the moment along the axis of the beam element.

2.3. Current Methods of Design

IStructE (1978) as well as CEB (1982) recommended a simple approach in fire resistance design that flexural failure is only related to the combination of stress and temperature in tension reinforcement. The required fire resistance can be obtained through tables incorporating concrete cover and temperature rise in the reinforcement. They also presented simple analytical methods based on the cross section analysis in which the moment capacity can be determine through the combination of fire time, cross section temperatures and material strengths.

Design of concrete structures subjected to fire in the UK has been published by British Standard Institution. BS 8110: Part 1 (1989) specifies minimum cross-section sizes of all structural members and nominal cover of reinforcement. This code assumes that if the reinforcement cover is less than 40 mm, severe spalling of the concrete does not occur.

Where the concrete cover is greater than 40 mm the designer is referred to BS 8110: Part 2 (1985) where the use of steel fabric is specified as additional reinforcement placing between the main bars and face of the member. BS 8110: Part 2 provides guidance on spalling of concrete, protection against spalling and the behaviour of aggregates in fire. BS 8110 presents three design methods to be used to calculate fire resistance requirements. The three design methods are: tabulated cover and member size data, application of fire test performance data and a basic fire engineering approach.

Along with the British Standards Institution (1989), a European Standard has been developed for structural fire design of concrete structures. Eurocode 2 (ENV 1992-1-2) provides similar prescriptive rules to those given in BS 8110. The latest draft of the EN version of the Eurocode 2 (2002) provides guidance on concrete spalling especially for high-strength concrete, namely the use of supplementary polypropylene fibres in the concrete mix for a minimum of 2.0 kg/m^3 dosage.

The current fire design methods are predominantly based on the fire resistance of individual members tested in small furnaces with the assumption that the fire resistance of the connected members on the entire structure will be at least equal to the fire resistance of its individual members. However, researchers such as Bailey (2002), Chana (2000), Izzuddin and Moore (2002), determined that the individual member-based approach is not likely adequate for the majority of entire structure since the behaviour of the most structure have significant beneficial and detrimental effects during fire. The fire performance of complete structures is significantly different than that of single elements from which fire resistance is universally assessed also recommended by Armer and Moore (1994). Therefore, considerable attentions should be given to the exploitation of full-scale fire testing.

Bailey (2002) described the limitations of the prescriptive approve and discussed the advantages of adopting performance based approach to ensure safe and economical building designs. He explained an obvious difference between whole building and individual member behaviour is that the structure will utilise actual load path mechanisms that cannot be identified from individual member testing. He gave an example that restraint to thermal expansion of a floor slab can induce high compressive stresses into a heated slab which can be beneficial by inducing compressive membrane

action to support the applied load. Another example, as a result of the large lateral movement caused by thermal expansion of floor slab the whole building can lead to premature collapse. This form of behaviour is not covered in current design codes.

In conclusion, Code of Practice methods of design for fire structure should provide the foundation for a full design approach rather than prescription. Current methods are based on isolated member behaviour. New methods, however, should look at the whole structure taking into account the inherent fire resistance and robustness of concrete construction. With respect to complete structures, it is likely the requirements for the design analysis of fire engineering will remain complex. The design engineers should be able to achieve solutions with validated experience in the field of fire engineering.

2.4. Overview of Concrete at High Temperatures

It has been reported in the literature that the behaviour of concrete exposed to fire depends on many simultaneous interacting factors. These factors range from the composition of the materials to the characteristics of the fire. Purkiss (1996) explained that the two main variables to be considered here are the specification of minimum overall dimensions of the member and the minimum concrete cover to the main steel-reinforcement. The minimum dimensions are specified to keep the temperature on the unexposed face below the insulation limit of 140°C as well as to ensure that spalling will not be severe enough to lose an amount of concrete. The minimum cover is specified to keep the temperature of the main reinforcement below a critical value generally considered as being around 500-550°C.

This chapter gives an overview of the standard fire test including the standard time-temperature curve and failure criteria of the tested members. The damage of concrete under fire, the thermal and mechanical properties of the concrete at elevated temperature are also presented.

2.4.1. Fire Development in Compartment Fires

Normally, a fire starts with the ignition of a single product then grows up into a fully developed fire. Conventionally, the development of fire presented in Figure 2.1 can be divided into three periods such as growth period, full development period and decay period.

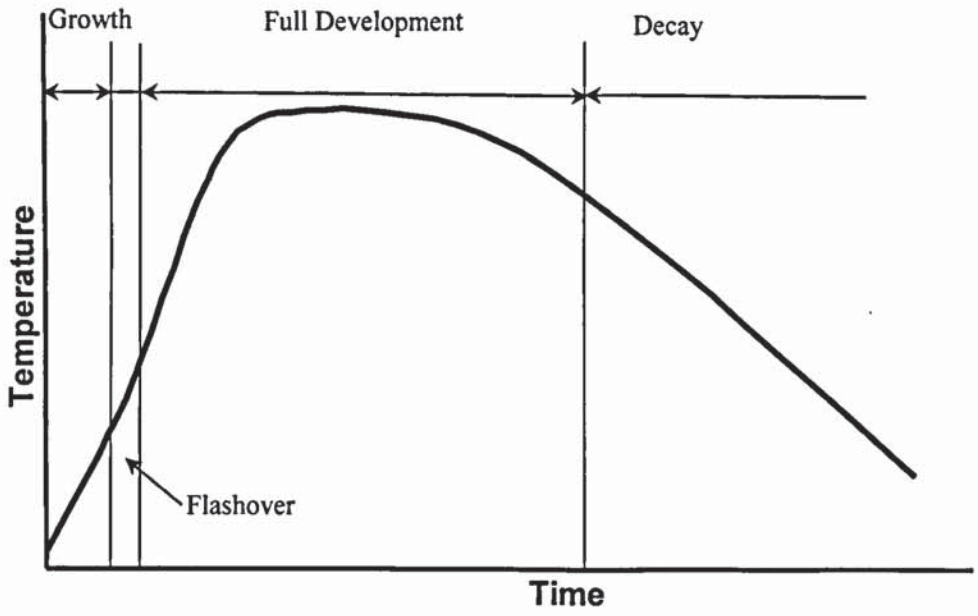

Figure 2.1 Generalized of fire development

The start of the full development period is usually preceded by a phenomenon referred to as flashover which is characterized by an almost instantaneous spread of

flame over all combustible surfaces. Harmathy (1993), however, indicated that the decay period begins when temperature decrease to 80% from maximum temperature after the peak.

2.4.2. Standard Fire Test

It has been found that the nature of fire depends substantially upon the nature of fuel. The fire resistance of structures in the compartment fire is determined by subjecting specimens of the compartment boundaries to standard test fires. Standard tests are idealized simulation of compartment fires presented in a unique temperature-time curve. According to ASCE (2002), there are no significant differences of standard temperature-time curved used in various countries of Europe, Australia and North America. Standard fire test used in the UK will be presented in the next discussion.

2.4.2.1 Fire time-temperature

The time-temperature curve used in fire resistance test is regulated on an international basis by ISO 834 (ISO, 1975). The thermal exposure is based upon an air temperature measured nominally 100mm from the fire exposed face of the element, either in a vertical or horizontal plane. The time-temperature curve specified for the furnace is defined in the following mathematical relationship:

$$T_g = 20 + 345\log(8t + 1) \tag{2.1}$$

Where: T_g is the furnace temperature (°C) and t is the time (minutes).

Equation (2.1) gives temperatures of about 842°C, 945°C, and 1049°C at the times of 30, 60, and 120minutes, respectively. This equation can also be plotted on Figure 2.1 as time-temperature response of standard furnace test according to BS476 (1987). The relationship between time and temperature results in a curve with a very steep initial rise in temperature which slows down as time progresses making a smooth transition into a nearly steady state heating relationship.

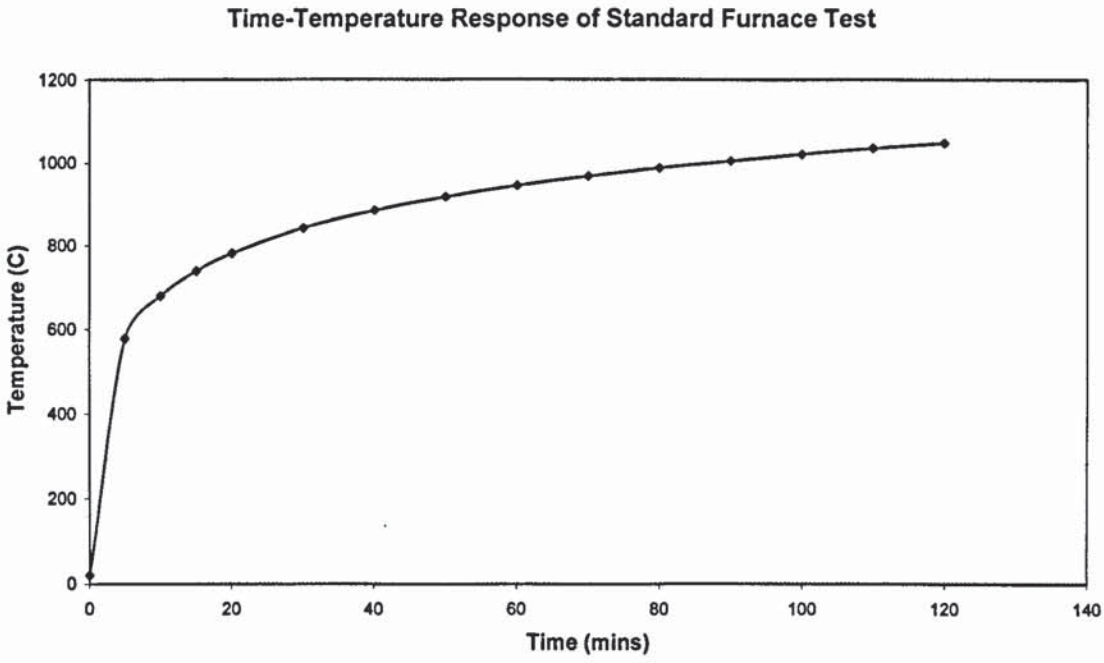

Figure 2.2 Time-temperature response of standard furnace test according to BS476

Concept of equivalent fire severity is used to relate the severity of standard fire test to an estimated real fire. First attempts at time equivalence compared the area under time-temperature curves was proposed by Ingberg (1928). Figure 2.3 illustrates the concept in which two fires are considered to have equal severity if the areas under each curve above a base of certain reference temperature are equal. However, the equal area

concept can cause a problem since it give a very poor comparison of heat transfer for fires with different time-temperature curve where the first curve gives low peak temperatures with a long duration and the second curve give high peak temperatures but has a short duration.

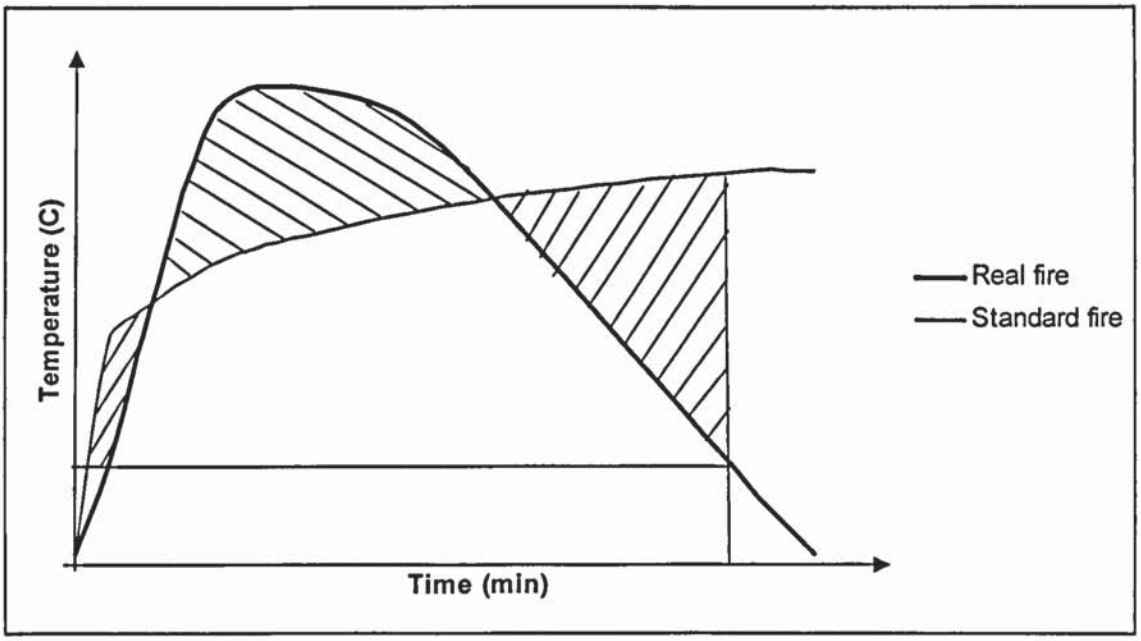

Figure 2.3 Equivalent of fire severity on equal area basis

2.4.2.2 Failure criteria

Failure criteria of the standard test depend on the type of member tested. These failure criteria are simply identified as:

- Stability (R)
- Insulation (I)
- Integrity (E)

Stability (R), or load bearing capacity, is a measure of the element ability to resist the applied loading over the duration of the test. The test procedures set a limit on

the maximum displacement or rate of displacement that is taken to the time at which the stability is lost. So, the test can be stopped before actual failure occurred to the test specimen in which would damage the furnace. The standard sets the following criteria for the maximum displacement and rate of displacements:

$\frac{l^2}{400d}\ mm$ or $\frac{l^2}{9000d}\ mm/\min$ for horizontal element, and $\frac{h}{100}\ mm$ or $\frac{3h}{1000}\ mm/\min$ for vertical element. However, Bailey (2004) states that these limits have primarily been set to reduce the probability of damage to the furnace and do not relate to true structural behaviour of the real structures.

Insulation (I) is a measure of ability to restrict heat transmission throughout the cross section of the element. The temperature on the unexposed face must not exceed a maximum of 180°C plus ambient (nominally 200°C) or an average of 140°C plus ambient (nominally 160°C). These limits have been set to prevent initiation of combustion of materials stored against that face.

Integrity (E) is ability of the element to resist the passage of flame and hot gasses from fire to unexposed face. The flame should not being able to reach unexposed face through any weakness in the construction or due to excessive deformation during the test. Failure by integrity is simply obtained by ignition of a cotton fibre pad held 25 mm in front of any gap or weakness (fissure, crack, etc.) in the construction.

The stability and insulation failure criteria are capable of being assessed on a calculation basis. However, the integrity failure criterion is not amenable to calculation and can only be determined by physical testing and, therefore, will not be considered further in this manuscript.

2.4.3. Concrete under Fire Damage

Al-Mutairi and Al-Shaleh (1997) inspected the fire damaged Kuwaiti structures resulting from the August 1990 Iraqi invasion. Fire damage was presented based on a field survey included inspection of damage to commercial buildings, apartment buildings, residential houses, and public buildings. The study summarised fire causes carbonation of exposed concrete surface that increases the suitable medium for the corrosion of the reinforcing steel imbedded inside the concrete.

Concrete exposed to fire causes spalling of the concrete cover and exposure of the reinforcing steel. This exposure will definitely cause a reduction in the resistance strength of the reinforcing steel, and thus reduce the ultimate capacity of the structural element. High-strength concrete is thought to be particularly susceptible to spalling. The incorporation of synthetic fibres such as polypropylene fibres which melt during the fire to produce channels where steam can escape is recommended by Purkiss (2000) and Kitchen (2001), and now has been codified at EN 1992-1-2 in Eurocode 2 (2002).

Purkiss (1990) stressed the importance of moisture effects on spalling in determining the overall behaviour of concrete structures exposed to fire. A better representation of actual behaviour can only be achieved if moisture effect on material properties and spalling are included in computer modelling. This necessitates the use of a variable finite element mesh to represent the variation in cross section due to spalling. Therefore, thermal response and structural response should be combined in one model incorporating one variable mesh.

Connolly (1995) presented the categorisation suggested by Gary in 1916 that spalling can be grouped as follows:

- Aggregate spalling, which is defined as a splitting of aggregates at the heated surface. This spalling occurs to areas on the heated surface within the first 20minutes of exposure to the standard heating test with maximum depth of the dislodged piece being 5 to 10 mm. Aggregate spalling has little effect on the fire resistance of concrete structures.
- Corner spalling, which defined as a gradual disintegration of parts of heated concrete at the corner of member such as beams and columns. This type of spalling occurs after 30 minutes of exposure to the standard test. Dougill (1971) and Malhotra (1984) attributed corner spalling to the loss of tensile strength leading to bond failure. Fortunately, corner spalling can usually be repaired easily after fire according to the Concrete Society (1990).
- Surface spalling, which defined as the violent removal of sizeable lumps from the heated surface up to 100x100 mm. The loss of sizeable parts of concrete means the effective area of concrete is reduced and the exposure of the steel-reinforcement to fire causes result in rapid rise of steel temperature. Therefore, the fire resistance of concrete structures decreases significantly.
- Explosive spalling, which is described as a very violent bursting of large parts of heated concrete. This type of spalling is extremely dangerous and may cause sudden and complete failure accompanied by a large release of energy and produces a typical explosive noise.

2.4.4. Thermal Properties of Concrete

The properties of materials at elevated temperatures can be divided into thermal properties and mechanical properties. The thermal properties are needed to calculate thermal response such as heat transfer problem within a structure or a structural element during fire. The heat transfer solution can be used to predict the temperature distribution history at any point within the cross-section. Therefore, the temperature-dependant mechanical properties can be evaluated to determine the structural response in the fire.

Even though some other materials can also be recognised, this chapter will only concentrate on two main structural materials, i.e. steel and concrete. Based on modelling material properties at high temperatures, Anderberg (1983) reported the properties of steel, whilst Schneider (1986) provided the properties of normal strength concrete. Both materials data have been published in two RILEM technical committee reports. However, Purkiss (1996) noted that these reports are compendia of existing data compiled on an *ad-hoc* basis using various test methods, which are not currently standardised. Also Schneider does not include high strength concrete.

The thermal properties of concrete are very complex. The values are dependent on the mix proportions, the type of aggregates (siliceous or calcarious in normal-weight or lightweight concrete), the original moisture content, and the age of concrete. Therefore, an assemblage of the element comprising the structure to determine the fire resistance must be considered on an individual basis. Purkiss (1996) summarised the data presented in the following which can only be taken as representative of typical concrete.

2.4.4.1. Thermal conductivity

The thermal conductivity of a material is required in order to calculate the temperature rise on the material subjected to fire. For temperatures below 100°C, thermal conductivity of concrete depends on nature of aggregate, porosity, and moisture contents. Presented in the Eurocode 4 at ENV 1994-1-2 (1994), the equations for the values of thermal conductivity, λ_c (W/m°C), for various normal-weight concrete were given in the following:

For siliceous aggregates:

$$\lambda_c = 2.0 - 0.24\left(\frac{T_c}{120}\right) + 0.012\left(\frac{T_c}{120}\right)^2 \tag{2.2}$$

In addition, a constant value of 1.6 W/m°C is also permissible.

For calcarious aggregates:

$$\lambda_c = 1.6 - 0.16\left(\frac{T_c}{120}\right) + 0.008\left(\frac{T_c}{120}\right)^2 \tag{2.3}$$

For light-weight concrete, the relationship is given as follows:

at $20 \le T_c \le 800°C$: $\lambda_c = 1.0 - \left(\frac{T_c}{1600}\right)$ (2.4)

at $T_c > 800$ °C : $\lambda_c = 0.5$ (2.5)

where: T_c = temperature of concrete (°C).

2.4.4.2. Thermal diffusivity

Thermal diffusivity of concrete, a_c (m^2/hour), defined as the ratio of thermal conductivity, λ_c, to volumetric specific heat, $c_c\rho$.

$$a_c = \frac{\lambda_c}{c_c \rho} \tag{2.6}$$

This value measures the effectiveness of heat dissipation through the material. Thermal diffusivity is variable since the thermal conductivity and volumetric specific heat vary with temperature. The heat transfer rate through the material increases proportionally to the increases of the thermal diffusivity.

2.4.4.3. Specific heat

Harmathy (1970) reported the value of volumetric specific heat of light-weight concrete and normal weight concrete increase slowly when temperature increases from 0 to 1000°C. For light-weight concrete, the value of volumetric specific heat increases from about 1 to1.5MJ/m^3°C, while for normal weight concrete the value of volumetric specific heat increases from about 2.0 to 2.7MJ/m^3°C. However, a significant increase happens in the temperature range of 400 - 600°C with the peak value of specific heat occurring at a temperature of 500°C. The peak value of volumetric specific heats of lightweight concrete and normal-weight concrete at 500°C are about 3.0MJ/m^3°C and 4.0MJ/m^3°C, respectively. The peak value of the specific heat of cement paste at around 500°C has also approved by Lie (1992).

Purkiss (1986) identified that specific heat is also affected substantially by water at temperature below 150°C. This fact implies that the moisture content has significant effect on the thermal properties of concrete.

The following equation for the specific heat of normal-weight concrete, c_c (J/kg°C), is given by ENV 1994-1-2 (1994):

$$c_c = 900 + 80\left(\frac{T_c}{120}\right) - 4\left(\frac{T_c}{120}\right)^2 \quad (2.7)$$

For lightweight concrete, may be taken a constant value of 840 J/kg °C.

2.4.4.4. Concrete strains

Commonly used engineering materials, such as steel, when subjected to elevated temperature under applied stress, will have only three strains components. The three strain components are free thermal-strain caused by temperature change, classical creep-strain caused by dislocation of microstructures of the material, and instantaneous stress-related strain caused by externally applied stresses.

Unlike steel, concrete experiences a characteristic marked increase in creep during first heating due to the changes of chemical composition. The total strain of concrete, therefore, has an additional transient-strain term which originates in the cement paste and is restrained by the aggregate. Mathematically, the total concrete strain subjected to elevated temperature can be express as follow:

$$\varepsilon_{tot,c} = \varepsilon_{th,c} + \varepsilon_{cr,c} + \varepsilon_{\sigma,c} + \varepsilon_{tr,c} \quad (2.8)$$

Where: $\varepsilon_{tot,c}$ = total concrete strain

$\varepsilon_{th,c}$ = free thermal-strain

$\varepsilon_{cr,c}$ = classical creep-strain

$\varepsilon_{\sigma,c}$ = stress-related strain

$\varepsilon_{tr,c}$ = transient-strain

- **Thermal-strain**

The value of thermal-strain, $\varepsilon_{th,c}$, during heating is a simple function of temperature and is not linear. This non-linear behaviour is in part due to chemical or physical changes in the aggregate. The initial moisture content will affect the results below 150°C since the water being driven off may cause net shrinkage. Although the cement paste contracted when subjected to elevated temperatures, the thermal expansion of concrete is dominated by the thermal expansion of the mineral aggregate.

Several investigators have measured the thermal-strain in concrete at elevated temperature up to 1200°C. Investigation by Schneider (1982) has indicated that thermal-strain of concrete generally increases with temperature. The relationship between elevated temperature and thermal strain of concrete made with various conventional aggregates is shown in Figure 2.3.

Figure 2.3 Thermal expansion of concretes made with various aggregates as a function of temperature (Schneider, 1982)

The following equation for the free thermal strain of normal-weight siliceous aggregate concrete is given by ENV 1994-1-2:

For $20 \leq T_c \leq 700\,^{\circ}\mathrm{C}$:

$$\varepsilon_{th,c} = 1.8\times10^{-4} + 9\times10^{-6}T_c + 2.3\times10^{-11}T_c^{\,3} \tag{2.9}$$

For $T_c \geq 700\,^{\circ}\mathrm{C}$:

$$\varepsilon_{th,c} = 1.4\times10^{-4} \tag{2.10}$$

Eurocode 4 also gave the following values for calcareous aggregate concrete:

For $20 \leq T_c \leq 800\,^{\circ}\mathrm{C}$:

$$\varepsilon_{th,c} = -1.2\times10^{-4} + 6\times10^{-6}T_c + 1.4\times10^{-11}T_c^{\,3} \tag{2.11}$$

For $T_c \geq 800\,^{\circ}\mathrm{C}$:

$$\varepsilon_{th,c} = 1.2\times10^{-4} \tag{2.12}$$

For over the whole temperature range, approximate calculations the coefficients of thermal expansion of siliceous and calcareous aggregate concretes may be taken as $1.8e^{-7}$ and $1.2\ e^{-7}$ micro-strain per °C respectively.

- **Classical creep-strain**

The creep of concrete at elevated temperatures has been investigated by Gross (1973), Schneider (1986) and Anderberg and Thelandersson (1976). Test results show that the creep of concrete is increases markedly with increasing temperature.

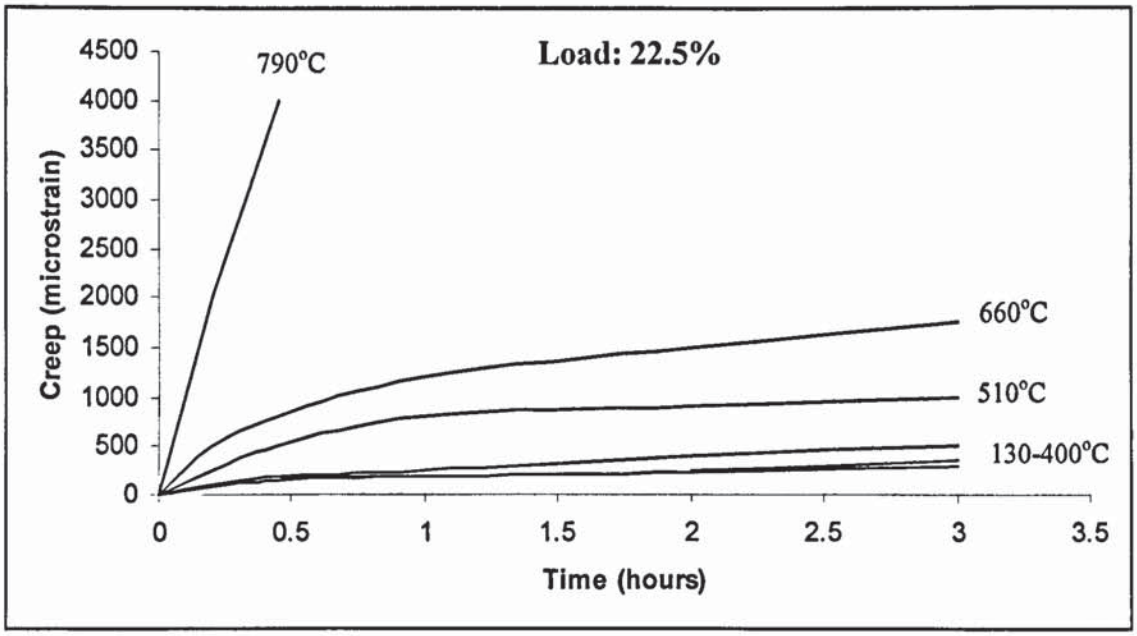

Figure 2.4.a Isothermal creep data at elevated temperatures with stress level 22.5% of original strength.

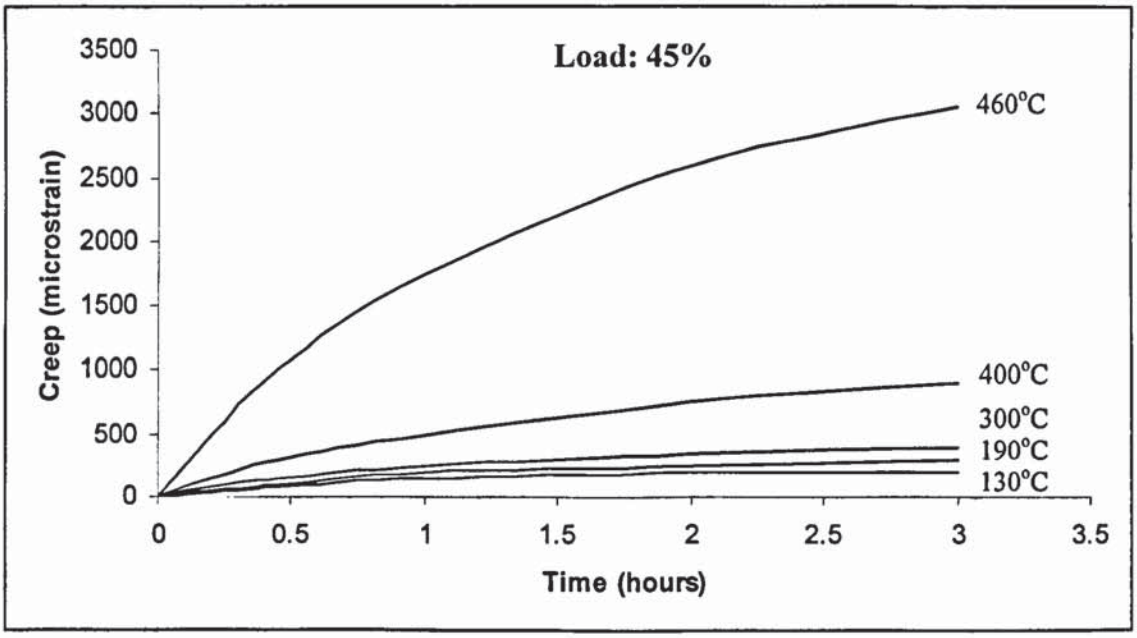

Figure 2.4.b Isothermal creep data at elevated temperatures with stress level 45% of original strength.

Figures 2.4.a and 2.4.b show the typical creep data for concrete given by Anderberg and Thelandersson. The creep curves are derived from steady state tests where the temperatures are stabilized at a given level throughout the test. Consequently, each curve corresponds to a given temperature and a given stress level.

- **Transient-strains**

Transient strains of concrete, $\varepsilon_{tr,c}$, were first identified by Anderberg and Thelandersson (1976). These strains are developed under constant applied stress when the temperatures increase. These strains are essentially irrecoverable and only occur under the first heating and cooling cycle of the concrete. Any subsequent heating and cooling cycle does not exhibit such strain.

Unlike the thermal-strain which is a function of only temperature, the transient-strain together with creep-strain and instantaneous stress-related strain are functions of stress and temperature. The transient-strain component can not be measured directly in the tests. Current existing models incorporate the effect of transient-strain will be reviewed in the following discussion.

- **Anderberg and Thelandersson**

Anderberg and Thelandersson presented two series of an experimental and theoretical basis for the analysis of stress and deformations of concrete subjected to high temperatures. The first part, Anderberg and Thelandersson (1973), embraced a general discussion of the problems and a critical review of literature. They concluded that an

appropriate analysis of concrete structures subjected to high temperature can only be done if the deformation behaviour can be understood.

The second and final part of the investigation, Anderberg and Thelandersson (1976), contains the experimental investigation and a material behaviour model of concrete at transient high temperature conditions which developed on a phenomenological level. They developed a constitutive model reflects the actual behaviour in a very appropriate way thus can be easily adopted in a computer analysis of concrete structure exposed to elevated temperature.

Based on the experimental data, the classical creep strain in Equation (2.8) at constant temperature and constant stress is expressed by:

$$\varepsilon_{cr,c} = \beta_O \cdot \frac{\sigma}{\sigma_u(T)} \cdot \left(\frac{t}{t_r}\right)^p \cdot e^{k_1 \cdot (T - 20)} \qquad (2.13)$$

where:

β_O = - 0.00053

σ = stress

$\sigma_u(T)$ = ultimate compressive stress at current temperature (T)

t = time (minutes)

t_r = 180 (minutes)

p = 0.5

k_1 = 0.00304

T = temperature

The transient strain is an important component in the model, accounting for the deformations occurring under stress upon a temperature rise. This component accounts

for the difference in behaviour between transient and steady-state temperature conditions and is normally considerably greater than both the stress-related strain and the creep strain components. The transient strain was assumed as:

$$\varepsilon_{tr,c} = - k_2 \left(\frac{\sigma}{\sigma_{uo}}\right) \varepsilon_{th,c} \tag{2.14}$$

where k_2 is a dimensionless constant and σ_{uo} is the peak compressive stress at room temperature.

When plotting $\varepsilon_{tr,c} / \left(\frac{\sigma}{\sigma_{uo}}\right)$ against $\varepsilon_{th,c}$ they obtain a reasonably straight line, and the regression analyses of the data give value of k_2 between 1.8 and 2.35. However, the correlation is not so good for temperature around and above 550°C because the behaviour at these high temperatures is difficult to interpret due to the scatter in strength between individual tests. For $T \geq 550°C$ they proposed the following expression for the incremental change in ε_{tr}:

$$\Delta\varepsilon_{tr} = - 0.0001 \, \Delta T \left(\frac{\sigma}{\sigma_{uo}}\right) \tag{2.15}$$

- **Schneider**

Schneider presented a model where transient and creep strains are taken together. So, the total strain will be the sum of three strains i.e. thermal-strain, stress-related strain, and transient-creep strain. The total concrete strain can be express as follows:

$$\varepsilon_{tot,c} = \varepsilon_{th,c} + \frac{1}{E}(1 + \chi) + \frac{\Phi}{E} \tag{2.16}$$

in which :

$$E = E_0 \, . \, f(T) \, . \, g(\sigma,T) \tag{2.17}$$

Where χ, g and Φ are empirical functions depend upon the stress and temperature.

These empirical functions can be defined in the following:

$$\chi = \frac{1}{n-1}\left(\frac{\varepsilon_\sigma}{\varepsilon_{ult}}\right)^n \tag{2.18}$$

where n = 2.5 for lightweight concrete and n = 3 for normal concrete. A reasonable approximation for χ is given by:

$$\chi = \frac{1}{n-1}\left(\frac{\sigma}{\sigma_{ult}}\right)^5 \tag{2.19}$$

The other functions used in Schneider's model can be defined:

$$g = 1 + 0.01 \cdot \frac{\sigma_c}{f_c}(T - 20) \cdot \tag{2.20}$$

whereby the boundary limit is $\frac{\sigma_c}{f_c} \leq 3$

$$\Phi = g \cdot \phi + 0.01 \cdot \frac{\sigma_c}{f_c}(T - 20) \tag{2.21}$$

whereby the boundary limit is $\frac{\sigma_c}{f_c} \leq 3$

$$\phi = C_1 \cdot \tanh \gamma_w (T - 20) + C_2 \tanh \gamma_0 (T - T_g) + C_3 \tag{2.22}$$

$$\gamma_w = (0.3\ w + 2.2) \cdot 10^{-3} \tag{2.23}$$

Parameters for transient creep functions of structural concretes such as C_1, C_2, C_3, n, T_g and γ_0, are given by Schneider in a table for various different concretes. While γ_w accounts for the moisture content w in % by weight.

- **Diederichs**

Diederichs proposed a very simple model where the three strains of stress-related strain, creep-strain and transient-strain are taken together as a single strain. This model ignored the classical creep-strain and the instantaneous stress-related strain calculated using the ambient modulus of elasticity. The model can be expressed as follows:

$$\varepsilon_{tot,c} = \varepsilon_{th,c} + \frac{\sigma}{E_0}\left[1 - \frac{E_0}{\sigma_{u0}} f(T)\right] \quad (2.24)$$

$$f(T) = 3.3 \times 10^{-7}(T - 20)^3 - 1.72 \times 10^{-4}(T - 20)^2 + 0.0412(T - 20) \quad (2.25)$$

Where: E_0 = initial tangent modulus of concrete at room temperature

$f(T)$ = empirical function obtained by fitting the experimental data

- **Khoury *et al***

Khoury *et al* (1985a and 1985b) presented a model where transient and creep strains are taken together, so the total concrete strain can be explained as:

$$\varepsilon_{tot,c} = \varepsilon_{th,c} + \varepsilon_{\sigma,c} + \varepsilon_{tr,c} \quad (2.26)$$

Where: $\varepsilon_{tot,c}$ = total concrete strain

$\varepsilon_{th,c}$ = free thermal-strain

$\varepsilon_{\sigma,c}$ = stress-related strain

$\varepsilon_{tr,c}$ = sum of classical creep and transient-strain

They measured creep strains during testing under constant temperature and stress. They also investigated transient thermal strain of concrete during the first heat cycle under load to 600°C but not on subsequent heating. They identified that the thermal strains

were shown to consist of 'free' and 'load-induced' components. Thus they concluded that the thermal strains of concrete at first-time heating under load can be predicted and explained in term of the free thermal strain of unloaded concrete and the load-induced thermal strain which have different and distinct properties.

The free thermal strains were non-linier function of temperature and dominated by the thermal expansion of the constituent aggregate. Since the $\varepsilon_{\sigma,c}$ at the elastic strain defined as σ / E_O, the transient creep strain at a temperature T and a stress level σ, called as load-induced thermal strains (LITS), can be defined as:

$$LITS(T,\sigma) = (\varepsilon - \varepsilon_{th,c} - \frac{\sigma}{E_O}) \qquad (2.27)$$

However, Khoury *et al* reported only the experimental results for various types of concretes without developing an empirical formula to calculate the load-induced thermal strain (LITS).

- **Li and Purkiss**

Li and Purkiss (2005) developed model based on the Anderberg and Thelandersson's model with considering the transient-strain and it is a full thermal strain-stress model. They developed an empirical formula based on the plotted results of the average Young's modulus. Considering as long as the stress is in compression, the transient strain is assumed to be similar for loading and unloading. The instantaneous stress-related strain was assumed as:

$$\sigma = E \left(\varepsilon_\sigma - \frac{\varepsilon_\sigma^2}{2\,\varepsilon_{uT}} \right) \text{ for } 0 \le \varepsilon_\sigma \le \varepsilon_1 \qquad (2.28)$$

$$\sigma = \sigma_1 + E^- (\varepsilon_\sigma - \varepsilon_1) \text{ for } \varepsilon_1 \leq \varepsilon_\sigma \leq \varepsilon_{ult} \tag{2.29}$$

in which

$$\sigma_1 = E\left(\varepsilon_1 - \frac{\varepsilon_1^2}{2\,\varepsilon_{uT}}\right),\ \varepsilon_1 = \varepsilon_{uT}\left(1 - \frac{E^-}{E}\right),\ \varepsilon_{uT} = \frac{2\,\sigma_{uT}}{E} \tag{2.30}$$

where:

E = initial tangent modulus of stress-strain curve at temperature T

E^- = tangent modulus of stress-strain curve in the descending branch

ε_{ult} = ultimate compressive strain at temperature T

The Equations (2.28), (2.29) and (2.30) are modification of the conventional nonlinear stress-strain equation of concrete at room temperature by taking the peak stress, initial tangent modulus and ultimate compressive strain as the function of temperature. The strain ε_{uT} at the peak point, the stress σ_1 and the strain ε_1 at the intersection point between Equations (2.28) and (2.29) on the stress-strain curve can be expressed in terms of E^-, σ_{uT}, and ε_{ult}. Thus there are only four independent parameters in the model. If these four parameters are defined then the instantaneous stress-related strain can be calculated. In the Anderberg and Thelandersson's model, the tangent modulus of the descending branch was assumed as $E^- = -880$ MPa and the other three parameters were assumed to be functions of temperature.

The normalized stress-strain curve with transient strain included which graphically shows the stress-strain curve described by Equations (2.28), (2.29) and (2.30) is presented in Figure 2.5.

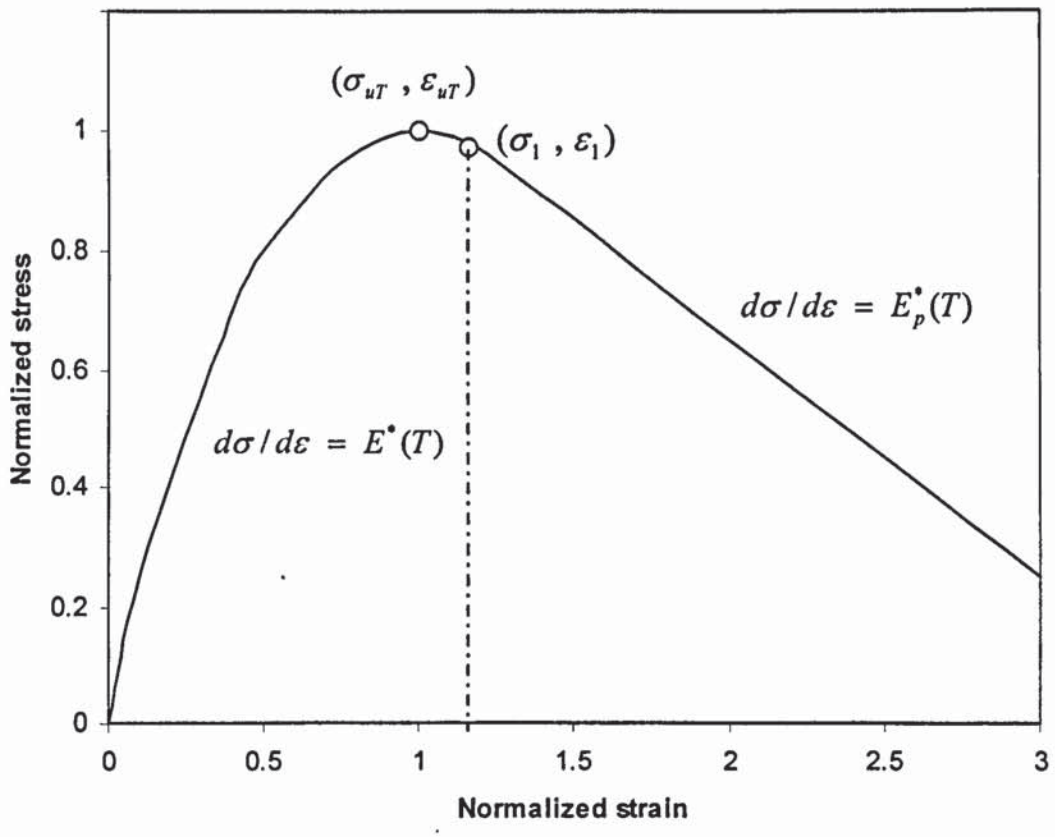

Figure 2.5 Normalized stress-strain curve with transient strain included

In the elastic ranges, temperature-dependent of Young's modulus is suggested in the following:

$$E^*(T) = E_0 \exp\left[-\frac{(T - 20)^{0.65}}{25}\right] \tag{2.31}$$

Where: E_0 = 32.2 GPa for normal-strength and E_0 = 40.6 GPa for high-strength.

For the Young's modulus in the plastic range the following equation is recommended:

$$E_p^*(T) = E_0^- \exp[k_p (T - 20)^{2.15}] \tag{2.32}$$

Where: $E_0^- = -0.045\, E_0$, and $k_p = 10^{-6}$.

2.4.4.5. Bond strength

Schneider (1986) investigated bond strength between the concrete and steel reinforcement. The magnitude of the loss is a function of the type of reinforcement and the type of concrete. Cold deformed steel is likely to be more loss of bond than plain round. As there is no standardized test procedure, the results obtained will be dependent on the test methods.

Although few failures have directly occurred due to loss of bond in pre-stressed concrete, bond strength is rarely critical in reinforced concrete. In reinforced concrete, the bottom face of beam or slab will be carrying only a small proportion of the applied load and the reinforcement at the support will be able to carry full bond stress as they will only be slightly temperature affected. In general, there is not a problem even though bond strengths are severely reduced in a fire.

2.4.4.6. Density

There will be a loss in weight when concrete is heated. The loss is caused by the evaporation of both free and combined water. Mustapha (1994) reported that the loss of density as the temperature increase exceeds 100°C is mostly caused by the loss of free moisture. However, this loss is not generally enough to cause substantial changes in density. Therefore, the effect of temperature is insignificant. Connolly (1995) suggested that it is usually considered accurate enough to take ambient values and can be assumed constant up to 800°C.

2.4.5. Mechanical Properties of Concrete

Mechanical properties of materials at elevated temperatures are necessary to determine structural response in a fire. A complete formulation is required to calculate deformations and displacement. However, to calculate load capacity, a more limited data set could be utilised. Indeed, much early work was directed to determining specific properties such as compressive strength of concrete or tensile strength of steel at elevated temperature.

Purkiss (1996) emphasised that it should be recognised that creep of concrete or relaxation of steel are much higher at elevated temperatures than at ambient temperatures. Thus, the rate of loading used in elevated temperature testing has a far more significant role than at ambient conditions. The rate of heating used to condition the test specimen will also affect the final test results.

The variation of temperature, rate of heating, and duration of heating affect concrete strength. High temperatures will result in concrete compressive strength reduction, concrete tensile strength reduction, disaggregation, spalling, and cracking. The effect of high temperatures can be described as follows:

- Tucker and Read (1981) reported the compressive strength of concrete is reduced significantly at temperatures above 300°C. While Cardoso (1992), declared tensile strength of concrete is reduced immediately and continues to decrease with an increase of temperature. In addition, differences in thermal properties between cement and aggregate create internal shearing stress. This phenomenon results in a breakdown in the cohesion of the aggregates, by means of cracking, leading to a rather accentuated phenomenon of disaggregation of the concrete.

- Concrete Society (1978), stated explosive spalling occurs within the first 30minutes of exposure to excessive heat. Most fine cracks are confined to the surface, while wide cracks or cracks near support may mean there has been a loss of anchorage of the reinforcement.
- Gustaferro (1985) represented concrete behaviour at high temperature depends on the type of aggregates such as carbonate aggregate, silicous aggregate, and lightweight aggregates. The carbonate aggregates (limestone, dolomite) undergo chemical changes at temperatures in the range of 700-1000°C, whereas silicous aggregates (granite, quartzite, sandstone) do not undergo chemical change at temperatures commonly encountered in fire. Lightweight aggregates (shale, slate) near the concrete surface may begin to soften after 4 hours of exposure in standard tests.
- However, Placido (1980) declared concrete has an advantage over other building materials in that it has remarkable ability to resist fire damage and can be easily repaired when subjected to severe fires. This is a result of the low thermal conductivity of concrete at high temperatures which can be as little as one-third of the value at room temperature, so that limiting the depth of penetration of fire damage.

2.5. Steel Reinforcement at High Temperatures

2.5.1. Thermal Properties of Steel-Reinforcement

The determination of thermal properties of steel-reinforcement is less complex than concrete. The values of the properties concerned are sensibly independent on the

strength or grade of steel-reinforcement. However, the relative temperature dependent strength reduction of reinforcing steel is very important because of its location which normally close to outer surface combined with its primary load bearing function.

The loss of strength at elevated temperature is likely to be more critical in pre-stressed concrete rather than in reinforced concrete. The modulus elasticity of cold-drawn steel used for pre-stressing tendon is typically 20% lower than the values for hot-rolled steel over a temperature range of 20-700°C. For this reason, the tabulated data given in codes described that the reinforcing steel must not exceed 550°C and the pre-stressing tendons must not exceed 450°C. This data is based on the conservative assumption that the structural elements are fully stressed at ambient temperature.

2.5.1.1. Thermal conductivity

Temperature rise in steel due to heating is a function of its thermal conductivity. The values of thermal conductivity are varies with chemical composition of the steel at room temperature and slightly dependent on the steel strength. Petterson, Magnusson, and Thor (1976) presented the variation of the thermal conductivity of steel at various temperatures. The values of thermal conductivity gradually decrease as the temperature increases to 800°C and then constant when the temperature exceeds 800°C. At this stage, the constant value of thermal conductivity is about 40% of the value at ambient temperature. While, Malhotra (1982) reported the value of thermal conductivity at temperature of 800°C is about 50% of the value at ambient temperature.

ENV 1993-1-2 (1994) gives the following expression for λ_s (W/m°C):

For $T_s \leq 800\,^{\circ}\mathrm{C}$: $\lambda_s = 54 - 3.33x10^{-2} T_s$ (2.33)

For $T_s > 800\,^{\circ}C$: $\lambda_s = 27.3$ (2.34)

However, for approximate calculations at elevated temperatures, it is permissible to take the thermal conductivity of steel as 45W/m °C.

2.5.1.2. Thermal diffusivity

Malhotra (1982) stated that thermal diffusivity of steel shows a sensibly linear relationship with temperature up to a temperature of 750°C. The relationship of the thermal diffusivity, a_s (m^2/hour), to the temperature of reinforcing-steel, T_s (°C), has been expressed as follow:

$$a_s = 0.87 - 0.84 \times 10^{-3} T_s \tag{2.35}$$

2.5.1.3. Specific heat

ENV 1993-1-2 (1994) gives the following equations for the specific heat of steel, c_s(J/kg°C) which hold a temperature up to 1200°C:

For $20 \le T_s \le 600\,^{\circ}C$:

$$c_s = 425 + 7.73 \times 10^{-1} T_s - 1.69 \times 10^{-3} T_s^{\,2} + 2.22 \times 10^{-6} T_s^{\,3} \tag{2.36}$$

For $600 \le T_s \le 735\,^{\circ}C$:

$$c_s = 666 - \frac{13002}{T_s - 738} \tag{2.37}$$

For $735 \le T_s \le 900\,^{\circ}C$:

$$c_s = 545 - \frac{17820}{T_s - 731} \tag{2.38}$$

For $900 \leq T_s \leq 1200\,^{\circ}C$:

$$c_s = 650 \tag{2.39}$$

For general type of reinforcing-steel, Malhotra (1982) suggested the specific heat may be taken as:

$$c_s = 475 + 6.010 \times 10^{-4} T_s^{\ 2} + 9.46 \times 10^{-2} T_s \tag{2.40}$$

2.5.1.4. Thermal strain

Many researchers have dealt with thermal strain of steel at elevated temperature. Anderberg (1976) has presented simple values for the steel as follows:

$$\varepsilon_{th,s}\ (20^{\circ}C) = 12.\ 10^{-6}\ .^{\circ}C^{-1} \tag{2.41}$$

$$\varepsilon_{th,s}\ (800^{\circ}C) = 20.\ 10^{-6}\ .^{\circ}C^{-1} \tag{2.42}$$

In the temperature interval between 20°C-800°C, a linear interpolation for $\varepsilon_{th,s}$ is suggested.

Malhotra (1982) suggested the value of free thermal strain of steel, $\varepsilon_{th,s}$, at elevated temperature, T_s, may be taken as:

$$\varepsilon_{th,s} = 0.4 \times 10^{-8}\ T_s^{\ 2} + 1.2 \times 10^{-5}\ T_s - 3 \times 10^{-4} \tag{2.43}$$

The slightly different version of above equations has been given by ENV 1993-1-2 as follows:

For $20 \leq T_s \leq 750\,^{\circ}C$:

$$\varepsilon_{th,s} = -2.416 \times 10^{-4} + 1.2 \times 10^{-5}\ T_s + 0.4 \times 10^{-8}\ T_s^{\ 2} \tag{2.44}$$

For $750 \leq T_s \leq 860\,^{\circ}C$:

$$\varepsilon_{th,s} = 11 \times 10^{-3} \tag{2.45}$$

For $860 \leq T_s \leq 1200\,^{\circ}C$:

$$\varepsilon_{th,s} = -6.2 \times 10^{-3} + 2 \times 10^{-5}\, T_s \tag{2.46}$$

2.5.1.5. Density

There is also insignificant affect to the value of density of steel-reinforcement subjected to high temperature. The density of steel-reinforcement may be taken as its ambient value of $7850 kg/m^2$ over the normally experienced temperature range.

2.5.2. Mechanical Properties of Steel-Reinforcement

Fire test on concrete structural member where the tensile reinforcement has primary load bearing function have shown that the strength and stiffness of reinforcing steel decrease significantly when reaching high temperatures. Therefore, the influence of high temperature on reinforcing steel in fire exposed concrete structural member is very importance.

Steel-reinforcement subjected to sustained high temperatures will suffer reduction in performance and instability. Lie (1972), Lie (1992), Green (1972), and Concrete Society (1978) reported the strength and stability of steel-reinforcement affected by high temperatures as follows:

- Significant loss of strength occurs at high temperatures, 50% of the original yield stress is lost at the temperature of about 550°C.

- Original yield stress is almost completely recovered on cooling from temperatures of 500-600°C for all steel-reinforcement.
- On cooling from 800°C, yield stress is reduced by 30% for cold-worked steels and 5% for hot-rolled steels.
- Buckling of steel-reinforcement often occurs as a result of compressive stress induced at high temperatures.
- Creep depends not only on temperature but is also strongly dependent on the stress level. The significant creep starts at 250°C for cold-worked steels and 400°C for hot-rolled steels.

2.6. Steel Structures under Elevated Temperature

In order to compare with frame-structures composed by leading materials other than concrete, behaviour of steel-frame structures under elevated temperature are briefly reviewed in this discussion. Attention will be given to the results of full-scale fire tests on eight-storey composite steel-frame building conducted in BRE Cardington, Bedfordshire. The comparison of the behaviour of steel structure and concrete structure under elevated temperature will be concluded in the last chapter.

2.6.1. Steel-Framed Test

Method for determination of the fire resistance of structural member element has been presented by BS 5950: Part 8 (1990) to ensure the strength and stability of a steel-structure during a fire. Based on this method ASFP (1992) addresses the cover of exposed areas of steel with a protective material and specified the required thickness of

insulating material for structural steel in building. These design codes have proved adequate for a single element since they were developed from standard fire test on isolated element. According to Bailey and Moore (2000a), Eurocode 3 (1995) and Eurocode 4 (1994) provide better scientific approach for the provision of fire resistance based on a method for determination of the fire resistance of structural member elements. However, again, these codes were developed from isolated member of single element without paying attention to the interaction between the members of the entire structure when the elements are connected together. They ignore the inherent fire resistance of the whole structure. Therefore, these methods are unlikely assess the optimum levels of fire safety design.

Up to 1995-1996 six full-scale fire tests have been carried out on eight-storey composite steel-frame building at the BRE laboratory at Cardington. Two of the tests were conducted by BRE while the other four tests were conducted by British Steel (now Corus). A seventh test was carried out in 2003. The results were clear that unprotected steel members can have significantly greater fire resistance than when they are tested as isolated member. When deflections were very large, the influences of membrane tensions in the floor slabs have played an important role in preventing failure of the structure during the tests. From these tests, Martin and Moore (1997) and Bailey *et al* (1999) confirmed that the performance of a steel-frame is significantly better than that of the single element.

Bailey *et al* (1999) explained that the two tests by BRE together with the four British Steel tests have shown comprehensively that the existing design codes are over conservative. According to the codes, the structure should collapse when the beam temperature reaches 680°C. In fact, no collapse was evident even though the

unprotected beams reached temperature of 903°C in the BRE tests and even over 1100°C were reached in the British Steel tests.

Based on the results from the series of full-scale tests on Cardington steel framed building, Bailey and Moore (2000a) suggested the development of new design methods for calculating the performance of steel-framed building with composite floor-slabs subjected to fire. The method uses a simple energy approach to calculate load carrying capacities of a composite flooring system and in the most cases the method gives accurate prediction. In all examined cases the proposed method predicts behaviour that is superior to that obtained using the existing design approaches.

A companion paper by Bailey and Moore (2000b) showed how the above method can be applied in design. This new design method which based on holistic approach would be a major improvement on current design methods. The new design method provides significant economical benefits while still maintaining adequate levels of safety. For example, in all the cases examined, significant number of steel composite beams can be left without protection for either 30 minutes or 60 minutes fire resistance.

Huang *et al* (2002) presented the modelling of six full-scale fire tests on the Cardington composite steel-framed building using computer program, called Vulcan, developed at the University of Sheffield. The computer program predicted the structural behaviour of the steel-framed building with a good accuracy. However, the modelling of the tension zones of the slabs at high deflections did not take account of possible localisation of failure by discrete slab cracking and reinforcement fracture. Therefore, a crack propagation mechanism would not be identified using the model.

2.6.2. Steel Work Connections

Based on postulated connection characteristics and a reasonable understanding of moment-rotation curves, El-Rimawi *et al* (1995) confirmed that connection rigidities can be significant in improving the performance of steel-frames in fire. Some previous connection tests of steel beam to column connections at elevated temperatures were conducted by Lawson (1990) which covered a range of connection types but providing insufficient data for the accurate construction of moment-rotation curves.

Leston-Jones *et al* (1997) conducted six tests consisted of one test at ambient temperature through out the entire moment-rotation range and five tests at elevated temperature of bare steel flush endplate beam to column connection. The main objective of the test was to postulate rules for the elevated temperature degradation of connection characteristics. The test concluded that there is a significant decrease in the moment capacity in the range of 500-600°C, suggesting a direct correlation between steel strength properties and the degradation of connection performance at elevated temperatures. Modified form of the classic equation from Ramberg-Osgood (1942) with regard to moment-rotation curves were effectively represented for various temperature increments.

In situations when a steel member penetrates a concrete fire wall, usually the member will be fire protected for a certain length on each side of the wall in order to minimise the heat flow within the steel member. However, Bennetts and Goh (2001) reported that a dramatic reduction is happened in steel temperature from the exposed side to unexposed side of the steel member, thus, the resulting temperatures are unlikely to reduce the stiffness and strength of the steel member on the non-fire side of the wall. Therefore, they suggested that it is not necessary to apply fire protection to each side of

the penetrating steel member. This is not surprising as previous testing conducted by Schwatz and Lie (1985) and Poh (1996) gave similar reports.

Chapter 3 FIRE TEST ON THE CARDINGTON CONCRETE BUILDING

3.1. Introduction

The Building Research Establishment (2002) reported that they carried out a full-scale reinforced concrete building subjected to fire at their laboratory in Cardington, Bedfordshire. The building was a seven storey representing a typical commercial office building. The design and construction of the in situ concrete building was part of the European Concrete Building Project designed to the limits of ENV 1992-1-1. The test building was constructed using normal-strength concrete for the floor slabs and high-strength concrete for the lower storey columns and was designed to provide a minimum of 60 minutes fire resistance period.

Bailey (2002) explained that the main aim of the fire test was to investigate the behaviour of a full-scale concrete framed building subjected to a realistic compartment fire together with realistic applied static design load. The observations obtained would be used to produce design guidance based on the realistic structural behaviour which will result in the construction of safer and economic buildings. Based on the above ultimate aim, the main objectives of the overall proposed research were identified as follows:

- To investigate the resistance of building against the effect of thermal expansions of the fire heated parts of the structure within a given fire compartment.
- To identify both beneficial and detrimental modes of whole-building behaviour that cannot be shown from standard small-scale fire test.

- To investigate the overall effects of any concrete spalling and to determine their significance on the behaviour of the whole building.
- To compare test results and observations from large-scale fire test with current methods of design.

The fire test is part of a wider programme of development work on the fire design of concrete structures in the UK and Europe. More economical concrete frame construction whilst maintaining high levels of safety could be achieved by developing new fire engineering methods from the study of whole concrete structures.

3.2. Brief Description of the Project

The full-scale seven-storey *in situ* reinforced concrete building was constructed at the BRE Laboratories in Cardington, Bedford. The building was designed to Eurocode 2 and BS 8110 and represented a commercial office building. As explained by Chana and Moss (2001), this design and construction approach was developed to enable the process involved in constructing this type of concrete building frame to be investigated, with the aim of producing design and best practice guidance, which ultimately increases construction economy. As a consequence, the finished building had a mixture of concrete strengths and different reinforcement layouts for each floor.

The completed concrete building was 25.20 m tall structure comprising 3 x 4 bays in plan, each square bay being 7.50 m x 7.50 m, with 2 core areas as shown in Figure 3.1. The slab was constructed with nominally 250 mm thick flat floor slab supported by internal columns of 0.40 m x 0.40 m and external columns of 0.40 m x

0.25 m. The column cross-sections were kept constant through out of the building. Minimum cover to the reinforcement was 20 mm in the slab and 40 mm on the columns.

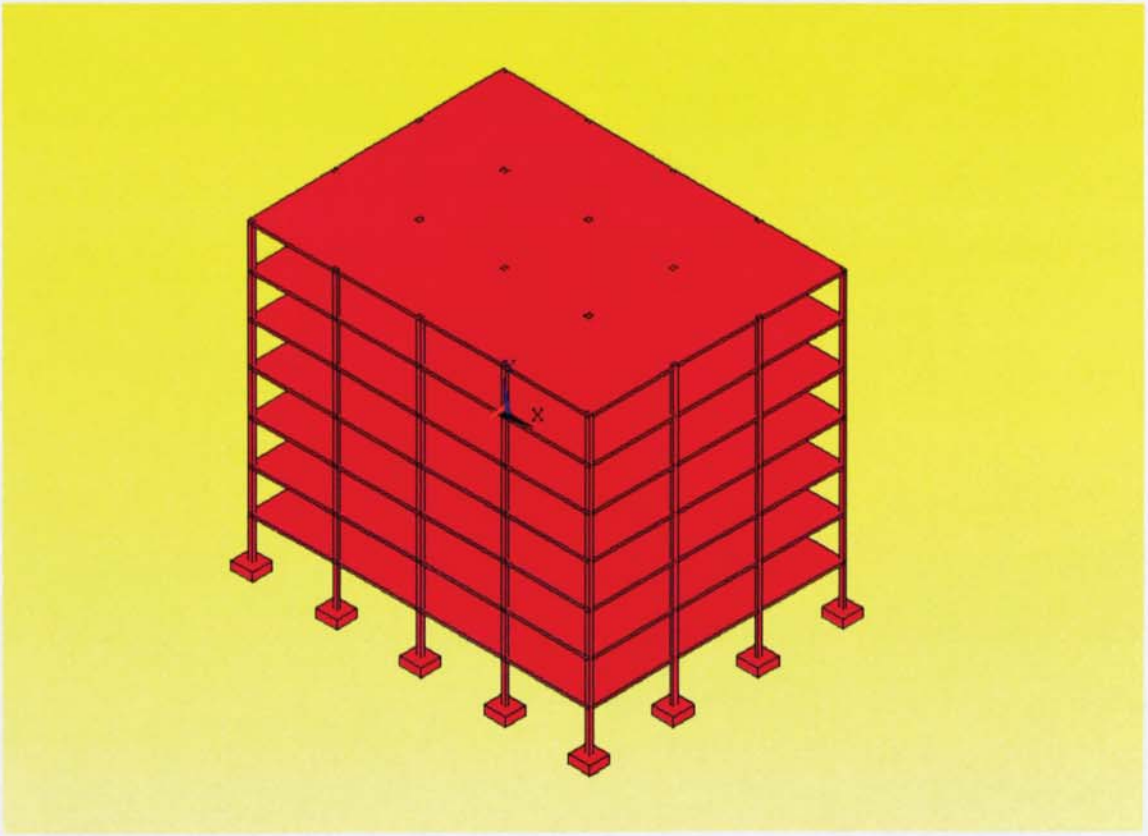

Figure 3.1 Seven-storey Cardington Concrete Building

The concrete floor slabs of the building were constructed using a grade C 37 normal-weight concrete with a flint aggregate. Tests on the wet properties showed that the average cement content was 407 kg/m^3 and average water content was 205 kg/m^3. However, a higher strength concrete for the first-floor slab of 61 MPa at 28 days and 74 MPa at the time of fire test was unexpected. Chana and Price (2003) explained that the concrete of the tested slab ought to have been considered essentially as a high-strength concrete, which would normally have required the addition of polypropylene fibres to

prevent spalling. All columns were high-strength concrete grade C 85 containing silica fume and limestone aggregates. At 28 days the average measured cube strength was 103 MPa. This concrete also contained 2.7 kg/m^3 of polypropylene fibres to reduce spalling in fire. At the time of construction, the draft version of the Eurocode did not provide any recommendations of the minimum dosage of fibre and the designers of the building had to estimate a required dosage based on the limited data available. Subsequently, however, this dosage of fibres was noted to be higher than the minimum value of 2.0 kg/m^3 specified in the latest EN draft version of the Eurocode 2 (2001).

3.3. Test Procedure

The test was carried out inside the main hanger at Cardington and was not exposed to normal outdoor drying. The average moisture content measured seven days before fire test was 3.8% by weight on the slabs and 4.2% by weight on the columns. These moisture contents are higher than a typical 2% for a conventional concrete building exposed to normal drying condition. The average measured permeability 48 mm into the floor slab was 6.75×10^{-17} m^2 while into the column was 1.92×10^{-19} m^2.

The fire test was undertaken in ground-floor in order to save time and removed the need of personnel and materials to be transported vertically up the building. The area of fire test was four-bays (2x2) with a total floor area of 225 m^2 and floor to soffit clear height of 4250 mm as shown in Figure 3.2 and Figure 3.3. One of the internal columns was fully exposed to the fire while other internal and edge columns were partially exposed. The compartment wall comprised of block-work, plasterboard and

ceramic fire blanket. The ceramic fire blankets were fixed to first floor soffit and compartment wall to ensure the fire would not escape from the compartment area.

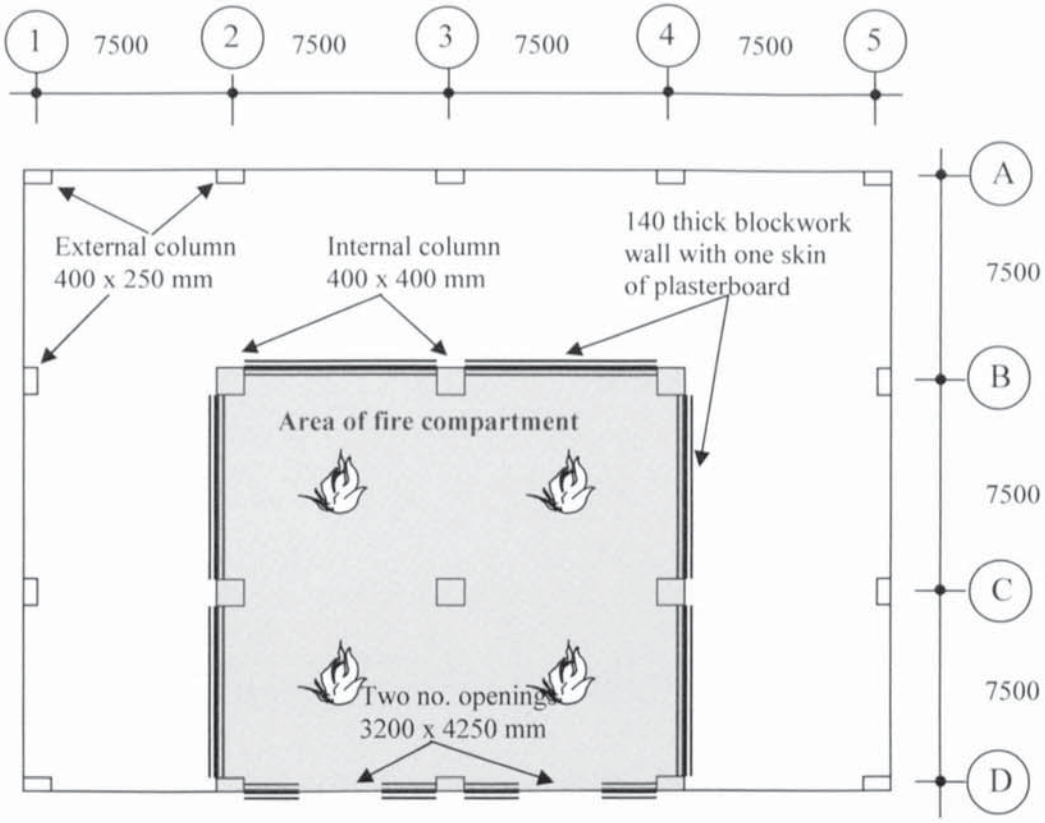

Figure 3.2 Plan of building showing location the area of fire compartment

In order to support the floor slab if the column should fail during the fire, a protected steel safety cage was placed around the exposed internal column. The cage comprised four steel columns which were tied together and were not actually in contact with the soffit of the floor slab. This cage was not required in the present modelling since the concrete column performed adequately during the fire test.

The first floor slab was loaded with 17 sandbags per-bay each weighing of 1100 kg (10.79 kN) to achieve a vertical uniform load over the fire compartment area of 3.25 kN/m^2. Additional sandbags were placed on the tested floor to produce an axial load of

925 kN in the fully exposed internal column. This design load is based on BS 6399 Part 1 for dead and imposed loads as a 40% reduction in the partition and imposed load. Realistic office fire would be obtained by providing ventilation from full height openings representing 12% opening of the compartment floor area. The fire load of 40 kg/m^2 (720 MJ/m^2) is created from timber cribs placed in the compartment area.

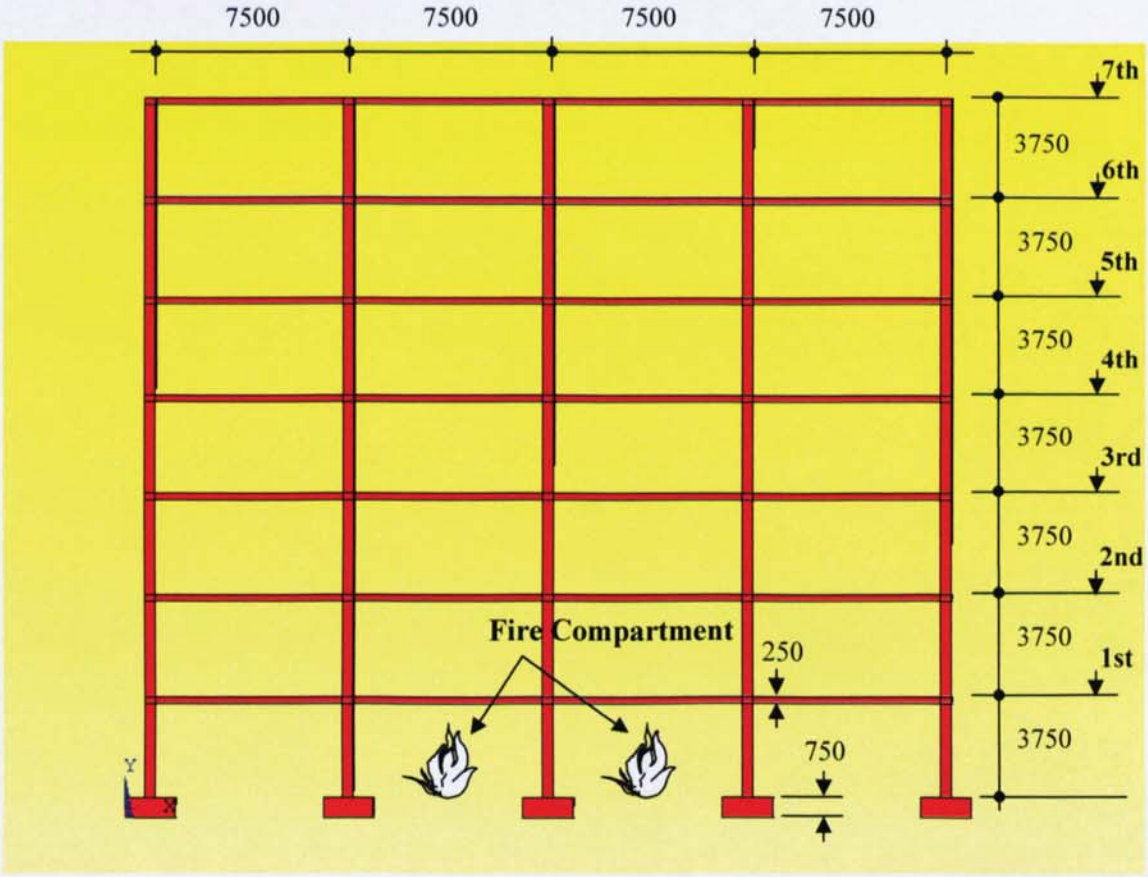

Figure 3.3 Cross-section through the building showing location of fire test

Instrumentation was installed to measure horizontal and vertical displacements, atmosphere temperatures, surface temperatures, temperatures within the slab, and surface strains on the slab. The atmosphere temperatures were measured using standard bead thermocouples. Four thermocouples were used to measured temperatures within

the slab i.e. temperature on the top surface, temperatures of the top and bottom reinforcing bars, and temperature at mid-depth of the slab. It was not decided to measure the temperature distribution within the column due to possible damage caused by drilling into the column. Therefore, only surface temperatures were measured on the column.

Prior to the fire test, a survey was carried out to check the sufficiency of nominal concrete cover to all reinforcement which should be at least 20 mm in the slabs and 40 mm in the columns according to BS 8110: Part 1 and Eurocode 2: Part 1.2. The results from the survey showed that the concrete cover to all reinforcement was more than sufficient to achieve at least 60 minutes fire resistance as specified in the codes. The survey had also showed that the section sizes on this building had a greater fire resistance than the minimum slab thickness of 95 mm and minimum column width of 200 mm as specified in current codes.

3.4. Test Results

The fire test was carried out on 26th September 2001 and was witnessed by a number of experts from UK, Europe and Australia. The instrumentation discussed in Section 3.3 was checked prior the fire test and shown should be working satisfactorily during the test. The design of the fire was based on the parametric approach from Annex A of the EN 1991-1-2 for actions on structures exposed to fire. As described in previous discussion, the fire load consisted of 40 kg/m^2 of timber cribs. The cribs were 1.00x1.00 m^2 and 0.50 m high with the timber having a moisture content of 12.5%. The predicted

time-temperature response of the design fire curve compared to standard fire curve is shown in Figure 3.4.

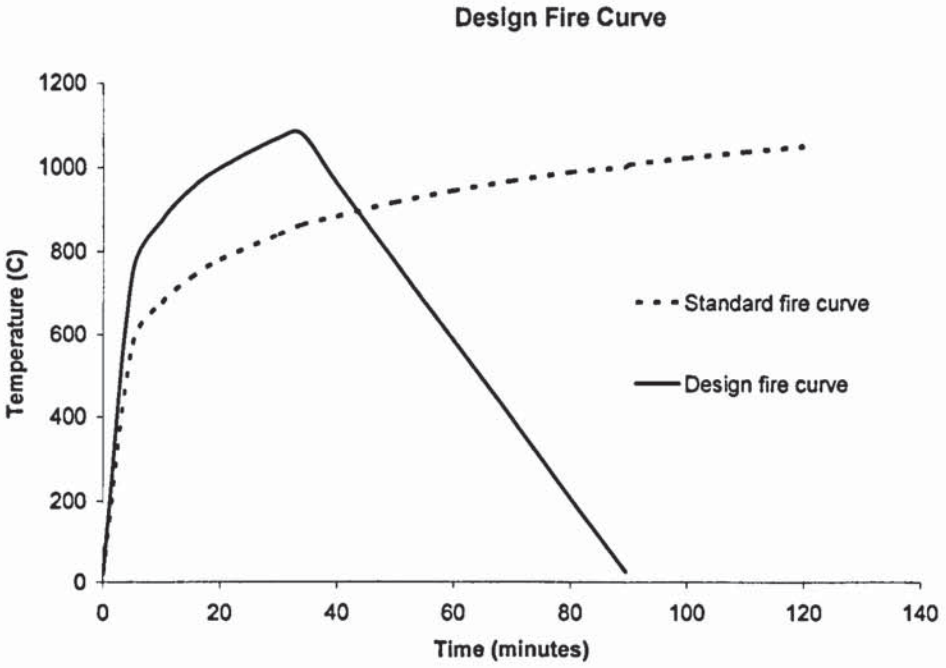

Figure 3.4 Design fire curve compared to standard fire curve

Unfortunately, all the instruments malfunctioned approximately 25 minutes into the test. Bailey (2002) explained the following description regarding the events leading to malfunction of the instruments. All the electrical wires of the instruments were run horizontally above the first floor to one point and then bound and run vertically at column A3 (see Figure 3.2). These vertical wires were 7.50 m from the fire compartment and were unprotected. The blanket of the compartment wall was shot fired to the soffit of the first floor and when the soffit started to spall the fixing to the blanket was lost. The fire escaped the compartment through the top opening and travelled horizontally 7.50 m and burnt through the electric cables. The melting of the instrumentation caused some data to be lost. At this stage the temperature of the

compartment below the soffit was 950°C and represented a time approximately 18 minutes after ignition. Above explanation has been presented in order to aid future researchers carrying out similar tests and to highlight practitioners the possible weakness of fixing into the soffit of concrete slabs during the fire, especially those fixings that provide restraint to compartment wall.

Recorded atmosphere temperatures measured 300 mm below soffit of slab and the time from the start until the malfunction of the instrumentations shown in Figure 3.5. The figure shows that the ignition of the test started to approximately 7 minutes from the start of fire. At this stage the temperature started to rise considerably to approximately 700°C in just 5-6 minutes. The temperature slightly dropped when the concrete slab started to spalling and then gradually increased to about 950°C in 13 minutes when the malfunction of instruments occurred.

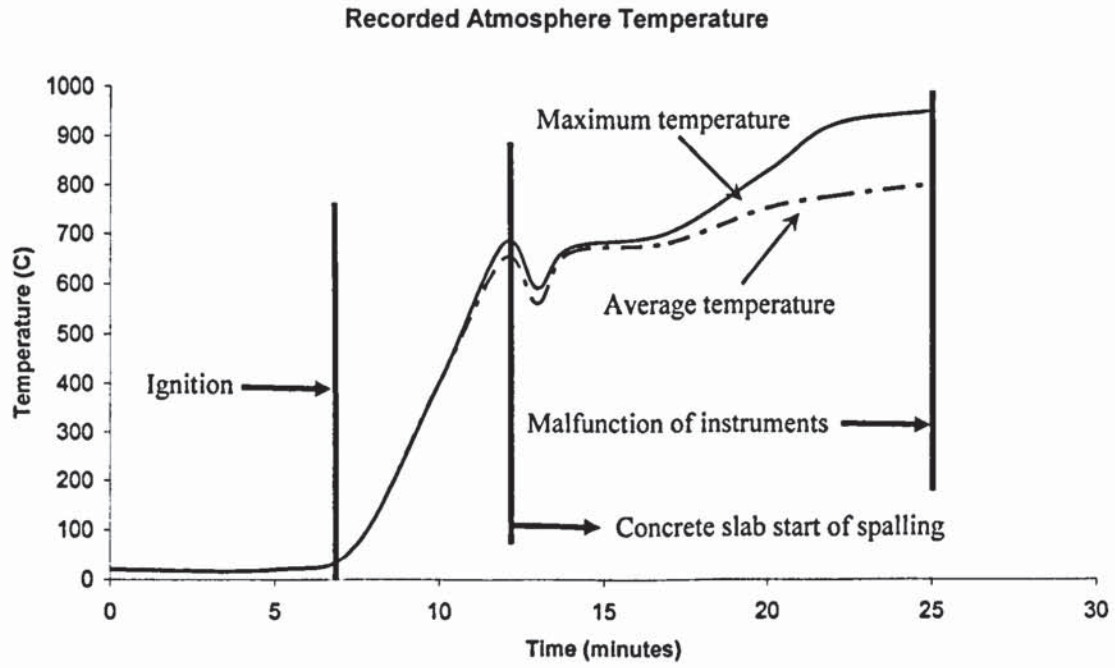

Figure 3.5 Recorded atmosphere temperatures measured 300 mm below slab soffit

3.5. Observations of the Test

The building was survived without signs of collapse during or after fire even though significant cracking occurred on the column and extensive spalling exposed over large area on the slab. The observations have also included displacements of each structural member where significant horizontal displacements were found due to irrecoverable thermal expansion of the concrete slab. The damage of the structure has also been observed to provide useful information on the holistic behaviour of concrete buildings subjected to fire.

3.5.1 Floor Slab

As described in previous discussion, malfunction of the instruments happened about 25 minutes into the test due to concrete spalling around the fixings. The maximum atmosphere temperature recorded before malfunction of some instrumentation was 950°C. Chana and Price (2003) suggested this confirms the severity of the fire test and it was probable that higher temperatures occurred. The extensive spalling of the floor slab exposed large area of the reinforcement. However, the building survived satisfactorily without a sign of collapse. Even it was not intended prior to the test; the spalling was not surprising and can be described as follows:

- Concrete floor slab was tending toward high-strength (cube strength of 61 MPa at 28 days and 74 MPa at 2 years 41 days) with flint aggregates which have a tendency to spall were used. No polypropylene fibres were included in the mix. These three factors gave a strong possibility of spalling. The uses of high strength in the concrete were unexpected. However, the main focus for constructing the structural

frame was to study the construction process issues and was not specially designed to conduct a programme of fire test. The frame design was optimised for construction speed and investigating early striking of the slab formwork. This could have led to the mix being adjusted to ensure a higher concrete strength at an early stage.

- Moisture contents in a dry environment typically are below 2%. However, as a result of the closed environment of the test building in the hangar, the moisture content in the concrete was found to be 3.8% by weight. This is unusually high and increased the likelihood of spalling due to the build up of high vapour pressure near the surface causing tensile failures in the concrete. According to Eurocode 2: Part 1.2, the spalling can be ignored when the moisture content does not exceed 3% by weight.

The horizontal displacements of the floor slab were significant. A maximum horizontal residual displacement due to thermal expansion was recorded of 67 mm. On the other hand, the residual vertical displacements of the floor slab were very low and a maximum vertical displacement of 78 mm was recorded. The slab was able to carry the imposed loads with this low vertical displacement.

Observations from the test suggested high compressive forces induced in the slab due to restraint and thermal expansion. Although these high compressive stresses almost certainly lead to the severity of the spalling, the floor slab was survived due to beneficial effect of compressive membrane action. The compressive membrane action of the floor slab is illustrated in Figure 3.6.

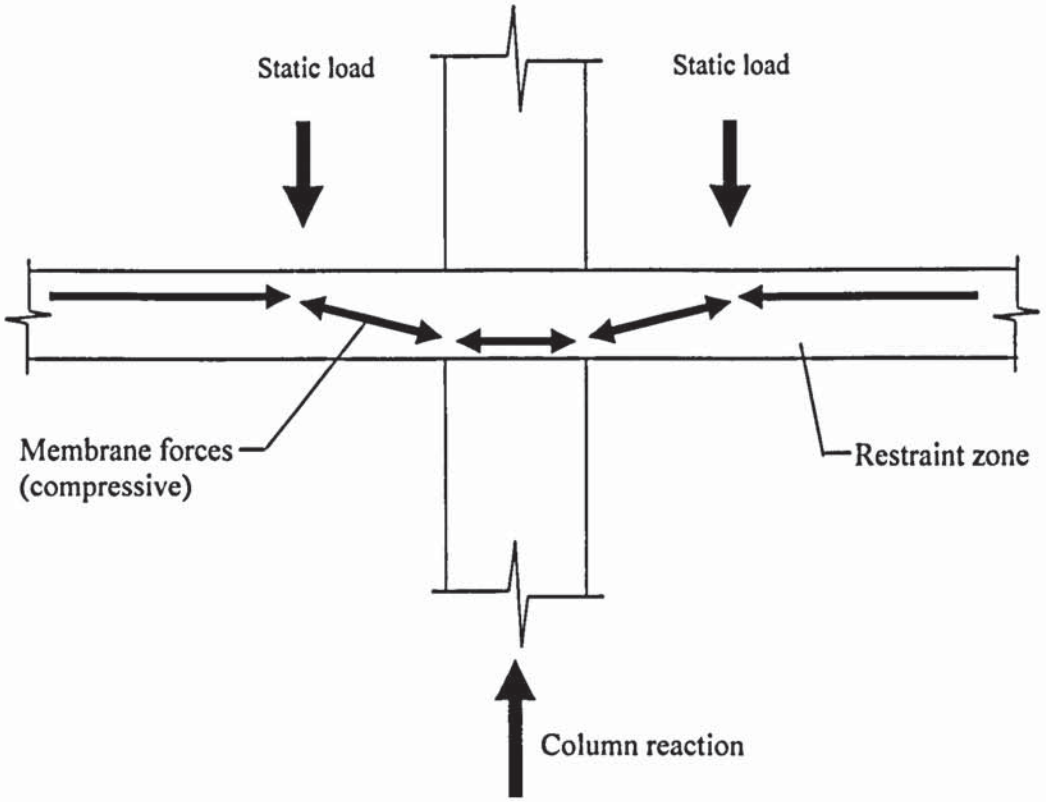

Figure 3.6 Compressive membrane actions

The European Committee for Concrete (1962) explained that the compressive membrane action on floor slab can only occur at small vertical displacements. Typically displacements less than half thickness of the slab and can occur in flat slabs. Provided the slab of the test does not reach vertical displacements greater than half of its depth, then the effect of compressive membrane action will considerably enhance the load carrying capacity of the slab.

Even though the concrete floor slab spalled extensively and totally exposed some bottom reinforcing bars to fire, the slab remained stable. The applied static load of the slab was supported by compressive membrane action when the sagging flexural capacity of the slab was extremely reduced.

3.5.2 High-Strength Concrete Column

All columns were grade C 85 high-strength concrete which had average cube strength of 103 MPa at 28 days. During the fire, the polypropylene fibres added to the concrete mix reduced spalling. It was predicted that the fibres would have melted at approximately 160°C and reduce the pore pressures.

Typical corner spalling was evident but this was considered to be insignificant to the column stability. This type of corner spalling can usually be repaired easily after the fire according to the Concrete Society (1990). Longitudinal cracks of approximately 50 mm into the column had also occurred and were found after the test. The longitudinal cracks were also considered to be insignificant to the column stability and it was relatively easy to remove and if necessary to repair the surface concrete after fire.

The lateral displacements of the external columns due to thermal expansion of the floor slab induced additional column moment. The lateral movement of the external columns has been identified as the cause of previous failure of concrete structures. Although the thin external columns of the Cardington building showed no signs of distress and was able to accommodate these movements, designer should be aware of this behaviour and ensure that the external columns can withstand the lateral displacement during fire.

3.6. Summary

The full-scale seven-storey BRE Cardington concrete building constructed with elements formed of normal and high-strength concrete using the UK Design Code with minimum of 60 minutes fire resistance period demonstrated excellent performance of

reinforced concrete structure subjected to fire. The results and observations from test on a complete frame concrete structure indicated that the current design methods are based on an incorrect model of structural behaviour. The current design codes and design methods do not incorporate the beneficial effects of compressive membrane action. The detrimental effect of lateral displacement of the external columns due to large thermal expansion of the heated floor has also not been accommodated in the current design codes. Therefore, the development of new fire engineering method from the study of whole concrete structures rather than individual member behaviour is required.

Consideration of materials characteristics and structural design are required to optimise the behaviour of real structures in a fire. Designers should consider the spalling of concrete when specifying fixing between compartment wall and the soffit of concrete slab. The effect of concrete spalling on fixings was not anticipated in this test with the consequence of the fire escaping the compartment area and destroying the cables resulting in the loss of valuable data.

Chapter 4 DESCRIPTION OF COMPUTER PROGRAM (ANSYS)

4.1. Introduction

In this chapter, a demonstration of heat transfer problem will be presented using ANSYS program, which based on finite element computer program. The finite element analysis is a numerical analysis technique for obtaining approximate solutions to a variety of problems in engineering. The idea of finite element method appeared in the early 1900s when some researchers approximated and modelled elastic continua using discrete equivalent elastic bars.

Courant (1943) has been credited with being the first person to develop the finite element method using an assemblage of triangular elements and the principle of minimum potential energy to investigate torsion problems. However, the first term of *finite element method* appeared in 1960 when Clough (1960) wrote a paper on plane elasticity problems. Beginning this decade, the finite element method is widely applied in many areas of engineering.

Huebner *et al* (1995) described that rapid advancements in computer hardware with substantial increases in computer memory and speeds at lower cost have meant that large mainframe computers are no longer required for finite element analysis. The availability of personal computers with advanced finite element software brings powerful simulation capability to the design process. Therefore, the finite element analysis has remained the most excellent approach for structural analysis.

In recent years, the use of finite element analysis as a design tool compiled in computer software has grown rapidly. Moaveni (2003) explained that comprehensive

package such as ANSYS has become the common tool in the hand of design engineers. ANSYS is a very powerful engineering tool that may be used to solve a variety of engineering problems. ANSYS has been a leading finite element analysis program for over 25 years.

To obtain all of the simulation capabilities needed for complex modelling scenarios normally meant combining several different software packages. ANSYS Multiphysics solution allows a user to combine the effects of two or more different physics within one and unified simulation environment. This program is unique and powerful with high performance and reliability to meet the analysis requirements. So, ANSYS program is employed to this research because of its capabilities to provide most advanced multi-physics solution to solve coupled-field of structural and thermal problem.

4.2. Conduction of Elements Used by ANSYS

ANSYS offer many two-dimensional thermal-solid elements that are based on linear and quadratic quadrilateral shape function. This chapter discusses a four-node quadrilateral element used in modelling two-dimensional heat transfer problem. The element has a single degree of freedom, which is temperature. Input data at the element is convection heat transfer flux, while the output data will include nodal temperatures and element data such as thermal gradient and thermal flux components. The two dimensional heat transfer problem of a two-storey concrete frame structure will be presented in the following example.

The dimension of two-storey concrete frame structure is shown in Figure 4.1. Material property of the concrete is given in Table 4.1 and thermal data for temperature dependant of the properties is given in Table 4.2. From this structure, the inside room temperature in the second floor and the surrounding air at the outside of the frame are assumed to be uniform at 20°C. The convection heat transfer coefficient $\alpha = 25$ W/m^2 is applied for air inside surfaces of first floor and $\alpha = 10$ W/m^2 are applied on all non heated surfaces at the inside surfaces of second floor as well as the outside surfaces the frame structure.

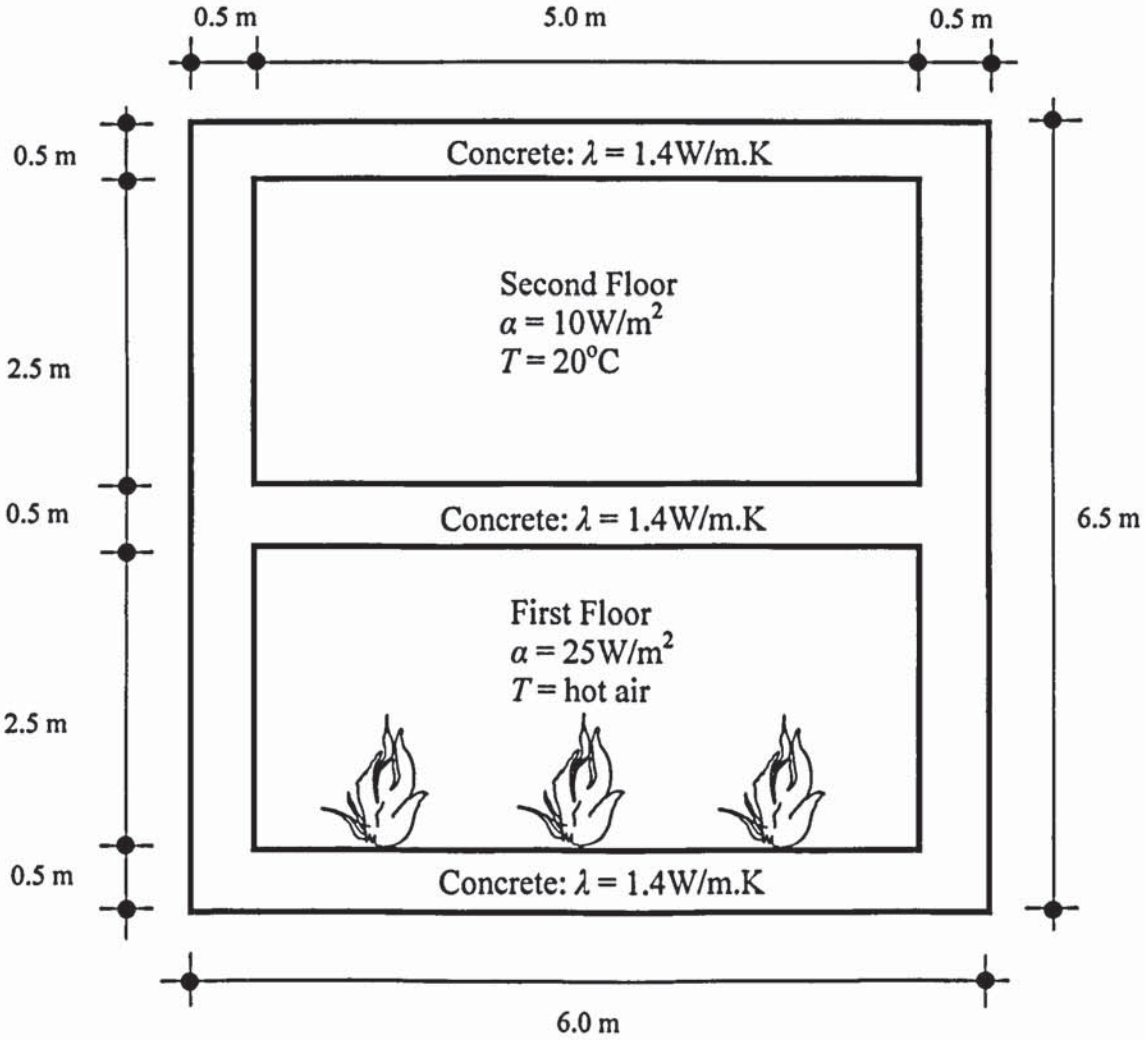

Figure 4.1 Dimension of concrete frame structure

Properties of concrete	Values
Specific heat (c)	1000 J/kg°C
Convection or film coefficient (α)	25 W/m^2°C and 10 W/m^2°C (non heated surfaces)
Thermal conductivity, λ	1.4 W/m.K
Initial condition: Temperature, T	20°C

Table 4.1 Thermal properties of concrete

The atmosphere temperature of a hot air in the inside surface of the first floor due to fire are 842°C, 945°C, and 1049°C which are assumed according to standard fire test at the exposure temperature of 30, 60, and 120 minutes, respectively.

4.3. Verification of the Results

The temperature distribution within the concrete frame for the exposure temperature of 30 minutes is shown in Figure 4.2. The figure shows that the value of maximum temperature of the concrete is 766°C. Temperature distributions within the concrete frame for various exposure temperatures can be obtained by repeating the above steps. The temperature distributions for exposure temperature of 60 minutes and 120 minutes are presented in Figure 4.3 and Figure 4.4 respectively. Similar tends appear that the maximum temperatures occur at about 50mm depth from concrete surface and decrease gradually within the cross-section of concrete elements to 20°C at the surface opposite of the fire. The maximum temperatures for exposure temperatures of 60 minutes and 120 minutes are about 860°C and 955°C respectively.

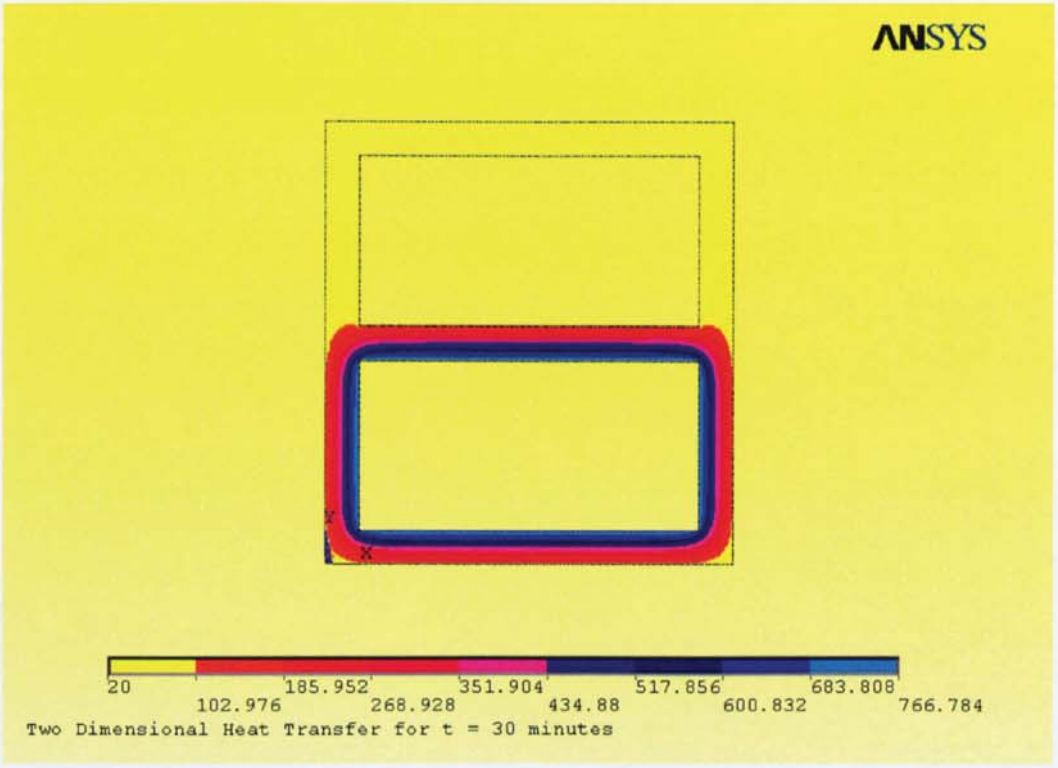

Figure 4.2 Temperature contour plot for the exposure temperature of 30 minutes

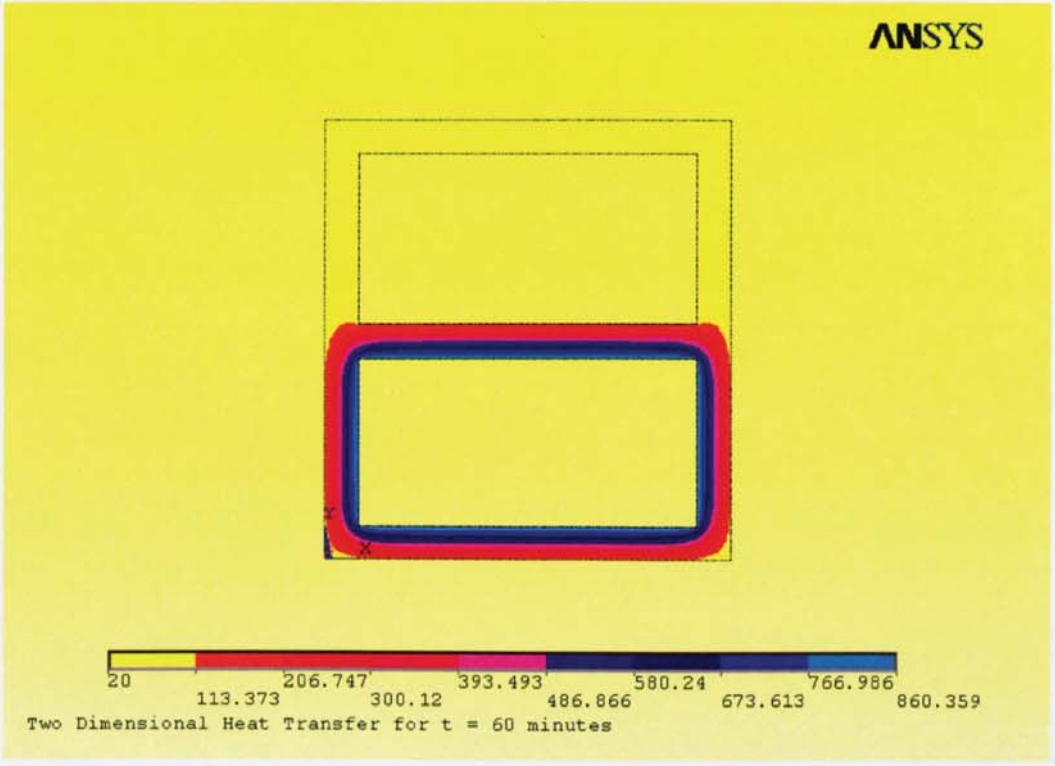

Figure 4.3 Temperature contour plot for the exposure temperature of 60 minutes

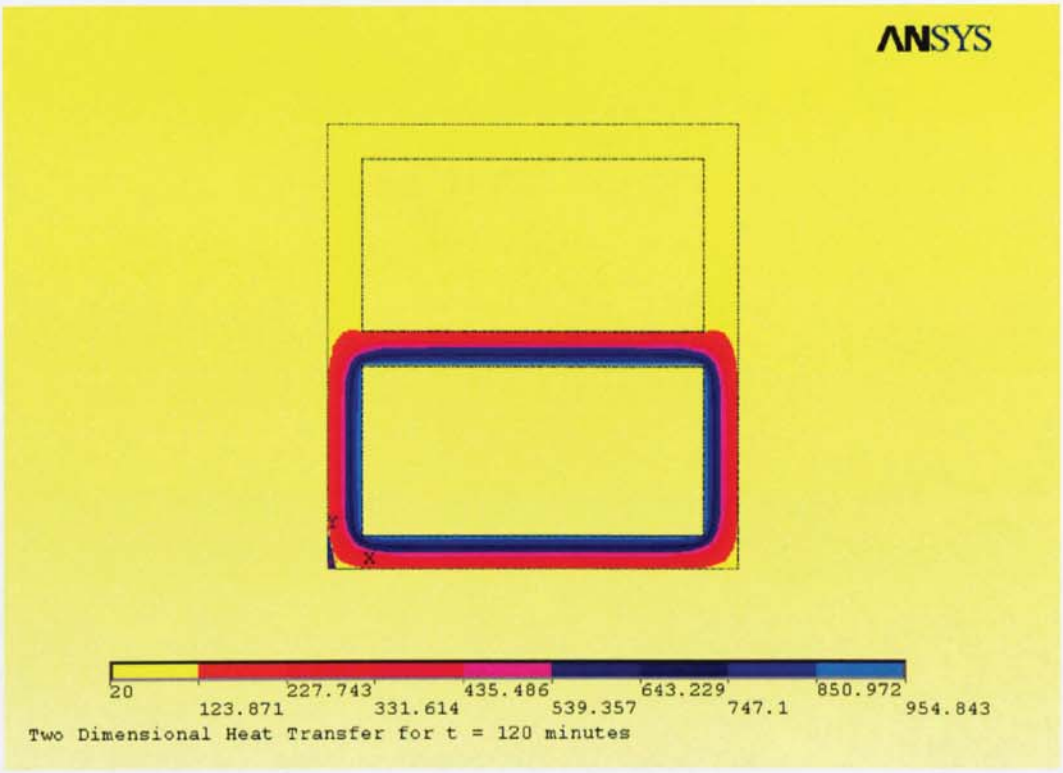

Figure 4.4 Temperature contour plot for the exposure temperature of 120 minutes

The above results have a reasonable agreement when a comparison with numerical calculation by Tenchev *et al* (2001) and experimental data from Ahmed and Hurst (1997) are made. At concrete surface, the agreement is very good. However, at another distances throughout the concrete element, the result is slightly higher because both the numerical and experimental results used couple heat and mass transfer rather than the use of heat transfer alone used by the program. The comparison of the results with numerical and experimental results is presented Table 4.2.

Temperature	Results (ANSYS)	Numerical (Tenchev *et al*)	Experimental (Ahmed and Hurst)
t = 60 min at concrete surface	860°C	840°C	850°C
t = 60 min at 15 mm from surface	580°C	520°C	510°C
t = 60 min at 30 mm from surface	393°C	310°C	340°C

Table 4.2 Comparison with numerical and experimental results

Full demonstration of the steps to create the appropriate element type and the geometry of the problem is presented in Appendix. The task includes applying boundary conditions and obtaining results for the problem using ANSYS Version 6.0. Transferring the results onto word document is also presented.

Chapter 5 THERMAL ANALYSIS OF STRUCTURAL ELEMENT

5.1. Introduction

The main objective of this chapter is to analyse temperature distribution within the member of a structural element. In order to measure temperature distribution within the member of structural element, usually four thermocouples would be placed on the top of concrete surface, on the top and bottom of reinforcing bars, and at mid-depth of the member of structural element.

In many cases, it was not decided to measure the temperature distribution within the member of structural element due to possible damage caused by drilling into the member of structural element. Therefore, the computation below would be satisfied to analyse the temperature distribution within the member of structural element.

5.2. Thermal Conductivity

Heat flows within a body or between two bodies in physical contact of material when temperature at one point is different from another point. The term of conduction is the transfer of heat in which heat passes from the hotter to the colder parts by an exchange of energy with negligible movement of particles of the body. This conduction may occur in solids, liquids and gasses; but occurs most efficiently in solids. The effect of conduction is thermal conductivity where quantity of heat exists between the faces of unit thickness of materials. Fundamental unit of thermal conductivity is W/m°C.

Shown in Figure 5.1 is the thermal conductivity within an element. In this figure, the left face of wall is maintained at a temperature T_i and the right face is maintained at

a temperature T_j. For simplicity will be assumed that T_i is greater than T_j. Since heat flows only in the x-direction, the problem can be treated as one-dimensional with a single degree of freedom is temperature.

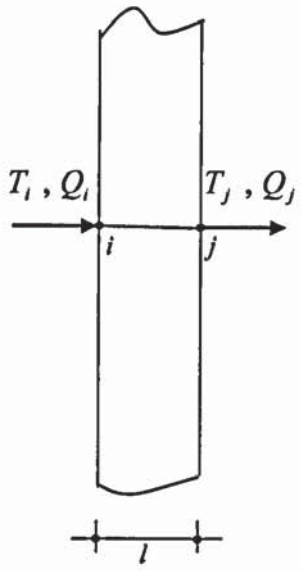

Figure 5.1 Thermal conductivity within an element

If the heat flows over an area A (m^2) with the thermal conductivity λ (W/m.K), then the quantity of heat Q(W) crossing the area per-unit time in the x-direction is given by the Fourier's law of heat conduction:

$$Q = -A\,\lambda\,\frac{dT}{dx} \tag{5.1}$$

Where $\frac{dT}{dx}$ is the temperature gradient, which for discrete systems its can be approximated as follows:

$$\frac{dT}{dx} \cong \frac{\Delta T}{\Delta x} = \frac{T_i - T_j}{l} \tag{5.2}$$

Where l is thickness of the wall (m).

If the heat flow into the node is positive and that leaving the node is negative,

$$Q_i = \left(\frac{T_i - T_j}{l}\right) \lambda A \tag{5.3}$$

$$Q_j = -\left(\frac{T_i - T_j}{l}\right) \lambda A \tag{5.4}$$

Expressing the above equation in a matrix form, we have:

$$\begin{Bmatrix} Q_i \\ Q_j \end{Bmatrix} = \left(\frac{\lambda A}{l}\right) \begin{bmatrix} 1 & -1 \\ -1 & 1 \end{bmatrix} \begin{Bmatrix} T_i \\ T_j \end{Bmatrix} \tag{5.5}$$

or in matrix form:

$$\{Q\} = [C]\{T\} \tag{5.6}$$

Where $[C]$ is the conductance matrix.

Equation (5.3) can also be written as:

$$Q = \frac{A\,(T_i - T_j)}{(l/\lambda)} \tag{5.7}$$

If $R = l/\lambda$ (m^2.K/W) is the thermal resistance of the wall, Eq. (5.7) becomes:

$$Q = \frac{A\,(T_i - T_j)}{R} \tag{5.8}$$

Reciprocal of R is known as the thermal conductance of the wall with unit W/m^2.K.

5.3. Convection

Convection happens when the heat is transferred from place to place due to the movement of a fluid (liquid or gas) in which the heat is carried with the particles of the

moving fluid. These processes may be natural or forced. The sketch how the thermal convectivity occurs within an element is illustrated in Figure 5.2.

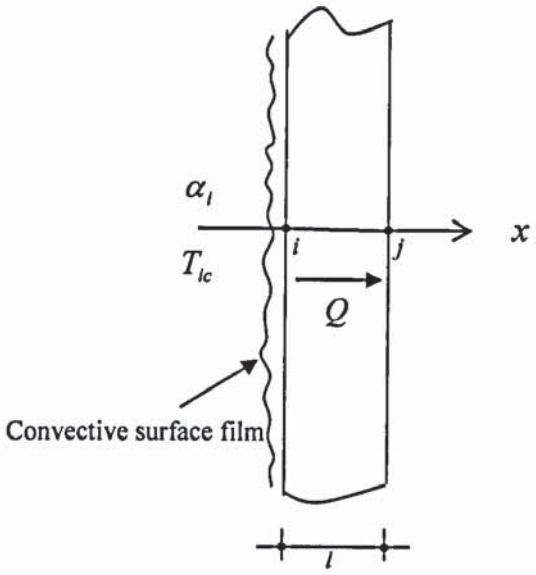

Figure 5.2 Thermal convectivity within an element

Heat flow into node *i* due to convection is given by:

$$Q_i = \alpha_i A (T_{ic} - T_i) \tag{5.9}$$

Where: α_i = convective heat transfer coefficient

T_{ic} = gas temperature

T_i = surface temperature

Heat flow out of the node *i* due to conduction is:

$$Q_i = -\frac{\lambda A}{l}(T_i - T_j) \tag{5.10}$$

Heat balance at node *i* lead to:

$$\alpha_i A (T_{ic} - T_i) - \frac{\lambda A}{l}(T_i - T_j) = 0 \tag{5.11}$$

Rearranging equation (5.11) we have:

$$\alpha_i A T_{ic} = \left(\frac{\lambda A}{l} + \alpha_i A\right) T_i - \left(\frac{\lambda A}{l}\right) T_j \quad \text{or}$$

$$\left(\frac{\lambda A}{l} + \alpha_i A\right) T_i - \left(\frac{\lambda A}{l}\right) T_j = \alpha_i A T_{ic} \tag{5.12}$$

The element conductance matrix $[C]$ at equation (5.6) including the convective heat transfer coefficient, in this case, therefore, can be written as:

$$[C] = \left(\frac{\lambda A}{l}\right) \begin{bmatrix} 1 & -1 \\ -1 & 1 \end{bmatrix} + \begin{bmatrix} \alpha A & 0 \\ 0 & 0 \end{bmatrix} \tag{5.13}$$

5.4. Radiation

Radiation is a dominant mode of heat transfer. For the solution of heat transfer problem, it is often more convenient to express the heat flow to the member in term of an effective heat transfer coefficient, α_{eff}, multiplied by the temperature difference between the gas and the member. Drysdale (1985) gave the theory for the calculation of the radiation factor, thus the α_{eff} can be calculated as:

$$\alpha_{eff} = \alpha_c + \frac{\Phi e_{res} \sigma \left(T_g^4 - T_m^4\right)}{T_g - T_m} \tag{5.14}$$

Where: α_{eff} = effective heat transfer coefficient

α_c = convective heat transfer

Φ = radiation factor of the angle of the heat source

e_{res} = resultant emissivity

σ = Stefan-Boltzmann constant

T_g = surface temperature (°K)

T_m = gas temperature (°K).

Li *et al* (2001) gave the simple equation for the calculation of combined convective-radiation heat transfer coefficient, α , as:

$$\alpha = \alpha_c + e\sigma\left(T + T_\infty\right)\left(T^2 + T_\infty^2\right) \tag{5.15}$$

Where: α = effective heat transfer coefficient

α_c = convective heat transfer

e = emissivity

σ = Stefan-Boltzmann constant

T = surface temperature (°K)

T_∞ = gas temperature (°K).

It is be noted that values of effective heat transfer coefficient, α, calculated from Equation (5.15) will be adopted as a convective heat transfer coefficient for all heat transfer analysis throughout this manuscript.

5.5. Temperature Distribution within Element Using ANSYS

ANSYS (2002) version 6.0 presented that the basis formula of thermal analysis is a heat balance equation obtained from the principle of conservation of energy. The finite element solution performed via ANSYS calculates nodal temperatures, and then uses the nodal temperatures to obtain other thermal quantities. The ANSYS program handles all three primary modes of heat transfer: conduction, convection, and radiation.

In the term of conduction, the energy is transported by molecular activities from the high-temperature region to the low temperature region. Using Fourier's Law, ANSYS determines the rate of heat transfer by conduction. The important property in this case is the value of thermal conductivity which is temperature dependant.

Convection is specified as a surface load on conducting solid elements. When the convection film coefficient and the bulk fluid temperature at a surface are specified, ANSYS then calculates the appropriate heat transfer across that surface. If the film coefficient is a temperature dependant, a function or a table of temperatures along with the corresponding values of film coefficient at each temperature should be specified.

ANSYS supports two types of thermal analysis i.e. steady-state and transient thermal analysis. Steady-state thermal analysis determines the temperature distribution and other thermal quantities under steady-state loading conditions. Steady-state loading condition is a situation where heat storage effects varying over a period of time can be ignored. In the other hand, transient thermal analysis determines the temperature distribution and other thermal quantities under conditions that vary over a period of time. The corresponding values of temperature varying over period of time may also be specified in a function or simplified in a table.

5.5.1. Thermal Properties

Material properties of concrete at elevated temperature (thermal properties) applied throughout this study are adopted from previous researchers. Li *et al* (2002) presented reasonable values of the properties used to this study. The thermal properties of concrete at elevated temperature are presented in Table 5.1.

Properties of concrete	Values
Density	2400 kg/m^3
Enthalpy	1
Emissivity	0.6
Convection or film coefficient: (α_f)	25 $W/m^2{}^oC$ (heated surface), and
(α_a)	10 $W/m^2{}^oC$ (non heated surfaces)
Young modulus (E)	2.5 x 10^{11} Pa
Poisson' ratio (υ)	0.20 (normal strength concrete)
Specific heat (c)	Temperature dependant (see Table 5.2)
Thermal conductivity (λ)	Temperature dependant (see Table 5.2)

Table 5.1 Thermal properties of concrete

In order to simplify the calculation, the use of heat transfer alone rather than coupled heat and mass transfer will continue to be the preferred method. Some researchers such as Tenchev *et al* (2001a) and (2001b), Li *et al* (2001), Lie and Woollerton (1988) analysed the effect of mass transfer on heat transfer in concrete. They concluded that the predicted temperature using combined heat and mass transfer has very good agreement with experimental results. Ang (2004) incorporated the effect of mass transfer in heat transfer analysis only by modifying the specific values of hydroscopic materials and the equivalent additional specific heat of 20% to 70% higher is obtained by converting the combined heat and mass transfer. In order to include the

effect of mass transfer in heat transfer analysis, the following specific heat is used when heat transfer only is considered:

$$c_p = c_{p,dry} + c_{add} \text{ , with:}$$

$$c_{add} = \frac{2.26 \, x \, 10^6 \, e_{free}}{\Delta T} \text{ (J/kg°C)}$$

Where: e_{free} = water content by weight

= 0.03 for the first dehydration reaction

= 0 for the second dehydration reaction

ΔT = magnitude of the temperature interval of evaporation or dehydration

= 95°C to 155°C for the first dehydration reaction

= 200°C to 220°C for the second dehydration reaction

In the combined heat and mass transfer the $c_{p,dry}$ = 950 J/kg°C is used by Mehaffey *et al* (1994). Axenenko and Thorpe (1996) and Thomas (2002) have also used it as the base value for specific heat in heat transfer only analyses. Even though it does not include the effects of re-condensation and water movement in concrete, ENV 1994-1-2, Part 1.2 suggests an additional specific heat to be included to the base value of dry concrete at temperature 100°C and 200°C. The heat transfer only analysis and the additional specific heat included to the base value of dry concrete as suggested by ENV 1994-1-2 will be used through out the analyses of this manuscript.

From Table 5.1, the coefficient of specific heat and thermal conductivities of concrete are temperature dependant. The relation between temperature and the properties according to ENV 1994-1-2 are as follows:

- Specific heat for normal concrete (J/kg °C):

$$c = 900 + 80\left(\frac{T}{120}\right) - 4\left(\frac{T}{120}\right)^2$$

- Thermal conductivity (W/m°C):

$$\lambda = 2.2 - \frac{1.2\,T}{150}, \quad \text{for: } T < 150°C$$

$$\lambda = 1 - \frac{0.8\,(T - 150)}{550}, \quad \text{for: } 150°C \leq T \leq 700°C$$

$$\lambda = 0.2, \quad \text{for: } T > 700°C$$

Using the additional specific heat to the base value of dry concrete at temperatures 100°C and 200°C as suggested by ENV 1994-1-2, then the corresponding values of the specific heat and thermal conduction of concrete at various temperatures are given in Table 5.2.

Temperature (°C)	**20**	**200**	**400**	**800**	**> 1000**
Specific heat (c)	963	1072	1122	1255	1289
Thermal conductivity, λ	2.04	0.93	0.64	0.2	0.2

Table 5.2 Temperature dependant of the properties of concrete

5.5.2. Temperature Distribution of One-Side Fire Exposed Surface

Consider a concrete structural element (column) in this investigation. The dimension shown on Figure 5.3 represents a rectangular cross-section of the column exposed to fire. The column was exposed to fire on one-side surface (BD) makes the problem one-dimensional thermal distribution along the horizontal axis. The material properties of

concrete specified in Table 5.1 and Table 5.2 are adopted. The time-temperature response of the design fire of standard fire curve is employed as:

$$T_g = 20 + 345\log(8t + 1)$$

Where: T_g = the furnace temperature (°C), and t = time (minutes).

From above equation, the corresponding values of temperature varying over period of time can be simplified in Table 5.3 as follows:

Time (minutes)	0	5	10	15	30	60	120
Temperature	20°C	576°C	678°C	739°C	842°C	945°C	1049°C

Table 5.3 Varying temperatures over period of time.

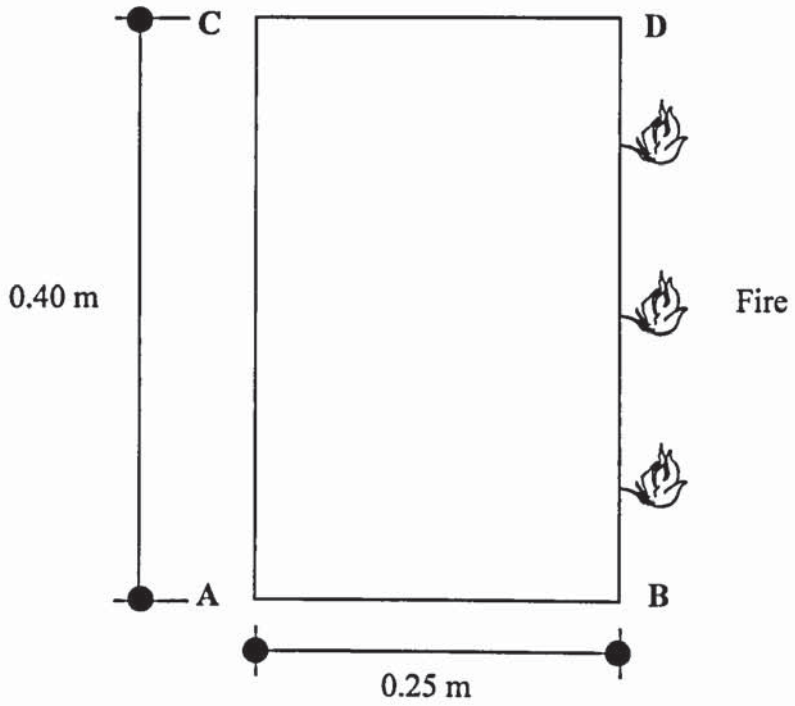

Figure 5.3 Cross-section of structural element with one-side fire exposed surface

5.5.2.1. Using ANSYS

Based on general finite element method recommendation, the square shaped elements are generated in this problem. The maximum size of the square element is 0.025 m. The corresponding boundary conditions in this problem are that the element surfaces at side AB, AC and CD are exposed to bulk air temperature of 20°C. The thermal load applies to the element surface at side BD is temperature dependant taken from Table 5.4.

The element surface at side BD is exposed to fire. The convective heat transfer coefficient of heated surface: α_f = 25 W/m^2°C, non heated surfaces: α_a = 10 W/m^2°C. The thermal conductivity of concrete, λ_c, is temperature dependant which can be taken from Table 5.3. Using ANSYS 6.0, result of the problem in the form of temperature distribution along the horizontal axis is presented in Figure 5.4.

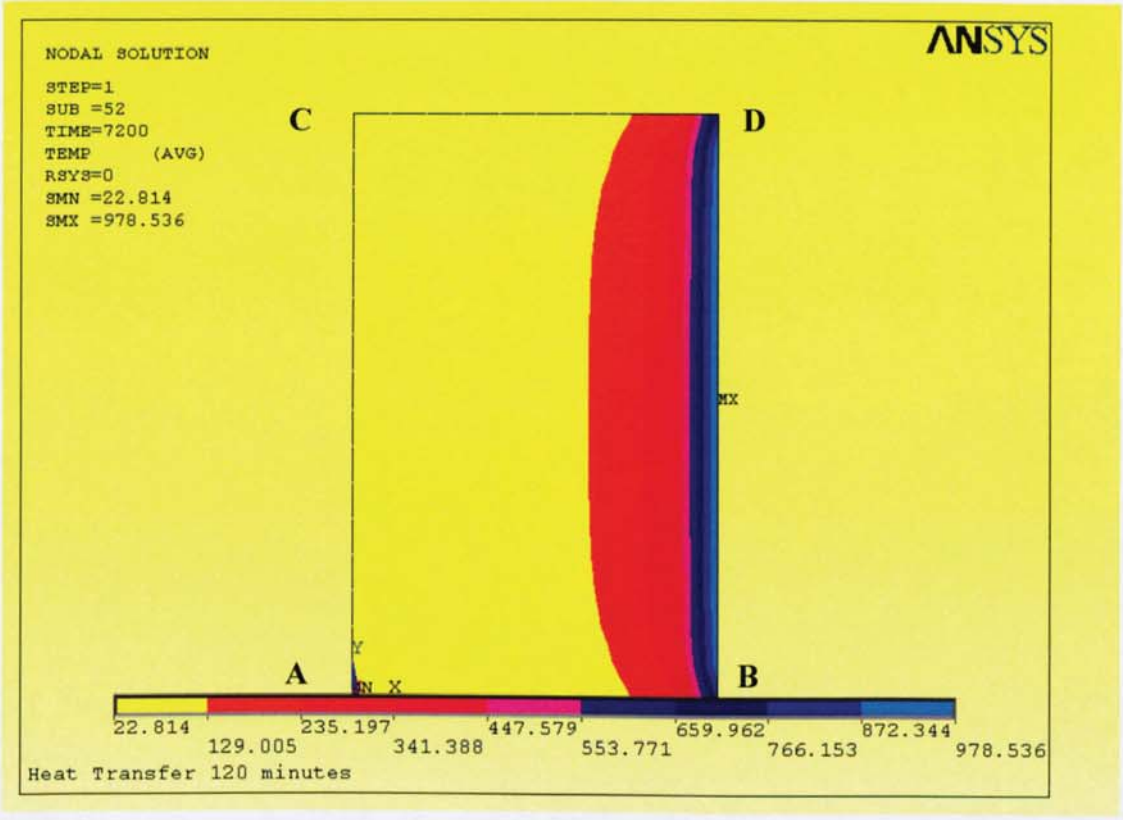

Figure 5.4 Temperature distribution of one-side fire exposed surface

5.5.2.2. Verification of the results using FEA

Consider a concrete structural element which heat flows in only the X direction. The heat flows within the element of one-side fire exposed surface is illustrated in Figure 5.5. The right face of the element is exposed to 120 minutes fire where the environment temperature in the furnace is T_f =1049°C. The temperature of the ambient air on the left face of the element is T_a=20°C.

Since the thermal conductivity of the concrete, λ, is temperature dependant, it can be assumed that λ_1= 0.20 W/m°C, λ_2= 0.64 W/m°C, λ_3 = 0.93 W/m°C, and λ_4= 2.04 W/m°C are thermal conductivities of element (1), (2), (3), and (4), respectively. The heat transfer coefficient pertaining the convective surface adjacent to the inside of the element is α_f= 25 W/m^2°C, while the heat transfer coefficient on non heated surface is α_a= 10 W/m^2°C.

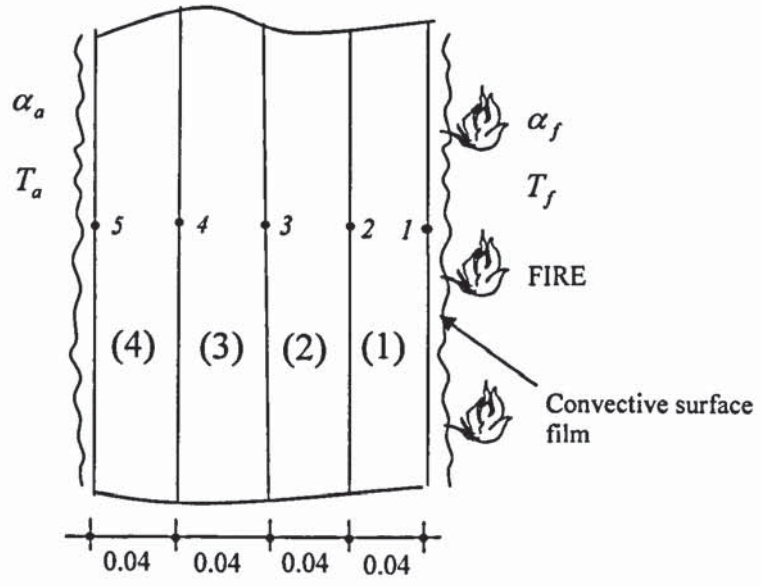

Figure 5.5 Heat flows through out the element of one-side fire exposed surface

Using finite element model, the temperature distribution through the element can be determined in the following descriptions.

The element conductance matrix:

$$[C] = \left(\frac{\lambda A}{l}\right)\begin{bmatrix} 1 & -1 \\ -1 & 1 \end{bmatrix}$$

The element conductance matrix including the convective heat transfer coefficient:

$$[C] = \left(\frac{\lambda A}{l}\right)\begin{bmatrix} 1 & -1 \\ -1 & 1 \end{bmatrix} + \begin{bmatrix} \alpha A & 0 \\ 0 & 0 \end{bmatrix}$$

The element matrix equation:

$$\{Q\} = [C]\{T\} \text{ or } [C]\{T\} = \{Q\}$$

Element (1):

Assume the area A is 1 square meter.

$$[C]^{(1)} = \left(\frac{\lambda A}{l}\right)\begin{bmatrix} 1 & -1 \\ -1 & 1 \end{bmatrix} + \begin{bmatrix} \alpha A & 0 \\ 0 & 0 \end{bmatrix} = \begin{bmatrix} 30 & -5 \\ -5 & 5 \end{bmatrix}$$

$$\{Q\}^{(1)} = \begin{Bmatrix} \alpha A T \\ 0 \end{Bmatrix} = \begin{Bmatrix} 26225 \\ 0 \end{Bmatrix}$$

Element (2):

$$[C]^{(2)} = \left(\frac{\lambda A}{l}\right)\begin{bmatrix} 1 & -1 \\ -1 & 1 \end{bmatrix} = \begin{bmatrix} 6.4 & -6.4 \\ -6.4 & 6.4 \end{bmatrix}$$

$$\{Q\}^{(2)} = \begin{Bmatrix} 0 \\ 0 \end{Bmatrix}$$

Element (3):

$$[C]^{(3)} = \left(\frac{\lambda A}{l}\right)\begin{bmatrix} 1 & -1 \\ -1 & 1 \end{bmatrix} = \begin{bmatrix} 9.3 & -9.3 \\ -9.3 & 9.3 \end{bmatrix}$$

$$\{Q\}^{(3)} = \begin{Bmatrix} 0 \\ 0 \end{Bmatrix}$$

Element (4):

$$[C]^{(4)} = \left(\frac{\lambda A}{l}\right)\begin{bmatrix} 1 & -1 \\ -1 & 1 \end{bmatrix} = \begin{bmatrix} 20.4 & -20.4 \\ -20.4 & 20.4 \end{bmatrix}$$

$$\{Q\}^{(4)} = \begin{Bmatrix} 0 \\ 0 \end{Bmatrix}$$

The assembled global-matrix can be expressed as:

$$\begin{bmatrix} 30 & -5 & 0 & 0 & 0 \\ -5 & 5+6.4 & -6.4 & 0 & 0 \\ 0 & -6.4 & 6.4+9.3 & -9.3 & 0 \\ 0 & 0 & -9.3 & 9.3+20.4 & -20.4 \\ 0 & 0 & 0 & -20.4 & 20.4 \end{bmatrix} \begin{Bmatrix} T_1 \\ T_2 \\ T_3 \\ T_4 \\ T_5 \end{Bmatrix} = \begin{Bmatrix} Q_1^{(1)} \\ Q_2^{(1)} + Q_2^{(2)} \\ Q_3^{(2)} + Q_3^{(3)} \\ Q_4^{(3)} + Q_4^{(4)} \\ Q_5^{(4)} \end{Bmatrix}$$

Where: $Q_1^{(1)} = 26225$, and $Q_2^{(1)} + Q_2^{(2)} = Q_3^{(2)} + Q_3^{(3)} = Q_4^{(3)} + Q_4^{(4)} = Q_5^{(4)} = 0$.

Then the matrix became:

$$\begin{bmatrix} 30 & -5 & 0 & 0 & 0 \\ -5 & 11.4 & -6.4 & 0 & 0 \\ 0 & -6.4 & 15.7 & -19.3 & 0 \\ 0 & 0 & -9.3 & 29.7 & -20.4 \\ 0 & 0 & 0 & -20.4 & 20.4 \end{bmatrix} \begin{Bmatrix} T_1 \\ T_2 \\ T_3 \\ T_4 \\ T_5 \end{Bmatrix} = \begin{Bmatrix} 26225 \\ 0 \\ 0 \\ 0 \\ 0 \end{Bmatrix}$$

Applying the base boundary condition $T_5 = T_a = 20°C$ to find that the final set of linear equation can be written as:

$$\begin{bmatrix} 30 & -5 & 0 & 0 & 0 \\ -5 & 11.4 & -6.4 & 0 & 0 \\ 0 & -6.4 & 15.7 & -19.3 & 0 \\ 0 & 0 & -9.3 & 29.7 & -20.4 \\ 0 & 0 & 0 & 0 & 1 \end{bmatrix} \begin{Bmatrix} T_1 \\ T_2 \\ T_3 \\ T_4 \\ T_5 \end{Bmatrix} = \begin{Bmatrix} 26225 \\ 0 \\ 0 \\ 0 \\ 20 \end{Bmatrix}$$

The solution of the above matrix-equation is:

$$\begin{Bmatrix} T_1 \\ T_2 \\ T_3 \\ T_4 \\ T_5 \end{Bmatrix} = \begin{Bmatrix} 974 \\ 602 \\ 311 \\ 111 \\ 20 \end{Bmatrix}$$

Presenting the above results in the following table, we have:

Nodes	T_f (atmosphere)	T_1 (concrete)	T_2	T_3	T_4	T_5
Distance from fire surface	0 mm	0 mm	60 mm	120 mm	180 mm	240 mm
Temperature	1049°C	974°C	602°C	311°C	111°C	20°C

Table 5.4 Temperature distribution within the element of one-side fire exposed surface

The agreement between the results computed by ANSYS presented in Figure 5.4 and the calculated result using FEA presented in Table 5.4 was reasonable. Therefore the use of ANSYS program can be continued to obtain approximate solutions in the variety problems of thermal analysis.

5.5.3. Temperature Distribution of Two-Side Fire Exposed Surfaces

The next investigation is temperature distribution of two-side exposed surfaces column subjected to fire. Dimension of the column and the two-side surfaces exposed to fire is shown on Figure 5.6. In this case, the problem is two-dimensional thermal distribution along the X and Y directions. The corresponding boundary conditions are that side BD and CD are exposed to convection heat while sides AB and AC are exposed to bulk air temperature of 20°C. The properties of concrete specified in Tables 5.1 and 5.2 and time-temperature design specified in Table 5.3 are also employed. Using ANSYS, the temperature distribution of two-side fire exposed surfaces is shown in Figure 5.7.

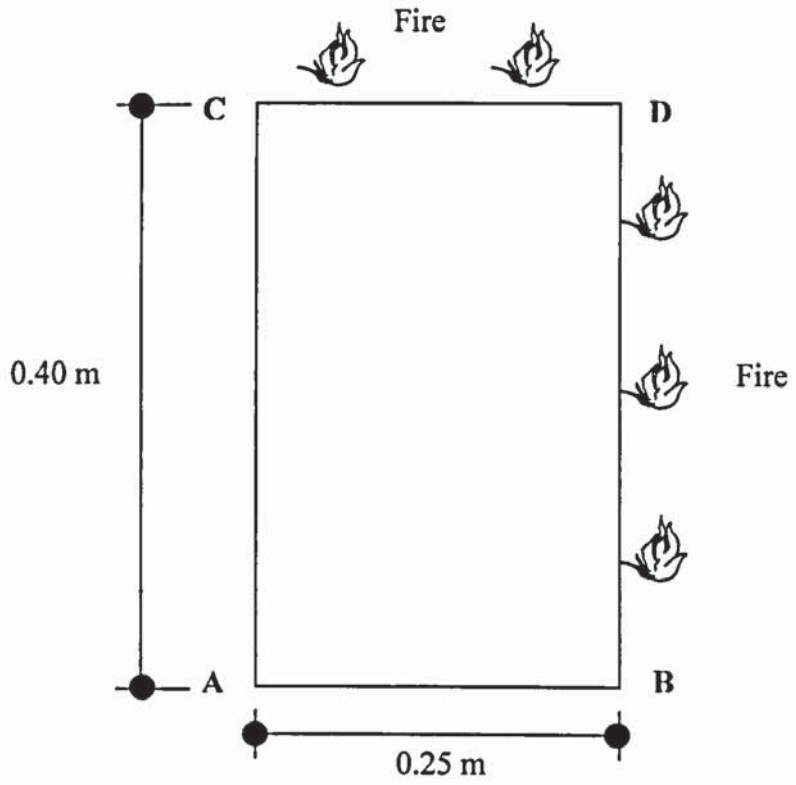

Figure 5.6 Cross-section of structural element with two-side fire exposed surfaces

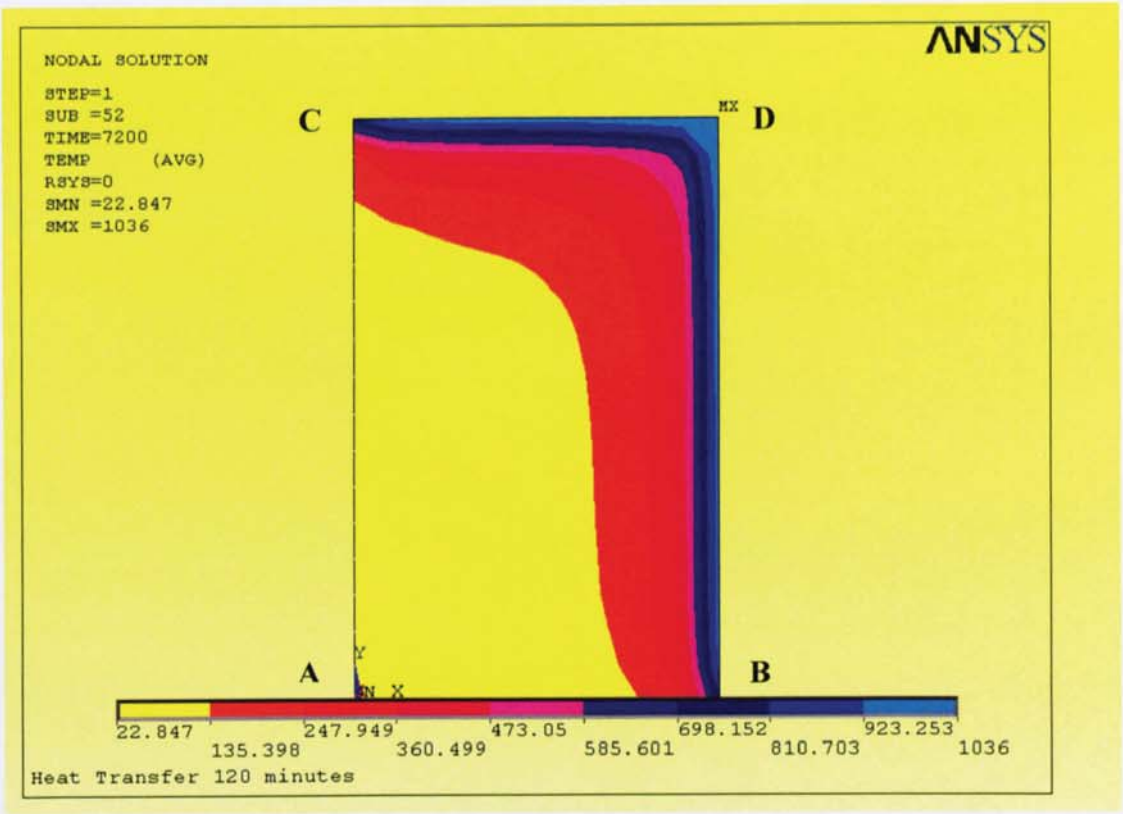

Figure 5.7 Temperature distribution of two-side fire exposed surfaces

5.5.4. Temperature Distribution of Three-Side and Four-Side Exposed Surfaces

Further investigations of this discussion are temperature distribution of three-side and four-side exposed surfaces column subjected to fire. Dimension of rectangular cross-section of the column exposed to fire at three-side and four-side are shown on Figure 5.8 and Figure 5.10 respectively.

Similar to the previous analysis, the material properties of concrete specified in Tables 5.1 and 5.2 are employed as well as the thermal load of the atmosphere exposed to fire varying over period of time simplified in Table 5.3. Using ANSYS, the two-dimensional thermal distribution along the X and Y directions within the element of three-side and four-side are presented in Figure 5.9 and Figure 5.11, respectively.

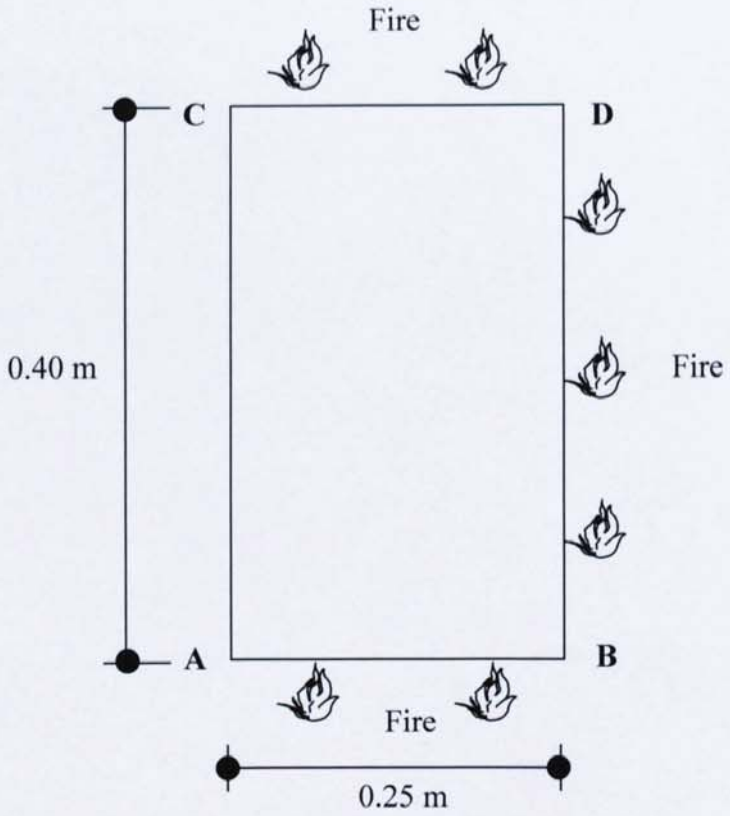

Figure 5.8 Cross-section of structural element with three-side fire exposed surfaces

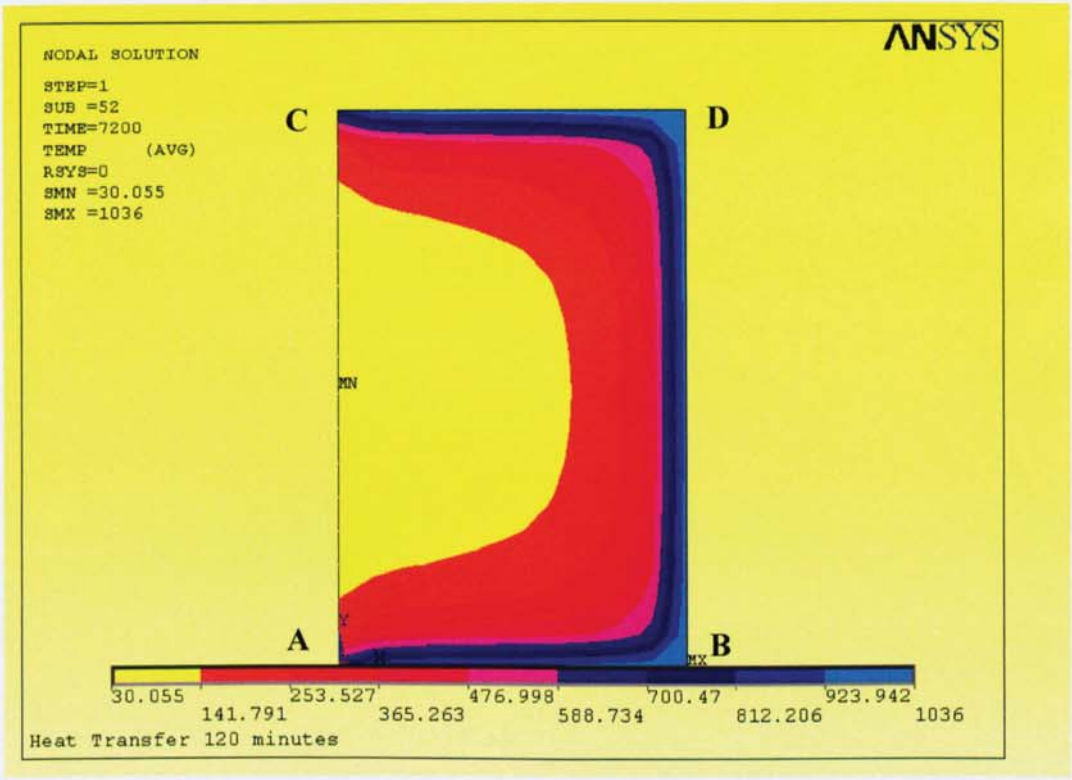

Figure 5.9 Temperature distribution of three-side fire exposed surfaces

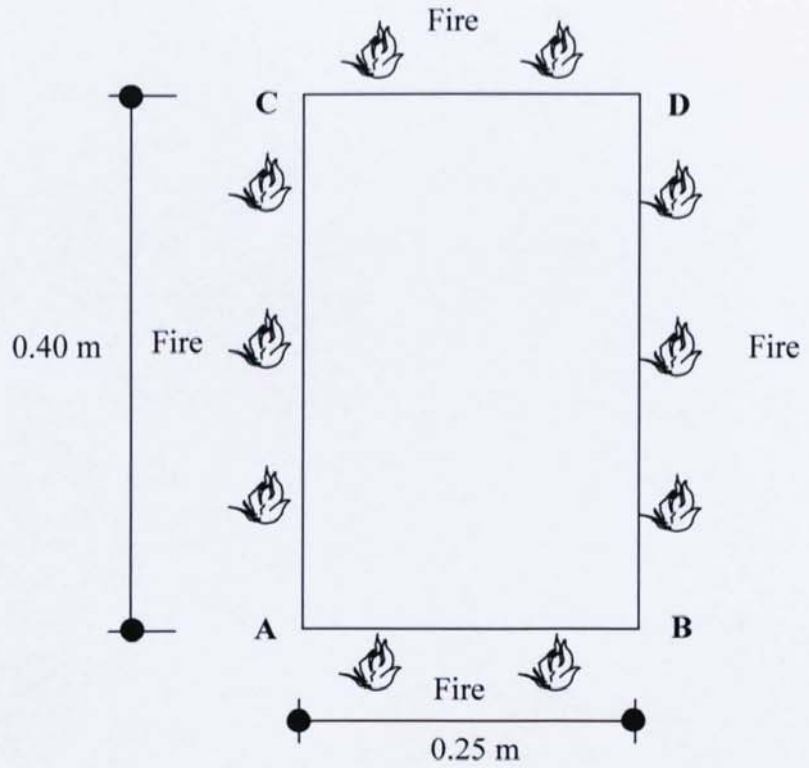

Figure 5.10 Cross-section of structural element with four-side fire exposed surfaces

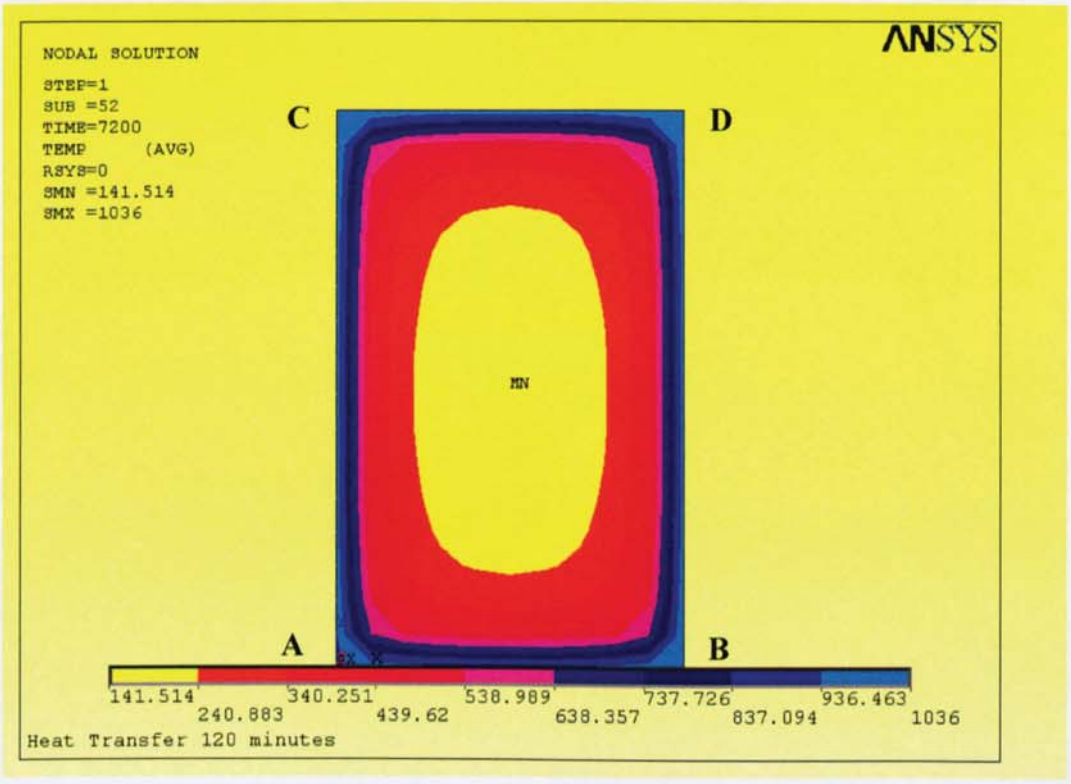

Figure 5.11 Temperature distribution of four-side fire exposed surfaces

5.6. The Effect of the Distances from Fire Surface within the Element

The temperature distributions as a function of time at several distances from the fire exposed surface are shown in the following figures. Figures 5.12 to 5.15 represent the temperature distributions at distances 0 mm, 25 mm, 50 mm, and 125 mm, respectively. These figures illustrate the rise of temperature at selected distances from concrete surface starting from time 0 to 120 minutes of the ignition of the fire.

Shown in Figure 5.12, the temperature at the concrete surface increased rapidly after ignition and reached above 600°C in 40 minutes. The surface temperature rose about 980°C at the end of 120 minutes, this means the different between atmosphere temperature of 1080°C, and concrete surface temperature was about 100°C or decreased by about 10%.

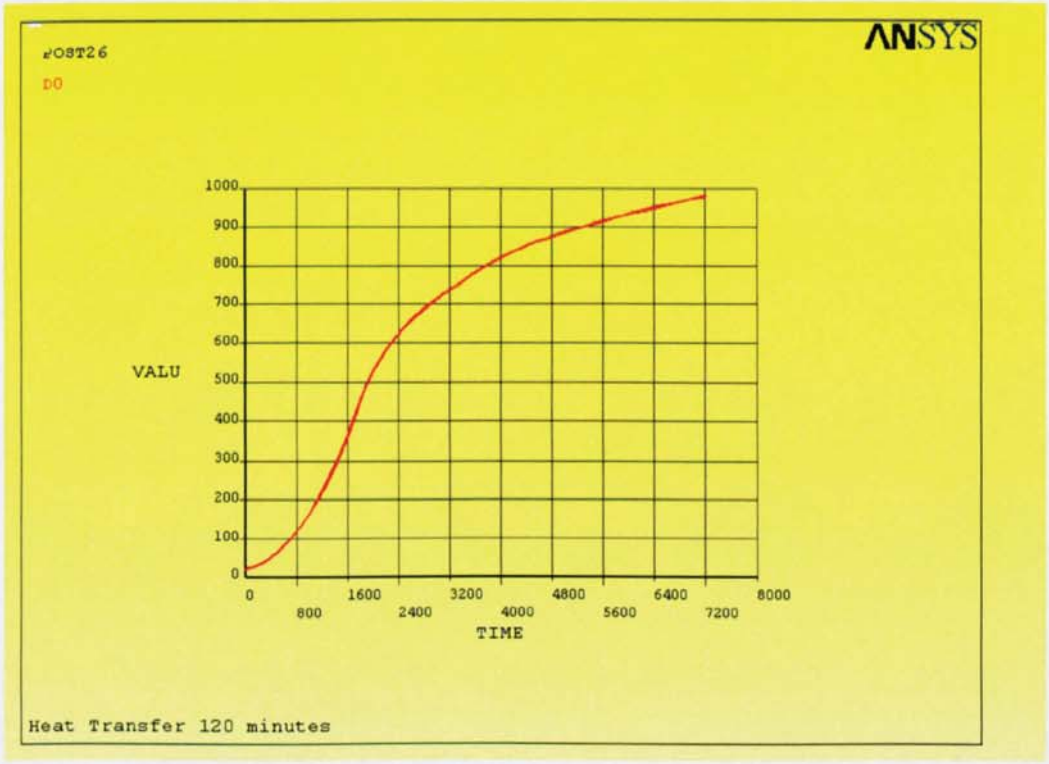

Figure 5.12 Time-temperature at distance 0 mm from concrete surface

Relationship between times vs. temperature at distance 25 mm from concrete surface inside the element is given in Figure 5.13. The 25 mm distance from the surface may represents the temperature of the bottom reinforcing bars. It can be seen from the figure that the temperature at this location increased gradually and reached above 400°C after 120 minutes exposed to fire. This smooth curve is representative assuming there was no concrete spalling occurred in the structure.

Similar tend of time-temperature curve appeared at the distance of 50 mm from concrete surface. The temperature at this location reached to about 240°C at the end of 120 minutes exposed to fire. The 50 mm distance from the concrete surface may also represents the temperature of the bottom reinforcing bars. The time-temperature curve at this location is shown in Figure 5.14, and again, assuming there was no concrete spalling occurred in the structure.

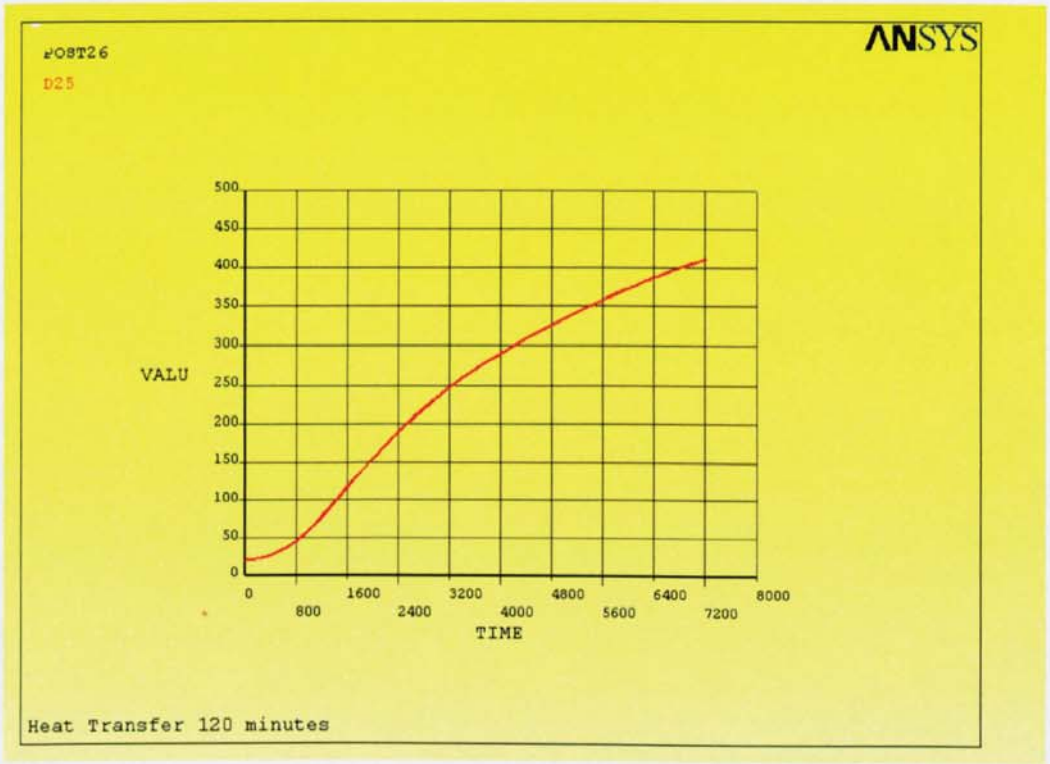

Figure 5.13 Time-temperature at distance 25 mm from concrete surface

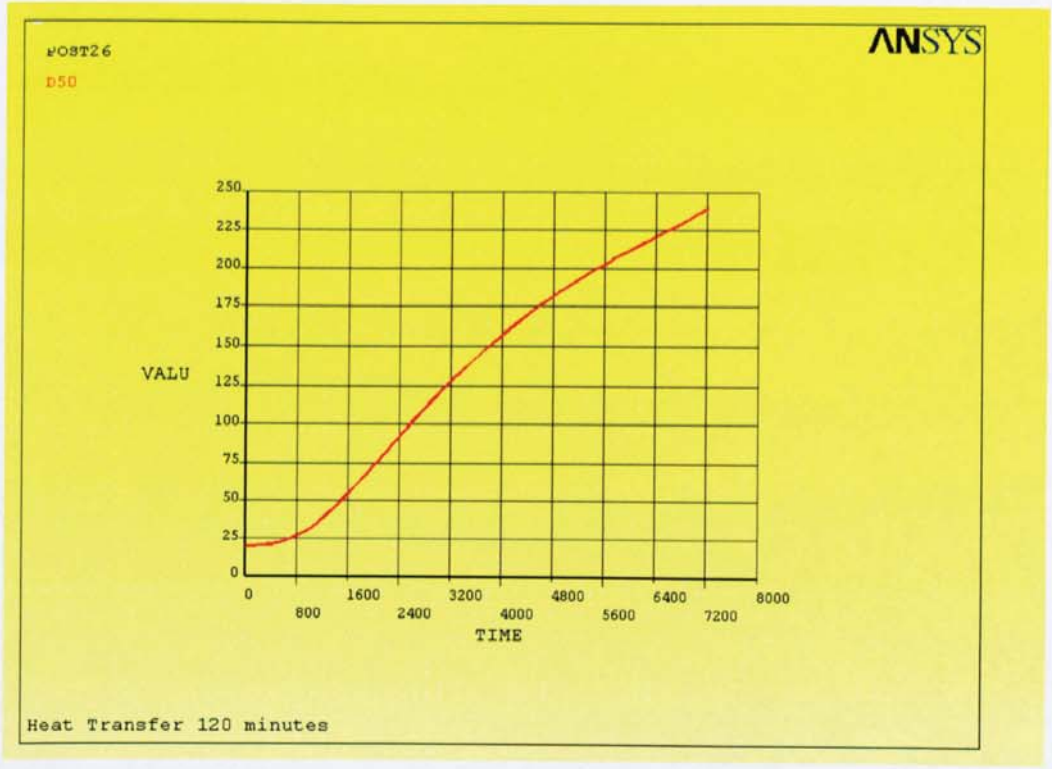

Figure 5.14 Time-temperature at distance 50 mm from concrete surface

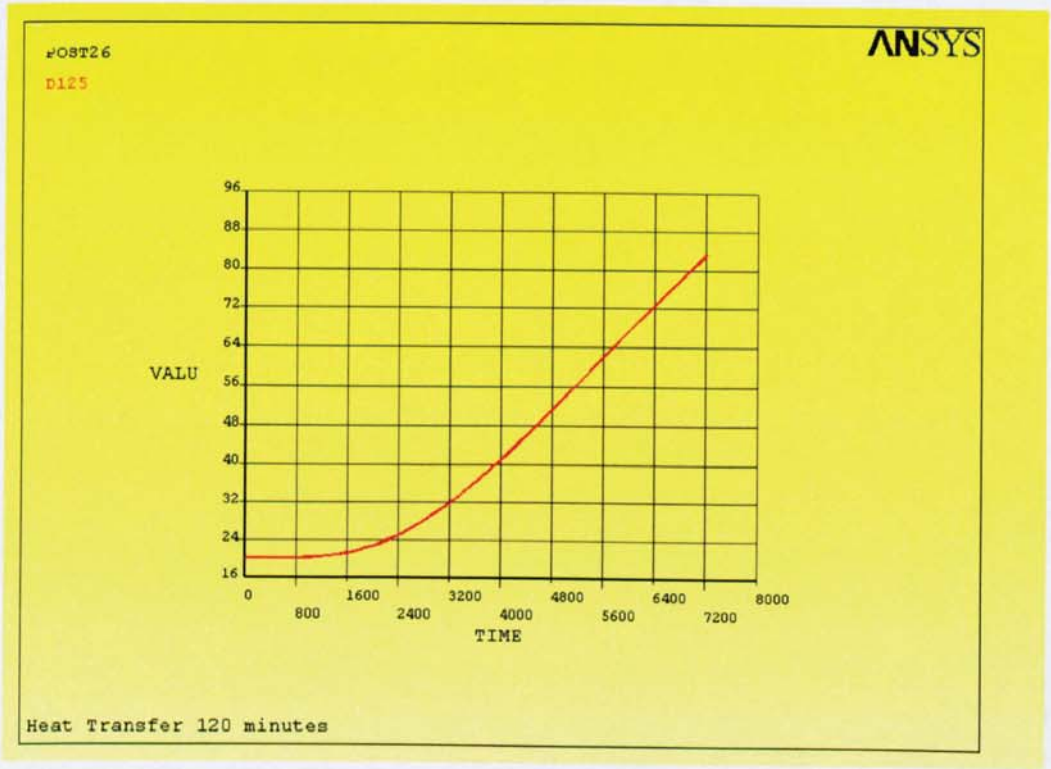

Figure 5.15 Time-temperature at distance 125 mm from concrete surface

Further selected location to be examined in this discussion is 125 mm inside of concrete surface. This location may represent the temperature at mid-depth of the structural element. Shown in Figure 5.15, the temperature at this location remained steady at its ambient temperature until 20 minutes exposed to fire. This means that the fire at the surface has no effect to the mid-depth of concrete element until 20 minutes exposed to fire. After that, the temperature increased linearly and reached about 80°C at the end of 120 minutes.

5.7. The Effect of the Number of Surfaces Exposed to Fire

Temperature distributions within the element at variety number of surface element side exposed to fire have been compared. The comparison of temperature versus distance between one-side and two-side surfaces exposed to fire at 120 minutes duration is presented in Figure 5.16. While Figure 5.17 presents the comparison of two-side and four-side. The distance from fire surface denotes location from a middle element surface crossing the element at X direction. Therefore, the distances were normal from left or right hand side surface only.

In Figure 5.17, the temperature's curve of four-side is symmetric exactly in the middle of the element, while the temperature's curve of two-side continuing drops since there was no fire exposed at the opposite surface. It is evident that the temperature distribution of a surface in the centre of normal direction is not affected by the temperature from exposing fire at another side. This indicates that the temperature distribution through normal direction from one surface is not affected by temperature distribution from another surface.

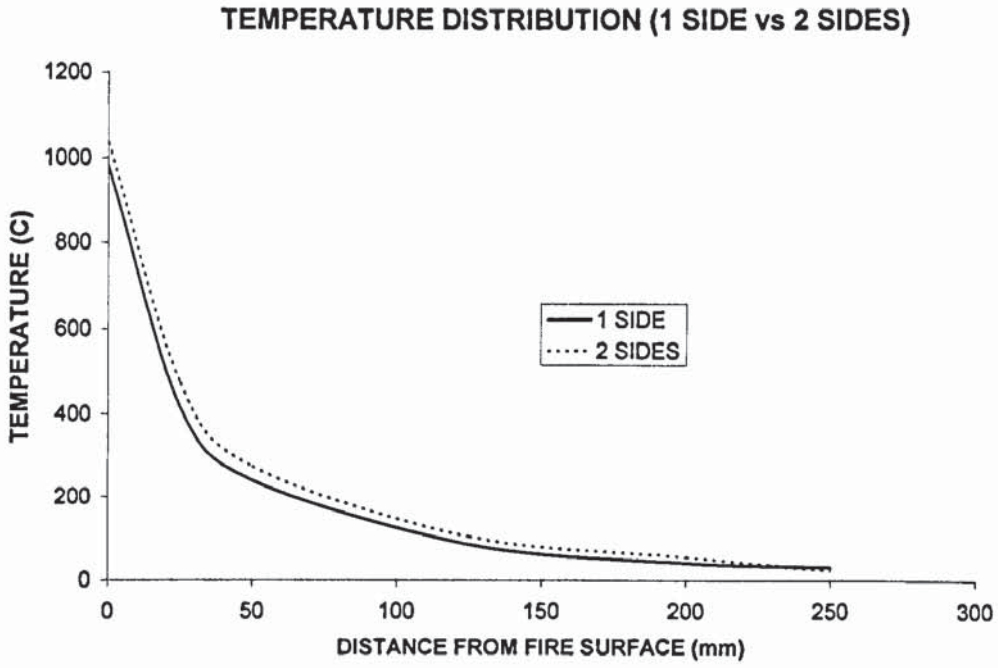

Figure 5.16 Temperature vs. distance of one-side and two-sides surfaces at 120 minutes exposed to fire

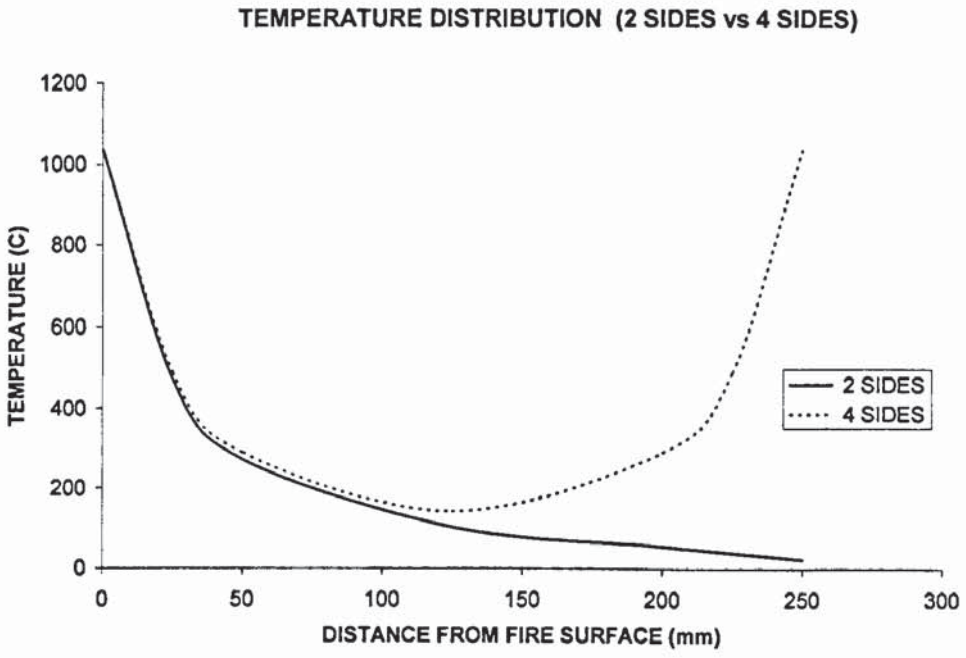

Figure 5.17 Temperature vs. distance of two-sides and four-sides surfaces at 120 minutes exposed to fire

5.8. The Effect of the Duration Exposed to Fire

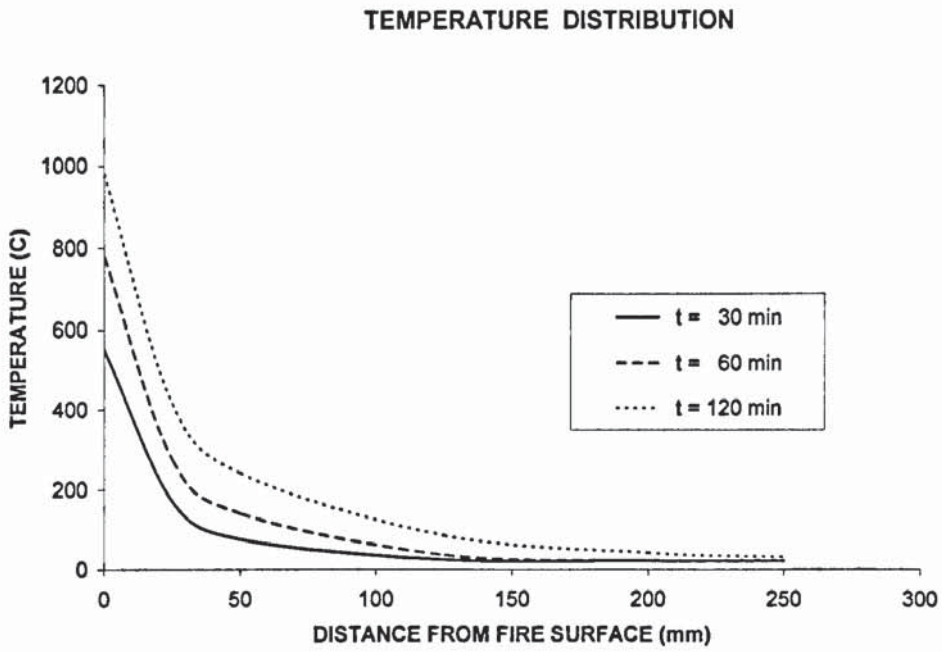

Figure 5.18 Temperature vs. distance in the variety of exposed fire duration

The temperature distributions as a function of the distance from the fire exposed surface at times t = 30 minutes, t = 60 minutes, and t = 120 minutes is shown in Figure 5.18. As it is to be expected the temperature rises with time, and for a given time, decreases exponentially with the distance from the fire exposed surface. The temperature within cross-section of the element remain 20°C at distances 150 mm, 160 mm and 250 mm from the fire surface for the fire durations of 30, 60, and 120 minutes, respectively.

The result simulated by ANSYS presented in Figure 5.18 has a good agreement with the publication by ISE and Concrete Society (1978) especially for normal weight concrete members. The isotherms for normal weight concrete member according to ISE and Concrete Society (1978) is presented in Figure 5.19.

Figure 5.19 Isotherms for normal weight concrete according to ISE and Concrete Society (1978)

Again the ANSYS program is evident to predict the general trend of transient thermal analysis and therefore the ANSYS simulations could be adapted to accurately simulate behaviour of concrete frame structure under fire scenario presented in further discussion.

5.9. Summary

The steady-state and transient analyses of temperature distribution within the member of structural element were simulated using ANSYS program and some of the results have been validated satisfactory by finite element analysis. The summary of the examined work are listed in the following:

- The temperature of concrete surface is approximately 10% lower than the atmosphere temperature.
- The temperature within the element remain 20°C at distances 150 mm, 170 mm, and 250 mm from the fire surface for the fire durations of 30, 60, and 120 minutes, respectively. This indicates that concrete is an insulated material.
- The temperature distribution through normal direction from one surface is not affected by temperature distribution from any other surface.
- The agreement between the computed results by ANSYS and the calculated result using finite element analysis as well as experimental results are reasonable. Therefore, the use of ANSYS program can be continued to obtain approximate solutions in variety problems of thermal analysis.

Chapter 6 CONCRETE FRAME UNDER STRUCTURAL AND THERMAL ANALYSIS

6.1. Introduction

Concrete structures are traditionally seen to have a favourable position in building industry with regard to their performance of fire resistance. So that modern concrete structures may often require special consideration for their fire performance. The special consideration may include the ability of building to fulfil its assigned function in the event of fire and the stability of building which providing adequate time for the occupants to escape and for fire fighting. In a large and complex building, this tends to be as more important as evacuation of the occupants to escape the building and fire fighting operations take much longer.

The Institution of Structural Engineers (2003) explained that there are two primary ways of achieving an adequate standard of fire safety in building, including the fire performance of structures. First is the simple application of the building codes and standards. The application of the building codes and standards gives little flexibility in the approach and therefore, require only a limited engineering approach. Secondly is there a fire safety engineering solution which requires greater skills involving the analysis, risk assessment and engineering judgement. The second way gives greater design flexibility to achieve a particular performance of the building.

This section is mainly concerned with the performance of concrete frame structures when exposed to localised fire scenarios. Special attention will be given to the fire test on the Cardington concrete frame structure. Preliminary analysis of the

Cardington concrete frame prior to the test carried out by a research group at Aston University will be presented and a simplified model of fire compartment subsequent to the test will be discussed. From the simplified model, load carrying mechanism of concrete frame will be identified and several design implications of the investigation will be discussed.

6.2. Preliminary Analysis of Cardington Test Frame

Led by Dr. Purkiss, a preliminary analysis of Cardington test frame was carried out at the School of Engineering and Applied Science, Aston University, prior to the fire test. For the initial analysis, it was decided to take a series of "snap-shot" analyses without attempting to model transient strain effects during the growth phase. This is likely to be conservative as no allowance is made for redistribution of internal forces due to transient effects. The decay phase was not modelled. The whole frame structure was analysed using both ANSYS and ALGOR. Both codes provide almost the same results and therefore only one of them is presented here.

Preliminary calculations from BCA indicated that the planned compartment fire had an equivalent fire endurance of around one hour. This figure has therefore been adopted. It was then decided to examine performance at 7.5, 15, 30, 45 and 60 minutes. However, when the 45 minutes results were compared with the room temperature results, there was no significant difference. Therefore, one room temperature case, three uniform compartment temperature cases, and one non-uniform temperature distribution case have been taken on this investigation.

6.2.1. Finite Element Model

All columns and the first floor slab of the seven story building are modelled using 3-D solid elements while the remainder slabs in other six floors were modelled using plate elements. The reason for this is because the temperature is defined at each node and in order to simulate the temperature gradient between the fired compartment and adjacent rooms the 3-D solid element has to be used. The detailed element mesh for the whole frame structure (140 columns and 84 slabs) is shown in Figure 6.1. The element of the frame has dimensions of 400 x 400 mm for internal columns, 250 x 400 mm for external columns, and 250 mm slab's thickness.

The material properties were assumed that the structure has a concrete density of ρ_c = 2450 kg/m^3, Young's modulus of E_c = 32 GPa (for room temperature), Poisson's ratio υ = 0.2, and thermal expansion of $\varepsilon_{th,c}$ = 12x10^{-6} per °C. It was also assumed that the concrete behaves like a linear material. Reinforcement was not considered in the model. The applied loads were acting on each floor, the value of which is 3250 N/m^2. Temperature is as an input parameter, which is defined at each node. For other than the room temperature the Young's modulus of concrete is given in Table 6.1, which is calculated based on those suggested by Purkiss (1996).

In order to match the influence of temperature on the Young's modulus, eleven different materials are used, ten of which are used to describe the nine columns and four first floor slabs in the fired compartment, and one is used for all of the remainder columns and slabs. The boundary conditions of the ground floor columns are assumed to be ideally fixed.

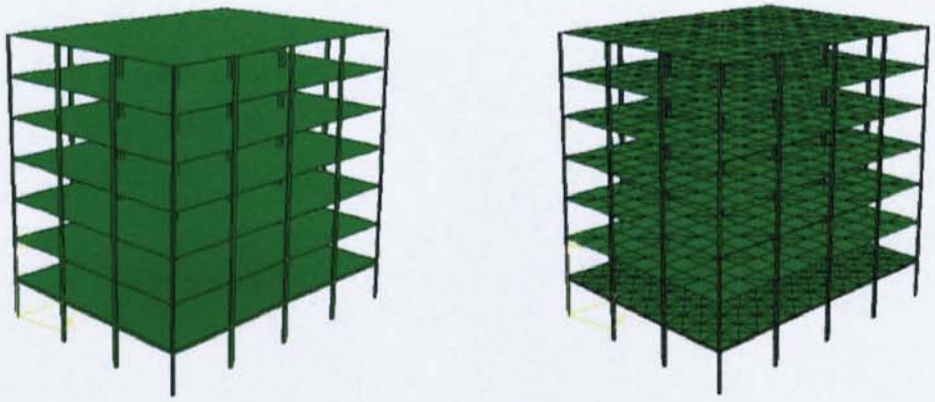

(a) Frame structure (b) Finite element mesh

Figure 6.1 Severn-story frame structure and corresponding fine element mesh

Temperature (°C)	Young's modulus (GPa)	Reduction factor
20	32	1.0
200	24	0.75
400	14.4	0.45
600	12	0.375

Table 6.1 Young's modulus of concrete for different temperature

6.2.2. Finite Element Analysis Results

The stress analyses were carried out for five different temperature distribution cases, in which four cases were assumed to have uniform temperatures (20, 200, 400, 600 °C) and one case is assumed to have a non-uniform temperature distribution in the fired compartment. The detailed results are presented below.

6.2.2.1. Case 1: Room temperature (T=20°C)

In this case all columns and slabs were assumed to have the same room temperature and thus no thermal stress need to be considered. The stress is caused purely due to the applied loads. In order to check the reliability of the proposed finite element model, a full three-dimensional finite element model is also employed. The three-dimensional solid element mesh is shown in Figure 6.2. The comparison of the two models showed that there is almost no difference in the results. This demonstrated that the plate element used for modelling the thick slab is acceptable. The use of plate element, however, can significantly reduce the degrees of freedom of problem and thus the computing cost.

Figure 6.2 Three-dimensional solid element mesh

Figures 6.3 and 6.4 show the maximum and minimum principal stresses in columns and slabs from which we can see the maximum principal stress and the minimum principal stress have almost the same value of 10.5 MPa, which is about 37.5% of the concrete strength (28 MPa, note that the tension stress is assumed to be taken by the reinforcement). The maximum tensile stress is located at the bottom

surface of the slab near to the column whereas the maximum compressive stress is located at the bottom of the ground floor columns.

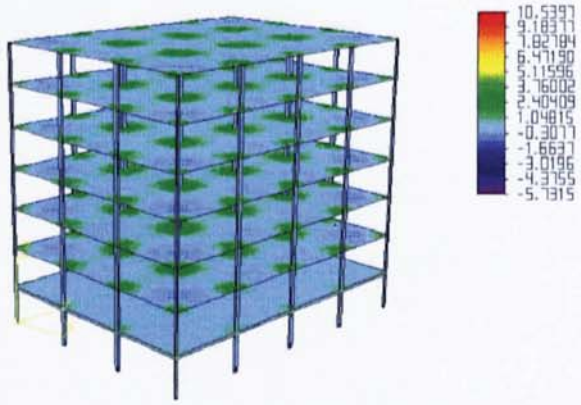

Figure 6.3 Distribution of the maximum principal stress (MPa)

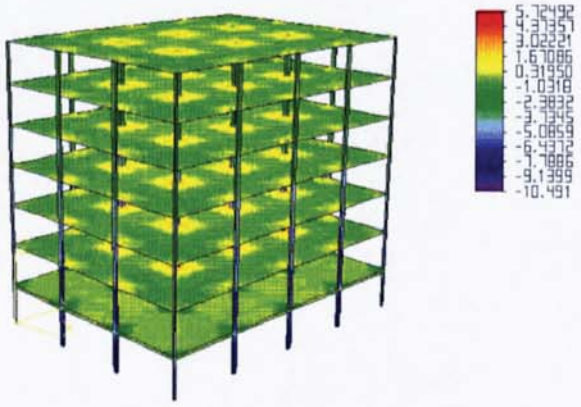

Figure 6.4 Distribution of the minimum principal stress (MPa)

Figure 6.5 shows the stress in z-direction. As it can be seen, for slabs, no matter what elements (solid or plate elements) are used, the z-direction stresses are always negligible. For columns, the axial compressive stress is dominant and the maximum compressive stress for the ground floor column (9.6 MPa) is very close to the minimum principal stress. The deformed shape of the structure subjected to the assumed

distributed loads is displayed in Figure 6.6, the maximum deflection is found in the top floor in which the value is 5.3 mm.

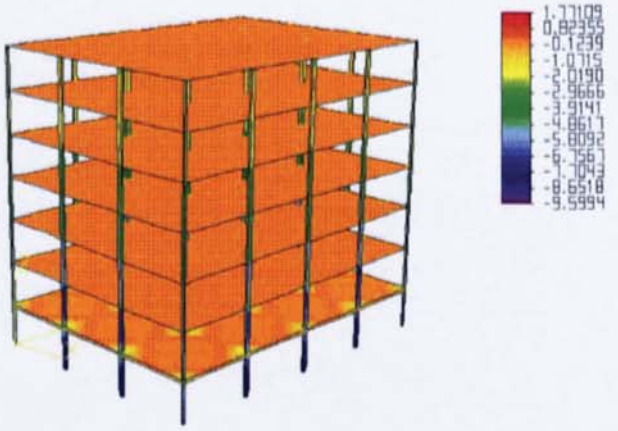

Figure 6.5 Distribution of the stress in z-direction (MPa)

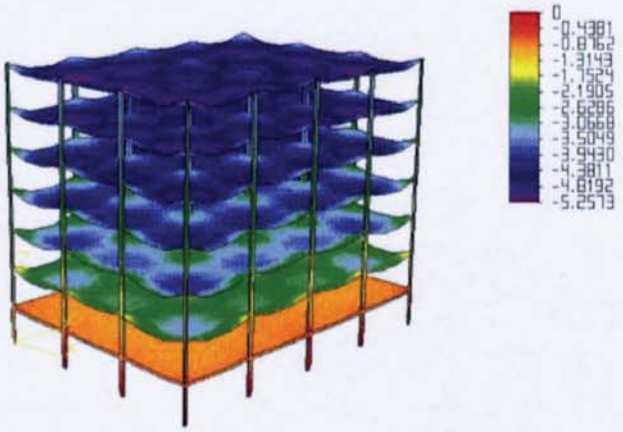

Figure 6.6 Distribution of the vertical displacement (mm)

6.2.2.2. Case 2: Firing compartment temperature (T=600°C)

In this case the temperature in the fired compartment is assumed to be 600°C and thus the surface temperature of columns and slabs exposed to the fired compartment is also 600°C; whereas all others are assumed to have a room temperature (20°C). Also, as the thickness of the slab is relatively high, it is unlikely the temperature will rise on the mid-plane of the slab during the first hour. Therefore the temperature distribution along

the cross-section of the slab is assumed to vary linearly from the bottom surface (600°C) to mid-plane (20°C) and for the upper half thickness slab the temperature is assumed with the room temperature.

For columns, however, since they are exposed to fire on more than one surface, the temperature distribution is assumed to be uniform within the whole section, as this may provide a worst case. The material properties (only the Young's modulus) are assumed to be temperature-dependent, which, again, are taken as a worst case (that is, if an element has different temperatures at its eight nodes, the material properties of this element will be taken as those related to the highest temperature).

Figures 6.7 and 6.8 show the maximum and minimum principal stresses in the columns and slabs. It is interesting to notice that, the influence of the temperature on the maximum principal stress seems to be small comparing to the minimum principal stress. With comparing to the reduced strength of the concrete material owing to the high temperature, it seems that the structure would not collapse at this stage.

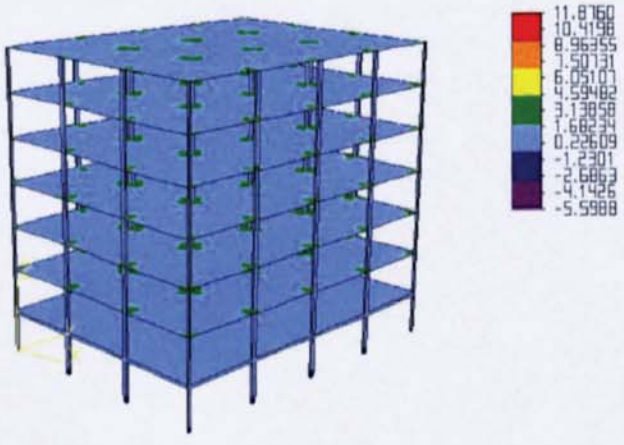

Figure 6.7 Distribution of the maximum principal stress (MPa)

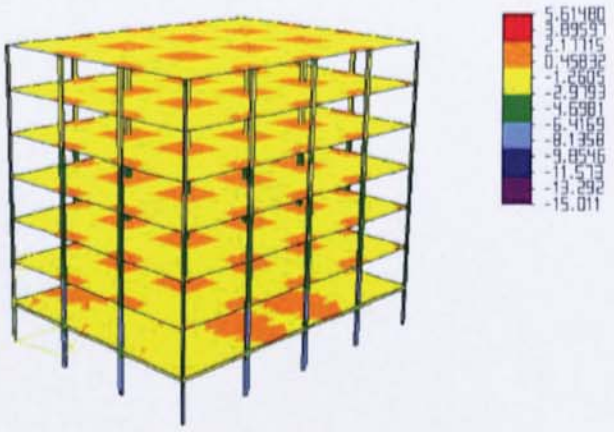

Figure 6.8 Distribution of the minimum principal stress (MPa)

Figure 6.9 shows the z-direction stress. As is expected, the maximum stress is located in the bottom of the ground floor columns, the value of which is close to the minimum principal stress. The stresses in x- and y-directions for the first floor slab are shown in Figures 6.10 and 6.11. Compared with the z-direction stress these two stresses are rather small. This indicates that if the structure were to collapse the columns would fail first assuming there is no spalling with slab strength reduction.

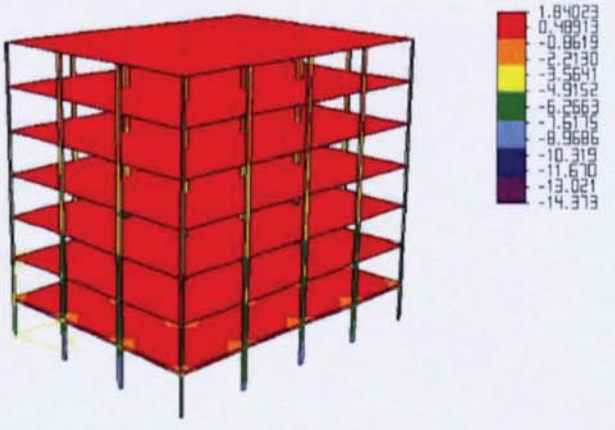

Figure 6.9 Distribution of the stress in z-direction (MPa)

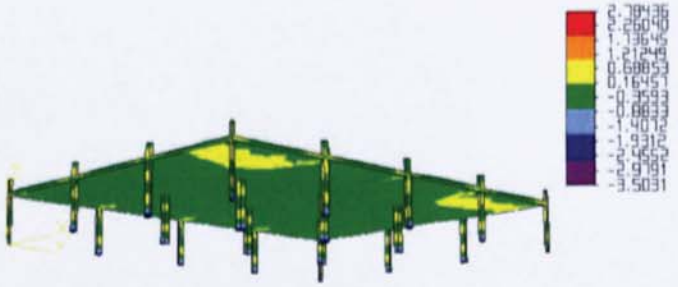

Figure 6.10 Distribution of the stress in x-direction (MPa)

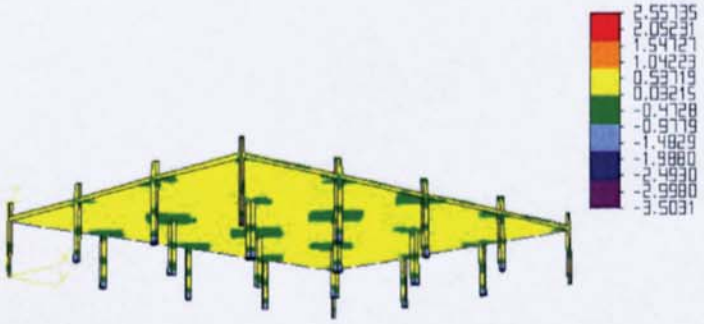

Figure 6.11 Distribution of the stress in y-direction (N/mm^2)

The vertical displacement of the structure is shown in Figure 6.12 consist of (a) vertical displacement for whole structure in mm, and (b) vertical displacement of the first floor slab. The maximum displacement is found of 6.33 mm in top floor.

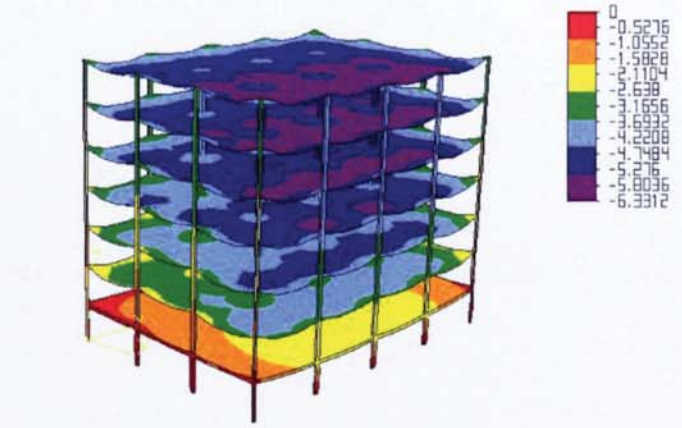

(a) Whole structure (mm)

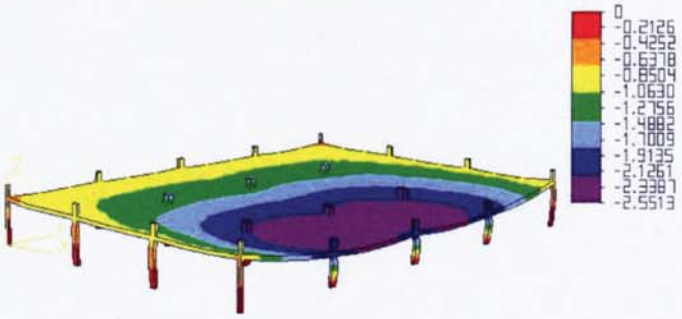

(b) The first floor slab (mm)

Figure 6.12 Distribution of vertical displacement for the whole structure and the first floor slab

6.2.2.3. Case 3: Non-uniform temperature distribution in fired compartment

In this case the temperature distribution in the fired compartment is assumed to be uniform in the vertical direction but non-uniform in the horizontal plane. The surface temperatures of the nine columns in the fire compartment are shown in Figure 6.13 and the lower surface temperature of the four slabs are assumed to be identical of 555°C. This assumed temperature distribution in the compartment is approximated to the firing time of 45 minutes.

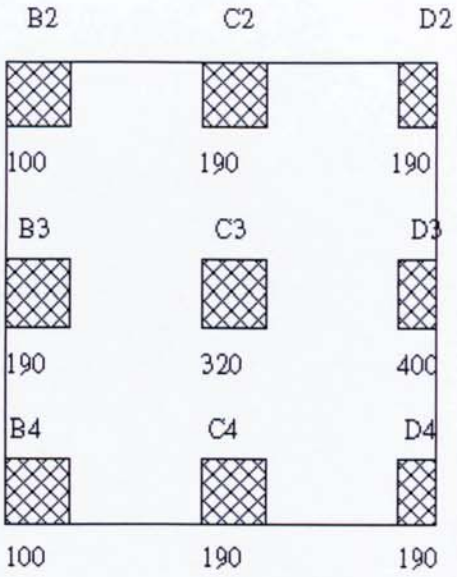

Figure 6.13 Temperature distributions in the fired compartment (^{o}C)

The maximum principal stress and minimum principal stress in the columns and slabs show in Figures 6.14 and 6.15, respectively. It can be seen that both the maximum and minimum principal stresses are almost the same as those in case one (room temperature case). This indicates that the temperature does not cause significant thermal stress.

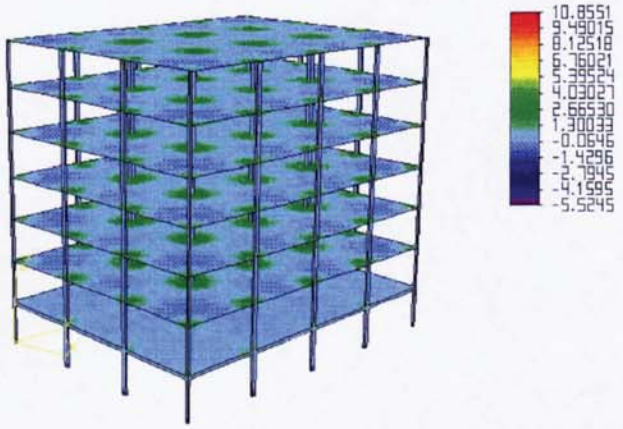

Figure 6.14 Distribution of the maximum principal stress (MPa)

Figure 6.15 Distribution of the minimum principal stress (MPa)

The horizontal z-direction stress and z-direction displacement are shown in Figures 6.16 and 6.17, respectively. Again, comparing to those shown in case one, insignificant differences are found between these two cases. Therefore, these results could be confirmed as another indication that the temperature does not cause significant thermal stress in this case.

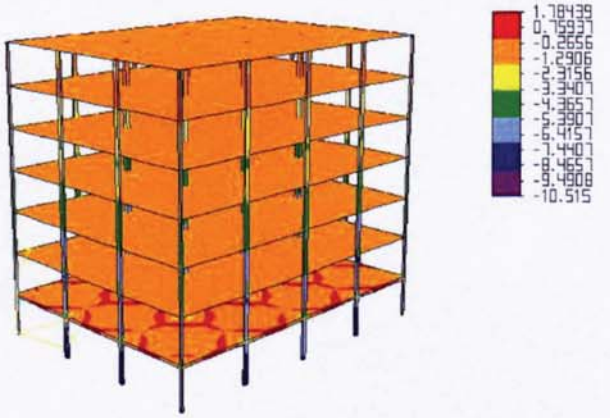

Figure 6.16 Distribution of the stress in z-direction (MPa)

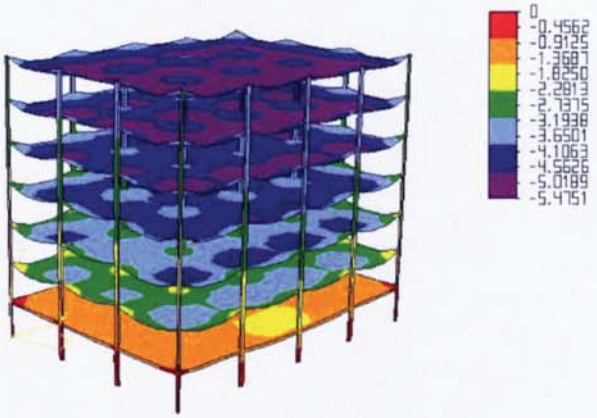

Figure 6.17 Distribution of vertical displacement (mm)

6.2.2.4. Other cases (T=200°C and T=400°C)

The analysis models for these two cases are similar to that in case 2 except for the surface temperature reduce and the Young's modulus increases. The results of these two cases are found to be lie between those in case 1 and 2. Therefore they are not being discussed further here.

6.2.3. Analysis with Transient Strain

In this analysis the constitutive model proposed by Li and Purkiss (2005) is employed because this simple constitutive model can easily be incorporated into various commercial finite element analysis codes. As described in the previous, Li and Purkiss (2005) developed an empirical formula based on the plotted results of the average Young's modulus. The normalized stress-strain curve with transient strain included is presented in Figure 6.18.

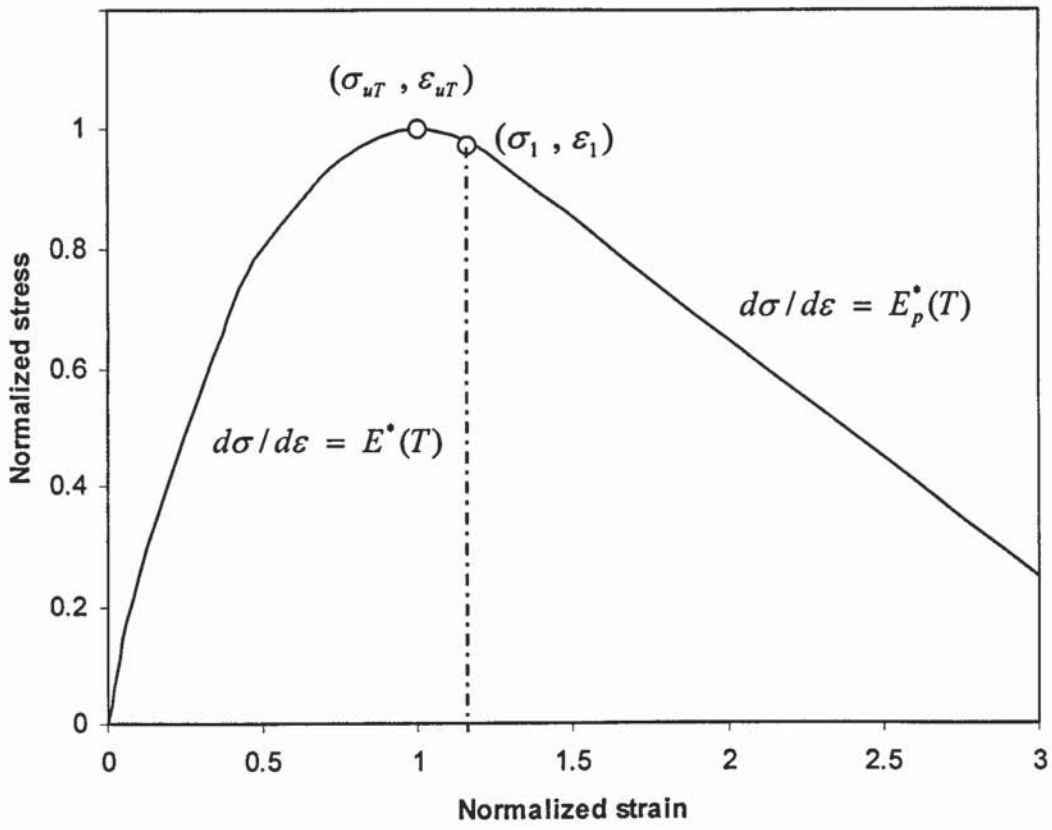

Figure 6.18 Normalized stress-strain curve with transient strain included

Temperature-dependent of Young's modulus in the elastic ranges are suggested in the following equations:

$$E^*(T) = E_0 \exp\left[-\frac{(T-20)^{0.65}}{25}\right]$$

For the Young's modulus in the plastic range the following equation is recommended:

$$E_p^*(T) = E_0^- \exp[k_p (T-20)^{2.15}]$$

Where: E_0 = initial Young's modulus, $E_0^- = -0.045 E_0$, and $k_p = 10^{-6}$.

It is important to consider transient strains in the analysis involving concrete in compression. However, when the exposure temperature is not high, the influence of the

transient strain may not be significant. Therefore, only the Case 2 of the above analysis, where the temperature in the fired compartment is assumed to reach 600°C, will be presented with transient strains included.

Figure 6.19 and 6.20 show the maximum and minimum principal stresses in column and slabs. The value of the maximum tensile stress occurred at the slab near to the column is 14.27 MPa. Since the tension stress is assumed to be taken by steel reinforcement, the attention will be given only to the distribution of compressive stress. In this case the maximum compressive stress of – 22.99 MPa occur at the bottom of the ground floor columns while the maximum compressive stress of the concrete slab of -18.32 MPa was found.

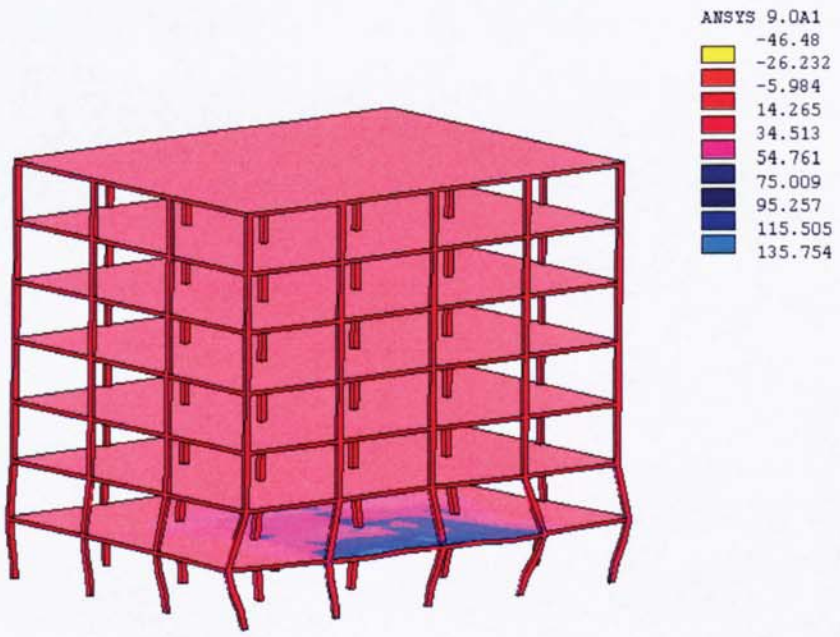

Figure 6.19 Distribution of the maximum principal stress (MPa)

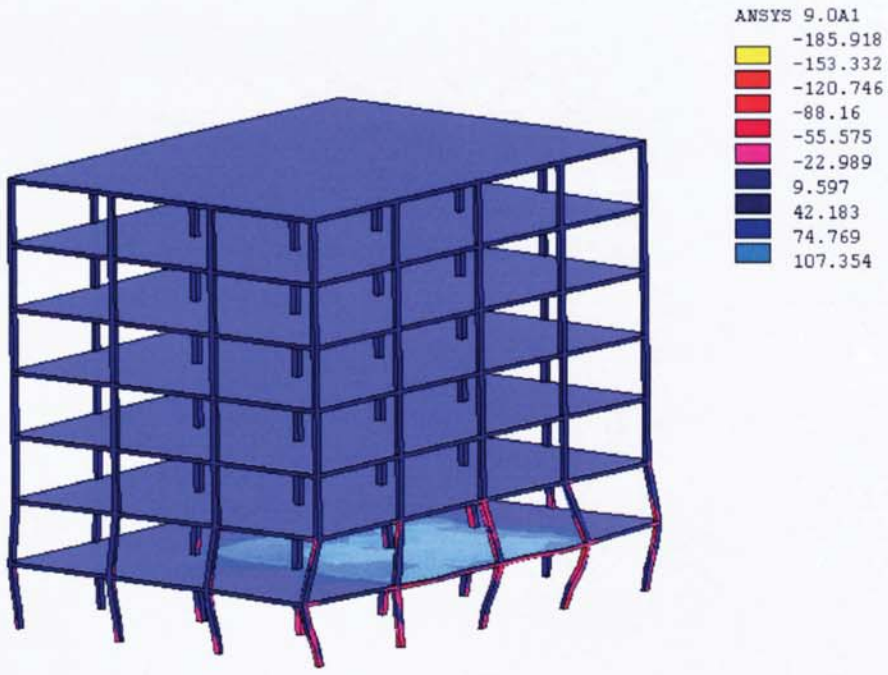

Figure 6.20 Distribution of the minimum principal stress (MPa)

Distribution of the stress in horizontal (z-direction) is presented in Figure 6.21. As is expected, the maximum compressive stress is located at the bottom columns of the ground floor. The value of -21.02 MPa is found in which is close to the minimum principal stress. The stresses in horizontal direction perpendicular to the fire compartment (x-direction) and vertical (y) directions are not presented here since the values of both directions of stresses are small compared to the z-direction stress.

Figure 6.21 Distribution of the stress in horizontal (z) direction (MPa)

The horizontal displacement in z-direction and vertical displacement of the structure are shown in Figure 6.22 and 6.23, respectively. Significant horizontal displacements are occurred to the heating slab mainly due to thermal expansion of the floor slab. The horizontal movement of the slab caused a maximum lateral displacement of 31.88 mm to the external columns of the ground floor. The horizontal displacement of 7.67 mm is also found to the unexposed fire external column at the opposite side. This large lateral displacement is significant and can not be ignored in design. A designer should be aware and ensure that the columns can withstand any significant lateral displacement during fire. On the other hand, vertical displacements of the structure are relatively low. The maximum vertical displacement of 8.52 mm is found in the middle of the concrete slab. So, its can be ignored and would not be concerned here.

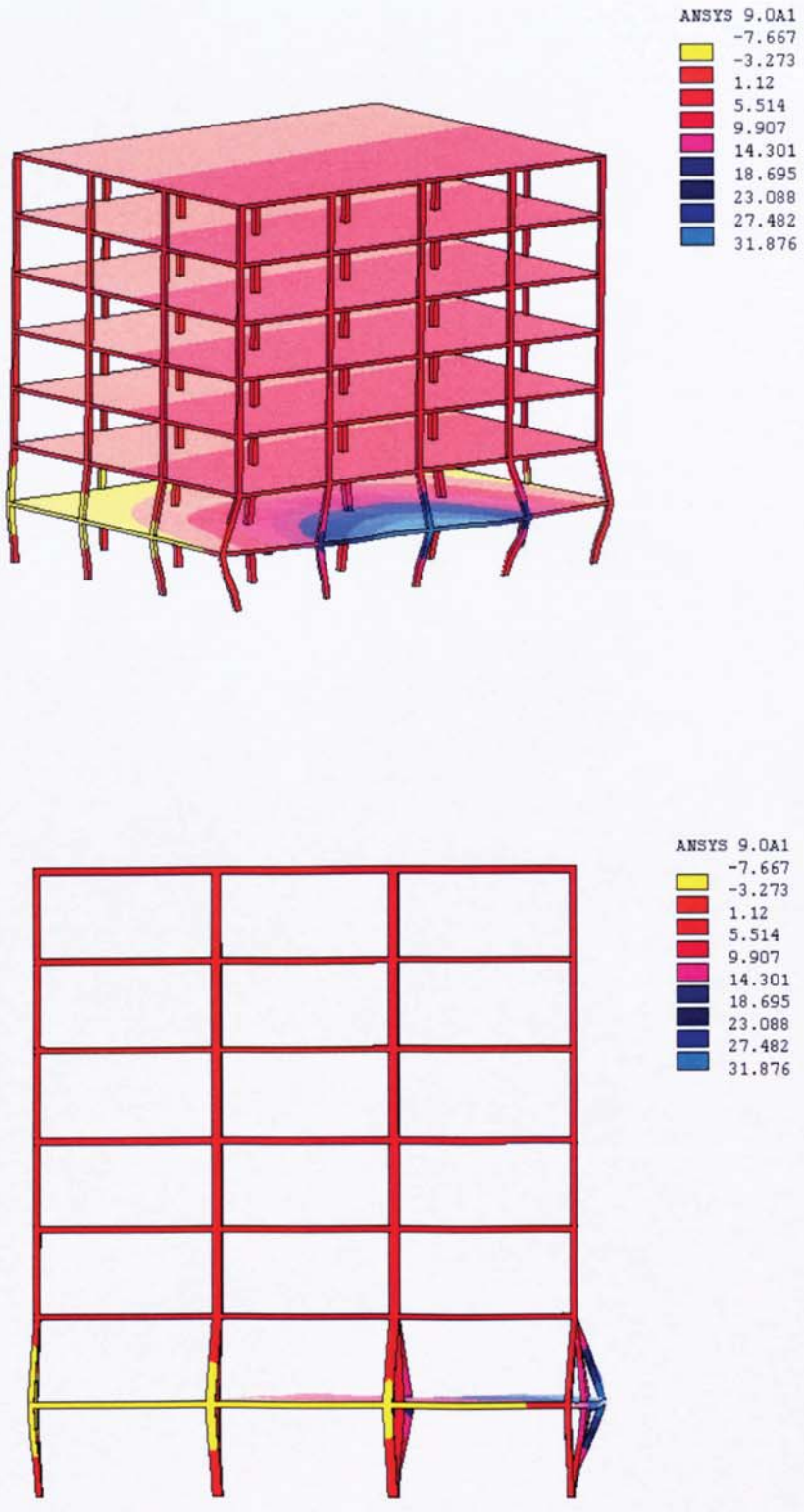

Figure 6.22 Horizontal displacement of the structure in z-direction (mm)

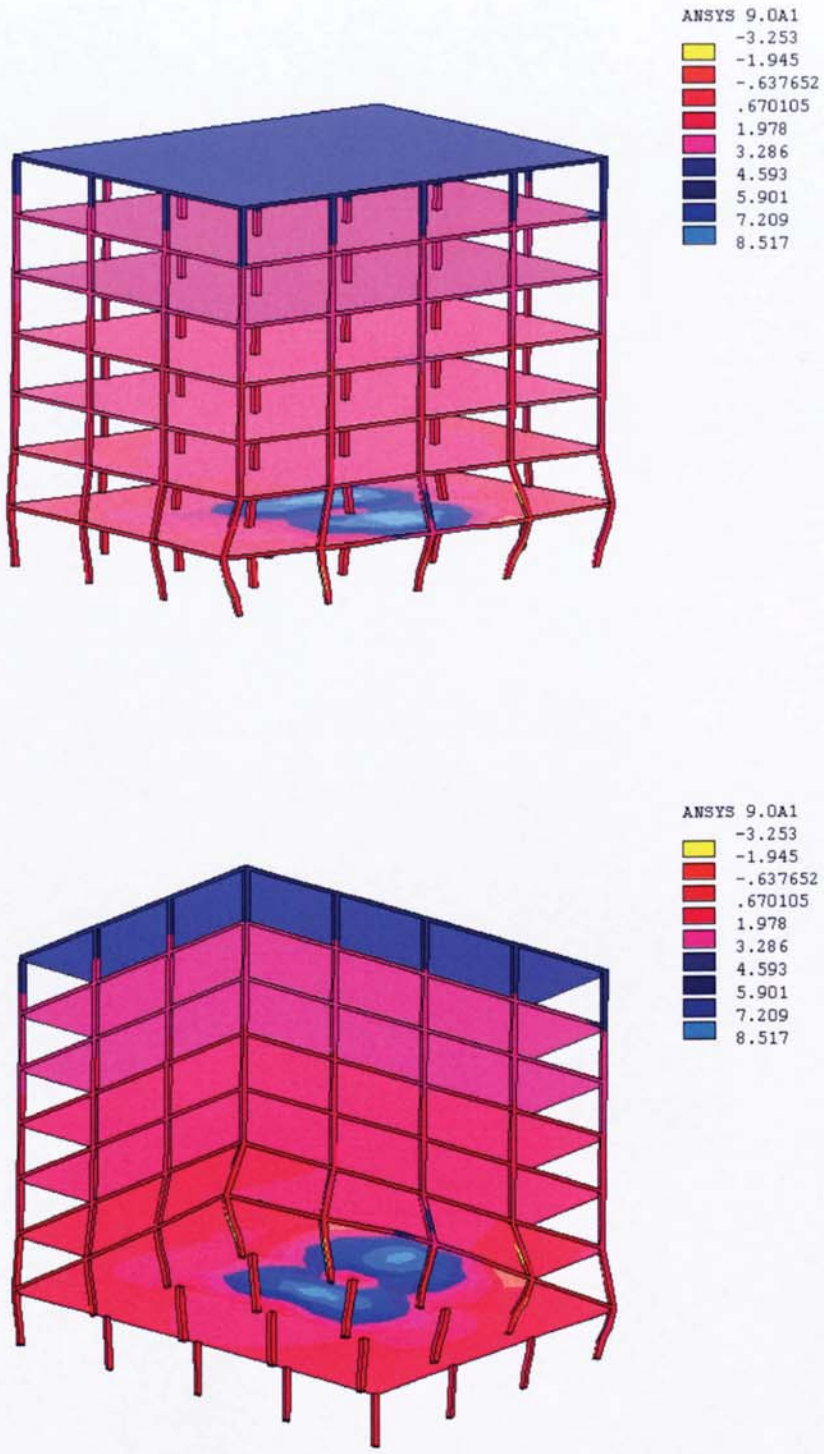

Figure 6.23 Vertical displacement of the structure in y-direction (mm)

6.2.4. Comparison of the analyses with and without transient strains included

The result of the analyses with and without transient strain included is presented in Table 6.2.

Temp	Without Transient	With Transient
20°C	Max compressive stress: 10.5 MPa	N/A
	Max tensile stress: 10.5 MPa	N/A
	Vertical displacement: 5.26 mm	N/A
600°C	Max compressive stress: 15.01 MPa	Max compressive stress: 22.99 MPa
	Max tensile stress: 11.88 MPa	Max tensile stress: 14.28 MPa
	Vertical displacement: 6.33 mm	Vertical displacement: 8.52 mm
	Horizontal displacement: 5.48 mm	Horizontal displacement: 31.88 mm

Table 6.2 Comparison of the results with and without transient strains included

Comparison of the different results between the first analysis (without transient strains) and the second analysis (with transient strains included) can be described as follows:

- Maximum compressive stress is increased about 153% from 15.01 MPa at the first analysis to 22.99 MPa at the second analysis. This significant increased can not be ignored in design. So, designers are encouraged to include transient strains in the thermal analysis especially for structures exposed to fire at high temperature $\geq 600°C$.
- The temperature distribution assumption in the first analysis where along the cross-section of the slab is change linearly from 600°C at the bottom plane (the fire

surface) to 20°C at the mid-plane and then steady at 20°C for the whole upper half slab's thickness was not right. In the second analysis, the temperature distribution was not changed linearly and the temperature distribution started steady to 20°C at about 170 mm from the fire surface. This dissimilar temperature distribution resulted significant different in lateral displacement of external columns from 5.48 mm at the first analysis to 31.88 mm at the second analysis. This significant different caused predominantly by thermal expansion of the heated slab. Therefore, the effects of thermal expansions of the slabs at high temperatures were very significant and can not be ignored in design.

- The vertical displacements and the maximum tensile stresses were not gave significant different in both analyses. The vertical displacement were considered very small thus will not be concerned here as well as the maximum tensile stresses since the most tensile stresses are assumed to be carried by steel reinforcement.

6.3. Modelling of Frame Structure from Fire Compartment

The fire tests at Cardington generated valuable data to evaluate the effect of real fires on large-scale structures. The data of this work could be used by researchers to predict the behaviour of concrete frame structures under fire conditions using Finite Element models. In this discussion, a concrete frame model of fire compartment is considered as a substructure of the seven-story Cardington concrete building. The central frame as a substructure of the whole building viewing both from the front direction and the top direction are shown in Figure 6.18 and Figure 6.19, respectively. The frame model consists of four columns connected together with a continues-beam as a replacement of concrete floor slab of the first floor.

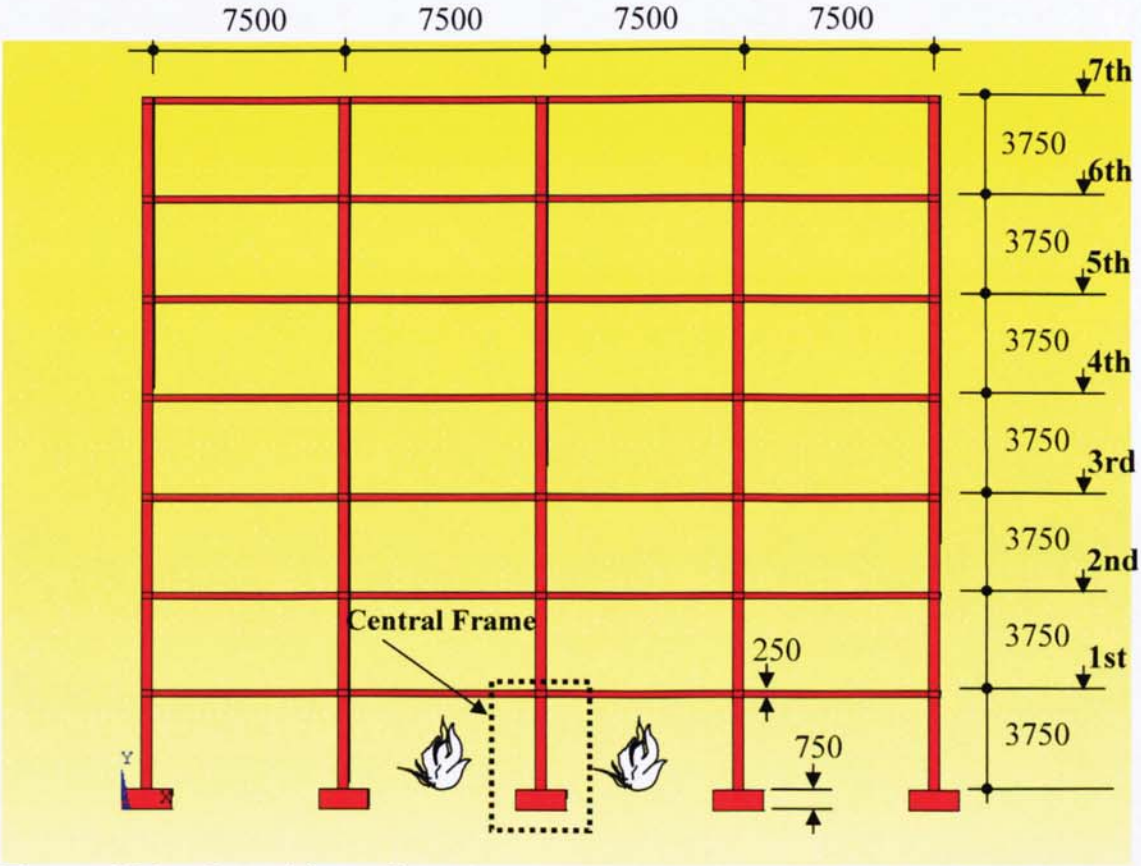

Figure 6.24 Central frame from the whole building viewing from the front direction

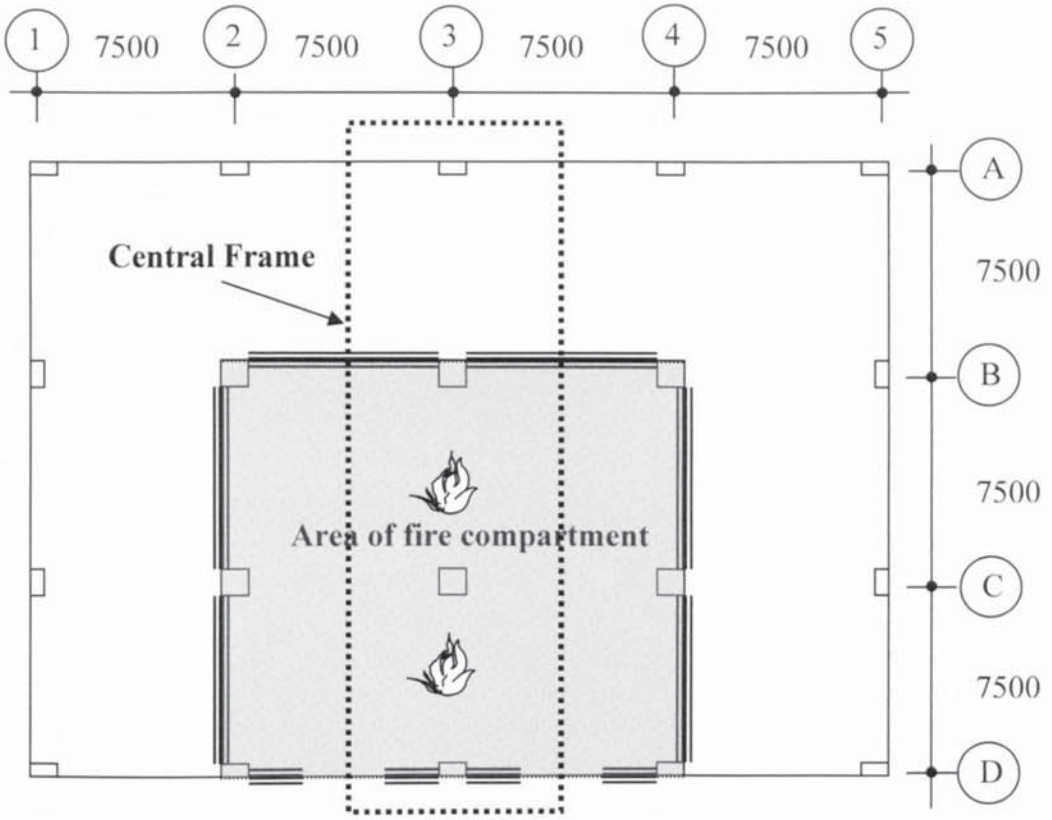

Figure 6.25 Central frame from the whole building viewing from the top direction

6.3.1. Concrete Frame

The frame model constructed of normal-strength reinforced concrete continuous beam and high-strength reinforced concrete columns. The frame is assumed to be fixed at the bottom of all columns while the top of columns can move horizontally both in the X and Z and vertically in the Y directions. The frame has 4.00 m height and 21.50 m length which divided by four columns with the distance of each column is 7.50 m. Dimension of the element at concrete frame model in 3-D is illustrated in Figure 6.20.

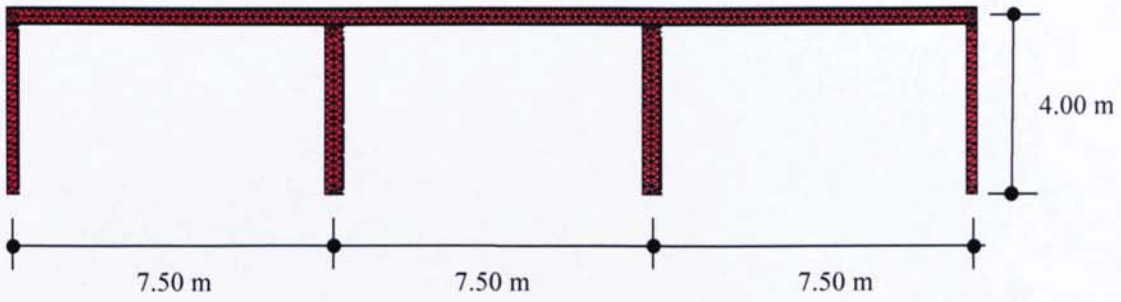

Figure 6.26 Dimension of the concrete frame model

Similar to the Cardington building, the internal columns have dimension of 0.40 x 0.40 m and the external columns of 0.25 x 0.40 m. The dimension of 0.40 m x 0.40 m for the beam is chosen in order to match the performance of the slab behaviour. To represent the steel-reinforcement, pairs of 0.01 m thick of steel have been layered longitudinal within the beam and vertical within the internal columns, and the 0.006 m thick are layered within the external columns. The steel layers have been positioned at the distance of 0.04 m from both sides of the top and bottom concrete surfaces. The 0.04 m distances from concrete surfaces represent the concrete cover to the reinforcement. The dimensions of steel layer were used so that the reinforcement ratio of concrete were not exceed to the maximum specified (4%) in the British Standard. The cross sections of the beam and columns are shown in Figures 6.21, 6.22 and 6.23, respectively.

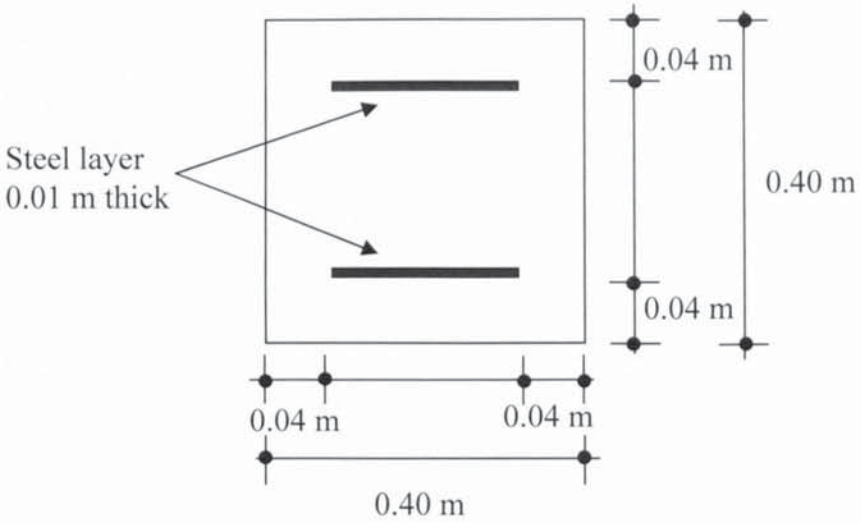

Figure 6.27 Cross section of the beams

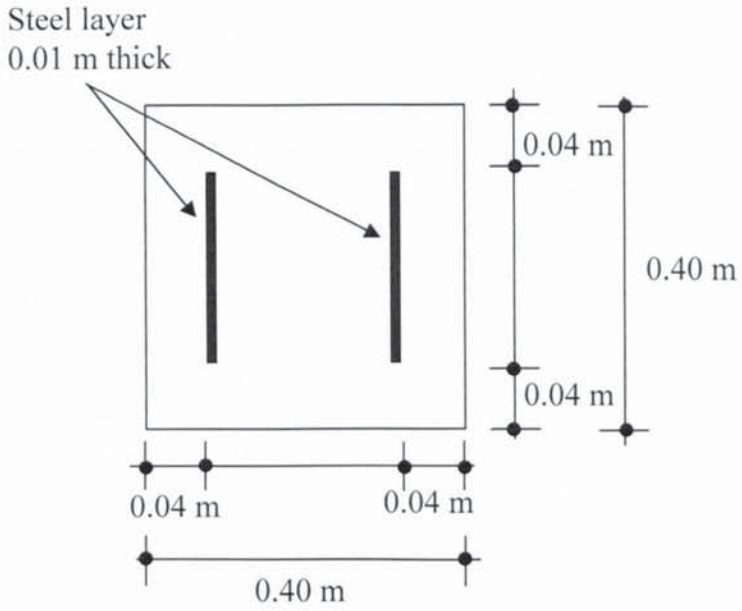

Figure 6.28 Cross section of the internal columns

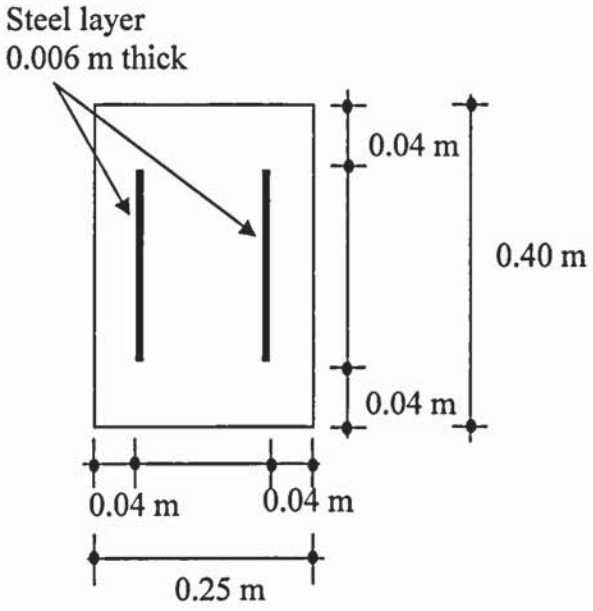

Figure 6.29 Cross section of the external columns

The use of the layered steel instead of steel reinforcement in thermal case is due to convenience in the model analysis used. Bending direction of the layered steel will have same results obtained from the steel reinforcement. The temperature distribution throughout the element will have little different between the layered steel and the reinforcement, but the effect can be considered minor.

6.3.2. Materials Properties

6.3.2.1. At elevated temperature

Similar to the BRE concrete building, the beam is constructed using normal-strength concrete with compressive strength of 61 MPa and all columns are high-strength concrete with compressive strength of 103 MPa. The density of the concrete can be assumed as 2400 kg/m^3 for normal strength and 2450 kg/m^3 for high-strength concrete.

All concrete members have Poisson's ratio (υ) of 0.2 at room temperature and the values of enthalpy and emissivity can be assumed as1.0 and 0.6, respectively.

The temperature dependant of the materials properties of concrete can be determined as follows:

- Specific heat in unit J/kg°C: $c_c = 900 + 80\left(\frac{T_c}{120}\right) - 4\left(\frac{T_c}{120}\right)^2$

As suggested by ENV 1994-1-2 Part 1.2 an additional specific heat will be included to the base value of dry concrete of $c_{p,dry} = 950$ J/kg°C at temperature 100°C and 200°C.

- Combined convective-radiation heat transfer coefficient:

  $\alpha = \alpha_c + \sigma . e . [(T + 273) + (T_\infty + 273)] [(T + 273)^2 + (T_\infty + 273)^2]$

  Where: α_c is the convective heat transfer coefficient; σ is Stefan-Boltzmann constant (5.67 x 10^{-8} W/m^{2}K^4); e is the emissivity; T is surface temperature and T_∞ is the temperature of surrounding environment, both T and T_∞ are in °C.

- Isotropic thermal expansion:

  $\varepsilon_{th,c} = 1.8\times10^{-4} + 9\times10^{-6}T_c + 2.3\times10^{-11}T_c^{\,3}, \qquad 20 \le T_c \le 700\,°C$

  $\varepsilon_{th,c} = 1.4\times10^{-4}, \qquad T_c \ge 700\,°C$

- Thermal conductivity in W/m°C:

  $\lambda_c = 2.2 - \frac{1.2\,T}{150}, \qquad T \langle 150\,°C$

  $\lambda_c = 1 - \frac{0.8\,(T - 150)}{550}, \qquad 150 \le T \le 700\,°C$

  $\lambda_c = 0.2, \qquad T \rangle 700\,°C$

The steel reinforcements have characteristic strength (f_y) of 460 MPa, density of 7850 kg/m^3 and Poisson's ratio (υ) of 0.3 at room temperature. The temperature dependant of the material properties of steel reinforcement can be determined from the following equations:

- Specific heat (J/kg°C):

$$c_s = 425 + 7.73\times10^{-1}T_s - 1.69\times10^{-3}T_s^{\ 2} + 2.22\times10^{-6}T_s^{\ 3}, \quad 20 \le T_s \le 600\,°C$$

$$c_s = 666 - \frac{13002}{T_s - 738}, \quad 600 \le T_s \le 735\,°C$$

$$c_s = 545 - \frac{17820}{T_s - 731}, \quad 735 \le T_s \le 900\,°C$$

$$c_s = 650, \quad 900 \le T_s \le 1200\,°C$$

- Isotropic thermal expansion, $\Delta l/l$:

$$\varepsilon_{th,s} = -2.416 \times 10^{-4} + 1.2 \times 10^{-5}\, T_s + 0.4 \times 10^{-8}\, T_s^{\ 2}, \quad 20 \le T_s \le 750\,°C$$

$$\varepsilon_{th,s} = 11 \times 10^{-3}, \quad 750 \le T_s \le 860\,°C$$

$$\varepsilon_{th,s} = -6.2 \times 10^{-3} + 2 \times 10^{-5} T_s, \quad 860 \le T_s \le 1200\,°C$$

- Thermal conductivity, W/m°C:

$$\lambda_s = 54 - 3.33x10^{-2}T_s, \quad T_s \le 800\,°C$$

$$\lambda_s = 27.3, \quad T_s > 800\,°C$$

The relative strengths and Young modulus of steel reinforcement at various temperatures can be obtained from Table 3.2 of ENV 1993-1-2 where the linear interpolation have been used for intermediate values between the tabulated temperatures.

6.3.2.2. At cooling phase

In this case the fired compartment are analysed under condition after cooling down to the ambient temperature of 20°C. The residual strength assessment of an element of a structure can be derived from specimens heated and cooled with no pre-load as this will be conservative. Typical residual strengths of concrete with temperature from Purkiss (1985) is plotted in Figure 6.24.

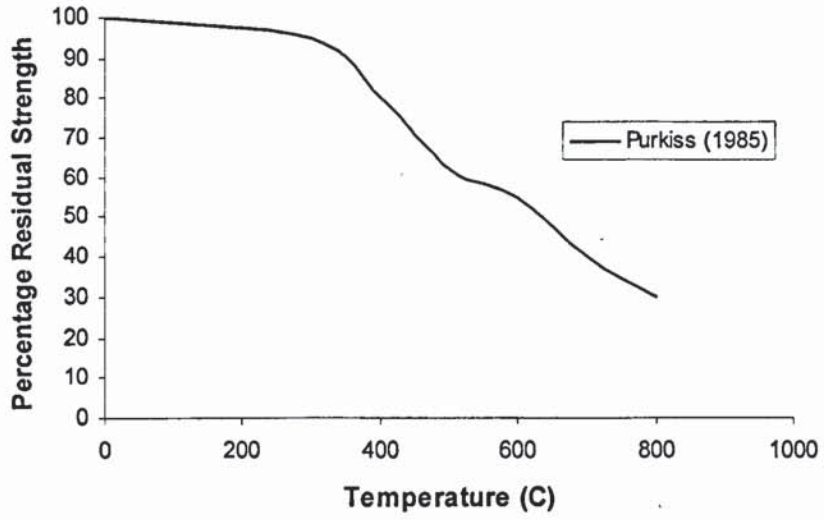

Figure 6.30 Residual concrete strength with temperature

Unfortunately, the ANSYS program can not back into prep7 after issuing a restart. Changing material properties to subsequent run between load steps or after restarts is not recommended. A warning will appear in the program and the validity of the results will be uncertain. This indicates that the material model at a certain temperature will only have certain value regardless the temperature was in ascent or descent phase. Regrettably, several commercial softwares such as FEMLAB have also been tried with similar unsuccessful results. Thus in the present study the model at cooling phases is not able to be presented appropriately due to the limitation of the

computer program. Since the behaviour of the element at maximum temperature is considered to be at the most severity condition, the behaviour of the structures based on the maximum temperatures are applied.

6.3.3. Transient Strains

Various existing constitutive models incorporating the transient strains for analysing concrete structures at elevated temperature have been reviewed in the previous chapter. It is important that the transient strains are included in this analysis to produce correct and safe results for the behaviour of the frame under first heating when temperature is high. In this analysis the constitutive model proposed by Li and Purkiss (2005) is employed because this simple constitutive model can easily be incorporated into various commercial finite element analysis codes.

As described in the previous, Li and Purkiss (2005) developed model based on the Anderberg and Thelandersson's model with considering the transient-strain and it is a full thermal strain-stress model. They developed an empirical formula based on the plotted results of the average Young's modulus. In the elastic ranges, temperature-dependent of Young's modulus is suggested in the following:

$$E^{*}(T) = E_0 \exp\left[-\frac{(T - 20)^{0.65}}{25}\right]$$

Where: E_0 = 32.2 GPa for normal-strength and E_0 = 40.6 GPa for high-strength.

For the Young's modulus in the plastic range the following equation is recommended:

$$E_p^{*}(T) = E_0^{-} \exp[k_p (T - 20)^{2.15}]$$

Where: E_0^{-} = - 0.045 E_0, and k_p =10^{-6}.

6.3.4. Boundary Conditions and Loadings

The boundary conditions assumed that all of the columns are fixed in their foundations, hence the bottom of the column are fully restrained against all translations and rotations. The connection between columns and beams are rigid and the beam can move in any directions. In order to simulate loading from the above floor, the beams are assumed to receive vertical uniform design load over the fire compartment area of 3.25 kN/m^2. Loading from the weight of concrete slab of 2400 x 9.81 x 0.25 = 5.89 kN/m^2 is added so that the total vertical uniform load would be 9.14 kN/m^2. Therefore, at 7.50 m runs a uniformly distributed load of q = 68.55 kN/m is applied. In addition, compressive forces of P_1 = 462.5 kN and P_2 = 925 kN are applied to internal and external columns, respectively. The above loadings represent total design load at the fire limit state applied at Cardington. Loading of the concrete frame is outlined in Figure 6.25.

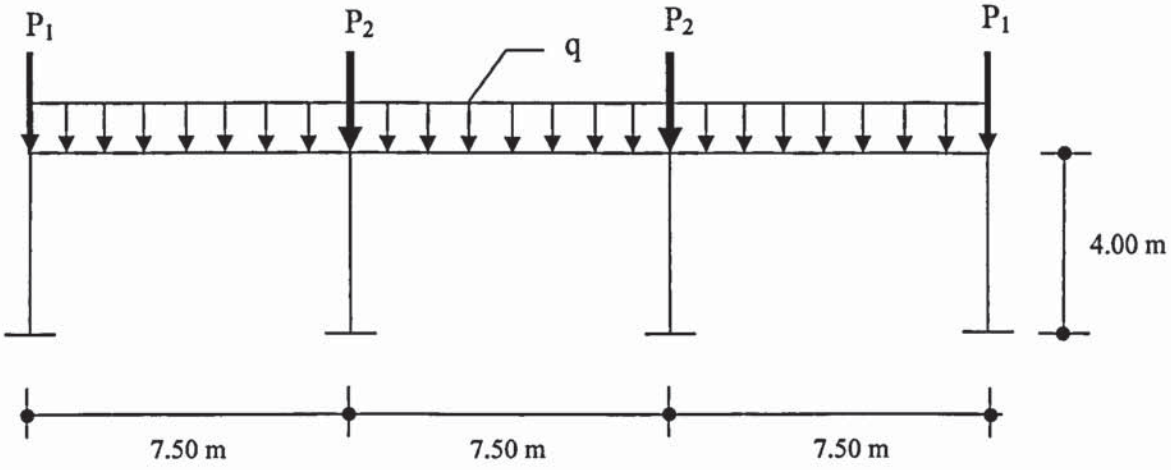

Figure 6.31 Loading of the concrete frame

Similar to the Cardington test, the time-temperature curve of the firing compartment is shown in Figure 6.26. This time-temperature response is predicted from the Eurocode (Bailey, 2002).

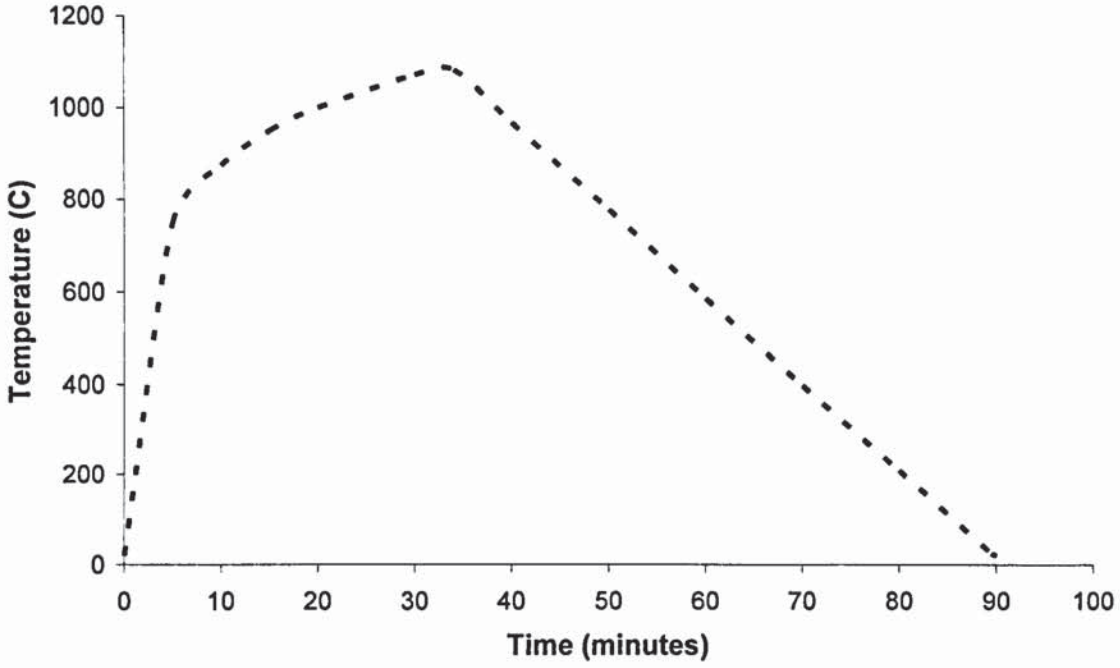

Figure 6.32 Time-temperature of the firing compartment

6.3.5. Element Type and Material Model

Finite element analysis software has been performed using ANSYS with coupled-field analysis. A coupled-field analysis is an analysis that takes into account the interaction between two or more disciplines of engineering. In this case, the coupled-field analysis is used for thermal-stress analysis.

All elements of the reinforced concrete frame are modelled using 3-D tetrahedral coupled-field solid element. The element is defined by ten nodes with four degrees of freedom (UX, UY, UZ, and TEMP) at each node. The total number of 38036 elements and 59080 nodes are used in the analyses with maximum size of the element is 130 mm. The geometry, node locations, and the coordinate system for this type of element are shown in Figure 6.27 and meshing of the element at concrete frame model in 3-D is illustrated in Figure 6.28.

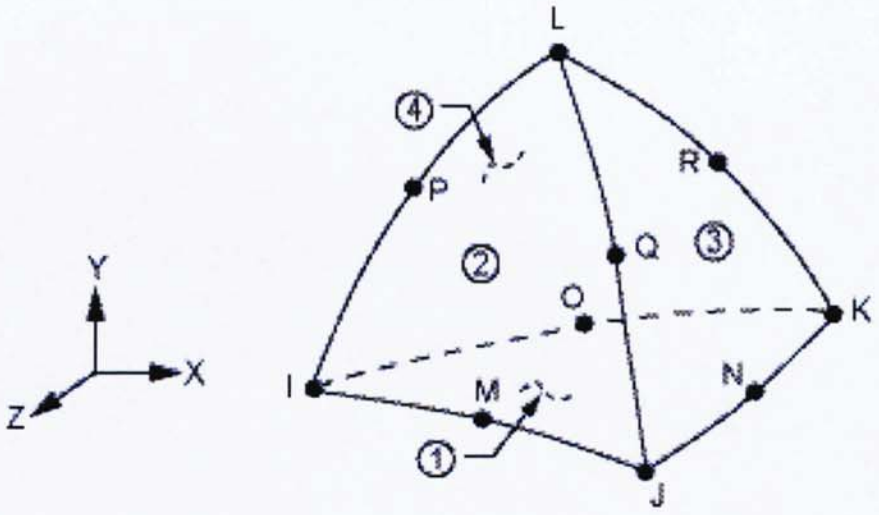

Figure 6.33 Geometry of the element

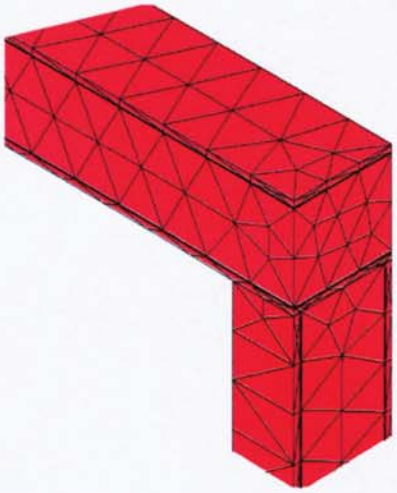

Figure 6.34 Meshing of the top corner of concrete frame model in 3-D

All materials defined with three different material models, i.e. Material Model Number 1 for layered steels, Material Model Number 2 for high-strength concrete of the columns, and Material Model Number 3 for normal-strength concrete of the beams. The properties of the models can be defined and tabulated in Tables 6.1, 6.2 and 6.3 as follows.

Time (minutes)	Temperature (°C)	c_s (J/kg°C)	$\varepsilon_{th,s}$ $\Delta l/l$	λ_s (W/m°C)	$E^*(T)$ (MPa)
0	20	440	0	53	2E+005
6	600	760	0.008	34	6.2E+004
18	950	650	0.013	27.3	1.125E+004
36	1050	650	0.015	27.3	6.75E+003
54	690	937	0.01	31	2.96E+004
72	350	584	0.004	42.3	1.5E+005
90	20	440	0	53	2E+005

Table 6.3 Material property of steel at elevated temperature

Time (minutes)	Temperature (°C)	c_c (J/kg°C)	α	$\varepsilon_{th,c}$ $\Delta l/l$	λ_c (W/m°C)	$E^*(T)$ (MPa)
0	20	963	25	0	2.04	40600
6	600	1200	56	0.0101	0.35	3332
18	950	1283	90	0.014	0.2	1355
36	1050	1294	100	0.014	0.2	1072
	Cooling Phase					
54	690	1228	80	0.0136	0.21	-6011
72	350	1099	49	0.004	0.71	-2370
90	20	963	25	0	2.04	-1827

Table 6.4 Material property of high-strength concrete at elevated temperature

Time (minutes)	Temperature (°C)	c_c (J/kg°C)	α	$\varepsilon_{th,c}$ $\Delta l / l$	λ_c (W/m°C)	$E^*(T)$ (MPa)
0	20	963	25	0	2.04	32200
6	600	1200	56	0.0101	0.35	2644
18	950	1283	90	0.014	0.2	1074
36	1050	1294	100	0.014	0.2	850
	Cooling Phase					
54	690	1228	80	0.0136	0.21	-4767
72	350	1099	49	0.004	0.71	-2273
90	20	963	25	0	2.04	-1449

Table 6.5 Material property of normal-strength concrete at elevated temperature

6.4. Results and Discussions

The analyses are carried out for five different fire scenarios. Case 1 analyses the frame structure before fire and then follows by Case 2, Case 3, Case 4 and Case 5 when the localised fire exposes at one external room, one internal room, one external and one internal rooms, and all three rooms, respectively. In all cases the temperature distribution in the fired compartment is assumed to be uniform both in the vertical and horizontal direction. Figure 6.29 shows the various localised fire scenarios from Case 1 to Case 5.

Case1:

Case2:

Case 3:

Case 4:

Case 5:

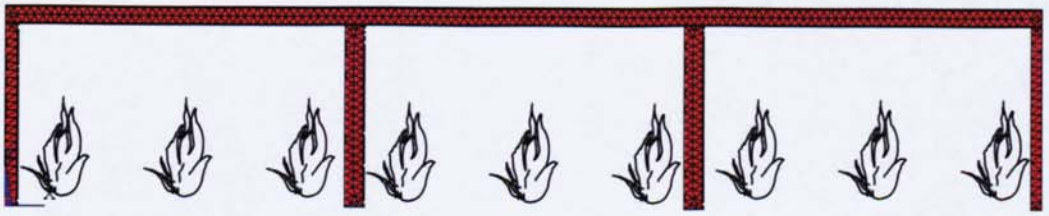

Figure 6.35 Various localised fire scenarios of cases 1 - 5.

6.4.1. Before Firing (Case 1)

Before firing the compartment, all columns and beams are assumed to have equal room temperature of 20°C. The stresses and displacements are caused purely due to applied loads from the above floors without considering any thermal stress. Full three-dimensional finite element model is employed using ANSYS and the plot of deformed shape of the frame subjected the distributed load only is discussed.

The maximum x-displacement of 3.5 mm occurs in the top of the right external column and due to symmetric loading the same value at the opposite direction is found in the left external columns as shown in Figure 6.30. While in Figure 6.31, the maximum vertical displacement of 13 mm is found in around the middle of external beams.

Figures 6.32 and 6.33 present the distributions of maximum principal stress and minimum principal stress of the beams and columns. The maximum principal stress in Figure 6.32 gives the most positive (tensile) stress while the minimum principal stress in Figure 6.33 gives the most negative (compressive) stress. The maximum principal stress of 23.881 MPa and the minimum principal stress of -17.226 MPa are found in the beam, while the minimum principal stress of -32.858 MPa is found in the column.

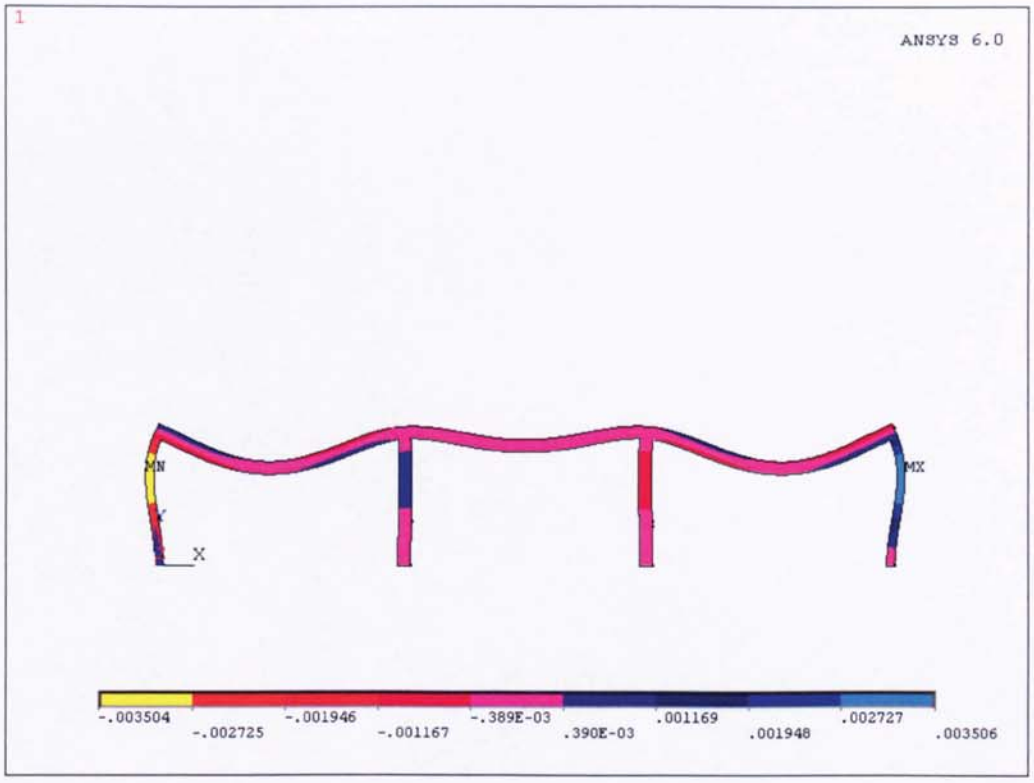

Figure 6.36 Displacements of the frame in the x direction (Case 1)

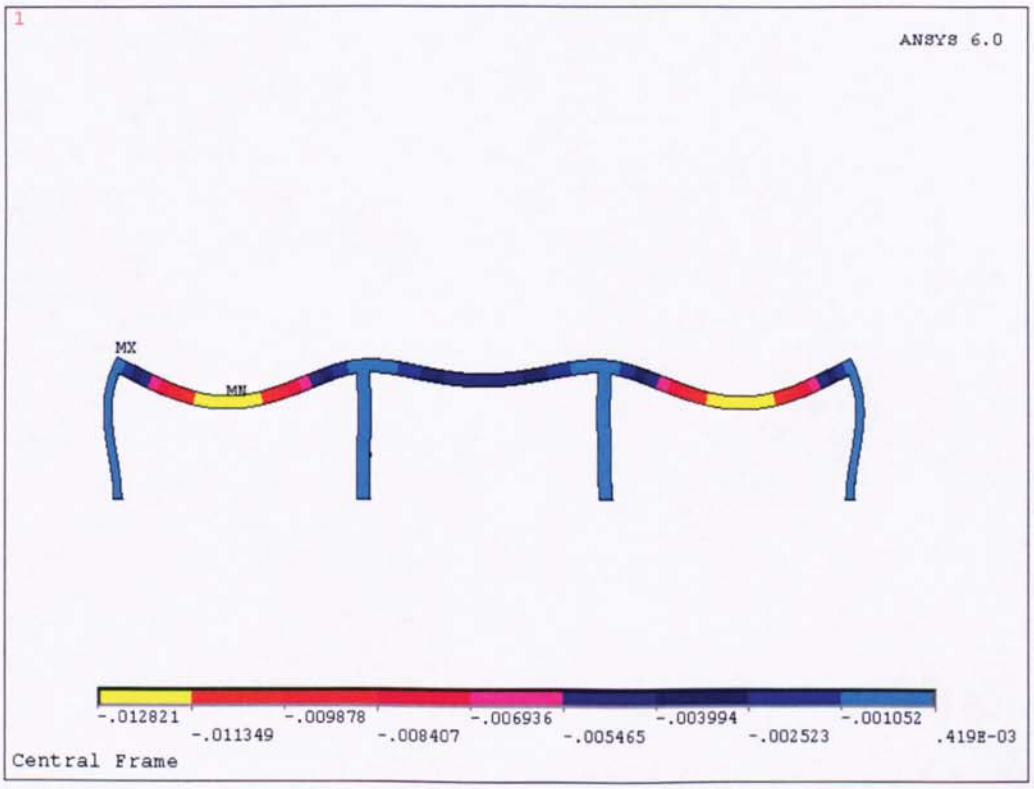

Figure 6.37 Displacements of the frame in the y direction (Case 1)

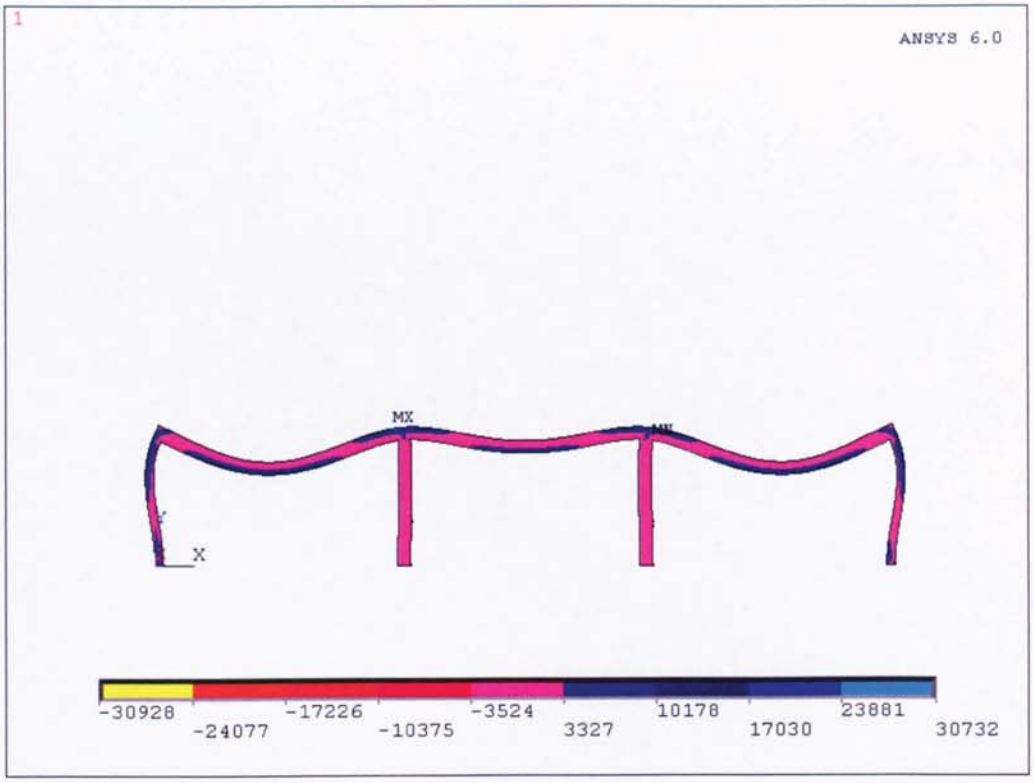

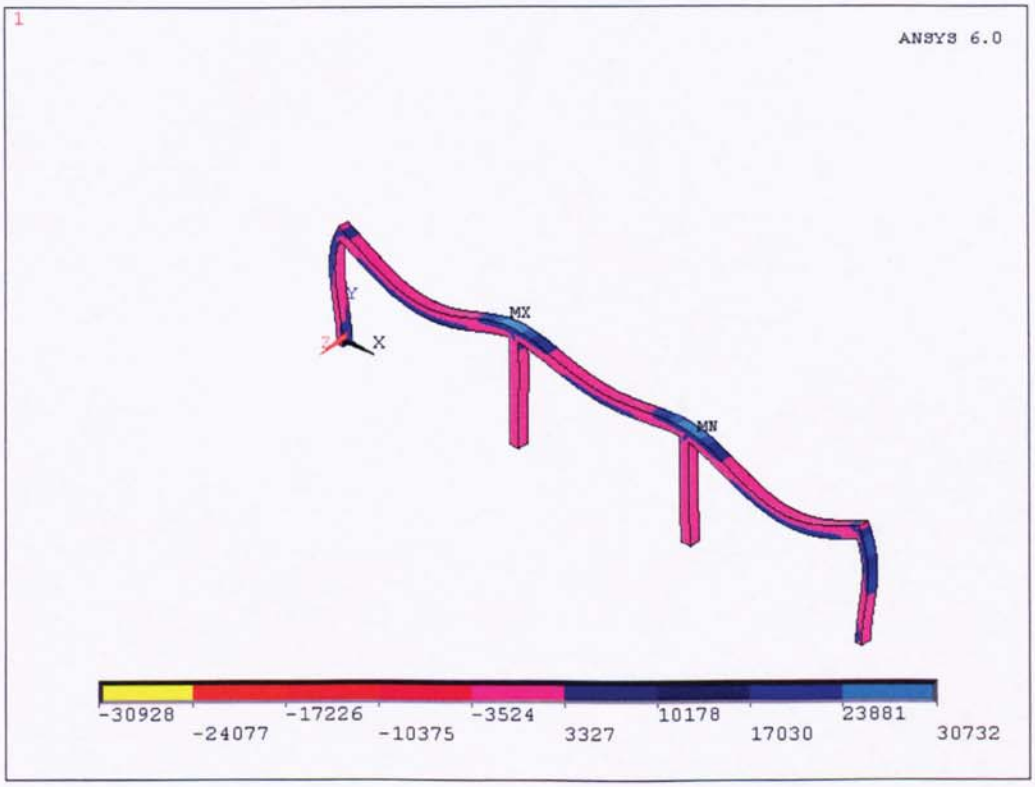

Figure 6.38 Distribution of maximum principal stress (Case 1)

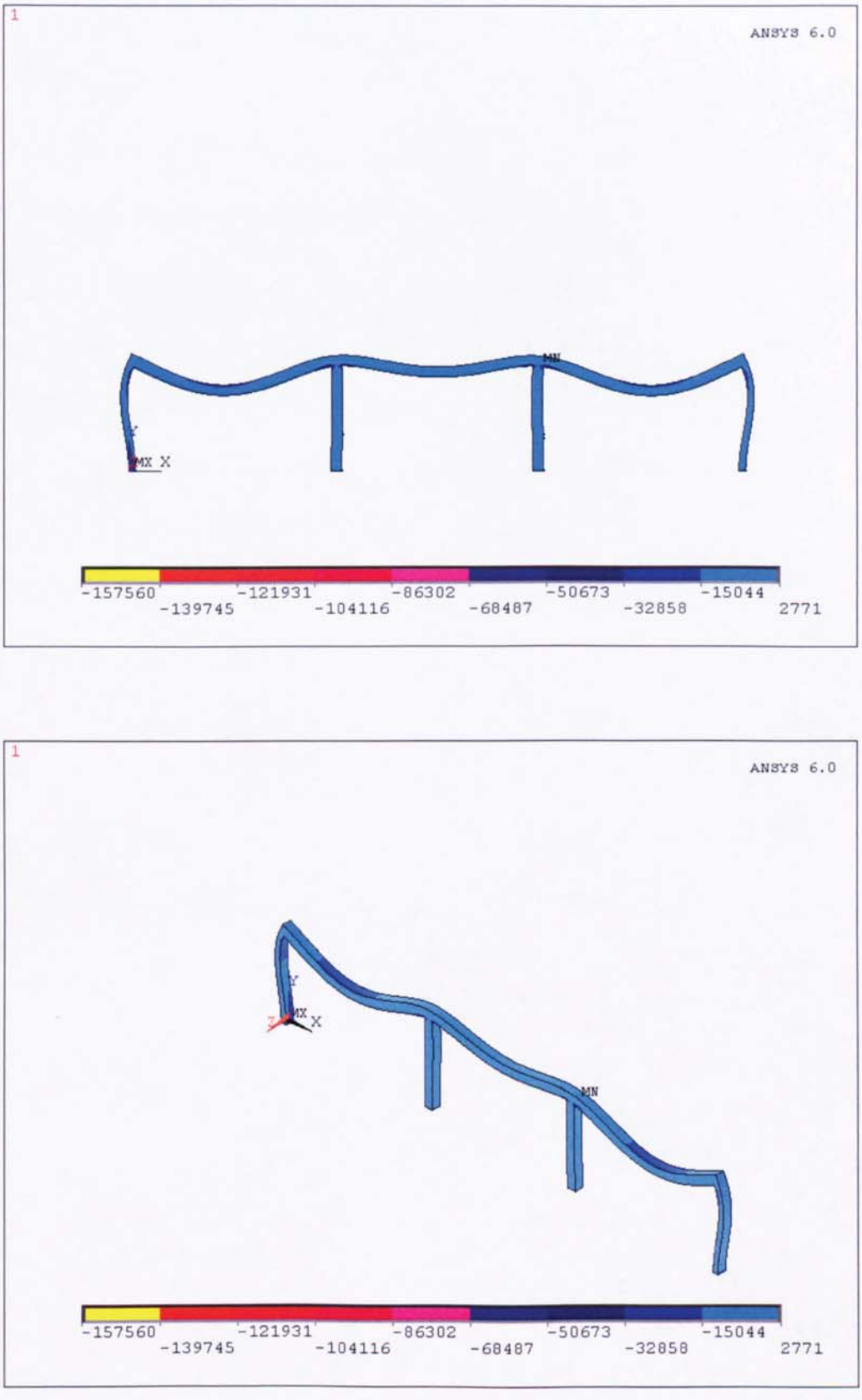

Figure 6.39 Distribution of minimum principal stress (Case 1)

6.4.2. Thermal Analyses after Firing

6.4.2.1. Case 2

In this case the fired compartment is localised at the external room in the right side of the frame. The temperature rises in this case is based on the time-temperature curve given in Figure 6.26 and is assumed to be uniform in the vertical direction. The distribution of maximum temperature of this case is given in Figure 6.34 where the maximum temperature of 935°C is occurred at the fired columns surfaces.

Figures 6.35 and 6.36 show the displacements of the frame in x and y directions, respectively. The maximum x-displacement of 21 mm is occurred in the top of the right external column, and the maximum y-displacement of 21 mm is found in the firing external beam.

Figures 6.37 and 6.38 give the distributions of the maximum and minimum principal stresses of the element. The maximum stress of 25.127 MPa and minimum stress of - are found in the beam, while the minimum principal stress of -60.799 MPa is found in the element of the concrete frame.

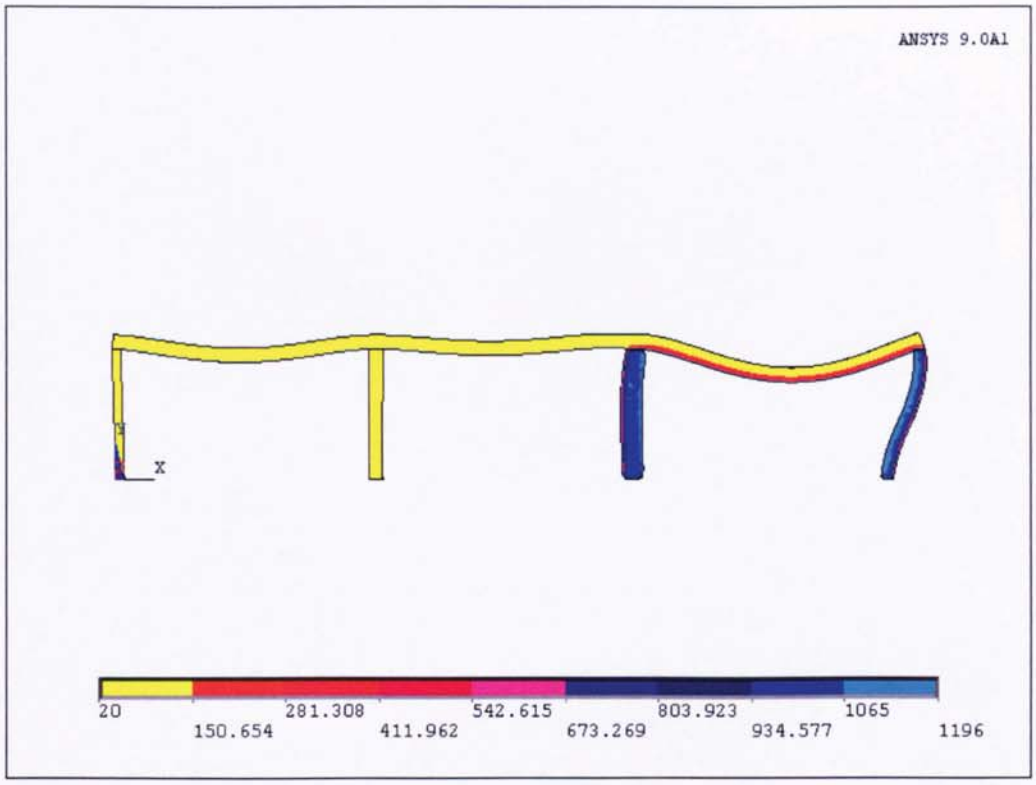

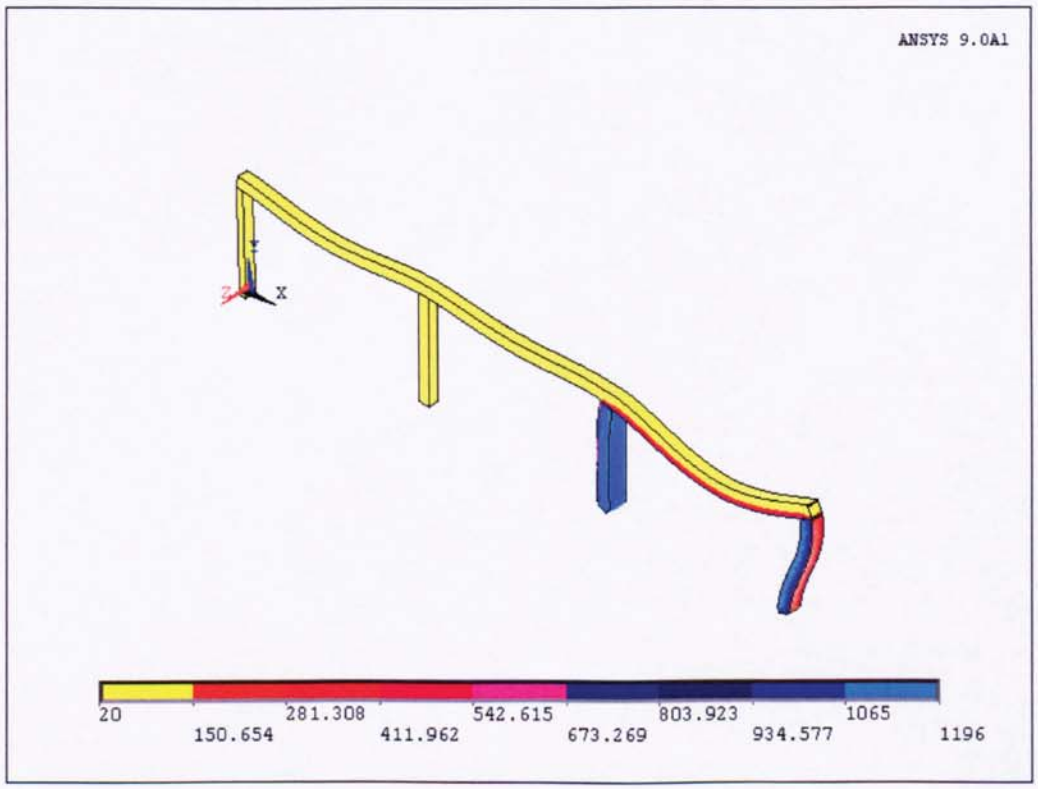

Figure 6.40 Temperature distributions (Case 2)

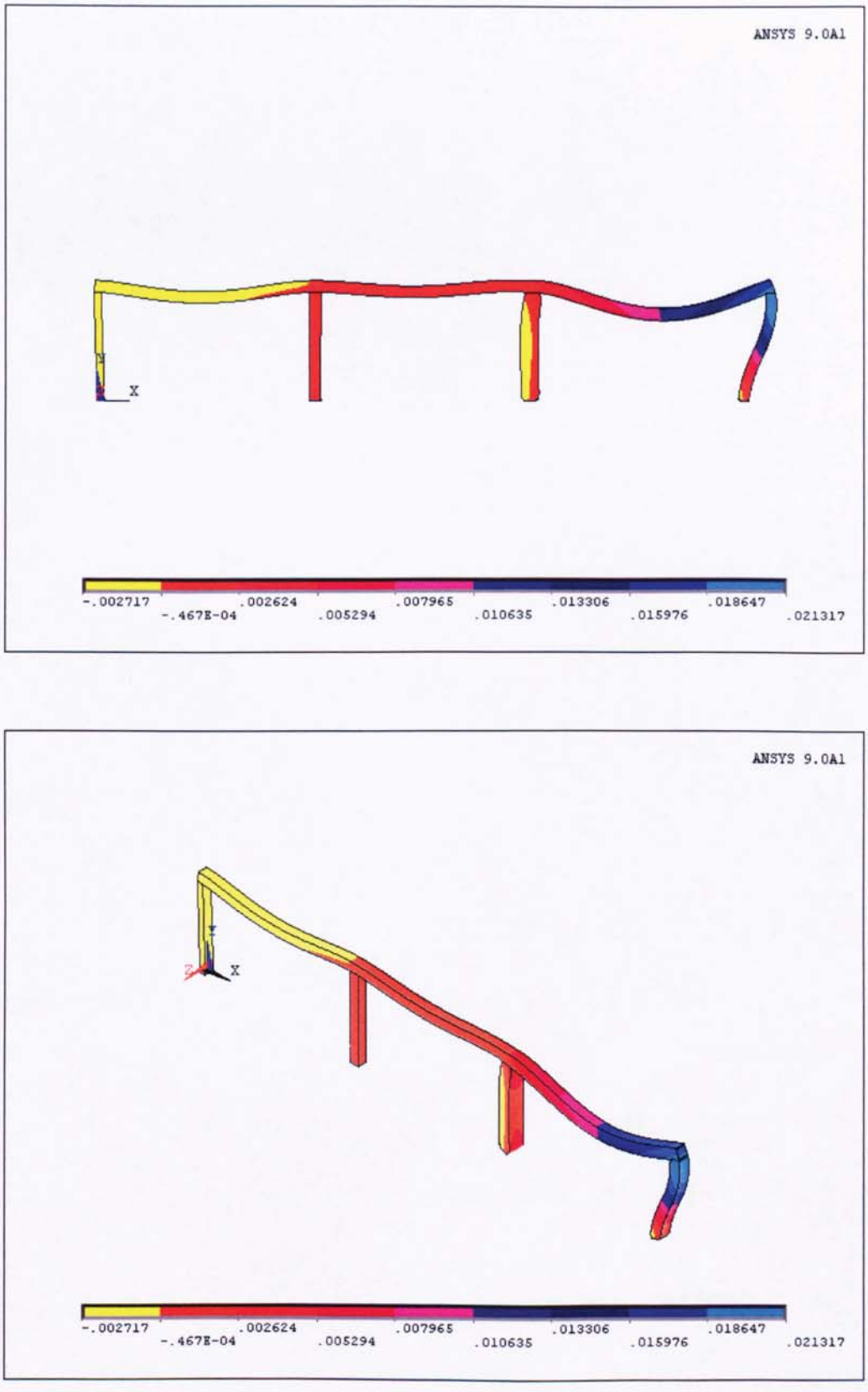

Figure 6.41 Displacements of the frame in the x direction (Case 2)

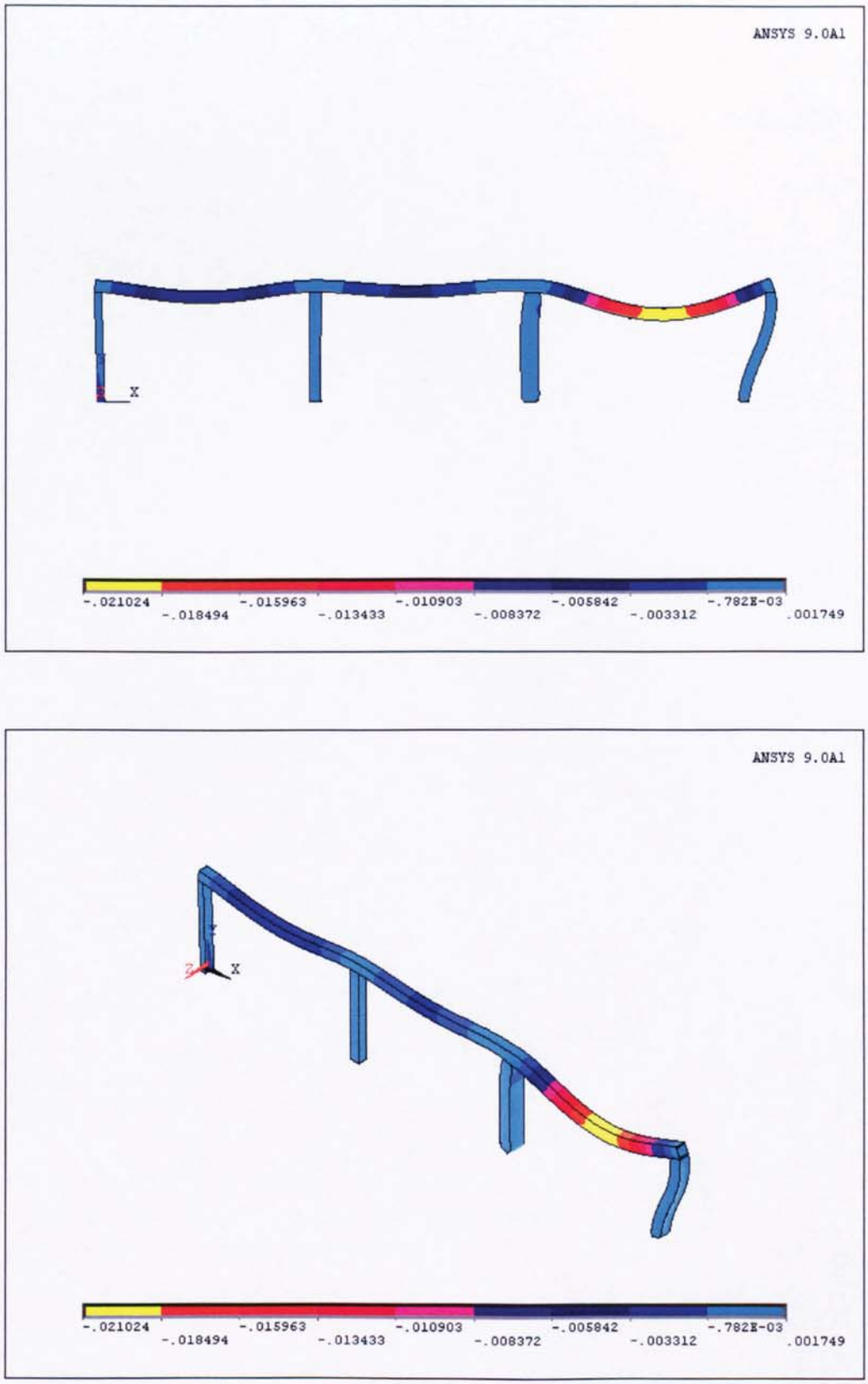

Figure 6.42 Displacements of the frame in the y direction (Case 2)

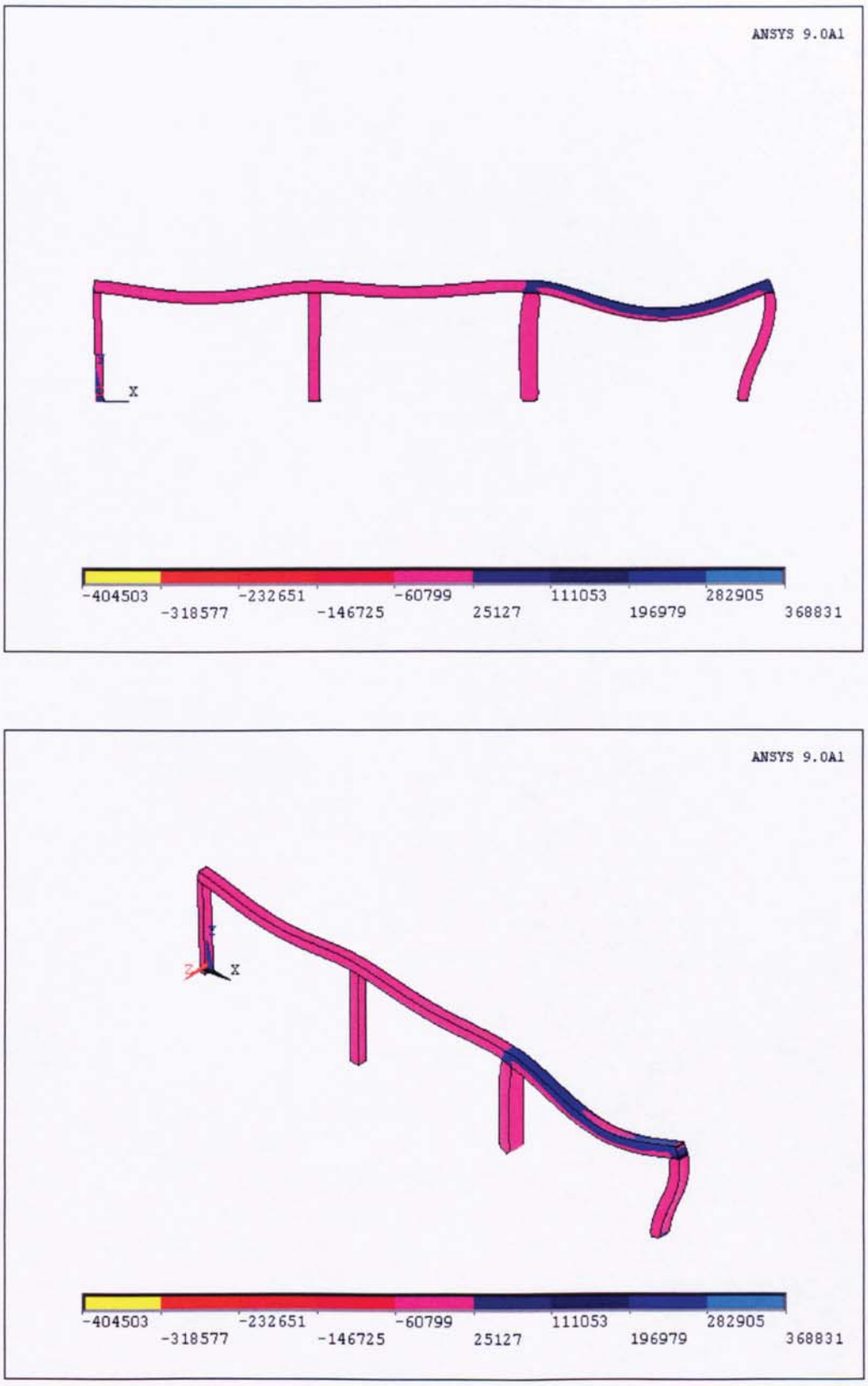

Figure 6.43 Distribution of maximum principal stress (Case 2)

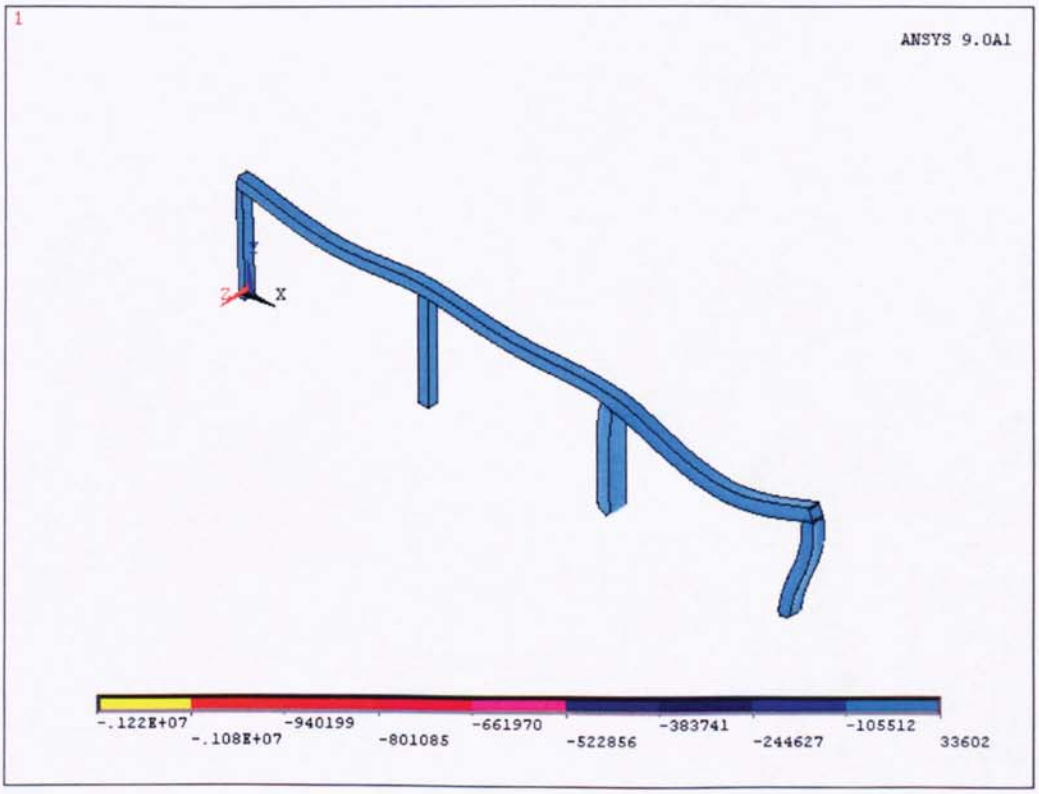

Figure 6.44 Distribution of minimum principal stress (Case 2)

6.4.2.2. Case 3

In this case the fired compartment is localised at one room only, i.e. the internal room in the middle of the frame. Similar to the previous case, the temperature distribution of this case is based on the time-temperature curve given in Figure 6.26. The temperature distribution of this case is given in Figure 6.39 where the maximum temperature of 890°C is found at the fired columns surfaces.

Figures 6.40 and 6.41 illustrate the horizontal and vertical displacements of the concrete frame structure, respectively. As a symmetric loading, the maximum x-displacements of 11 mm are occurred in the top of the right and left external column. The maximum y-displacements of 12 mm are found in both external beams.

Figure 6.42 and 6.43 show the distribution of the maximum and minimum principal stress of the element. Maximum stress of 23.063 MPa and minimum stress of -64.456 MPa are found in the element of reinforced concrete frame.

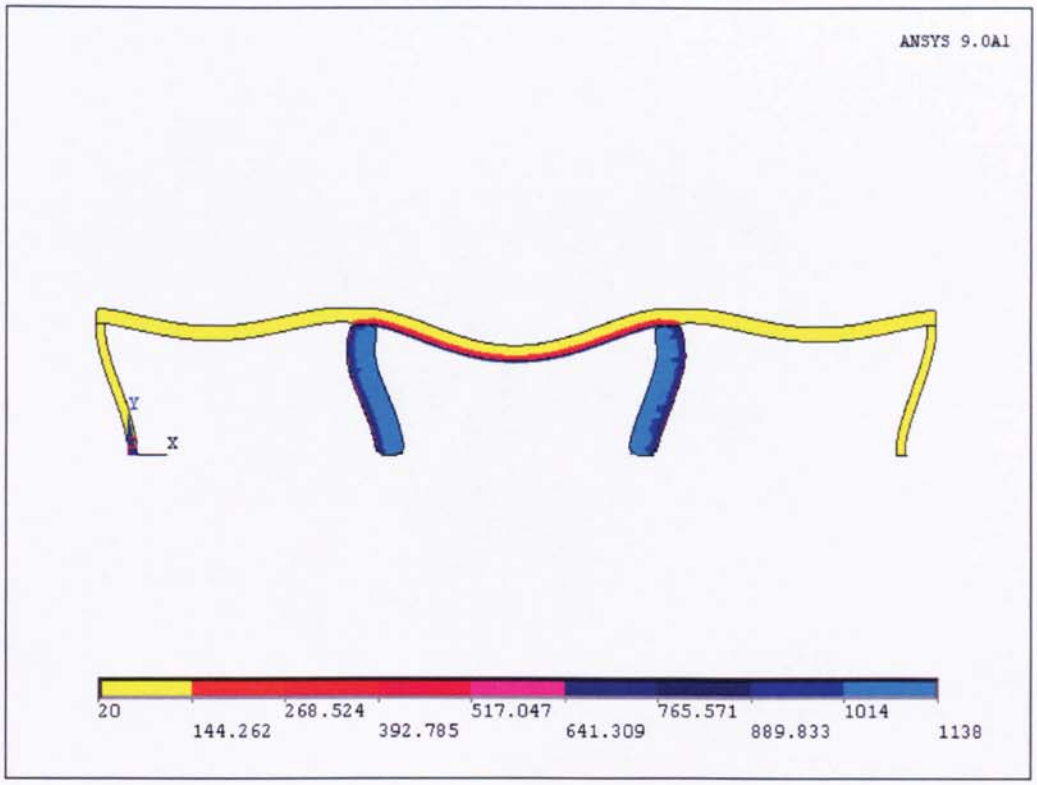

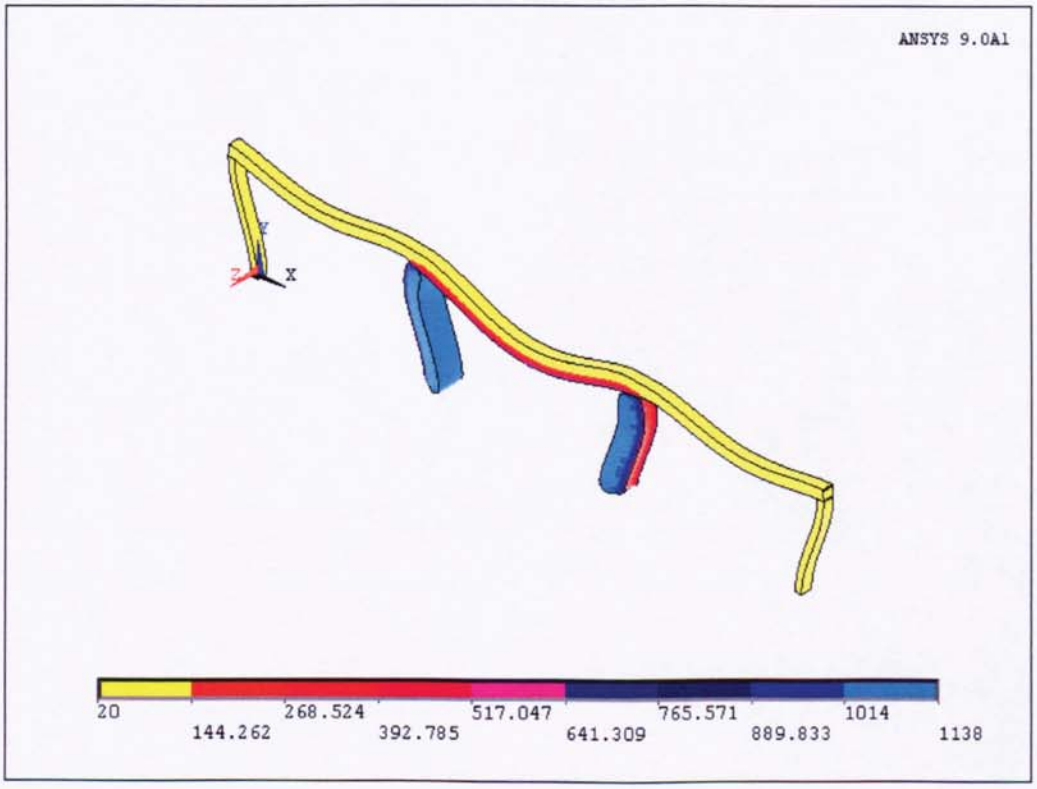

Figure 6.45 Temperature distributions (Case 3)

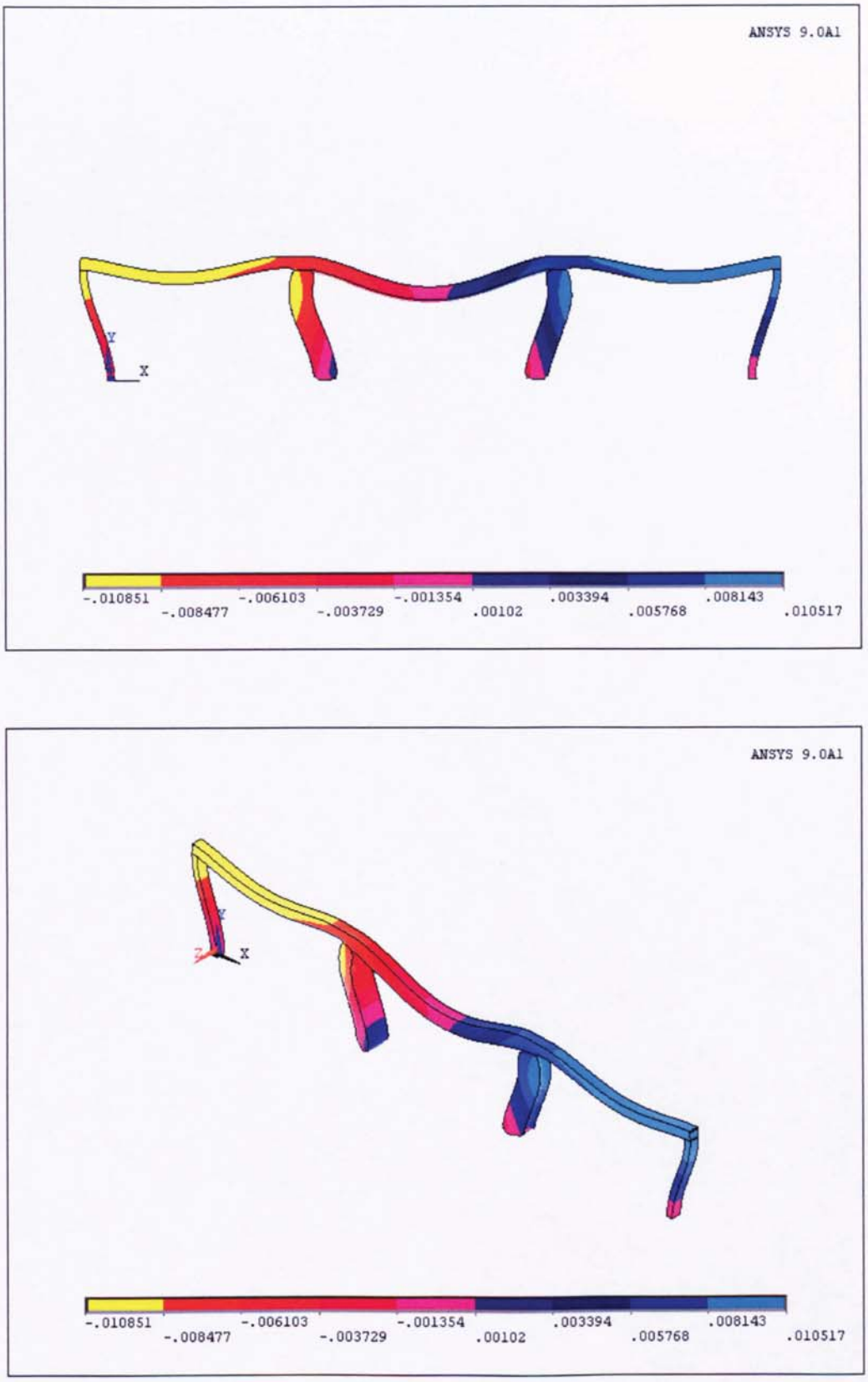

Figure 6.46 Displacements of the frame in the x direction (Case 3)

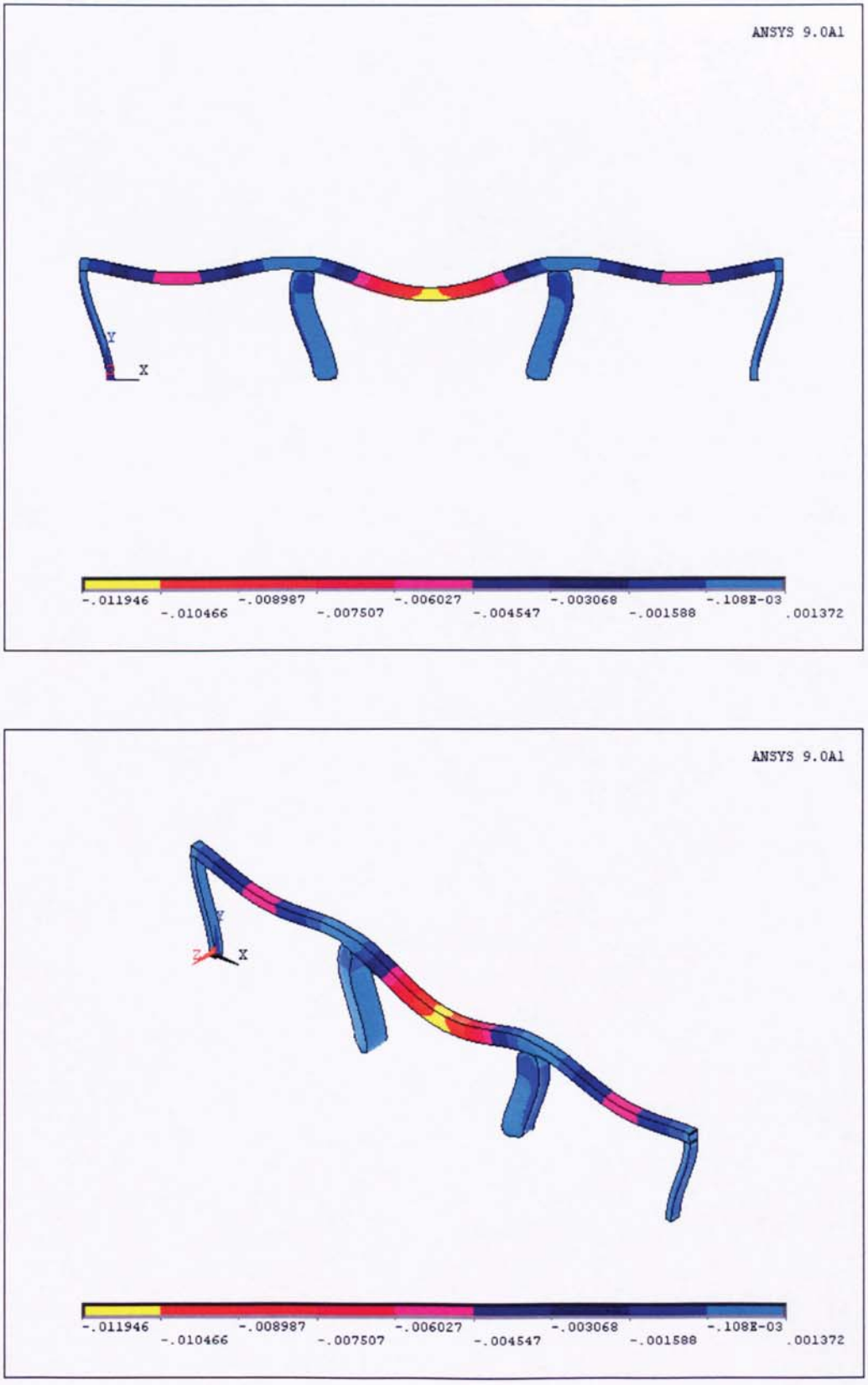

Figure 6.47 Displacements of the frame in the y direction (Case 3)

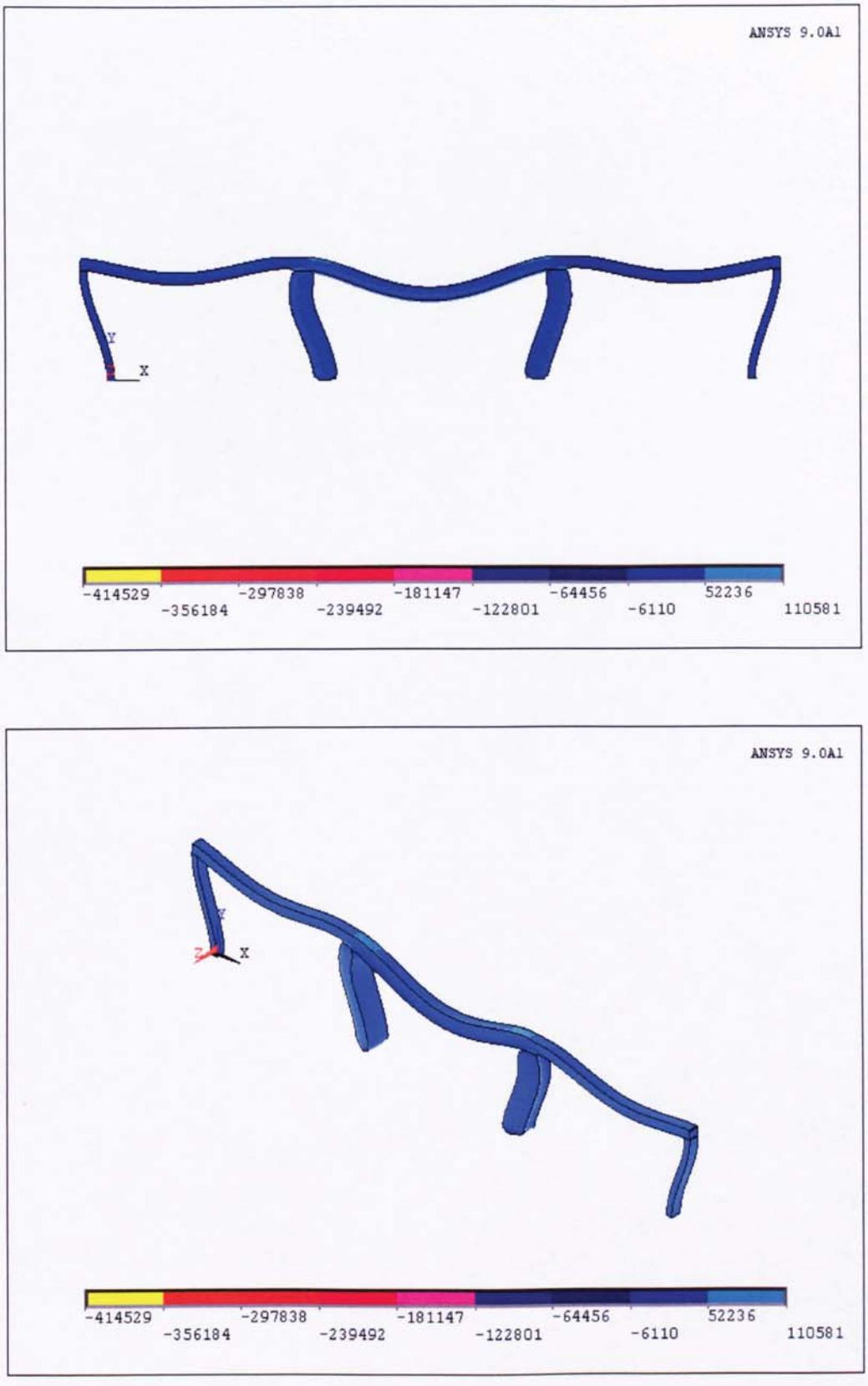

Figure 6.48 Distribution of maximum principal stress (Case 3)

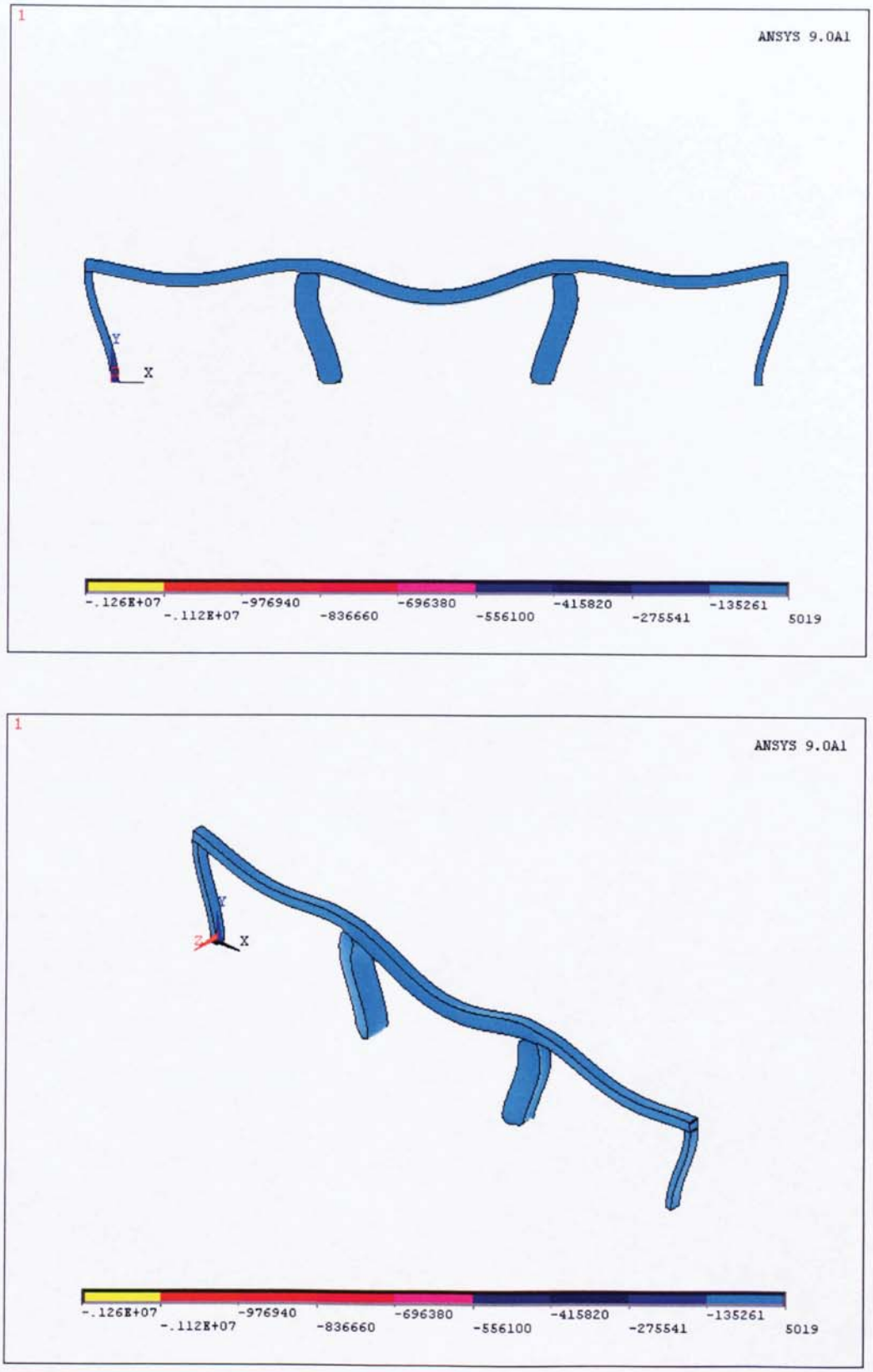

Figure 6.49 Distribution of minimum principal stress (Case 3)

6.4.2.3. Case 4

In this case the fired compartment is localised at two rooms, i.e. the internal and external rooms of the frame. As previous case, the temperature distribution of this case is based on the time-temperature curve given in Figure 6.26. The distribution of temperature of this case is shown in Figure 6.44 and, similar as previous cases, the maximum temperature of 935°C is found at the fired columns surfaces.

Figures 6.45 and 6.46 show the displacements of the elements. The maximum x-displacement of 33 mm occurs in the top of the right external column, and the maximum vertical deflection of 19 mm is found in the firing external beam.

Figure 6.47 and 6.48 show the distribution of the maximum and minimum principal stresses of the element. Maximum stress of 19.223 MPa and minimum stress of -66.499 MPa are found in the element of the concrete frame.

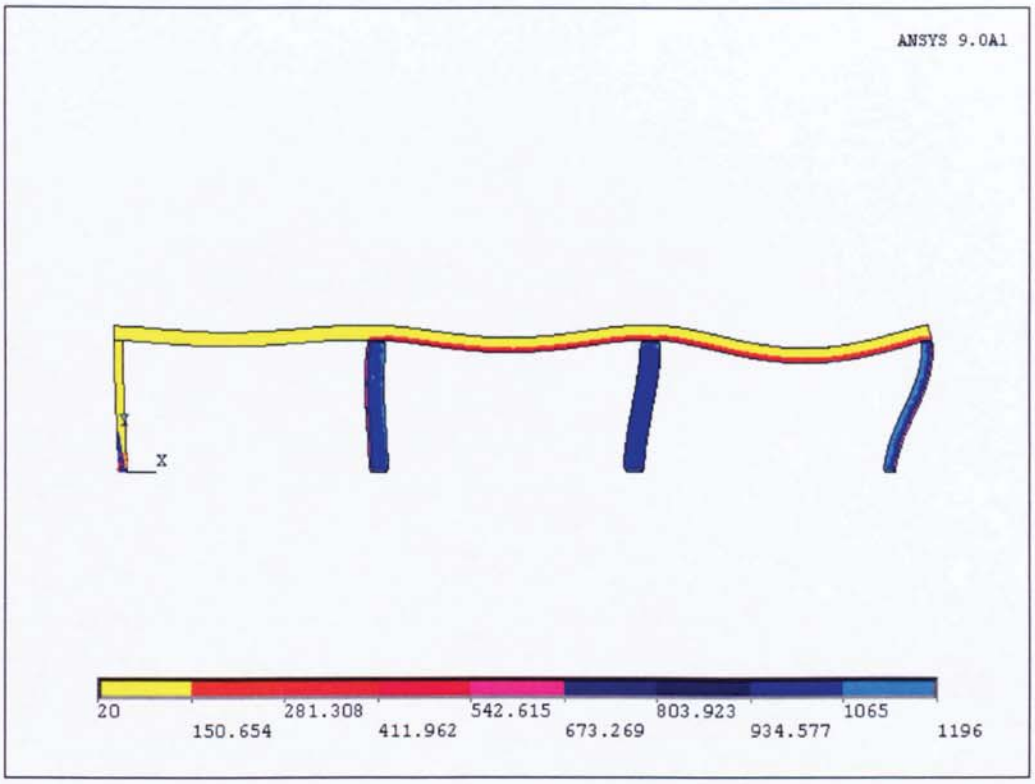

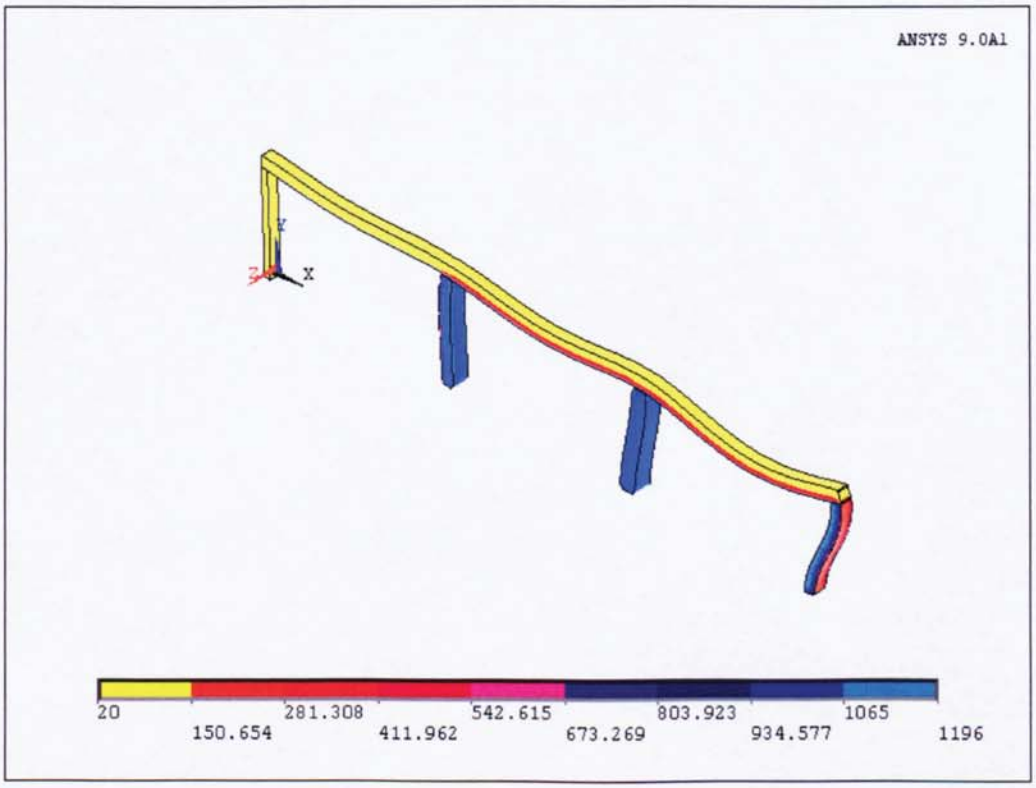

Figure 6.50 Temperature distributions (Case 4)

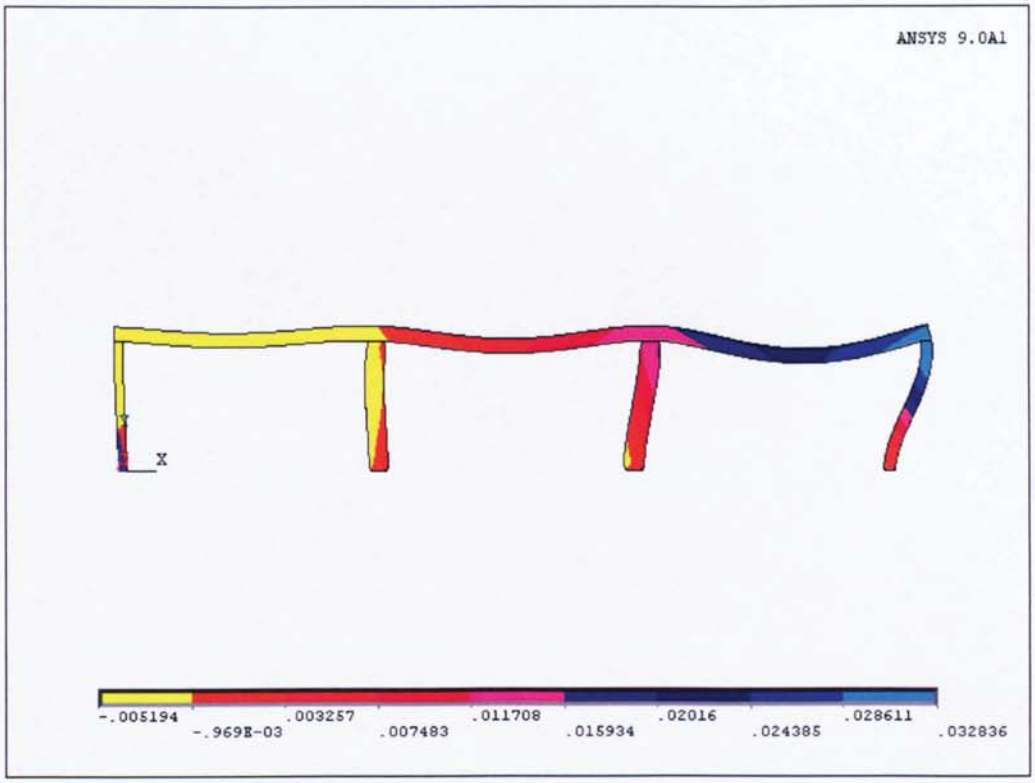

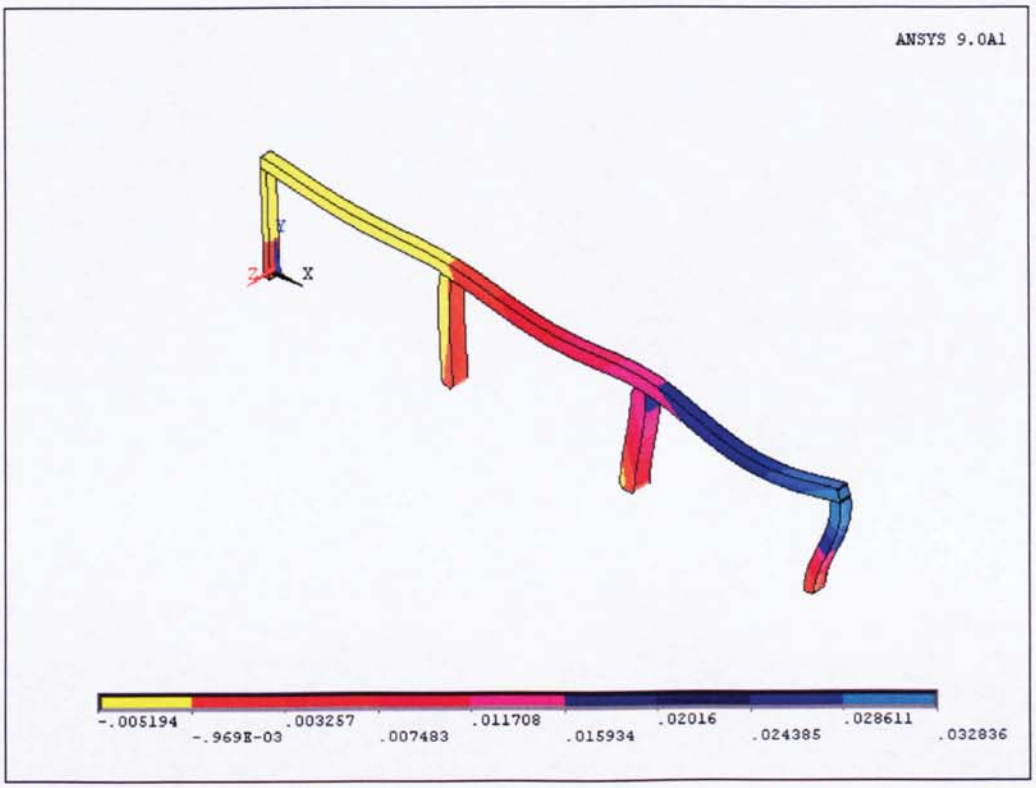

Figure 6.51 Displacements of the frame in the x direction (Case 4)

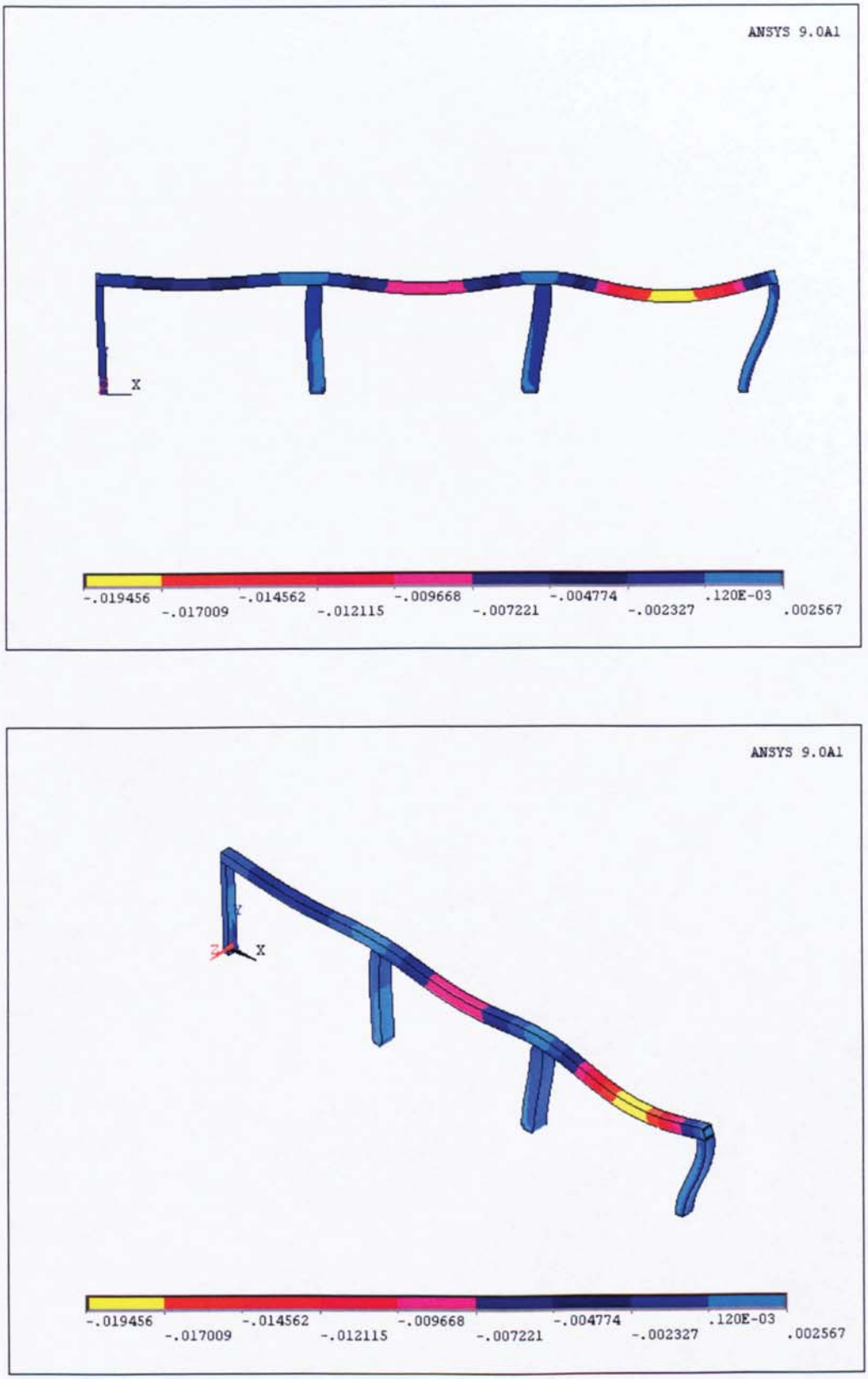

Figure 6.52 Displacements of the frame in the y direction (Case 4)

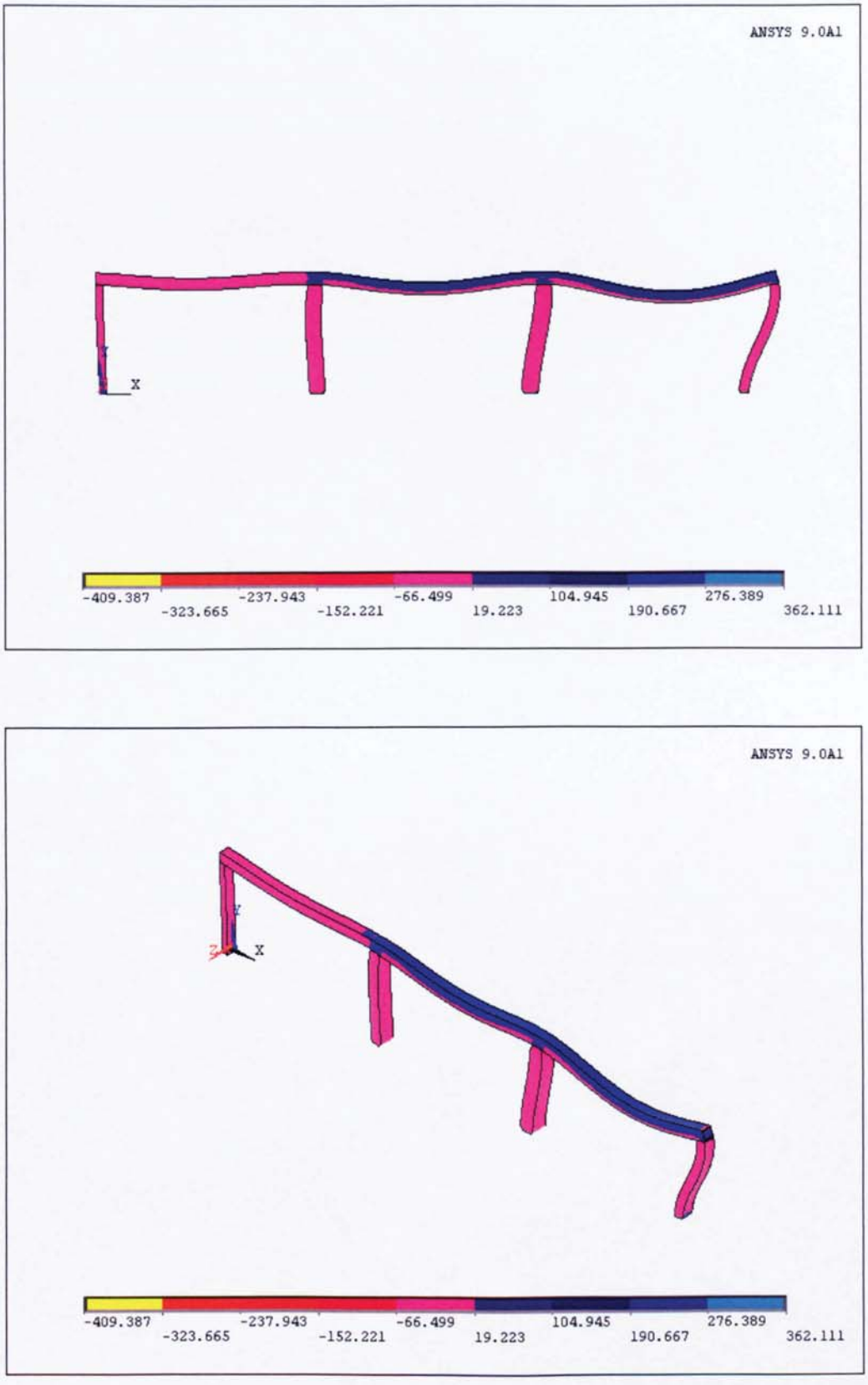

Figure 6.53 Distribution of maximum principal stress (Case 4)

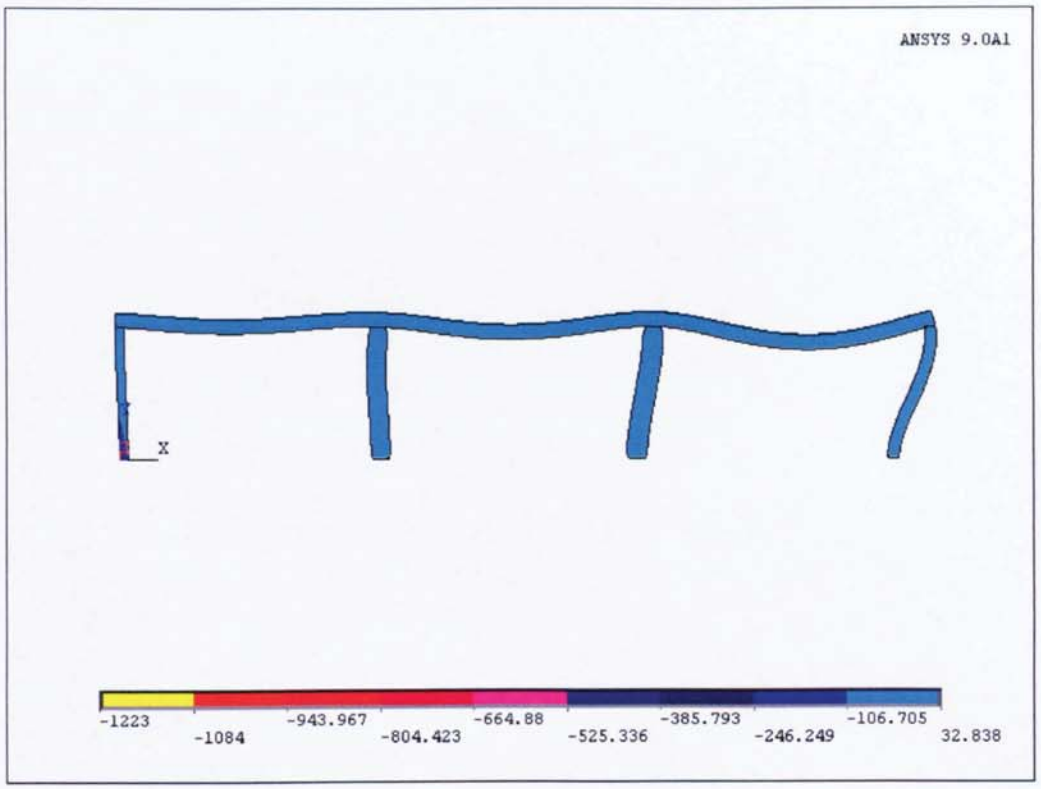

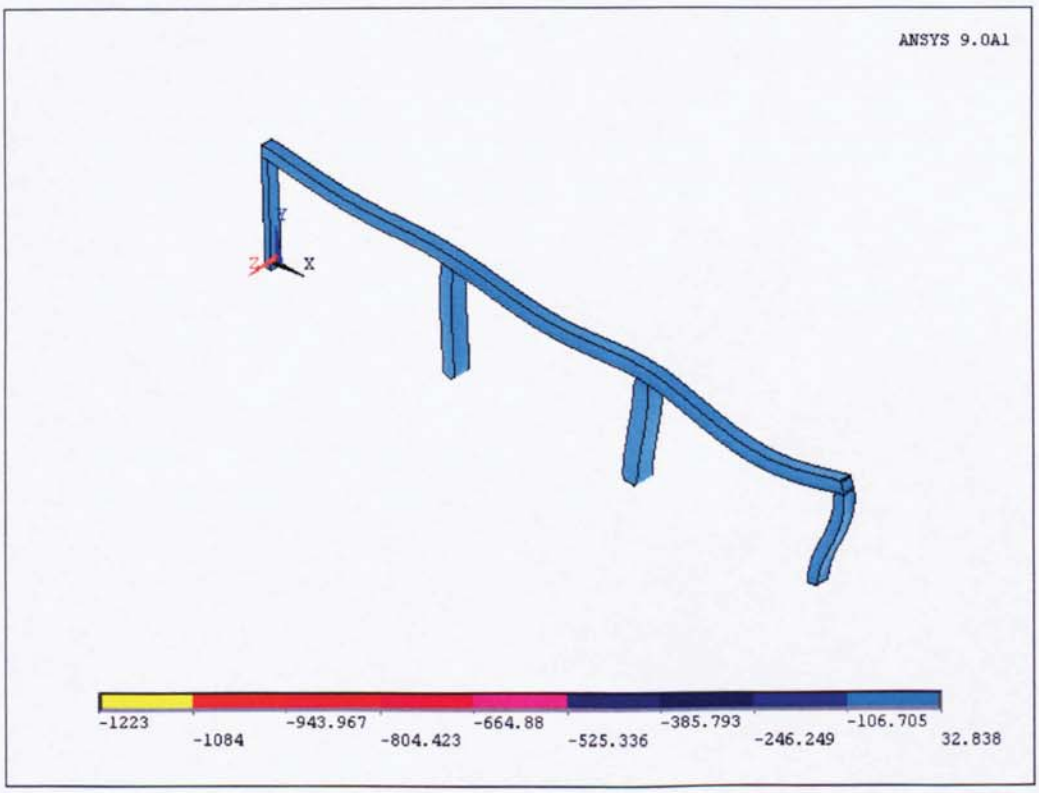

Figure 6.54 Distribution of minimum principal stress (Case 4)

6.4.2.4. Case 5

In this case the fired compartment is happened to all the rooms of the frame. Similar as previous cases, the temperature distribution of this case is based on the time-temperature curve given in Figure 6.26. The distribution of temperature of this case is given in Figure 6.49. From this figure a maximum temperature of 935°C is found at the fired columns surfaces.

Figures 6.50 and 6.51 present the horizontal and vertical displacements of the elements, respectively. The maximum x displacement of 33 mm is occurred in the top of the right external column, and the maximum y deflection of 19 mm is found in the firing external beam.

Figure 6.52 and 6.53 give the distribution of the maximum and minimum principal stresses of the element. From this figure, maximum stress of 23.336 MPa and minimum stress of -62.672 MPa are found in the element of the concrete frame.

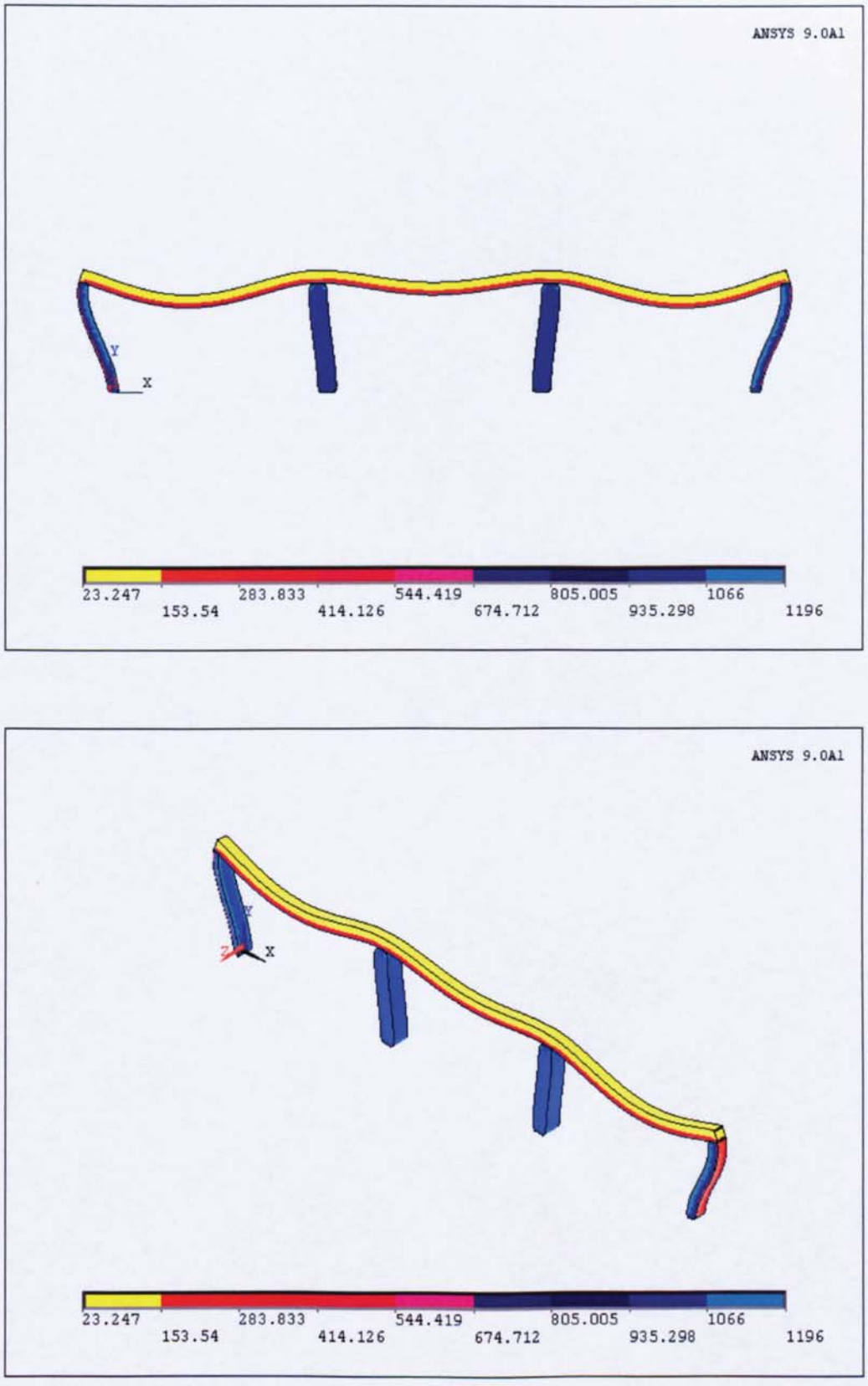

Figure 6.55 Temperature distributions (Case 5)

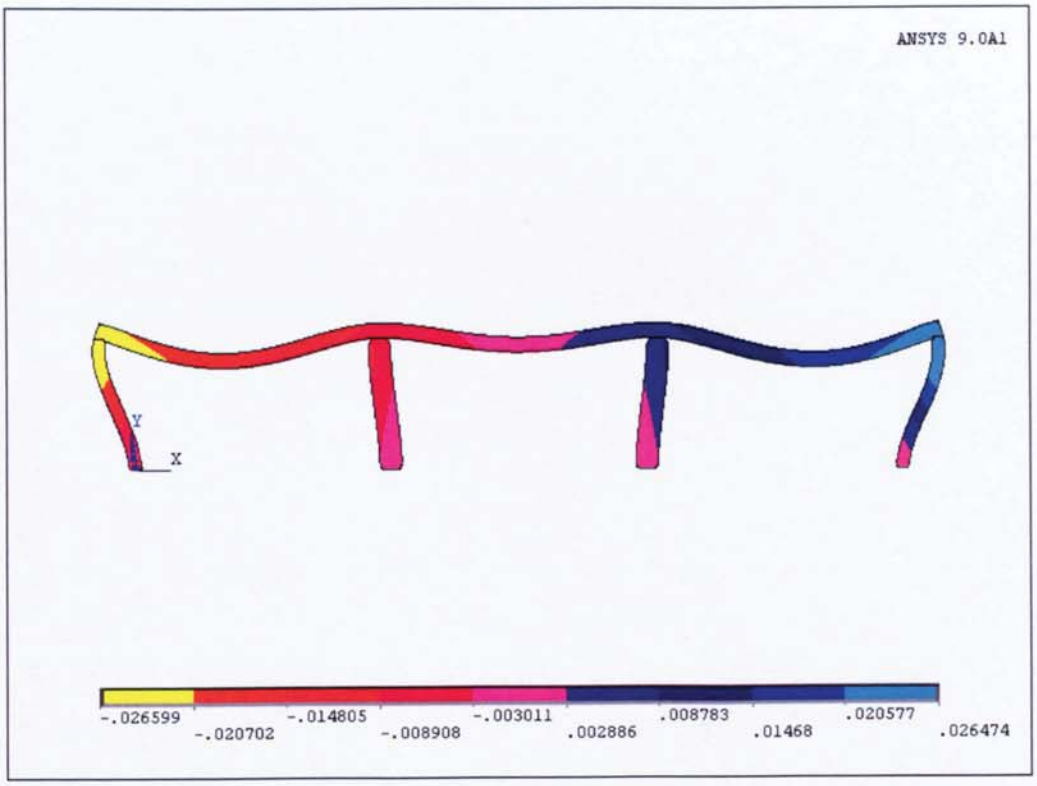

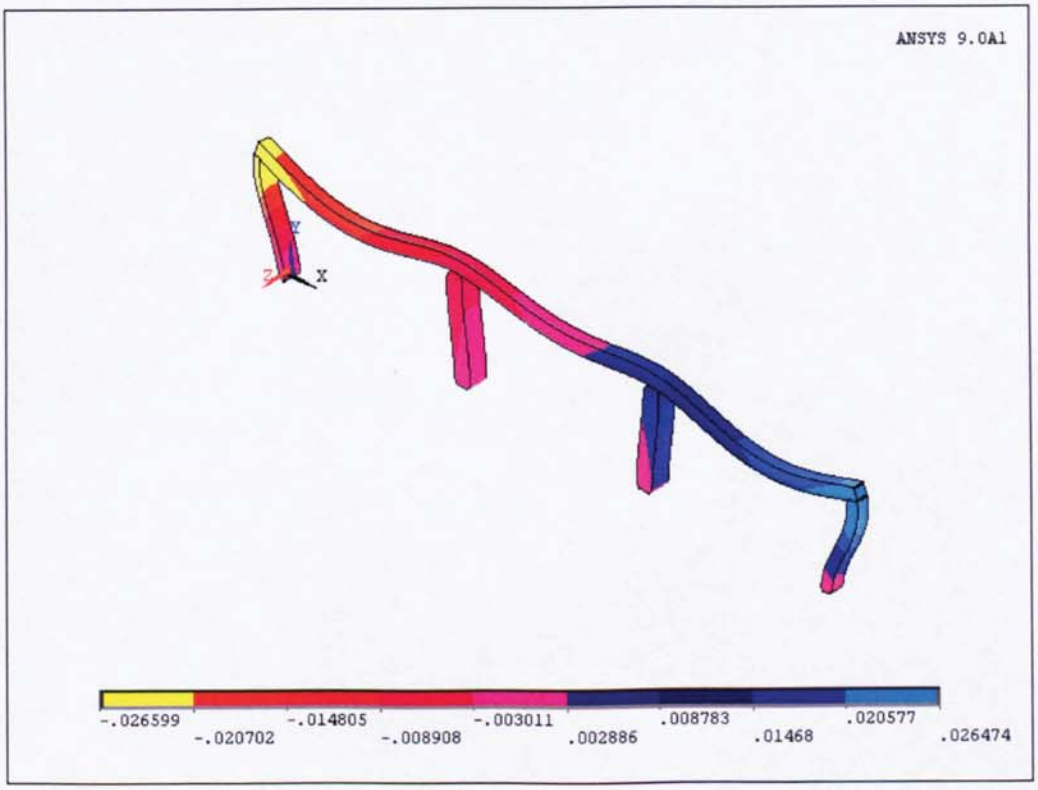

Figure 6.56 Displacements of the frame in the x direction (Case 5)

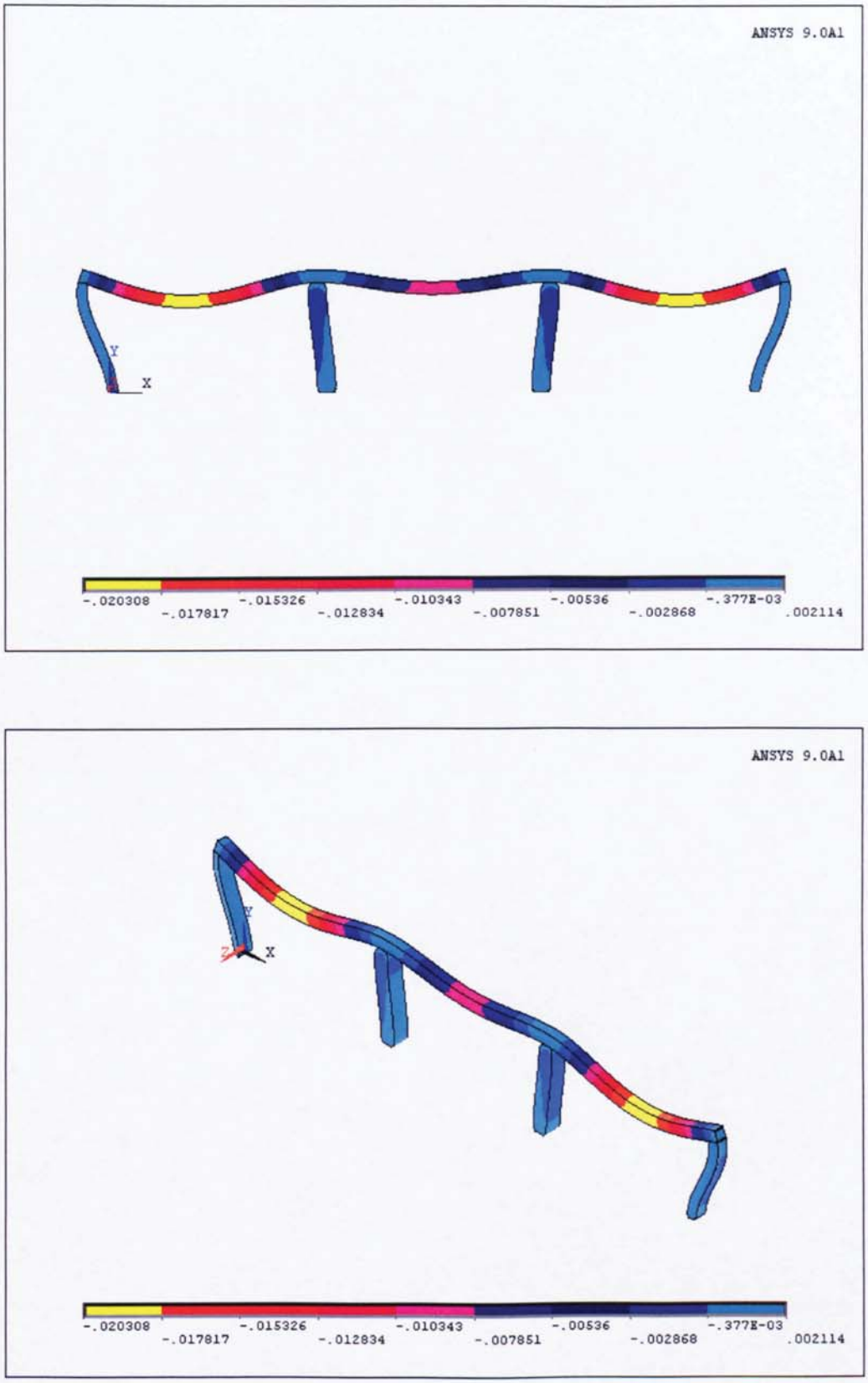

Figure 6.57 Displacements of the frame in the y direction (Case 5)

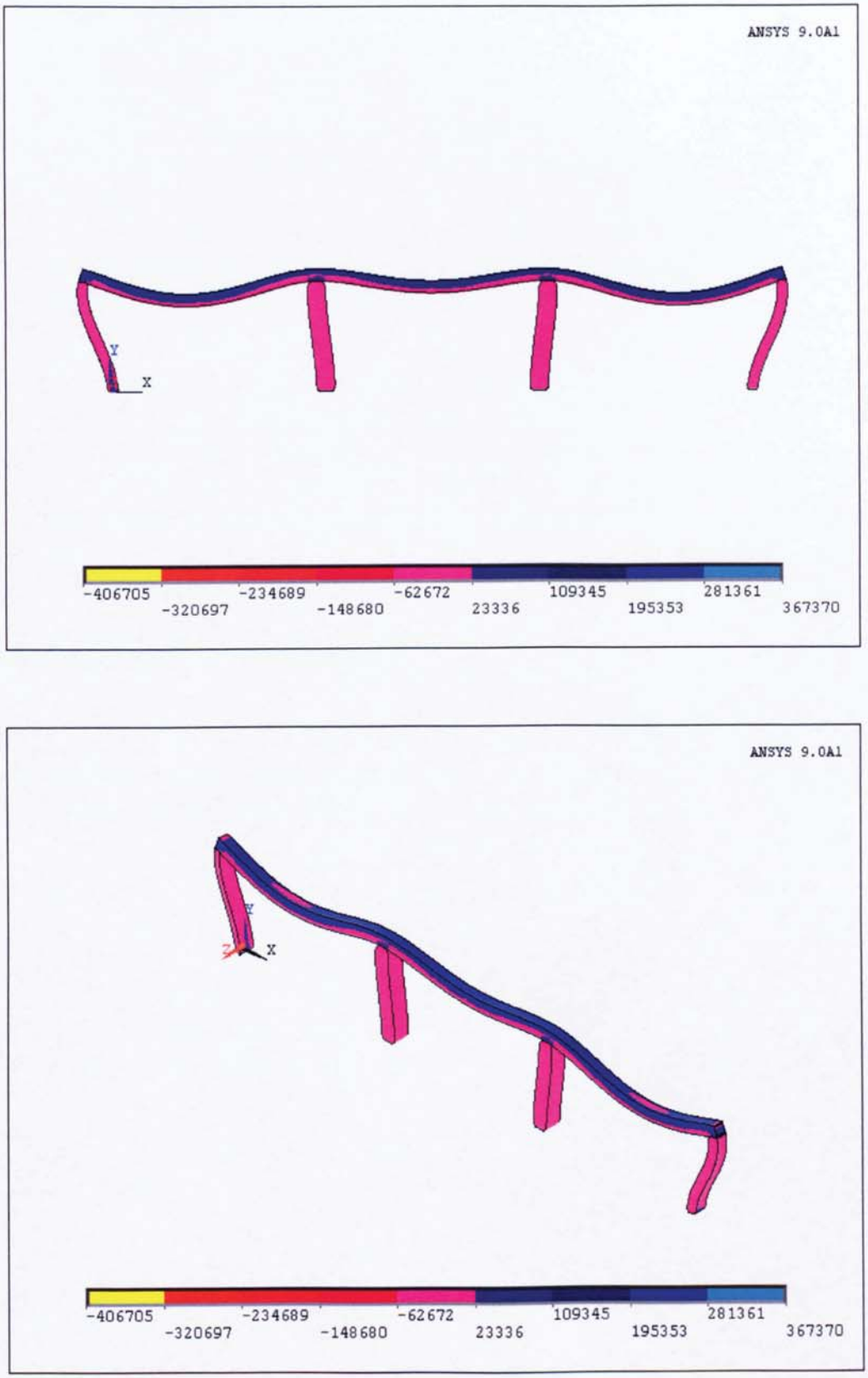

Figure 6.58 Distribution of maximum principal stress (Case 5)

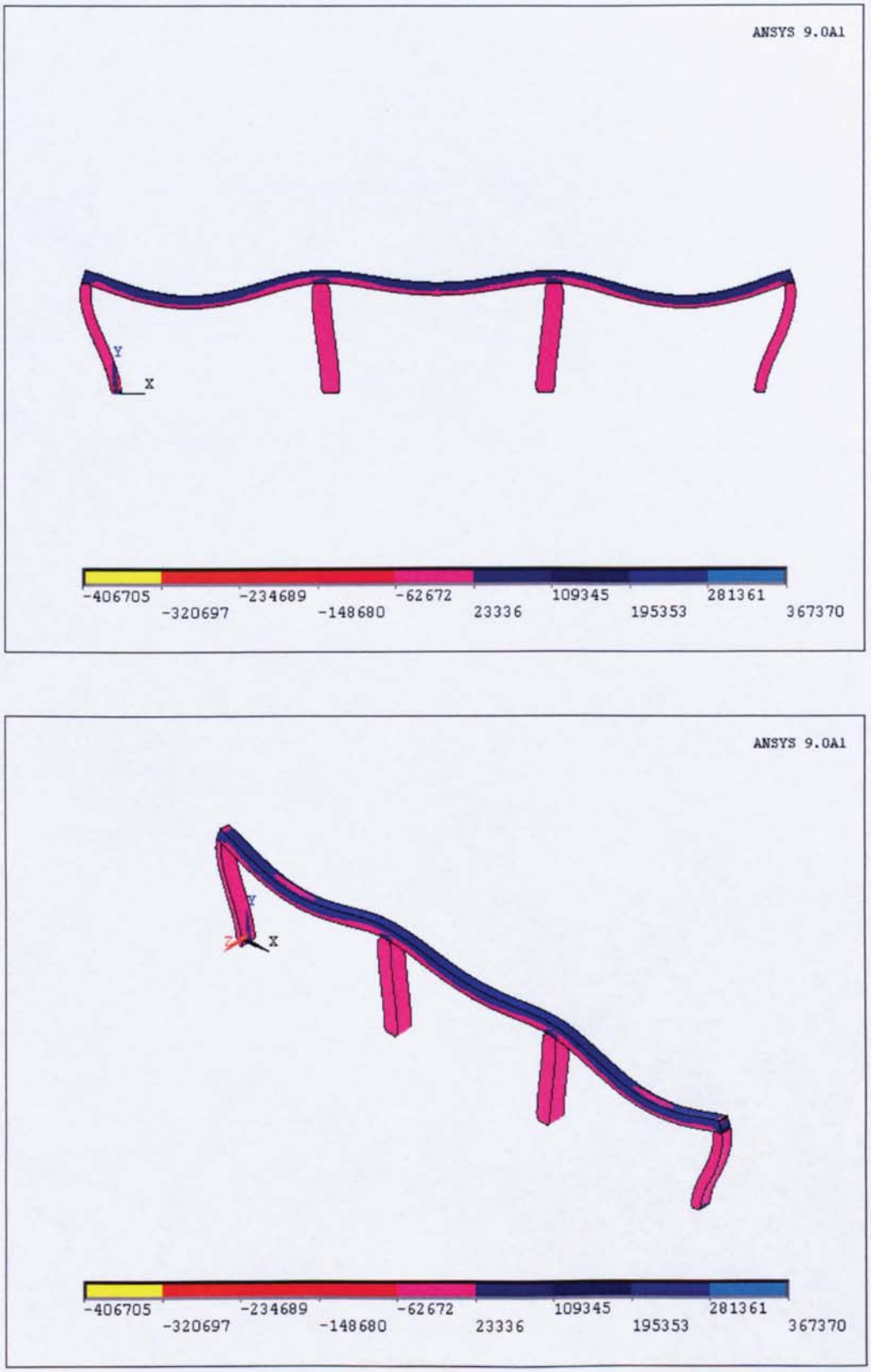

Figure 6.59 Distribution of minimum principal stress (Case 5)

6.4.3. Thermal Analyses without Transient Strains Included

In this case the fired compartment in the Case 4, where fired compartment is localised at two rooms of the internal and external rooms, is analysed without transient strains included. Concrete strength and Young's modulus at various temperatures can be obtained from the curves presented by Abrams (1968) and Philleo (1958), respectively. Thermal data for steel reinforcement from Holmes et al (1982) will also be employed. The reduction factor of strength and Young's modulus for concrete and steel reinforcement can be presented in Table 6.4 as follows:

Temperature	20°C	200°C	400°C	600°C	800°C
Concrete strength	1	0.9	0.8	0.3	0.2
Concrete Young's modulus	1	0.75	0.45	0.375	0.3
Steel strength	1	1	0.85	0.3	0.1
Steel Young's modulus	1	0.9	0.7	0.3	0.1

Table 6.6 Reduction factor of strength and Young's modulus of concrete and steel

Similar to previous cases, the temperature distribution of this case is based on the time-temperature curve given in Figure 6.26. The distribution of temperature of this case is shown in Figure 6.54 where the maximum temperature of about 929°C is found at the fired columns surfaces.

Figures 6.55 - 6.58 show the displacements and principal stresses of the elements. The maximum x-displacement of 28 mm occurs in the top of the right

external column, and the maximum vertical deflection of 47 mm is found in the firing external beam. In the beam, the maximum principal stress of 36.211 MPa and minimum principal stress of -21.464 MPa are found. While in the column, the minimum principal stress of -47.344 is found.

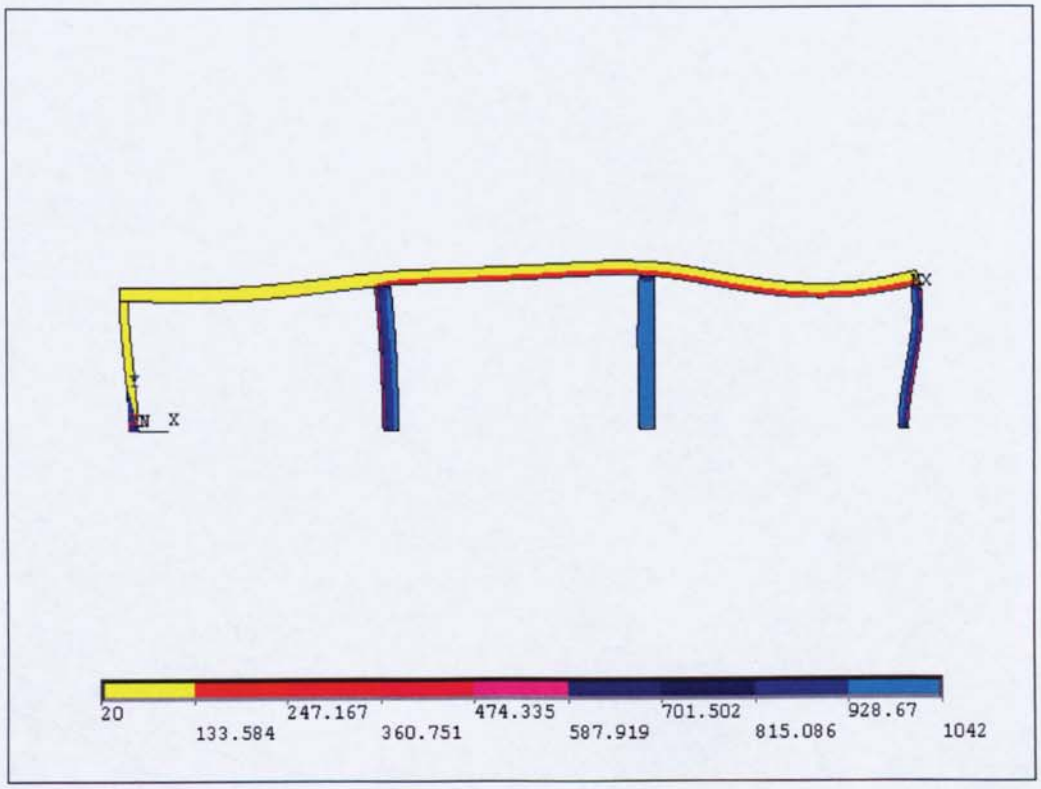

Figure 6.60 Temperature distributions (Case 4*)

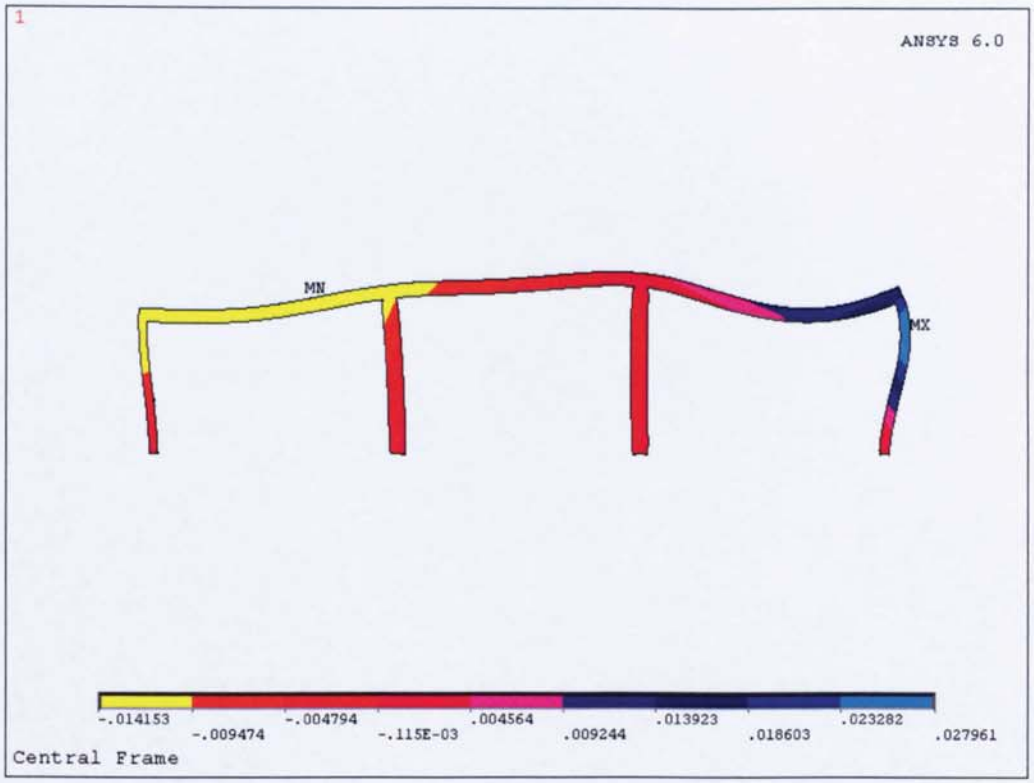

Figure 6.61 Displacements of the frame in the x – direction (Case 4*)

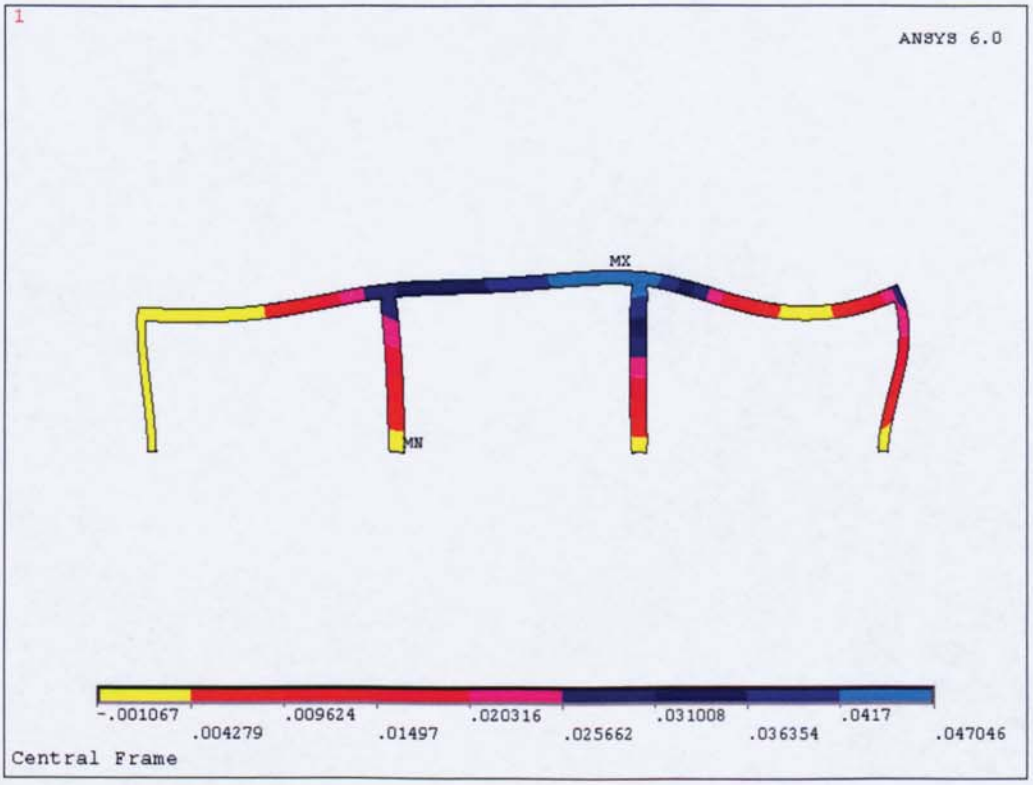

Figure 6.62 Displacements of the frame in the y – direction (Case 4*)

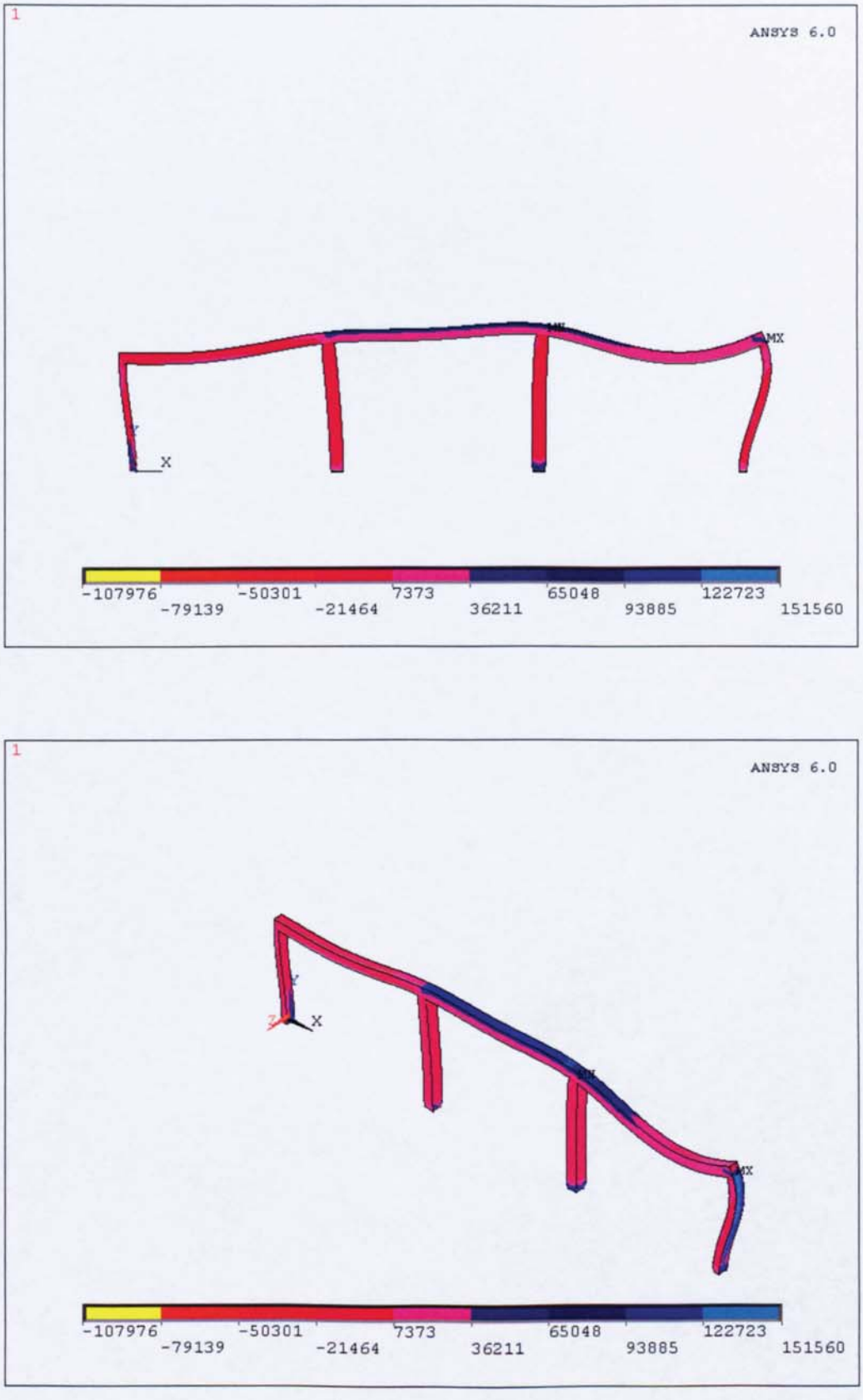

Figure 6.63 Maximum principal stress (Case 4*)

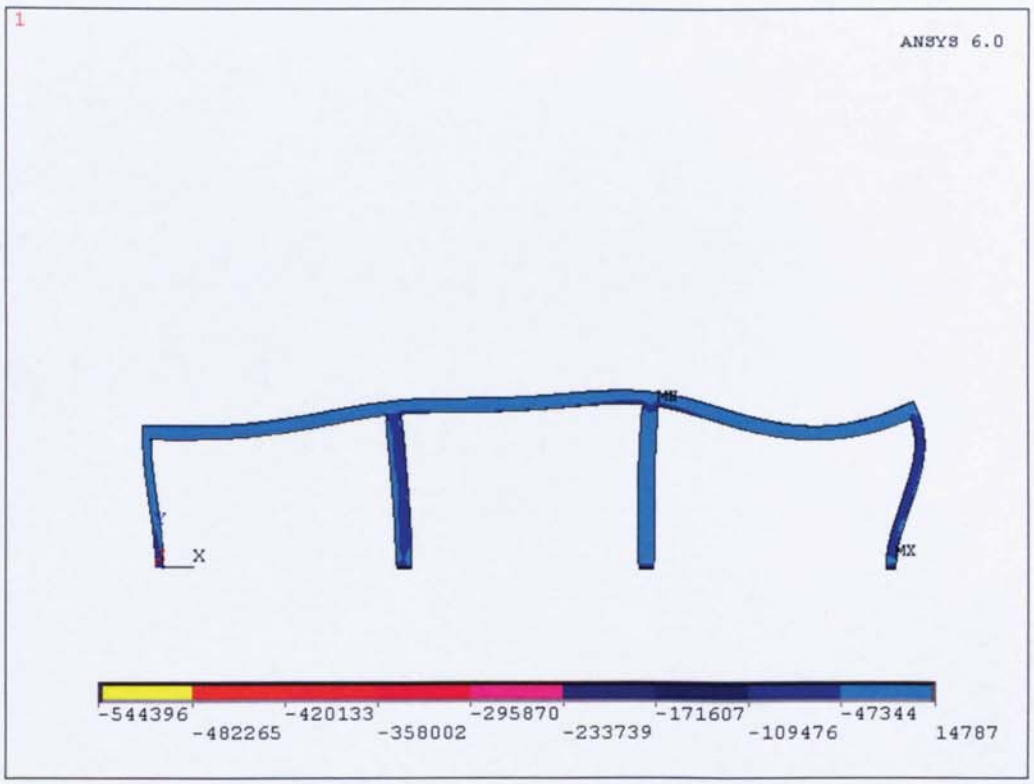

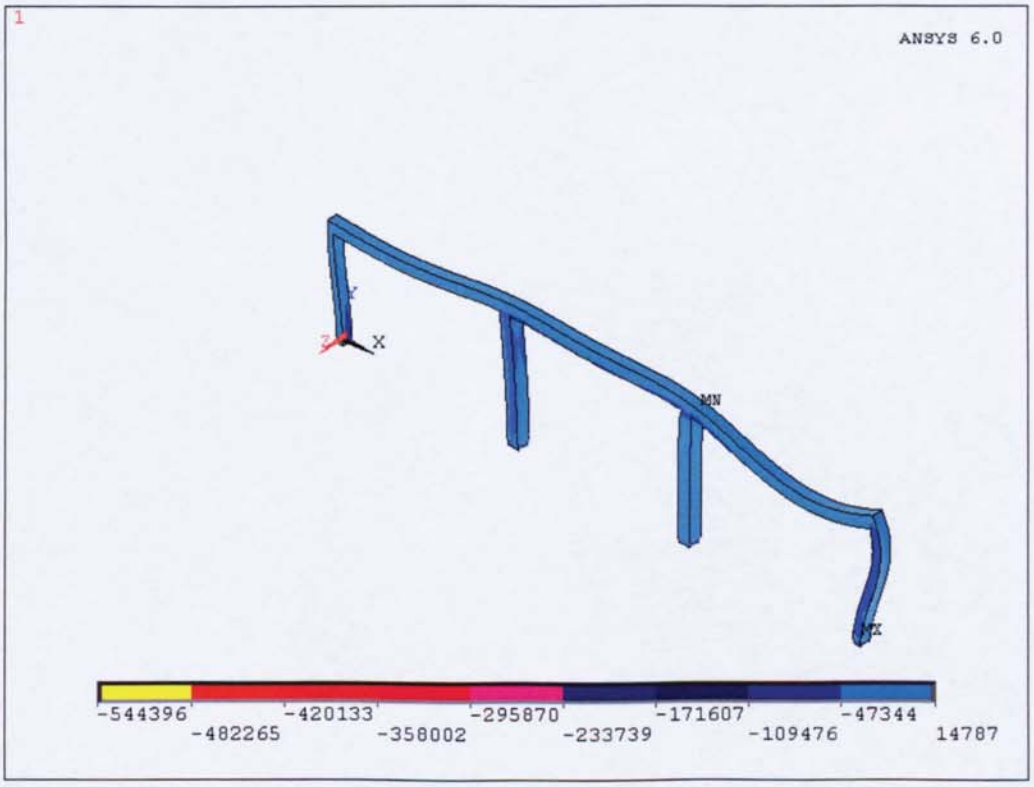

Figure 6.64 Minimum principal stress (Case 4*)

6.4.4. Observation of the Results

6.4.4.1. Summary of the results

Summary of the results of the all cases from the above analyses can be presented in Table 6.7 as follows:

	Case 1	Case 2	Case 3	Case 4	Case 5	Case 4*
Beam:						
Max T	20°C	935°C	890°C	935°C	935°C	929°C
Max Δx	3.5 mm	21 mm	11 mm	33 mm	27 mm	28 mm
Max Δy	13 mm	21 mm	12 mm	19 mm	21 mm	47 mm
f'_{max} (MPa)	23.881	25.127	23.063	19.223	23.336	14.787
f'_{min} (MPa)	-17.226	-35.672	-41.393	-47.276	-39.336	-32.557
Column:						
Max T	20°C	935°C	890°C	935°C	935°C	929°C
Max Δx	3.5 mm	21 mm	11 mm	33 mm	27 mm	28 mm
f'_{min} (MPa)	-32.858	-60.799	-64.456	-66.499	-62.672	-47.344

Table 6.7 Maximum/minimum stresses and displacements of all cases

Where: Max T is the maximum temperature of the element

Max Δx is the maximum displacement in the x (horizontal) direction

Max Δy is the maximum displacement in the y (vertical) direction

f'_{max} is the maximum tensile stress

f'_{min} is the maximum compressive stress

Case 4* is the Case 4 without transient strains included

6.4.4.1.1. Displacements

From Table 6.5 the maximum values of horizontal-displacement of 33 mm occurred in external column of the Case 4 and maximum vertical-displacement of 21 mm occurred in the external beam of the Case 2 and Case 5. The less significant values of the displacements are found in the Case 3 where the fire only exposed at one room in the middle.

The maximum displacements in all cases are satisfied to the normal limiting conditions for the stability performance criterion in BS 476 where the failure criteria for load bearing capacity in terms of deflection for beam is ≥ span/20 and for lateral column is ≥ 120 mm. However, the value of 33 mm lateral displacement in the column in Case 4 can be considered very significant since the initial displacement before fire was only 3.5 mm. This means that the lateral displacement of the column increased over 900% from the initial displacement before fire. This large lateral displacement of the external column is caused mainly by thermal expansion of the heated beams.

In fact, both BS 8110 and Eurocode 2 do not require the actual displacement to be calculated explicitly in ambient conditions and one is not concerned with deflection in an accidental situation. However, they recommend that the span/depth ratios should be satisfied. In this case the beams span/depth ratio of 18.75 (calculated from 7500/400) is satisfied both BS 8110 and Eurocode 2.

6.4.4.1.2. Stresses

It is interesting to notice that, from the Table 6.5, the highest maximum concrete compressive stresses of -47.276 MPa in the beam and -66.499 MPa in the column are both found in the Case 4 where the firing compartment localised at two rooms, i.e. the

internal and external rooms of the frame. On the other hand, the lowest maximum concrete compressive stresses of -35.672 MPa in the beam and -60.799 MPa in the column are both occurred in the Case 2 when the fire exposed only at one external room. The improvement of compressive stresses in the beams from the condition before firing in the Case 1 to after firing in the Case 2, Case 3, Case 4, Case 5 are 207%, 240%, 274%, and 228%, respectively. While in the column the improvement of the compressive stresses are 185%, 196%, 202%, and 191%, respectively.

The tension stress is assumed to be taken by the steel reinforcement. The critical temperature at the steel reinforcement is less than 400°C. According to Table 6.4, the temperature reduced steel strength is 0.85 f_y, thus, for all cases the steel strength are not significantly reduced. Therefore, further discussion would be focussed mainly on the compression stresses which will be taken by concrete strength.

The average concrete temperature within the element can be determined from arithmetic mean of concrete temperature at the surface, quarter depth-temperature and centre line temperature. In all cases, the critical average temperature is 402°C on the beams and 433°C on the column. Applying linear interpolation for strength reduction factor given in Table 6.4, the residual concrete strength reduction factors are 0.80 for the beam and 0.72 for the column. Assuming that concrete design strength of the beam f_{cu} = 61 MPa and column f_{cu} = 103 MPa, the temperature reduced permissible stresses, $\bar{f}_c$, of concrete beam and column would be:

- Beam : $\bar{f}_c = 0.80 \times 61 = 48.8$ MPa
- Column : $\bar{f}_c = 0.72 \times 103 = 74.2$ MPa

In order to identify how close each case to the failure, the values of compressive stresses given in Table 6.5 then be compared with the temperature reduced permissible stress. The fractional of the applied stresses compare to the reduced permissible stresses at the beams in Case 1, Case 2, Case 3, Case 4 and Case 5 are $0.28\,\bar{f}_c$, $0.73\,\bar{f}_c$, $0.85\,\bar{f}_c$, $0.97\,\bar{f}_c$ and $0.81\,\bar{f}_c$, respectively. And the applied stresses at the columns in the Case 1, Case 2, Case 3, Case 4, and Case 5 are $0.32\,\bar{f}_c$, $0.82\,\bar{f}_c$, $0.87\,\bar{f}_c$, $0.90\,\bar{f}_c$, and $0.84\,\bar{f}_c$, respectively. For all cases, the applied stresses are found lower than the permissible stresses. These indicate that the structure will not collapse assuming there is no spalling with beam and column further strength reduction.

6.4.4.1.3. Stress-strain model

The typical of stress-strain model of the concrete element of this investigation is illustrated in the curve presented in Figure 6.59. The curve of the stress-strain model is resulted from an element of concrete under compressive stress of the firing compartment. Adopting the transient analysis result, the stress-strain of the element can then be determined from the initial stress-strain before fire to the stress-strain under fire. In this case, the pre-load of 0.3 is adopted. Different element in every case will gives different values of the results, but the trends of the stress-strain curves are similar for the most all cases.

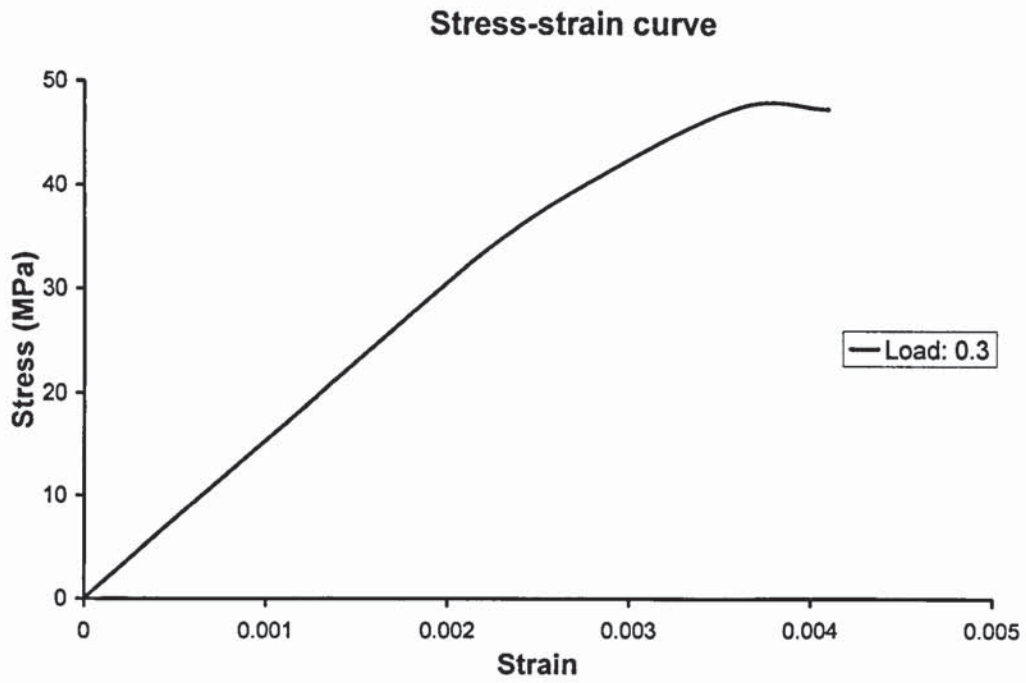

Figure 6.65 Typical of concrete stress-strain curve

6.4.4.2. Comparison of the models with and without transient strains included

In order to identify how significant the transient strains should be included to the analyses, a comparison between the applied stresses with and without transient strains included is presented. The stresses resulted from the analyses with transient strains included (Case 4) and without transient strain included (Case 4*) is given in Table 6.6.

From Table 6.6, the maximum tensile stress of the beam with transient strains included in the Case 4 is 130% higher than the result without transient strains included in the Case 4*. And, the maximum compressive stress is increase to 145% from -32.557 MPa in the Case 4* to -47.276 MPa in the Case 4. At the column, the maximum compressive stress with transient strains included in the Case 4 is 140% higher than the result of without transient strains included in the Case 4*. These significant increased of

the stresses can not be ignored in design. Therefore, designers are encouraged to include transient strains in the thermal analysis especially for structures exposed to fire at very high temperature.

	Case 4 (a)	Case 4* (b)	$\left(\frac{a}{b} \times 100\%\right)$
Beam:			
Max tensile stress (f'_{max})	19.223 MPa	14.787 MPa	130%
Max compressive stress (f'_{min})	-47.276 MPa	-32.557 MPa	145%
Column:			
Max compressive stress (f'_{min})	-66.499 MPa	-47.344 MPa	140%

Table 6.8 Comparison of max stresses with and without transient strains included

6.4.4.3. Load carrying mechanism

The objective of this section is to study the mechanism by which the structure sustains the applied load at elevated temperature. The comparison is made between Case 1 at condition before fire and Case 2 at elevated temperature when the thermal expansion is taken into account. It has been shown in previous section that the thermal expansion effects play considerable role with regard to the significant increase of displacement achieved, especially the horizontal displacements of the beam.

Comparison of maximum principal stress before fire and under fire is represented in Figure 6.56. This show the increases of horizontal displacements of the

beams indicate that the load carrying mechanism has been modified by thermal expansion at elevated temperature. The location of maximum tensile stress distribution in the middle span of beam at elevated temperature is moved upward compared to the initial maximum tensile stress before fire. These indicate that sagging moment occurred after fire is higher than before fire. It should be noted that the moment capacity of the beam will also reduce in real structures under fire due to concrete spalling at the bottom of the beams.

(a) Tensile stress before fire on Case 1 (b) Tensile stress under fire on Case 2

Figure 6.66 Comparison of maximum principal stress before fire and under fire

6.5. Summary

Performance of concrete frame structures when exposed under localised fire scenarios have been discussed in present investigation. Initial analysis of Cardington concrete frame carried out at Aston University prior to the test is presented. Three-dimensional finite element computer model using ANSYS is created as a subsequent fire compartment model of Cardington concrete frame building. The comparison of the analyses with and without transient strains included for both analyses of the Cardington concrete building and the created concrete frame structure are presented. The obtained conclusions from the present investigation are summarised in the following:

- The initial analysis carried out prior to the test was not included transient effects during the fire. The only temperature dependant of material property was Young's modulus. Therefore the result was likely to be conservative as no allowance is made for redistribution of internal forces due to transient effects.
- Further investigation using three-dimensional finite element computer model of concrete frame structure as a subsequent of Cardington concrete frame building considering transient effects gave reasonable results. The transient analysis of this model included additional specific heat to the base value of dry concrete at temperature 100°C and 200°C. The combined convective-radiation heat transfer coefficient and transient thermal expansion have also considered in this analysis. For the analysis with the transient strains included, the constitutive model proposed by Li and Purkiss (2005) is employed because this simple constitutive model can easily be incorporated into various commercial finite element analysis codes.
- When the comparison between the models with and without transient strains included is made, the maximum compressive stress of the beam of the model with transient strains included is increase to 145% from the model without transient strains included. At the column, the maximum compressive stress with transient strains included is 140% higher than the result of without transient strains included.
- The tension stress is assumed to be taken by the steel reinforcement. The critical temperature at the steel reinforcement is less than 400°C. In this condition, the

temperature reduced steel strength is 0.85 f_y, thus, for all cases the steel strength are not significantly reduced.

- The result of the present investigation indicated that the behaviour of complete structure is different from the behaviour of individual isolated member. Therefore, it is essential to develop new fire engineering methods from the study of complete structures rather than from isolated member behaviour.

Chapter 7 CONCLUSIONS AND FURTHER WORKS

7.1. Concluding Remarks

This research programme was carried out at the Aston University to investigate the behaviour of concrete frame structures under localised fire scenarios. The investigation included material properties, thermal and structural behaviour of concrete structures at elevated temperature. The conclusion of the present works are summarised below.

7.1.1. Literature Review

Chapter 2 examined the general review of structures under fire damages. The review commenced from early investigations to current investigations including the approaches of design methods, material properties at elevated temperature and thermal behaviour of the structures. The most significant findings in the literature review were:

- Demands on more sophisticated design methods of structures under elevated temperatures should be accommodated following the development in technology and its applications. The current codes were developed from isolated member of single element without paying attention to the interaction between the members of the entire structure when the elements are connected together. They ignore the inherent fire resistance of the whole structure. Therefore, development of new design methods based on holistic approach would be a major improvement on current design methods.
- Unlike the thermal-strain which is a function of only temperature, the transient-strain together with creep-strain and instantaneous stress-related strain are functions of stress and temperature. The transient-strain component can not be measured directly in the tests. Li and Purkiss (2005) developed model based on

the Anderberg and Thelandersson's (1976) model with considering the transient-strain and it is a full thermal strain-stress model in an empirical formula based on the plotted results of the average Young's modulus. This simple constitutive model can be easily adopted into various finite element analysis codes using commercial computer program.

- Predicted temperature using coupled heat and mass transfer analyses have very good agreement with experimental results. However, the use of heat transfer alone rather than coupled heat and mass transfer can be considered by including additional specific heat to the base value of dry concrete.
- In order to simplify the calculation on heat transfer analyses, a combined convective-radiation heat transfer coefficient can also be considered in the analysis by modified the value of convective heat transfer coefficient.

7.1.2. Fire Test on the Cardington Concrete Building

The full-scale seven-storey BRE Cardington concrete building constructed with elements formed of normal and high-strength concrete. The building was part of the European Concrete Building Project designed to the limits of ENV 1992-1-1. This building was also designed to provide a minimum of 60 minutes fire resistance period. The results obtained from this study have shown that:

- The results and observations from test on a complete frame concrete structure indicated that the current design methods are based on an incorrect model of structural behaviour. The current design codes and design methods do not incorporate the beneficial effects of compressive membrane action of the heated floor slab. The detrimental effect of lateral displacement due to large thermal expansion of the heated slab has also not been accommodated in the current

design codes. The large lateral movement of the heated floor can cause failure of the vertical members of the structures such as external columns and walls.

- The lateral displacements of the external columns due to thermal expansion of the floor slab induced additional column moment. The lateral movement of the external columns has been identified as the cause of previous failure of concrete structures. Although the thin external columns of the Cardington building showed no signs of distress and was able to accommodate these movements, designer should be aware of this behaviour and ensure that the external columns can withstand the lateral displacement during fire.
- Consideration of materials characteristics and instrumental design are required to optimise the behaviour of real fire in a structure. Designers should also consider the spalling of concrete when specifying fixing between compartment wall and the soffit of concrete slab. The effect of concrete spalling on fixings was not anticipated in this test with the consequence of the fire escaping the compartment area and destroyed the cables resulting in the loss of valuable data.

7.1.3. Description of the Computer Program (ANSYS)

The description of computer program has illustrated with conduction elements used by ANSYS. When a comparison with numerical calculation by Tenchev *et al* (2001) and experimental data from Ahmed and Hurst (1997) are made, the result has a reasonable agreement.

At concrete surface, the agreement is very good. However, at another distances throughout the concrete element, the result is slightly higher because both the numerical and experimental results used couple heat and mass transfer rather than the use of heat transfer alone used by the program. However, finite element analyses remain the most excellent approach for both structural and thermal analyses.

7.1.4. Thermal Analysis of Structural Element

The steady-state and transient analyses of temperature distribution within the member of structural element were simulated using ANSYS and some of the results have been validated satisfactory by finite element analysis. The main findings of the examined work are listed in the following:

- At an elevated temperature, the temperature of concrete surface is approximately 10% lower than the atmosphere temperature.
- The temperature within the element remain 20°C at distances 150 mm, 170 mm, and 250 mm from the fire surface for the fire durations of 30, 60, and 120 minutes, respectively. This indicates that concrete is an insulated material where the temperature at the surface of unexposed fire depend upon the thickness of the element, the properties of the materials and the duration of the fire.
- When the element is exposed to fire at multi surfaces, the temperature distribution through normal direction from one surface is not affected by temperature distribution from any other surface.
- The agreement between the computed results by ANSYS and the calculated result using finite element analysis as well as experimental results are reasonable. Therefore, the use of ANSYS program can be continued to obtain approximate solutions in variety problems of thermal analysis.

7.1.5. Concrete Frame Structure under Structural and Thermal Analyses

Preliminary analysis carried out at Aston University prior to the test of Cardington concrete frame is presented with and without transient strains. And modelling of concrete frame structure as a substructure of the whole building is investigated under variety of fire compartment scenarios. The comparison of the analyses with and without

transient strains included for both analyses of the Cardington concrete building and the created concrete frame structure are discussed. The conclusions of the concrete frame structure under structural and thermal analyses can be described as follows:

- The initial analysis carried out prior to the test was not included transient strains. The only temperature dependant of material property was Young's modulus. Therefore the result was likely to be conservative as no allowance is made for redistribution of internal forces due to transient effects.
- Further investigation using three-dimensional finite element computer model of concrete frame structure as a subsequent of Cardington concrete frame building considering transient effects gave reasonable results. The transient analysis of this model included additional specific heat to the base value of dry concrete at temperature 100°C and 200°C. The combined convective-radiation heat transfer coefficient and transient thermal expansion have also considered in this analysis. For the analysis with the transient strains included, the constitutive model proposed by Li and Purkiss (2005) is employed because this simple constitutive model can easily be incorporated into various commercial computer programs.
- When the comparison between the models with and without transient strains included is made, the maximum compressive stress of the beam of the model with transient strains included is increase to 145% from the model without transient strains included. At the column, the maximum compressive stress with transient strains included is 140% higher than the result of without transient strains included.
- The tension stress is assumed to be taken by the steel reinforcement. The critical temperature at the steel reinforcement is less than 400°C. In this condition, the

temperature reduced steel strength is 0.85 f_y, thus, for all cases the steel strength are not significantly reduced.

7.1.6. Design Implications

The result and observation of this study support the suggestion of previous researchers that the current fire design methods, which are predominantly based on the fire resistance of individual members used to construct the structure, is not likely adequate for the entire structure. The result of this study indicated that the behaviour of the complete structure is significantly different from the behaviour of individual isolated member. It is essential to develop new fire engineering methods from the study of complete concrete structures rather than from isolated member behaviour.

Although the current tabulated design procedures are conservative when the entire building performance is considered, it should be noted that the beneficial and detrimental effects of thermal expansion in complete structures should be taken into account. Design method to incorporate the beneficial effects of compressive membrane action due to thermal expansion of the slabs can then be explored. Design method to integrate the detrimental effects from the inability of vertical members to resist against the large lateral displacements caused by the thermal expansion of the heated floor slab can also be accommodated. The design method can then be used as design guidance for practitioners.

7.2. Suggestion for Further Works

Concrete slabs supported directly by high-strength concrete columns are widely used in the European buildings. In the event of fire, shear failure often occurred within the slabs near the connection to the columns. However, to the best of the author's knowledge,

there are very limited documented researches on the slab-column connection. In the last decade, some research efforts were directed towards the structural behaviour of complete structures and paying little attentions to the shear failure of slab-column connections. Therefore, considerable attention for further works may be given to the behaviour of concrete slab-column connection under fire as illustrated in Figure 7.1.

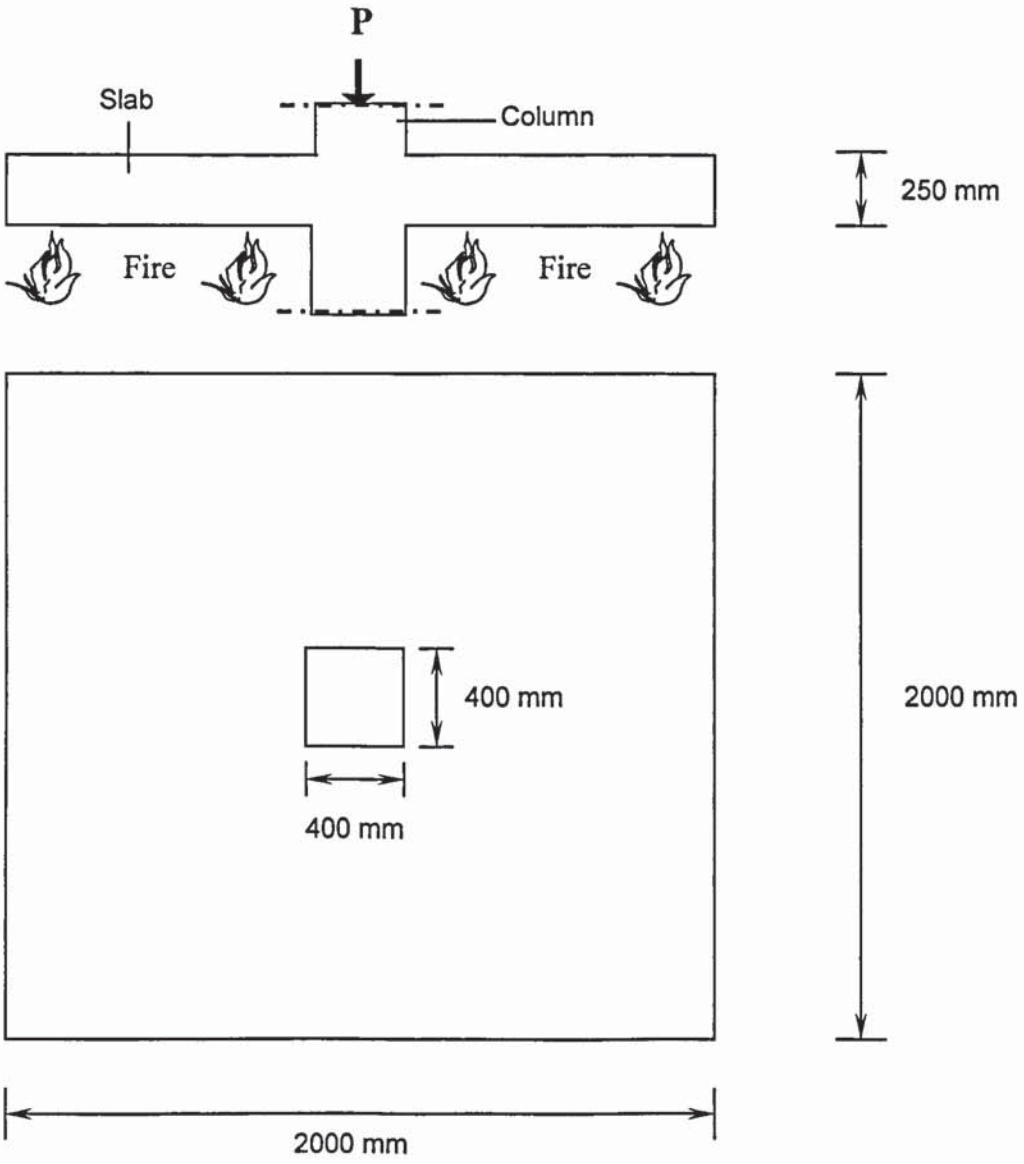

Figure 7.1 Concrete slab-column connection under fire

In modelling the reinforced concrete slabs, special nonlinear spring elements are employed along four edges of the slabs. The stiffness of the spring elements can be

assumed to be infinity when in compression and zero when in tension. The proper simulation of the boundary condition becomes very important in order to obtain the satisfactory prediction of the slab response. The reinforcing steels can be simply represented by layers of uniform thickness located at constant relative depth inside the concrete element. The model can be simplified using one-quarter slab. The purpose finite element model of one-quarter slab is illustrated in Figure 7.2.

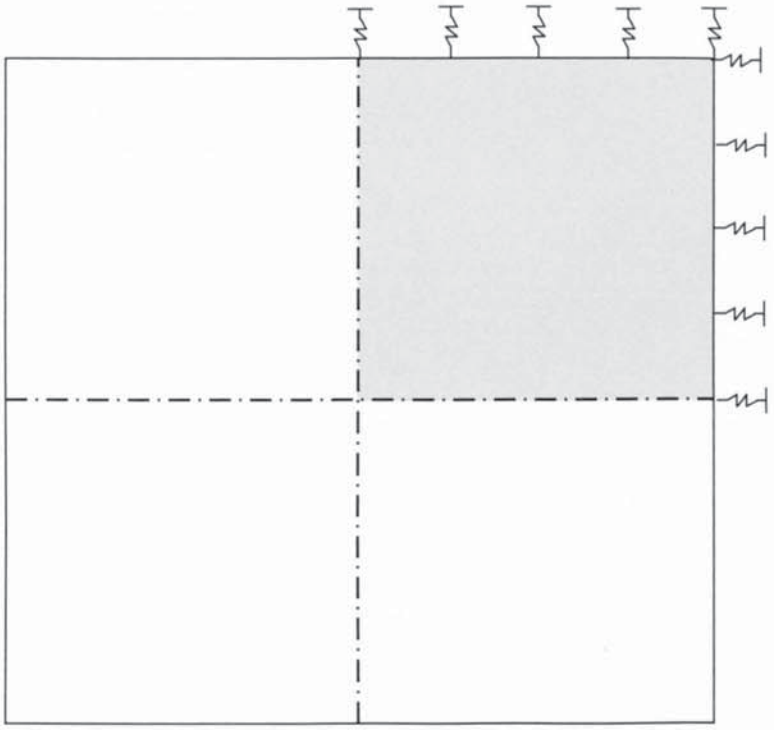

Figure 7.2 Finite element model of one-quarter slab

Additional simulation can also be made to the large lateral displacement of the high-strength concrete column. The large lateral displacement can be caused by thermal expansion of the slab. The effect of large lateral displacement may lead to premature collapse of the whole building at elevated temperature. This form of behaviour can be used by designers and practitioners to predict accurately the behaviour of the whole building under fire.

REFERENCES

Abrams, M.S (1968) *Compressive strength of concrete up to 1600°F (871°C)*, in Temperature and Concrete, Special Publication SP-25, American Concrete Institute, Detroit, pp.33-58.

Ahmed, G.N. and Hurst, J.P. (1997) *An analytical approach for investigating the cases of spalling of high-strength concrete at elevated temperatures*, International Workshop on Fire Performance of High-Strength Concrete, NIST Gaithersburg, MD, 13-14 February 1997, Paper B.6, pp. 95-108.

Al-Mutairi, N.M., and Al-Shaleh, M.S. (1997) *Assessment of fire-damaged Kuwaiti structures*, Journal of Materials in Civil Engineering, ASCE, Vol. 9, No.1, pp.7-14.

Ang, C.N. (2004) *Combined heat and mass transfer analysis in hydroscopic material under fire conditions*, PhD Thesis, University of Manchester, Manchester Centre for Civil and Construction Engineering.

Armer, G.S.T. and Moore, D.B. (1994) *Full-scale testing on complete multi-storey structures*, the Structural Engineer, Vol. 72, No. 2, pp. 30-31.

Anderberg, Y. (1976) *Fire exposed hyperstatic concrete structures – an experimental and theoretical study*, Bulletin 55, Lund Institute of Technology, Lund, Sweden.

Anderberg, Y. (1983) *Properties of material at high temperatures – Steel*, RILEM Technical Committee Report, Division of Building Fire Safety and Technology, Lund Institute of Technology, Lund, Sweden.

Anderberg,Y., and Thelandersson, S. (1973) *Stress and deformation characteristics of concrete at high temperatures*: *General discussion and critical review of*

literature, Bulletin 34, Division of Structural Mechanics and Concrete Construction, Lund Institute of Technology, Lund, Sweden.

Anderberg,Y., and Thelandersson, S. (1976) *Stress and deformation characteristics of concrete at high temperatures: Experimental investigation and material behaviour model*, Bulletin 54, Division of Structural Mechanics and Concrete Construction Lund Institute of Technology, Lund, Sweden.

ANSYS (2002) *Version 6.0 documentation*, Swanson Analysis Systems, Inc. USA.

ASCE (2002) *Structural fire protection*, ASCE Manuals and Reports on Engineering Practice, No 78, the American Society of Civil Engineers, USA.

ASFP (1992} *Fire protection for structural steel in buildings*, the Association of Specialist Fire Protection, Ascot, the Steel Construction Institute.

ASTM (1985) *Standard methods of fire tests of building construction and materials*, ASTM E119, American Society for Testing and Materials, Philadelphia, USA.

Axenenko, O. and Thorpe, G. (1996) *The modelling of dehydration and stress analysis of gypsum plasterboards exposed to fire*, Computational Material Science, No. 6, pp. 281-294.

Bailey, C. (2002) *Holistic behaviour of concrete buildings in fire*, Proceedings of the Institution of Civil Engineers, Structures & Buildings, Vol. 152 Issue 3, August 2002, pp. 199-212.

Bailey, C. (2004) *A simplistic or holistic approach to structural fire engineering?*, One Day Conference, School of Engineering and Applied Science, Aston University, Birmingham, 16 September 2004, pp. 1-9.

Bailey, C.G., Lennon, T. and Moore, D.B. (1999) *The behaviour of full-scale steel-framed buildings subjected to compartment fires*, The Structural Engineer, London, Vol. 77 No 8, 20 April 1999, pp. 15-21.

Bailey, C.G. and Moore, D.B. (2000a) *The structural behaviour of steel frames with composite floor slabs subject to fire: Part 1: Theory*, The Structural Engineer, London, Vol. 78 No 11, 6 June 2000, pp. 19-27.

Bailey, C.G. and Moore, D.B. (2000b) *The structural behaviour of steel frames with composite floor slabs subject to fire: Part 2: Design*, The Structural Engineer, London, Vol. 78 No 11, 6 June 2000, pp. 28-33.

Becker, J., and Bresler, B. (1974) *FIRES-RC, a computer program for the fire response of structures – reinforced concrete frame*, Report No UCB – FRG 74-3, Department of Civil Engineering, University of Berkeley, California, USA.

Bennetts, I.D. and Goh, C.C. (2001) *Fire behaviour of steel members penetrating concrete walls*, Electronic Journal of Structural Engineering, Vol. 1, pp. 38-51.

Bishop, P. (1991) *Blaze adds to insurer unease*, New Civil Engineer, 15th August 1991, pp.4.

Bottke, H. (1931) *Behaviour of reinforced concrete structures in fire*, Beton und Eisen, 30, Germany.

British Standards Institution (1978-1991) *Fire precaution in the design and construction of buildings*, British Standards Institution, London, BS 5588, Part 1-11.

British Standards Institution (1985) *Structural use of concrete: Code of practice for special circumstance,* British Standards Institution, London, BS 8110, Part 2.

British Standards Institution (1987), *Method for the determination of the fire resistance of elements of construction*, British Standards Institution, Luton, BS 476, Part 20.

British Standards Institution (1989), *Structural use of concrete: Code of practice for design and construction,* British Standards Institution, London, BS 8110 Part 1.

British Standards Institution (1989), *Structural use of concrete: Code of practice for special circumstances,* British Standards Institution, London, BS 8110 Part 2.

British Standards Institution (1990) *Structural use of steelwork in buildings: Code of practice for fire resistant design*, British Standards Institution, London, BS 5950, Part 8.

British Standards Institution (1996), *Loading for buildings: Code of practice for dead and imposed loads,* British Standards Institution, London, BS 6399, Part 1.

Building Research Establishment (2002), *Fire test on the Cardington concrete frame,* Building Research Establishment Ltd.

Byrd, T. (1992) *Sprinklers dry as Expo burned*, New Civil Engineer, 27th February 1992, pp.5.

Byrd, T. (1992) *Burning question*, New Civil Engineer, 27th February 1992, pp.12-13.

Cardoso, J.L. (1992) *Rehabilitation of works in reinforced and prestressed concretes*, Proceeding Rehabilitation of Damaged Buildings, *International Conference*: Sick Building Syndrome, Kuwait, Council of Tall Buildings and Urban Habitat, Bethlehem, pp. 180-200.

CEB (1982) *Design of concrete structures for fire resistance,* Bulletin D'Information, No.145, Paris.

Chana, P. (2000) *The European concrete building project*, The Structural Engineer, Vol. 78 No.2, January 2000, pp. 12-13.

Chana, P., and Moss, R.M. (2001) *Re-engineering the design and construction processes for in-situ concrete frames*, Structural Concrete, No. 2, pp. 49-61.

Chana, P., and Price, B. (2003) *The Cardington fire test*, Concrete, The Concrete Society, Berkshire, January 2003, Vol. 37, No. 1, pp. 28-33.

Clough, R.W. (1960) *The finite element method in plane stress analysis*, Proceedings of ASCE, 2nd Conference on Electronic Computations, Pittsburgh, Vol. 23, pp. 345-378.

Concrete Society (1978) *Assessment of fire damaged concrete structures and repair by gunite*, The Society, Technical Report No. 15, London, England.

Concrete Society (1990) *Assessment and repair of fire damaged concrete structures,* The Society, Technical Report No. 33, Slough, England.

Connolly, R.J. (1995), *The spalling of concrete in fires*, PhD Thesis, University of Aston in Birmingham.

Courant, R. (1943) *Variational methods for the solutions of problems of equilibrium and vibrations*, Bulletin of the American Mathematical Society, Providence, Vol. 49, pp. 1-23.

Department of the Environment (1992), *Building regulation and fire safety: procedural guidance*, Department of the Environment, London.

Dougill, J.W. (1971) *The effect of high temperature on concrete with reference to thermal spalling*, PhD Thesis, Imperial College, London.

Drysdale, D. (1985) *An introduction to fire dynamics*, John Willey and Sons, Chicester.

El-Rimawi, J.A., Burgess, I.W. and Plank, R.J. (1995) *The analysis of semi-rigid frames in fire – a secant approach*, Journal of Construction Steel Research, Vol. 33, pp. 125-146.

Eurocode 1 (2001) *Action on structures: General actions – Actions on structures exposed to fire,* European Committee for Standardisation, Brussels, 19 December 2001, prEN 1992-1-2, Final Draft, Part 1.2.

Eurocode 2 (1994) *Supplementary rules for structural fire design*: *Design of concrete structures – Structural fire design* (Draft), European Committee for Standardisation, ENV 1992-1-2, N 232 E, Part 10.

Eurocode 2 (1994) *Supplementary rules for structural fire design*: *Design of steel structures – Structural fire design* (Draft), European Committee for Standardisation, ENV 1993-1-2, N 232 E, Part 10.

Eurocode 2 (2001) *Design of concrete structures: General rules – Structural fire design,* European Committee for Standardisation, Brussels, July 2001, prEN 1992-1-2, 2nd Draft, Part 1.2.

Eurocode 2 (2002) *Design of concrete structures: General rules – Structural fire design,* European Committee for Standardisation, Brussels, prEN 1992-1-2, Part 1.2.

Eurocode 3 (1995) *Design of steel structures: Supplementary rules for structural fire design*, British Standards Institution, London, ENV 1993-1-2, Part 1.2.

Eurocode 4 (1994) *Supplementary rules for structural fire design*: *Design of composite steel and concrete structures*, British Standards Institution, London, ENV 1994-1-2, Part 1.2.

European Committee for Concrete (1962) *The application of the yield-line theory to calculation of the flexural strength of slabs and flat-slab floors*, Information Bulletin No.35, Cement and Concrete Association, London.

FIP/CEB (1978) *Report on methods of assessment of the fire resistance of concrete structural members*, Cement and Concrete Association.

Fire Protection Association (1965) *Introduction to fire: Nature, effect, control,* Planning for Fire Safety in Buildings Series: 1, Fire Protection Association, London, England.

Fire Protection Association (1999) *Design-guide for the fire protection of building 2000: A code of practise for the protection of business*, Loss Prevention Council, Fire Protection Association, London, England.

Forsen, N.E. (1982) *A theoretical study on the fire resistance of concrete structures*, Cement and Concrete Research Institute, Report STF65 A82062, Norwegian Institute of Technology, Trondheim, Norway.

Green, B. (2003) *Fire protection: Burning issues,* Construction Product, Construction News, London, April/May 2003, pp. 6-8.

Green, J.K. (1971) *Reinstatement of concrete structures after fire*, The Architect Journal, London, UK, 141(2), pp. 93-99.

Gross, H. (1973) *On high temperature creep of concrete,* 2nd International Conference on Structural Mechanics in Reactor Technology, Vol. 3, Part H 6/5, Berlin.

Gustaferro, A.H. (1985) *Fire resistance*, Handbook of Concrete Engineering, 2nd ed., M. Fintel, ed., Chapman and Hall, Ltd., London, UK, pp. 212-228.

Harmathy, T.Z. (1970) *Creep deflection of beam*, ASTM National Structural Engineering Meeting Pre-print 2216.

Harmathy, T.Z. (1993) *Fire safety design and concrete*, Longman Scientific and Technical, Harlow, England.

Holmes, M., Anchor, R.D., Cooke, G.M.E. and Crook, R.N. (1982) *The effects of elevated temperatures on the strength properties of reinforcing and prestressing steels*. The Structural Engineer, London, Vol. 60B, pp. 7-13.

Huang, Z.H., Burgess, I.W. and Plank, R.J. (2002) *Modelling of six full-scale fire tests on a composite building*, The Structural Engineer, London, Vol. 80 No.19, pp. 30-37.

Huebner, K.H., Thornton, E.A. and Byrom, T.G. (1995) *The finite element method for engineers*, 3rd Edition, John Wiley & Sons Inc., New York, USA.

Hyatt, T. (1877) *An account of some experiments with Portland cement concrete,* Chiswich Press, London.

Iding, R.J., Bresler, B., and Nizamuddin, Z. (1977) *FIRES-RCII, A computer program for the fires response of structures – reinforced concrete frames*, Report No UCB – FRG 77-8, University of Berkeley, California, USA.

ISE and Concrete Society (1978) *Design and detailing of concrete structures for fire resistance,* The Institution of Structural Engineers, London, UK.

ISO 834 (1987) *General requirements for fire resistance testing – Elements of building construction,* British Standard Institution, London.

IStructE (2003) *Introduction to the fire safety engineering of structures*, The Institution of Structural Engineers, September 2003, London.

Ingberg, S.H (1928) *Test of the severity of building fires,* US National Fire Protection Quarterly, Vol. 22, pp. 43-61.

Institution of Structural Engineers and Concrete Society (1978) *Design and detailing of concrete structures for fire resistance,* the Institution of Structural Engineer, April 1978, London.

Izzuddin, B.A. and Moore, D.B. (2002) *Lessons from a full-scale fire test*, Proceedings of the Institution of Civil Engineers, Structures & Buildings, Vol. 152, Issue 4, November 2002, pp. 319-329.

Khoury, G. (2000) *Effect of fire on concrete and concrete structures*, Progress in structural engineering and materials, Vol. 2, 2000, pp. 429-447.

Khoury, G.A., Grainger, B.N., and Sullivan, P.J.E. (1985a) *Transient thermal strain of concrete: literature review, conditions within specimen and behaviour of individual constituents*, Magazine of Concrete Research, Vol. 37, No. 132, September 1985, pp. 131-144.

Khoury, G.A., Grainger, B.N., and Sullivan, P.J.E. (1985b) *Strain of concrete during first heating to 600°C under load*, Magazine of Concrete Research, Vol. 37, No. 133, December 1985, pp. 195-215.

Kitchen, A. (2001) *Polypropylene fibres reduce explosive spalling in fire*, Concrete, Vol. 35, No.4, April 2001, pp. 40-41.

Lawson, R.M. (1990) *Behaviour of steel beam-to-column connection in fire*, Structural Engineer, Vol. 63 No. 14, pp. 263-271.

Lennon, T., Bullock, M. and Enjily, V. (2000) *The fire resistance of timber frame building*, BRE Report No. 79486-1, Garston, BRE.

Leston-Jones, L.C., Burgess, I.W., Lennon, T. and Plank, R.J. (1997) *Elevated temperature moment-rotation tests on steelwork connections*, Proceeding of the Institution of Civil Engineers for Structures & Buildings, No. 122, November 1997, pp. 410-419.

Li, L.Y. and Purkiss, J.A. (2005) *Stress-strain constitutive equations of concrete material at elevated temperatures*, Fire Safety Journal, Vol. 40, No.4, October 2005, pp. 669- 686.

Li, L.Y., Purkiss, J.A., and Tenchev, R.T. (2002) *An engineering model for coupled heat and mass transfer analysis in heated concrete*, Proceeding of Institution of Mechanical Engineers, Vol. 216 Part C: Journal of Mechanical Engineering Science, London, UK, pp. 213- 224.

Lie, T.T. (1972) *Fire and building*, Applied Science Publishers Ltd., London, UK.

Lie, T.T. (1977) *A method of assessing the fire resistance of laminated timber beams and columns*, Canadian Journal of Civil Engineering, Vol. 4, pp. 161-169.

Lie, T.T. (1992) *Principles of structural fire protection*, In Lie T.T. (Ed.), Structural Fire Protection, ASCE Manual and Report on Structural Engineering Practice, No 78.

Lie, T.T. and Woollerton, J.L. (1988) *Fire resistance of reinforced concrete column – Test results*, Internal Report No. 569, National Research Council Canada.

Malhotra, H.L. (1982) *Design of fire resisting structures*, Surrey University Press, London.

Malhotra, H.L. (1984) *Spalling of concrete in fires*, Technical Note 118, CIRIA, London.

Malhotra, H.L. (1986) *A survey of fire protection developments for buildings*, in *Design of structure against fire*, Eds RD Anchor, HL Malhotra and JA Purkiss, Elsevier Applied Science, London, pp. 1-13.

Mehaffey, J.R., Cuerrier, P. and Carisse, G. (1994) *A model for predicting heat transfer through gypsum-board/wood-stud walls exposed to fire*, Fire Material, Vol. 18, pp. 297-305.

Moaveni, S. (2003) *Finite element analysis: Theory and application with ANSYS*, Prentice-Hall, Upper Saddle River, New Jersey, USA.

Muirhead, J. (1993) *Making it safely through construction*, Fire Surveyor, No.22, pp.5-7

Petterson, O., Magnusson, S.E. and Thor, J. (1976) *Fire engineering design of steel structures*, Publication No. 50, Swedish Institute of Steel Construction, Sweden.

Philleo, R. (1958) *Some physical properties of concrete at high temperatures*, Proceedings of the American Concrete Institute, No. 54, pp. 857-64.

Placido, F. (1980) *Thermoluminescence test for fire damaged concrete*, Magazine of Concrete Research, 32 (111), pp. 112-116.

Poh, K.W. (1996) *Modelling elevated temperature properties of structural steel*, BHP Research, Report No. BHPR/SM/R/055, September 1996, Australia.

Purkiss, J.A. (1985) *Some mechanical properties of glass fibre reinforced concrete at elevated temperature*, In Marshall, I.H (Ed.), Composite-3, Elsevier Applied Science Publisher, London, pp. 230-241.

Purkiss, J.A. (1986) *High temperature effects*, In Anchor, R.D., Malhotra, H.L., and Purkiss J.A (Eds.), Design of Concrete Against Fire, Elsevier Applied Science Publisher, London, pp. 41-51.

Purkiss, J.A. and Bali (1988) *The transient behaviour of concrete at temperatures up to 800°C*, In Proceeding of the 10th Ibausil, Hochschule fur Architektur und Bauwesen, Weimar, Section 2/1 pp. 234-239.

Purkiss, J.A. (1990) *Computer modelling of concrete structural elements exposed to fires,* Interflam'90, 5th International Fire Conference, Interscience Communications Limited, London, 3-6 September 1990, pp. 67-73.

Purkiss, J.A. (1996) *Fire safety engineering design of structures*, Butterworth-Heinemann. Oxford, England.

Purkiss, J.A. (2000) *High-strength concrete and fire*, Concrete, Vol. 34, No.3, March 2000, pp. 49-50.

Ramberg, W. and Osgood, W. (1942) *Description of stress-strain curve by three parameters*, National Advisory Committee for Aeronautics, Technical Note No. 902.

Read, R.E.H. and Morris, W.A. (1993) *Aspect of fire precautions in buildings*, 3rd Edition, Department of the Environment, London.

Robbins, J. (1990) *Baptism of fire*, New Civil Engineer, 12th July 1990, pp. 17-19.

Rosato, C. (1992) *London Underwriting Centre*, Fire Prevention, No.248, pp 33-35.

Schaffer, E.L. (1967) *Charring rate of selected wood – transverse to grain*, FPL 69, US Department of Agriculture, Forest Service, Forest Products Laboratory, Madison, Wisconsin, USA.

Schneider, U. (1982) *Behaviour of concrete at high temperature*, Report to RILEM Committee 44-PHT, The Hague, April, p. 72.

Schneider, U. (1986) *Properties of material at high temperatures – Concrete*, 2nd Edition, RILEM Technical Report, University of Kassel, Germany.

Schneider, U. (1990) *Repairability of fire damaged structures,* CIP W14 Report, Fire Safety Journal, Vol 16, No. 4.

Schwatz, K.J. and Lie, T.T. (1985) *Investigating the unexposed surface temperature criteria of standard ASTM E119*, Fire Technology, February 1985, pp. 169-180.

Tenchev, R.T., Li, L.Y. and Purkiss, J.A. (2001) *Finite element analysis of coupled heat and moisture transfer in concrete subjected to fire*, Numerical Heat Transfer, Taylor & Francis, Part A, Vol. 39, No.7, pp. 685-710.

Tenchev, R.T., Li, L.Y., Purkiss, J.A. and Khalafallah, B.H (2001) *Finite element analysis of coupled heat and mass transfer in concrete when it is in a fire*, Magazine of Concrete Research, Vol. 53, No.2, pp 117-125.

Terro, M.J. (1998) *Numerical modelling of the behaviour of concrete structures*, ACI Structural Journal, Vol. 95, No. 2, pp. 183-193.

Thomas, G. (2002) *Thermal properties of gypsum plasterboard at high temperatures*, Fire Materials, Vol. 26, pp. 37-45.

Tucker, D.M. and Read, R.E.H. (1981) *Assessment of fire damaged structures*, Building Research Establishments Information Paper (IP 24/81), Building Research Establishment, Department of Environment, Watford, UK.

APPENDIX

EXAMPLE OF HEAT TRANSFER SOLUTION USING ANSYS

A.1. Element Type

Run the interactive of **ANSYS** to enter the program. Create a title for the problem. This title will appear on ANSYS display windows. To create the title, issue the following command:

Utility menu: **File** ⟶ **Change Title**

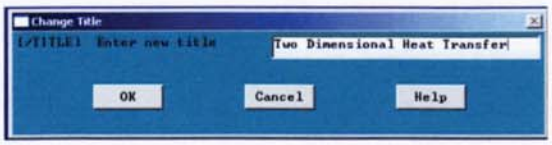

Define the element type with the command:

Main menu: **Preprocessor** ⟶ **Element type** ⟶ **Add/Edit/Delete ...**

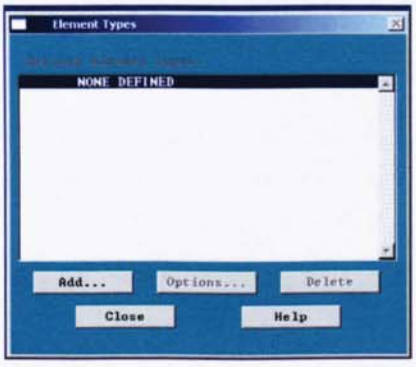

Click **Add** to get a Library of Element Types. From the Library of Element Types, under **Thermal Mass**, choose **Solid**, then choose **Quad 4node 55** and Close:

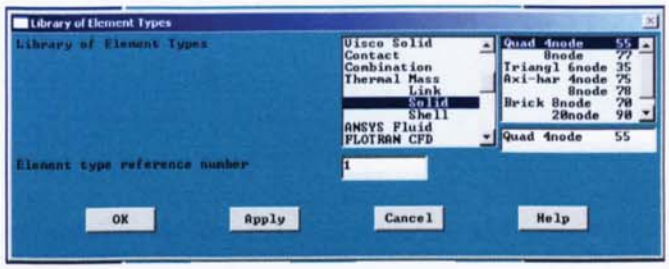

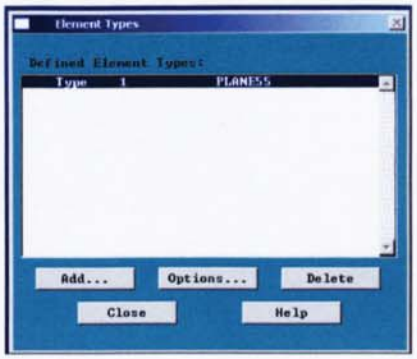

A.2. Material Model

Material properties of the element can be obtained with assign the thermal conductivity values for concrete using following commands:

Main menu: **Preprocessor** ⟶ **Materials Props** ⟶ **Material Models ...**

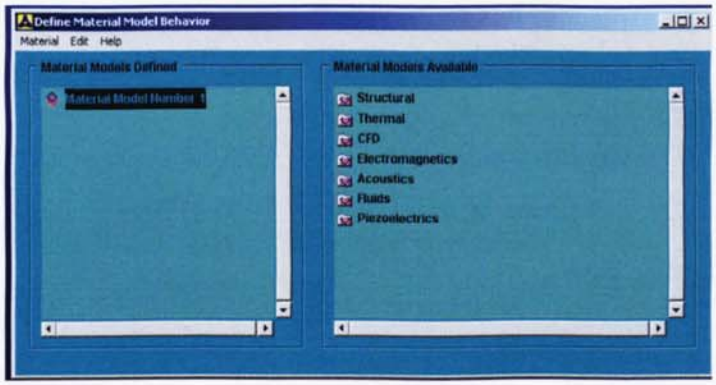

From **Material Model Number 1**, under **Thermal** and under **Conductivity**, choose **Isotropic**

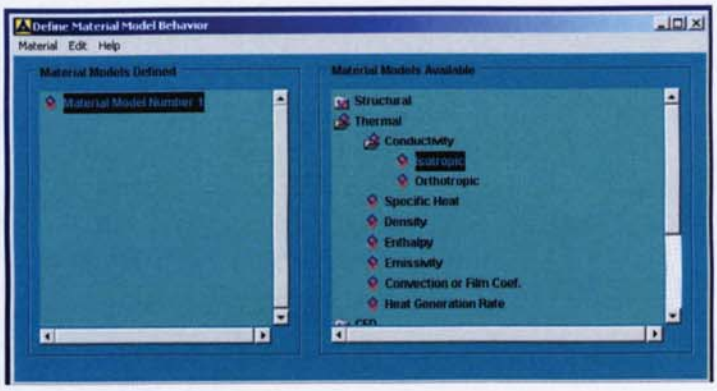

And put in the value of concrete thermal conductivity: KXX = 1.4, click OK and exit from Material Models.

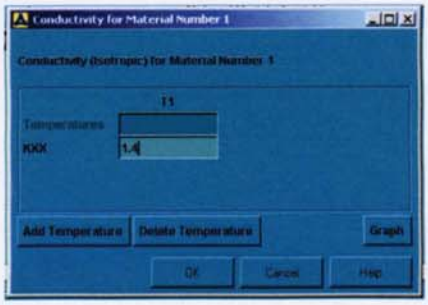

ANSYS Toolbar: **SAVE_DB**.

A.3. Modelling Dimension of the Frame

Set up the graphics area with the command:

Utility menu: **Workplane** ⟶ **WP Settings …**

Toggle on the workplane by issuing the command:

Utility menu: **Workplane** ⟶ **Display Working Plane**

Bring the workplane to view with the command:

Utility menu: **PlotCtrls** ⟶ **Pan, Zoom, Rotate …**

Click on the **small circle** and operate the moving buttons until the workplane can be view properly on the ANSYS display windows.

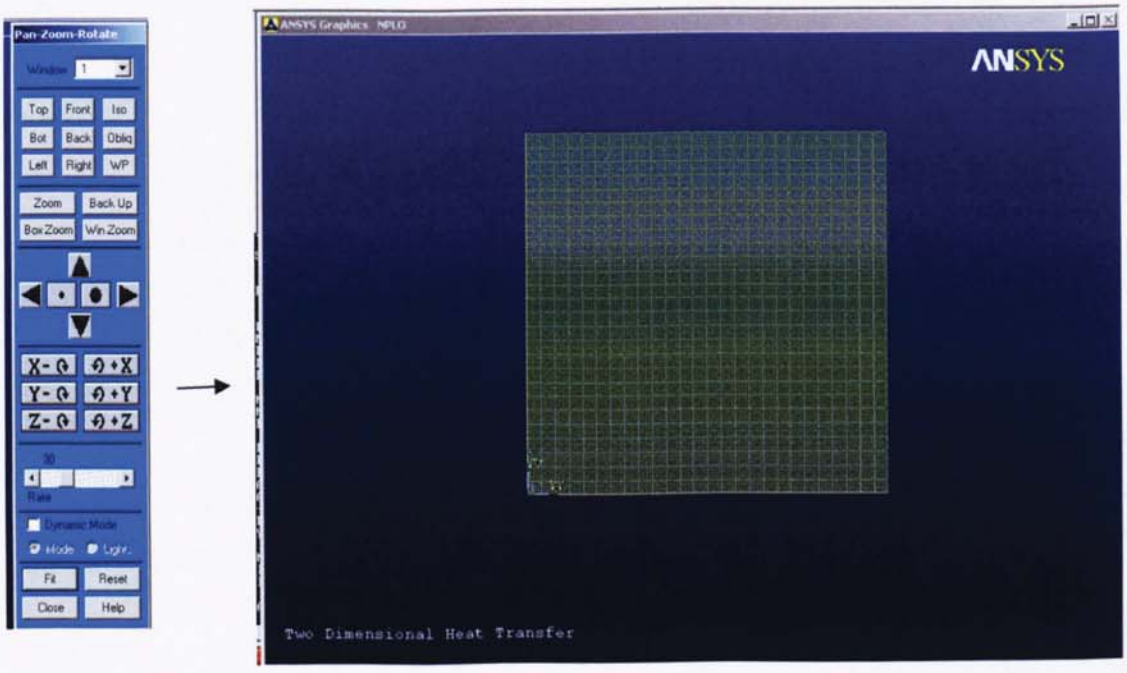

Create the two-storey concrete frame structure by issuing the commands:

Main menu: **Preprocessor** → **Modeling-Create** → **Areas-Rectangle** → **By Dimensions ...**

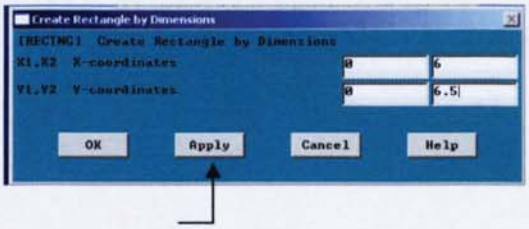

In the X,Y Offsets box, type in X (0.0,6.0) and Y (0.0,6.5) then click **Apply** to create area number 1

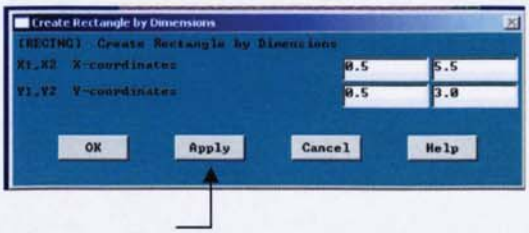

In the X,Y Offsets box, type in X (0.5,5.5) and Y (0.5,3.0) then click **Apply** to create area number 2

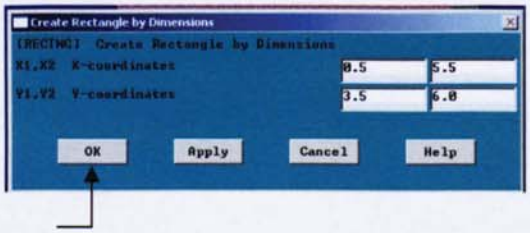

In the X,Y Offsets box, type in X (0.5,5.5) and Y (0.5,3.0) then click **OK** to create area number 3

Next, substract the two inside areas with command:

Main menu: **Preprocessor** → **Modeling-Operate** → **Booleans-Substract** → **Areas +**

Pick the area number 1, **OK**. Then pick area number 2 and area number 3 and **OK**.

To check the work thus far, plot the area by the command:

Utility menu: **Workplane** → **Display Working Plane**

ANSYS Toolbar: **SAVE_DB**.

A.4. Meshing

Before meshing the area to create elements and nodes, the element sizes need to be specified by issuing the commands:

Main menu: **Preprocessor** ⟶ **Meshing-SizeCntrls** ⟶ **-Global-Size ...**

Type in element edge length = 0.05 and **OK**.

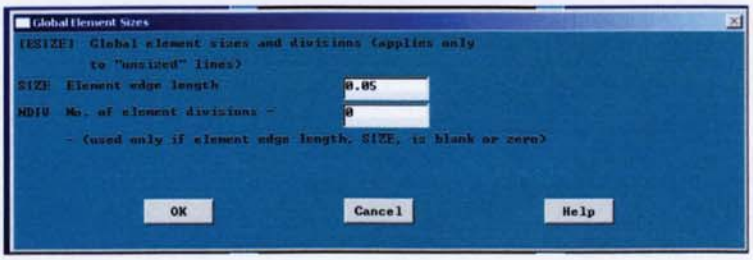

Before proceed with meshing, the material attribute for the concrete need to be checked by issuing the commands:

Main menu: **Preprocessor** ⟶ **-Attributes-Define** ⟶ **All Areas ...**

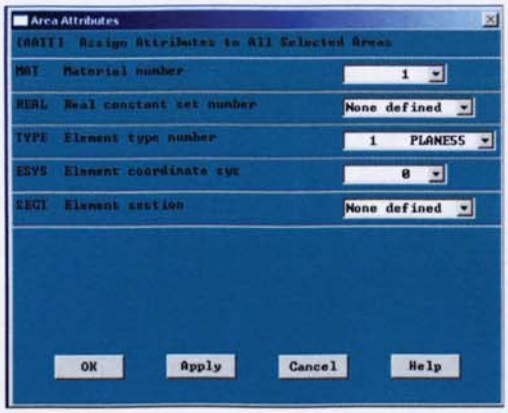

Proceed with meshing the area by issuing the commands:

Main menu: **Preprocessor** ⟶ **-Meshing-Mesh** ⟶ **-Areas-Free +**

Select **Pick All** and proceed meshing.

A.5. Boundary Conditions

Apply boundary conditions using the commands:

Main menu: **Solution** ⟶ **-Loads-Apply** ⟶ **-Thermal-Convection**

⟶ **On Lines +**

Pick the interior lines of first floor concrete frame and press the **OK** button to specify the convection coefficient and the temperature:

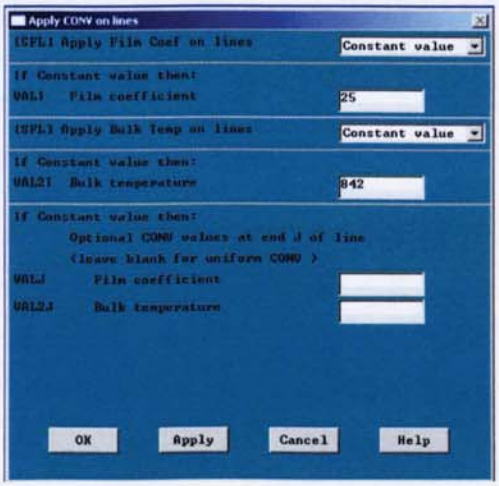

Main menu: **Solution** ⟶ **-Loads-Apply** ⟶ **-Thermal-Convection**

⟶ **On Lines +**

Pick the rest of lines of the concrete frame and press the **OK** button to specify the convection coefficient and the temperature:

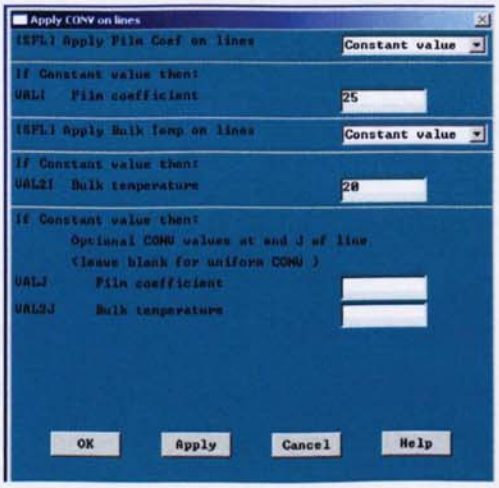

ANSYS Toolbar: **SAVE_DB**.

A.6. Solving the Problem

Solve the problem with the following commands:

Main menu: **Solution** ⟶ **-Solve-Current LS** ⟶ **OK**

Close (the solution is done!) window, and

Close (the /STATUS Command) window

Begin the postprocessing phase to obtain information such as nodal temperatures with the command:

Main menu: **General Postproc** ⟶ **Plot Results** ⟶ **-Contour Plot-Nodal Solu ...**

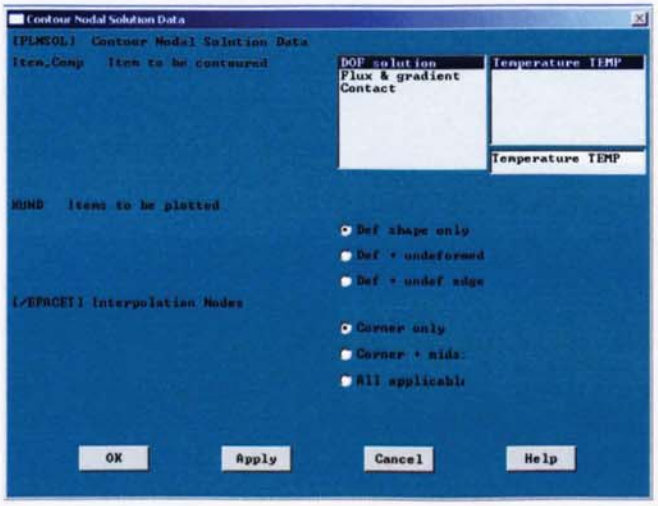

To view the contour plot of the temperature distribution on ANSYS display window, issue the following command:

Utility menu: **PlotCtrls** → **Window Controls** → **Window Options …**

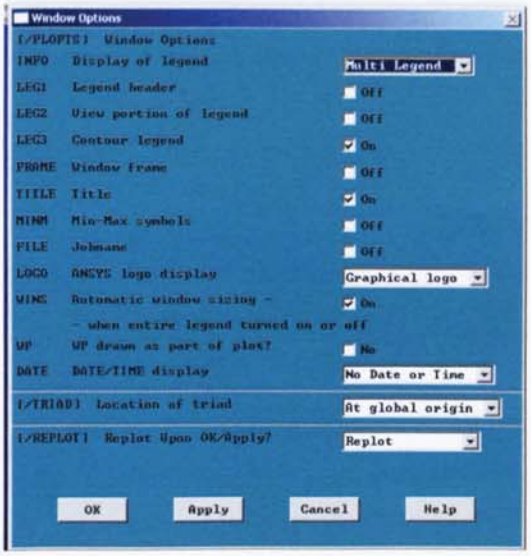

Turn **On** the Contour legend, Title and Automatic window sizing; and click **OK** to display the following temperature distribution result:

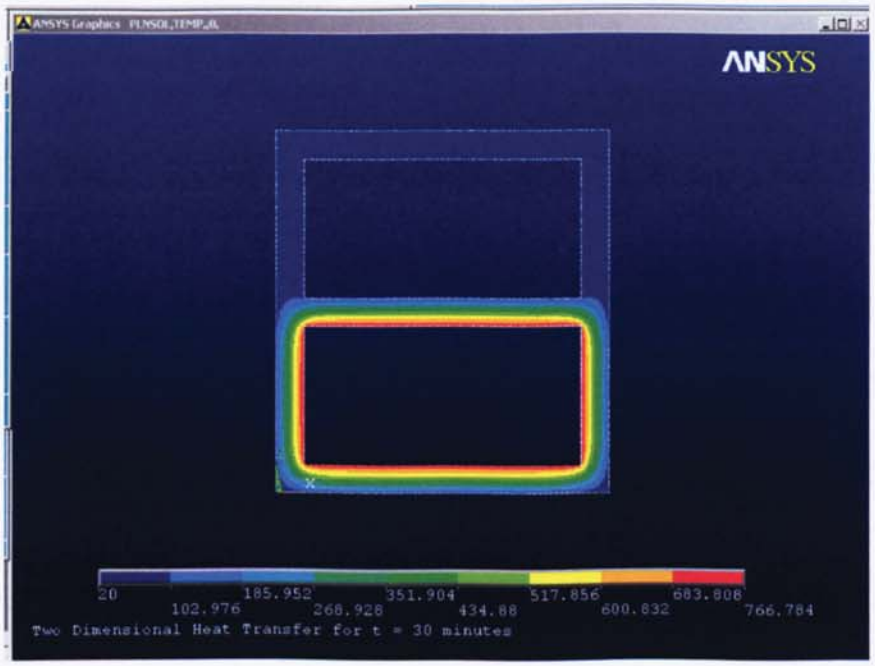

A.7. Transferring the Results onto Word Document

Transferring the results onto the Word.doc with the following commands:

Utility menu: **PlotCtrls** ⟶ **Capture Image**

From the image of figure displayed on the screen, click **File** ⟶ **Save As**

Save the file as a **file.bmp** to **My Documents**.

Open My Documents and click on File.

Edit the picture with following commands:

Utility menu of file.Bmp: **Image** ⟶ **Invert Colors**

This utiliy menu also has facility to edit or alter the picture.

Utility menu: **Edit** ⟶ **Select All**

Utility menu: **Edit** ⟶ **Copy**

Open the Word and **Paste Special** as a **Picture**, then, save the picture as a **word.doc**.

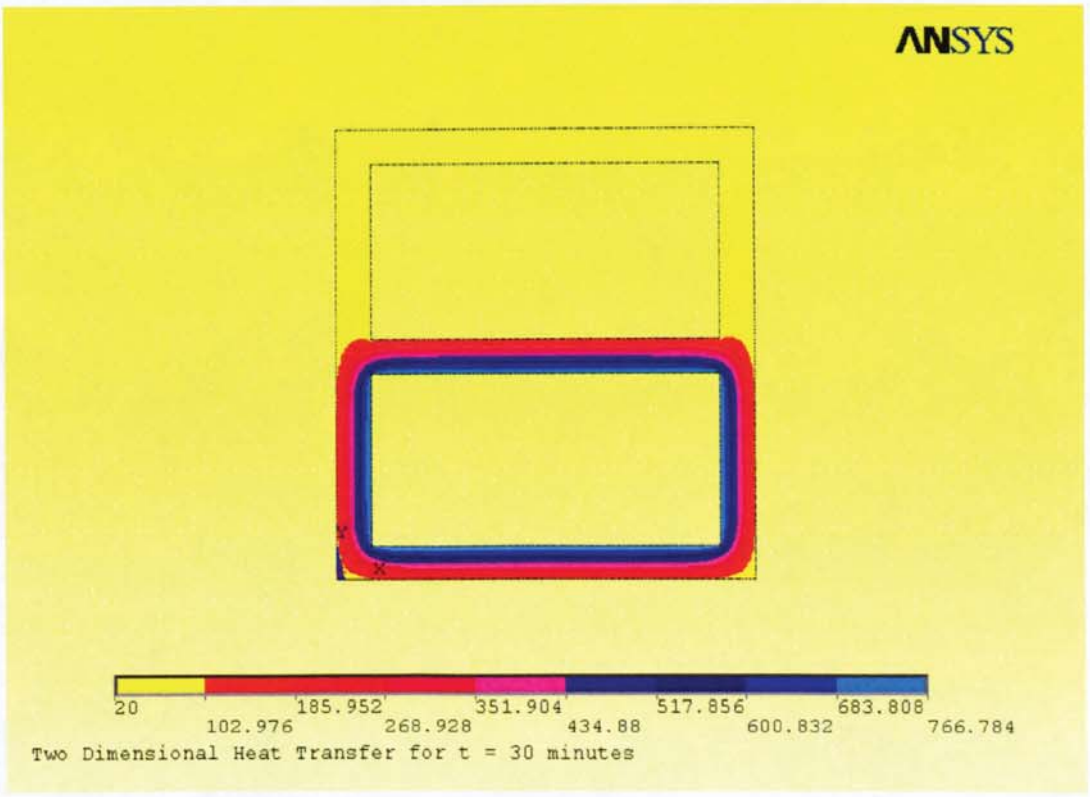

Figure: Temperature contour plot for the exposure temperature of 30 minutes